VOLUME 3

ADVANCED PETROPHYSICS

Solutions

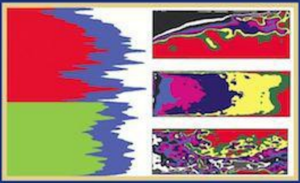

Ekwere J. Peters, PhD, PE

VOLUME 3

ADVANCED PETROPHYSICS

Solutions

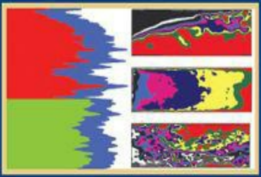

Ekwere J. Peters, PhD, PE

LIVE OAK
BOOK COMPANY

Published by Live Oak Book Company
Austin, TX
www.liveoakbookcompany.com

Distributed by Live Oak Book Company

For ordering information or special discounts for bulk purchases, please contact Live Oak Book Company at PO Box 91869, Austin, TX 78709, 512.891.6100.

Design and composition by Greenleaf Book Group LLC
Cover design by Greenleaf Book Group LLC

LCCN: 2012935369
Ebook ISBN: 978-1-936909-49-0

Ebook Edition

TABLE OF CONTENTS

Appendix B Solutions

PREFACE

Volume 3 of *Advanced Petrophysics* presents the solutions to the 150 end-of-chapter exercises and projects in Volumes 1 and 2. I recommend that you attempt the problem first before you consult my solution to check your progress and mastery of the subject. The solutions for the projects in Appendix B that involve log analysis require some professional judgment and experience to accomplish. Therefore, I do not expect your solutions for these projects to be identical to mine but they should be close.

Ekwere J. Peters, PhD, PE

Austin, Texas, 2012

CHAPTER 1 SOLUTIONS

PROBLEM 1.1

The solution to this problem depends on your background in geology, chemistry, physics, and your familiarity with various laboratory instruments. Here are some possibilities.

Acid Test:
Cut a fresh piece of each sample. Drop cold HCL on the freshly cut surface and observe. The limestone (Core A) will react vigorously with the cold HCL, releasing CO_2 in the process. The sandstone (Core B) and dolomite (Core C) will not react with the cold acid. This

simple test identifies the limestone conclusively.

Next, heat the HCL almost to its boiling point and repeat the test with the hot HCL on the two remaining samples (Cores B and C). The dolomite will react with the hot acid but the sandstone will not. This test distinguishes the dolomite from the sandstone.

Grain Density/Specific Gravity Measurements:

Cut a piece of each sample and grind into a powder. Weigh the powder in air (W). Determine the volume of the powder by fluid displacement (*V*). Compute the grain density in g/cc (*W/V*) and compare with the standard grain densities for quartz (2.65 g/cc), limestone (2.71 g/cc), and dolomite (2.85 g/cc) to identify the samples.

More Sophisticated Measurements:

X-ray diffraction spectroscopy can be used to identify the mineral constituents of each sample conclusively.

Infrared spectroscopy can be used to identify the mineral constituents of each sample conclusively.

Photoelectric effect measurements can be used to identify each sample conclusively. Here are the typical values:

Sandstone: 1.81 barns/electron

Dolomite: 3.14 barns/electron

Limestone: 5.08 barns/electron

By the way, the photoelectric log is used to distinguish dolomite and limestone in well logging.

CHAPTER 2 SOLUTIONS

PROBLEM 2.1

2.1a

$$V_b = \pi r^2 h_1 \tag{2.1.1}$$

$$V_s = \pi r^2 \left(h_2 - h_1\right) \tag{2.1.2}$$

$$\phi = \frac{V_p}{V_b} = 1 - \frac{V_s}{V_b} = 1 - \frac{\pi r^2 \left(h_2 - h_1\right)}{\pi r^2 h_1} = 2 - \frac{h_2}{h_1} \tag{2.1.3}$$

2.1b

$$\phi = 2 - \frac{h_2}{h_1} = 2 - \frac{8}{5} = 0.40$$

2.1c

From Carman-Kozeny equation for granular particles,

$$k = \frac{\phi^3}{5S^2} \qquad (2.1.4)$$

where *S* is the surface area per unit bulk volume and is given by

$$S = \frac{3(1-\phi)}{r} \qquad (2.1.5)$$

$$r = \frac{D}{2} = \frac{15\times10^{-3}}{2}\ \text{cm} = 75\times10^{-4}\ \text{cm}$$

$$S = \frac{3(1-0.4)}{75\times10^{-4}} = 240\ \text{cm}^2/\text{cm}^3$$

Substituting for S in Eq.(2.1.4) gives

$$k = \frac{(0.4)^3}{5(240)^2}\ \text{cm}^2 = 2.222\times10^{-7}\ \text{cm}^2 \times \frac{1}{9.869\times10^{-9}} \times \frac{D}{\text{cm}^2} = 22.5D$$

PROBLEM 2.2

2.2a

FIGURE 2.2.1 shows a sketch of the problem.

> R_e = external radius of the ping pong balls
> R_i = internal radius of the ping pong balls

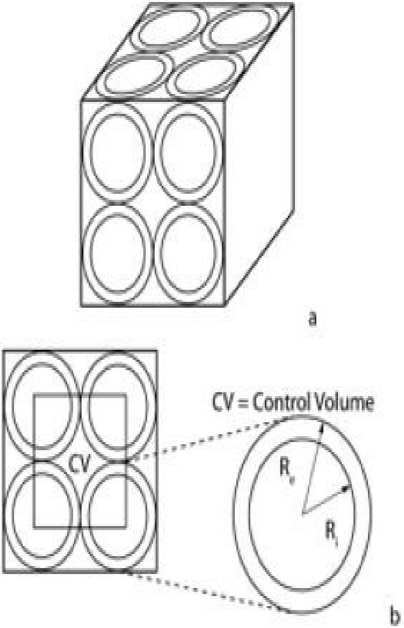

FIGURE 2.2.1 Schematic of packing. (a) 3D packing; (b) 2D plan view.

The total porosity is given by

$$\phi_T = \frac{V_{pore}}{V_{bulk}} = \frac{V_{bulk} - V_{solid}}{V_{bulk}} \tag{2.2.1}$$

$$V_{bulk} = (2R_e)^3 = 8R_e^3 \tag{2.2.2}$$

$$V_{solid} = \frac{4}{3}\pi R_e^3 - \frac{4}{3}\pi R_i^3 = \frac{4}{3}\pi\left(R_e^3 - R_i^3\right) \tag{2.2.3}$$

Substituting Eqs.(2.2.2) and (2.2.3) into (2.2.1) gives

$$\phi_T = \frac{8R_e^3 - \frac{4}{3}\pi\left(R_e^3 - R_i^3\right)}{8R_e^3} = 1 - \frac{\pi}{6} + \frac{\pi}{6}\left(\frac{R_i}{R_e}\right)^3 \tag{2.2.4}$$

Assume values of $R_e = 2$ cm and thickness of the ping pong ball of 0.025 cm. $R_i = R_e$-thickness = 2 cm – 0.025 cm

= 1.975 cm. Substituting these values in the equation (2.2.4) gives

$$\phi_T = 1 - \frac{\pi}{6} - \frac{\pi}{6}\left(\frac{1.975}{2}\right)^3 = 0.98 \text{ or } 98\%$$

2.2b

We know that the effective porosity of the cubic pack is 47.6%. If we filled the interconnected pores with solid spherical grains, we have the following new arrangement.

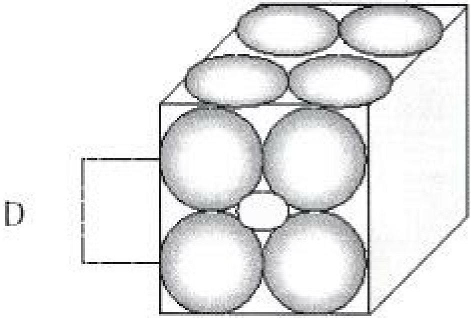

FIGURE 2.2.2 3D view.

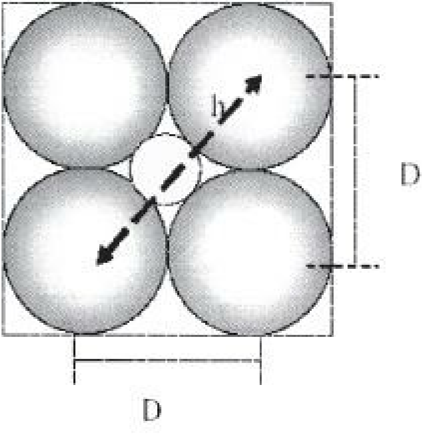

FIGURE 2.2.3 Plan view.

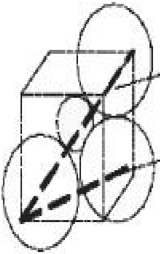

FIGURE 2.2.4 3D Schematic with diagonals.

The diagonal of the base (h) can be determined as follows (see plan view):

$$h=\sqrt{D^2+D^2}=D\sqrt{2} \tag{2.2.5}$$

The diagonal H, can be determined as follows:

$$H=\sqrt{h^2+D^2}=\sqrt{2D^2+D^2}=D\sqrt{3} \tag{2.2.6}$$

Then, the diameter of the quartz grain

located in the middle of the cube can be determined as:

$$D_g = H - 2\left(\frac{D}{2}\right) = H - D = D\sqrt{3} - D = D\left(\sqrt{3} - 1\right) \quad (2.2.7)$$

$$\phi = 1 - \frac{V_{solid-balls} + V_{solid-quartz}}{V_{bulk}} = 1 - \frac{\frac{\pi}{6}D^3 + \frac{\pi}{6}D^3(\sqrt{3}-1)^3}{D^3}$$

$$= 1 - \left[\frac{\pi}{6}\left(1 + (\sqrt{3}-1)^3\right)\right] = 0.271$$

The change in effective porosity with respect to the original effective porosity can be computed as:

$$\Delta\phi\ (\%) = \left|\frac{\phi_{original} - \phi_{final}}{\phi_{original}}\right| \times 100 = \left|\frac{0.476 - 0.271}{0.271}\right| \times 100 = 43.07\%$$

The poor sorting has reduced the effective porosity by 43.07%, a significant reduction in porosity.

2.2c

Without the holes in the ping-pong balls, the Boyle's Law porosimeter will measure the volume of the ping-pong balls as solid volume. Once the holes are drilled, the gas can penetrate inside the ping-pong balls and the porosimeter will measure the solid volume of the skin of the ping-pong balls. Hence, the volumes measured in both cases will be quite different. Let's consider 8 ping-pong balls in the porosimeter as case 1. The volume measured by the porosimeter, based on the ping-pong ball dimensions assumed in part (b), will be $8 \times 4/3 \times \pi \times Re^3_e = 268.08$ cc (the volume of the entire balls). Then, let's consider case 2, when the holes are drilled in the ping-pong balls. The volume of solids that will be measured will be as follows: $8 \times 4/3 \times \pi \times (Re^3_e - Re^3_t) = 9.92$ cc. The volumes measured are significantly different. In this case, the volume measured in case 1 is 27 times greater than that measured in case 2.

PROBLEM 2.3

Let the mass of the dry sample be M.

$$V_b = \frac{M}{\rho_b} \tag{2.3.1}$$

$$V_s = \frac{M}{\rho_s} \tag{2.3.2}$$

$$\phi_T = \frac{V_b - V_s}{V_b} = 1 - \frac{V_s}{V_b} = 1 - \frac{M / \rho_s}{M / \rho_b} = 1 - \frac{\rho_b}{\rho_s}$$

Weigh the dry sample in air. Determine the bulk volume using any of the methods described in the text. Calculate the bulk density using Eq.(2.3.1). Pulverize the sample into a powder. Determine the grain volume of the powder by fluid displacement. Calculate the grain density using Eq.(2.3.2). Substitute for the bulk density and grain density in Eq.(2.3.3) to determine the total porosity. Pulverizing the sample into a powder destroys any isolated pores that may be present. Therefore, the porosity determined above is the total porosity.

PROBLEM 2.4

2.4a

$$V_b = \pi\left(\frac{5}{2}\right)^2 (10) = 196.35 \text{ cm}^3$$

$$V_s = \frac{350}{2.65} = 132.08 \text{ cm}^3$$

$$V_p = V_b - V_s = 196.35 - 132.08 = 64.27 \text{ cm}^3$$

$$\phi_T = \frac{V_p}{V_b} = \frac{64.27}{196.35} = 0.3273 = 32.73\,\%$$

2.4b

No. What has been calculated is the total porosity because the pore volume determined by subtracting the mineral grain volume from the bulk volume is the total pore volume, which includes the isolated pores if present.

PROBLEM 2.5

Mass of dry sample = m_d
Mass of saturated sample = m_{sat}
Mass of kerosene saturating the sample $(m_k) = m_{sat} - m_d$
$m_k = 27.575 \text{ g} - 26.725 \text{ g} = 0.85 \text{ g}$

$$V_p = \frac{m_k}{\rho_k} \qquad (2.5.1)$$

$$\rho_k = \frac{141.5}{131.5 + API} = \frac{141.5}{131.5 + 44} = 0.806 \text{ g/cc}$$

Substituting the numerical values for m_d and ρ_k into Eq.(2.5.1) gives

$$V_b = \frac{27.575 - 16.385}{0.806} = 13.88 \text{ cc}$$

Mass of dry sample = m_d

Mass of saturated sample immersed in kerosene = m_{imm}

$$V_b = \frac{m_{sat} - m_{imm}}{\rho_k} \quad (2.5.2)$$

$$V_b = \frac{27.575 - 16.385}{0.806} = 13.88\text{cc}$$

$$\phi_e = \frac{V_p}{V_b} = \frac{1.0546}{13.88} = 0.076$$

PROBLEM 2.6

$$V_b = 23.60 \text{ cc}$$
$$V_s = 51.05 / 2.65 = 19.264 \text{ cc}$$
$$V_p = V_b - V_s = 23.60 - 19.264 = 4.336 \text{ cc}$$
$$\phi = V_p / V_b = 4.336 / 23.60 = 0.1837$$
$$m_w = \rho_w V_w = (1)(1.5) = 1.50 \text{ g}$$
$$m_{w+o} = 53.50 - 51.05 = 2.45 \text{ g}$$
$$m_o = 2.45 - 1.50 = 0.95 \text{ g}$$
$$V_o = m_o / \rho_o = 0.95 / 0.85 = 1.118 \text{ cc}$$
$$S_w = V_w / V_p = 1.50 / 4.336 = 0.3459$$
$$S_o = V_o / V_p = 1.118 / 4.336 = 0.2578$$
$$S_g = 1 - S_w - S_o = 1 - 0.3459 - 0.2578 = 0.3963$$

PROBLEM 2.7

2.7a

$$V_{bi} = \frac{AL}{N} \tag{2.7.1}$$

where A is the cross-sectional area of the core.

$$V_{pi} = V_{bi}\phi_i = \frac{AL}{N}\phi_i \tag{2.7.2}$$

$$V_{pT} = \sum_{i=1}^{i=N} \frac{AL}{N}\phi_i = \frac{AL}{N}\sum_{i=1}^{i=N}\phi_i \tag{2.7.3}$$

$$V_{bT} = AL \tag{2.7.4}$$

$$\phi_T = \frac{V_{pT}}{V_{bT}} = \frac{\frac{AL}{N}\sum_{i=1}^{i=N}\phi_i}{AL} = \frac{\sum_{i=1}^{i=N}\phi_i}{N} \qquad (2.7.5)$$

2.7b

Method 1

Apply the integrated form of Darcy's Law to the core before it was cut.

$$\Delta P_T = \frac{q\mu L}{k_T A} \tag{2.7.6}$$

Apply Darcy's Law to each piece after the core has been cut into *N* equal pieces.

$$\Delta P_i = \frac{q\mu L_i}{k_i A} \tag{2.7.7}$$

Because the core was cut into equal pieces,

$$L_i = \frac{L}{N} = \text{a constant} \tag{2.7.8}$$

Substituting Eq.(2.7.8) into (2.7.7) gives

$$\Delta P_i = \frac{q\mu L}{N k_i A} \tag{2.7.9}$$

But

$$\Delta P_T = \sum_{i=1}^{i=N} \Delta P_i \tag{2.7.10}$$

Substituting Eqs.(2.7.6) and (2.7.9) into Eq.(2.7.10) and cancelling common terms gives

$$\frac{1}{k_T} = \frac{1}{N} \sum_{i=1}^{i=N} \frac{1}{k_i} \tag{2.7.11}$$

Solving Eq.(2.7.11) for k_T gives

$$k_T = \frac{N}{\sum_{i=1}^{i=N} \frac{1}{k_i}} \tag{2.7.12}$$

2.7b

Method 2

The total permeability of the core is the harmonic average of the permeabilities of the pieces in series. Eq.(3.159) in the textbook gives the harmonic average for beds in series as

$$k_T = \frac{\sum_{i=1}^{i=N} L_i}{\sum_{i=1}^{i=N} \frac{L_i}{k_i}} = \frac{L}{\sum_{i=1}^{i=N} \frac{L_i}{k_i}} \tag{2.7.13}$$

Substituting Eq.(2.7.8) into (2.7.13) gives

$$k_T = \frac{L}{\frac{L}{N}\sum_{i=1}^{i=N}\frac{1}{k_i}} = \frac{N}{\sum_{i=1}^{i=N}\frac{1}{k_i}} \tag{2.7.14}$$

PROBLEM 2.8

2.8a

Ideal gas law:

$$PV = nRT \tag{2.8.1}$$

At initial conditions,

$$n_1 = \frac{\left(P_{1g} + P_a\right)}{RT} V_r \tag{2.8.2}$$

$$n_2 = \frac{P_a\left(V_c - V_s\right)}{RT} \tag{2.8.3}$$

At final conditions, the total amount of moles is:

$$n_T = \frac{\left(P_{2g} + P_a\right)\left(V_r + V_c - V_s\right)}{RT} \qquad (2.8.4)$$

From mass balance,

$$n_T = n_1 + n_2 \qquad (2.8.5)$$

Substituting Eqs.(2.8.2), (2.8.3), and (2.8.4) into Eq.(2.8.5) gives

$$\frac{(P_{2g} + P_a)(V_r + V_c - V_S)}{RT} = \frac{P_{1g} + P_a}{RT} V_r + \frac{P_a}{RT}(V_c - V_S)$$

$$P_{2g}V_r + P_aV_r + P_{2g}V_c + P_aV_c - P_{2g}V_S - P_aV_S = P_{1g}V_r + P_aV_r + P_aV_c - P_aV_S$$

$$P_{2g}(V_r + V_c - V_S) = P_{1g}V_r$$

$$V_r + V_c - V_S = \frac{P_{1g}}{P_{2g}} V_r$$

Therefore,

$$V_s = V_c + V_r - \frac{P_{1g}}{P_{2g}} V_r \tag{2.8.6}$$

2.8b

To generate the calibration curve, use the given data to plot a graph of V_s vs P_1/P_2. This should be a straight line. It is always advantageous to plot a linear calibration curve if possible. **FIGURE 2.8.1** shows the calibration curve.

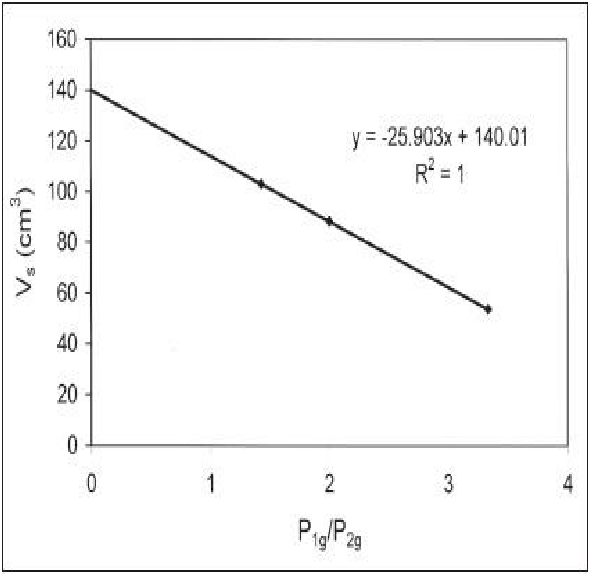

FIGURE 2.8.1 Calibration curve for the porosimeter.

2.8c

From the calibration curve,

$$V_r = 25.90 \text{ cm}^3$$

$$V_r + V_c = 140.010 \text{ cm}^3$$

$$V_c = 140.01 - 25.90 = 114.11 \text{ cm}^3$$

2.8d

L – 3.4 *in* – 8.636 cm

d = 1.5 *in* = 3.81 cm

V_b= 98.46 cm^3

P_{1g}=48 psig

P_{2g}=100 psig

P_{2g}/P_{1g} 100/48 = 2.08

V_r = 25.90 cm^3

V_c = 114.11 cm^3

From the calibration curve,

$$V_s = 86.05 \text{ cm}^3$$

$$\phi = \frac{V_p}{V_b} = \frac{V_b - V_s}{V_b} = \frac{98.46 - 86.05}{98.46} = 0.126$$

2.8e

Only the gas in the connected pores participates in this gas expansion experiment. Therefore, the porosity from this gas expansion experiment is the effective porosity.

PROBLEM 2.9

2.9a

$$V_p = \pi r^2 L = \pi \left(\frac{L}{4} \right)^2 L = \frac{\pi L^3}{16}$$

$$\phi = \frac{V_p}{V_b} = \frac{\pi L^3 / 16}{L^3} = \frac{\pi}{16} = 0.1963$$

2.9b

For resistors in parallel,

$$\frac{1}{r_t} = \frac{1}{r_w} + \frac{1}{r_m} \qquad (2.9.1)$$

$$r \propto \frac{L}{A}$$

$$r = \frac{RL}{A} \qquad (2.9.2)$$

where

A = cross-sectional area of the conductor

L = length of conductor

R = resistivity of the conductor

$$r_t = \frac{R_t L_t}{A_t} \qquad (2.9.3)$$

$$r_w = \frac{R_w L_w}{A_w} \qquad (2.9.4)$$

$$r_m = \frac{R_m L_m}{A_m} \tag{2.9.5}$$

Substituting Eqs.(2.9.3), (2.9.4), and (2.9.5) into Eq.(2.9.1) gives

$$\frac{A_t}{R_t L_t} = \frac{A_w}{R_w L_w} + \frac{A_m}{R_m L_m} \tag{2.9.6}$$

$$\frac{L^2}{R_t L} = \frac{\pi\left(\frac{L}{4}\right)^2}{R_w L} + \frac{L^2 - \pi\left(\frac{L}{4}\right)^2}{R_m L} \tag{2.9.7}$$

$$\frac{L}{R_t} = \frac{\pi\left(\frac{L}{16}\right)}{R_w} + \frac{L - \pi\left(\frac{L}{16}\right)}{R_m} \tag{2.9.8}$$

$$R_m \rightarrow \infty$$

$$\frac{L}{R_t} = \frac{\pi\left(\frac{L}{16}\right)}{R_w} \qquad (2.9.9)$$

$$\frac{R_t}{R_w} = \frac{1}{(\pi/16)} = \frac{16}{\pi} = 5.093$$

For this case, $R_t = R_0$.

2.9c

$$F = \frac{1}{\phi} = \frac{a}{\phi^m}$$

$$a = 1, m = 1.$$

2.9d

$$A_p = 2\pi r L = 2\pi\left(\frac{L}{4}\right)L$$

$$V_b = L^3$$

$$S = \frac{A_p}{V_b} = \frac{2\pi\left(\frac{L}{4}\right)L}{L^3} = \frac{\pi}{2L}$$

2.9e

Hagen-Poiseulle's Law:

$$q = \frac{\pi r^4}{8\mu}\frac{\Delta P}{L} \qquad (2.9.10)$$

$$q = \frac{kA_T}{\mu}\frac{\Delta P}{L} \qquad (2.9.11)$$

A comparison of Eqs.(2.9.10) and (2.9.11) gives

$$\frac{kA_T}{\mu} = \frac{\pi r^4}{8\mu} \qquad (2.9.12)$$

$$k = \frac{\pi r^4}{8A_T} \qquad (2.9.13)$$

$$r = \frac{L}{4} \qquad (2.9.14)$$

$$A_T = L^2 \qquad (2.9.15)$$

Substituting Eqs.(2.9.14) and (2.9.15) into (2.9.13) gives

$$k = \frac{\pi \left(\frac{L}{4} \right)^4}{8L^2} = \frac{\pi L^2}{2048} = \frac{\pi L^2}{2^{11}}$$

PROBLEM 2.10

Archie's equation:

$$F = \frac{R_o}{R_w} = \frac{a}{\phi^m}$$

The given data are used to determine the best values for *a* and m. **FIGURE 2.10.1** shows the log-log plot of *F* versus f. From the regression line, *a* = 0.7981 and *m* = 1.5131.

$$F = \frac{1.29}{0.056} = \frac{0.7981}{\phi^{1.5131}}$$

$$\phi = \left[0.7981\left(\frac{0.056}{1.29}\right)\right]^{\frac{1}{1.5131}} = 0.1084 \text{ or } 10.84\%$$

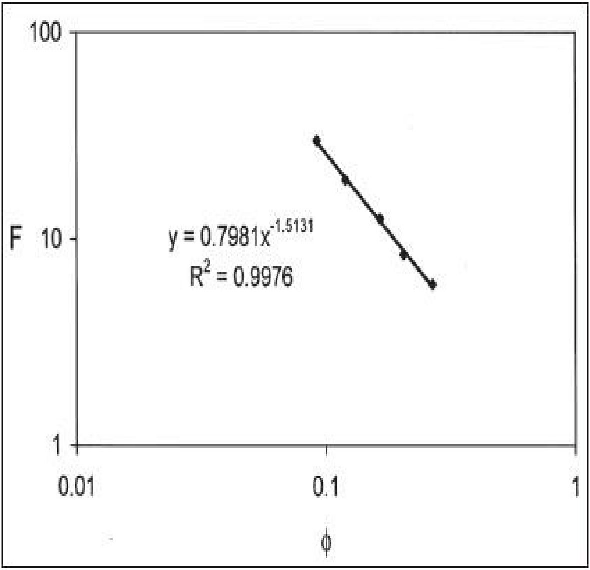

FIGURE 2.10.1 Log-log plot of F versus ϕ.

PROBLEM 2.11

Matrix densities:
Sandstone: 2.65 g/cm^3
Limestone: 2.71 g/cm^3
Dolomite: 2.87 g/cm^3
Pf = 1 g/cm^3

$$\rho_b = \rho_f \phi + (1-\phi)\rho_m \tag{2.11.1}$$

Eq.(2.11.1) was used to calculate the entries in **TABLE 2.11.1**.

TABLE 2.11.1 Bulk Density Variation with Porosity.

ϕ	ρ_b (g/cm^3) Sandstone	ρ_b (g/cm^3) Limestone	ρ_b (g/cm^3) Dolomite
0.05	2.571	2.625	2.777
0.10	2.489	2.539	2.683
0.15	2.406	2.454	2.590
0.20	2.323	2.368	2.496
0.25	2.241	2.283	2.403
0.30	2.158	2.197	2.309

PROBLEM 2.12

$a = 1$
$m = 2$
$n = 2$
$S_w = 0.25$
$R_w = 0.025$ ohm-m

$$F = \frac{a}{\phi^m} = \frac{R_o}{R_w} \tag{2.12.1}$$

$$R_o = F \times R_w \tag{2.12.2}$$

Archie's Equation:

$$\frac{R_t}{R_o} = \frac{1}{S_w^n} \tag{2.12.3}$$

$$R_t = \frac{R_o}{S_w^n} = \frac{F \times R_w}{S_w^n} \tag{2.13.4}$$

The entries in **TABLE 2.12.1** were calculated using Eqs.(2.12.1), (2.12.2), and (2.12.4).

TABLE 2.12.1 Variation of F, R_o, and R_w with Porosity.

ϕ	F	R_0 (ohm-m)	R_t (ohm-m)
0.05	400.00	10.00	160.00
0.10	100.00	2.50	40.00
0.15	44.44	1.11	17.78
0.20	25.00	0.63	10.00
0.25	16.00	0.40	6.40
0.30	11.11	0.28	4.44

PROBLEM 2.13

2.13a

Wyllie's average equation:

$$\phi = \frac{\Delta t - \Delta t_m}{\Delta t_f - \Delta t_m} \qquad (2.13.1)$$

$$\Delta t_m = 55.5 \ \mu\text{sec/ft}$$

$$\Delta t_f = 189 \ \mu\text{sec/ft}$$

From the log,

$$\Delta t = 100 \ \mu\text{sec/ft}$$

Substituting the numerical values into

Eq.(2.13.1) gives

$$\phi = \frac{100 - 55.5}{189 - 55.5} = 0.33$$

Archie's saturation equation:

$$S_w^n = \frac{aR_w}{\phi^m R_t} \qquad (2.13.2)$$

where

S_w = water saturation
R_w = formation water resistivity (in this case equal to 0.06 Ω*m*)
R_t= Formation resistivity (obtained from the resistivity log)
R_t =2Ωm, a = 1, m = 1.5 and n = 2.

$$S_w = \sqrt{\frac{0.06}{0.33^{1.5} \times 2}} = 0.398$$

$$S_o = 1 - S_w \tag{2.13.3}$$

Hence, the hydrocarbon saturation is 0.602.

2.13b

Humble formula for formation resistivity factor:

$$F = \frac{0.62}{\phi^{2.15}} \tag{2.13.4}$$

Eq.(2.13.2) can be rewritten as

$$S_w = \frac{0.62 R_w}{\phi^{2.15} R_t} \tag{2.13.5}$$

The water saturation is given by

$$S_w = \sqrt{\frac{0.62 \times 0.06}{0.33^{2.15} \times 2}} = 0.449$$

$$S_o = 1 - S_w = 1 - 0.449 = 0.551$$

The hydrocarbon saturation from the Humble formula is 0.551.

$$\%Difference = \frac{S_{o,Archie} - S_{o,Humble}}{S_{o,Archie}} \times 100 = \frac{0.602 - 0.551}{0.602} \times 100 = 8.5\%$$

Humble formula gives a hydrocarbon saturation that is 8.5% less than Archie's equation in this case.

PROBLEM 2.14

Porosity is given by

$$\phi = \frac{\rho_b - \rho_m}{\rho_f - \rho_m} \tag{2.14.1}$$

$$\rho_m = 2.67\ g/cm^3$$
$$\rho_f = 1\ g/cm^3$$

The bulk density (ρ_b) is read from the density log in each zone. The results for all the zones are shown in **TABLE 2.14.1**.

TABLE 2.14.1 Porosity Value in Each Zone.

Zone	ρ_b (g/cm^3)	ϕ (%)
A	2.4	16.168
B	2.32	20.958
C	2.36	18.563
D	2.35	19.162
E	2.35	19.162
F	2.37	17.964
G	2.4	16.168
H	2.37	17.964
I	2.27	23.952
J	2.4	16.168

PROBLEM 2.15

The datum from core 3 did not fit the trend of the other data, so it was treated as an outlier and left out. **FIGURE 2.15.1** shows the resistivity factor versus porosity for the remaining data.

From the regression line,

$$a = 0.674$$

$$m = 2.0625$$

The new and improved Humble formula is

$$F = \frac{0.67}{\phi^{2.06}}$$

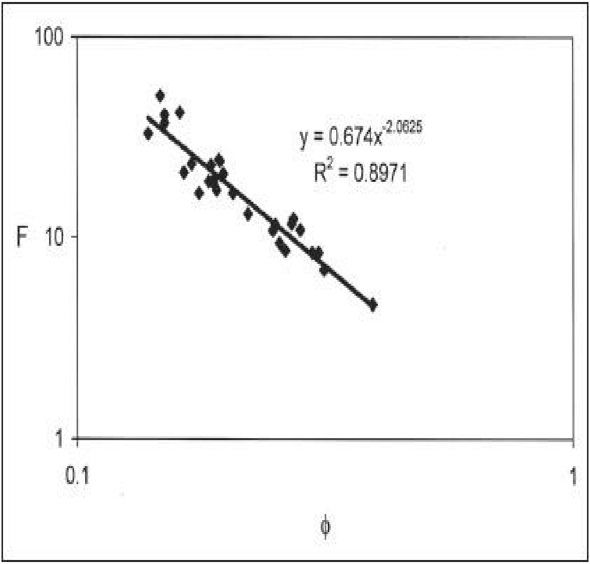

FIGURE 2.15.1 Log-log plot of resistivity factor versus porosity.

PROBLEM 2.16

2.16a and b

$\O_A > \O_B$ because B has closer packing than A.

$\O_A = \O_c$ because A and C have the same cubic packing.

$\O_A > \O_d$ because D has smaller pores than A due to poor sorting.

$\O_A > \O_F$ because E has smaller pores than A due to poor sorting.

$\O_A > \O_F$ because F has smaller pores than A due to compaction and deformation of grains.

CHAPTER 3 SOLUTIONS

PROBLEM 3.1

$L = 2.54$ cm
$d = 2.54$ cm
$A = 5.067$ cm^2
$\mu = 0.018$ cp
1 atm = 760 mm Hg
$P_{sc} = 1$ atm

The uncorrected gas permeability in Darcy units is given by

$$k_g = \frac{2q_{sc}\mu L P_{sc}}{A\left(P_1^2 - P_2^2\right)} \tag{3.1.1}$$

The Klinkenberg correction shown in

FIGURE 3.1.1 gives the absolute permeability of the core as 2.94 mD.

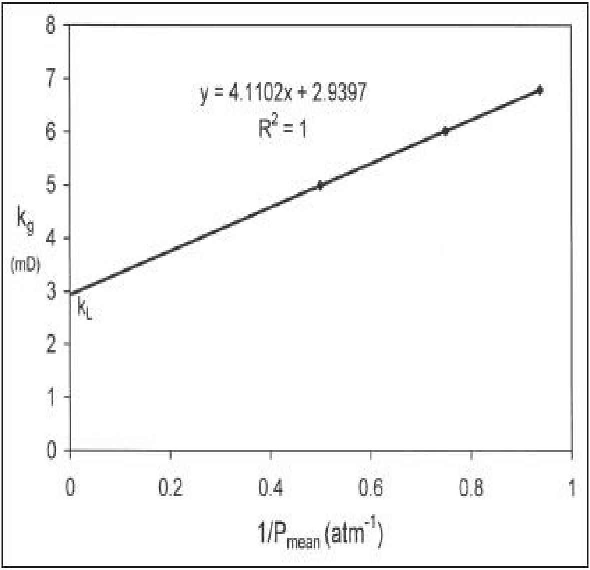

FIGURE 3.1.1 Klinkenberg correction.

PROBLEM 3.2

$L = 5.0$ cm
$d = 2.523$ cm
$A = 4.9995\ \text{cm}^2$
$\mu = 0.0175$ cp
$P_{sc} = 1$ atm

The Klinkenberg correction shown in **FIGURE 3.2.1** gives the absolute permeability of the core as 2.10 mD.

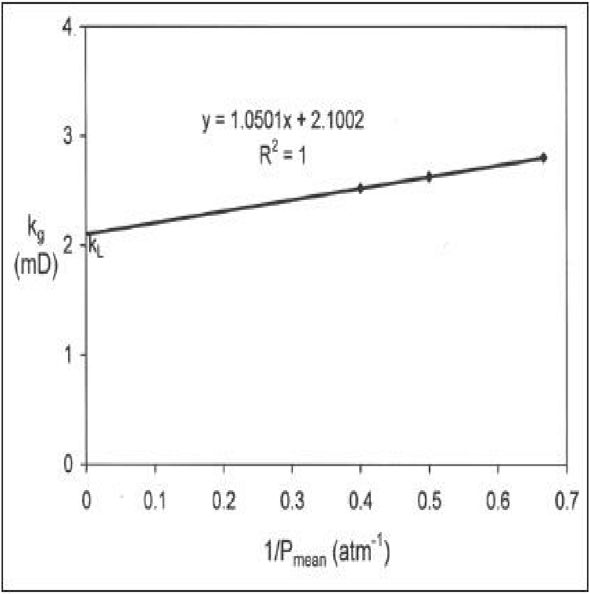

FIGURE 3.2.1 Klinkenberg correction.

PROBLEM 3.3

Applying the integrated form of Darcy's law in Darcy units, the pressure drop across the core is given by

$$\Delta P = \frac{q\mu L}{kA} \tag{3.3.1}$$

Everything on the right side of Eq.(3.3.1) is known except the permeability of the sandpack. We can estimate the permeability of the sandpack using the Carman-Kozeny equation. The surface area per unit bulk volume is given by

$$S = \frac{3(1-\phi)}{r} = \frac{6(1-\phi)}{D} \tag{3.3.2}$$

Carman-Kozeny equation gives

$$k = \frac{\phi^3}{5S^2} = \frac{\phi^3 D^2}{5 \times 6^2 (1-\phi)^2} \tag{3.3.3}$$

Given: $D = 18\mu m$, $\varnothing = 0.28$

Substituting the numerical values into Eq.(3.3.3) gives the permeability as

$$k = \frac{(0.28)^2 (18^2)}{5 \times 6^2 (1-0.28)^2} = 0.0762\ \mu\text{m}^2 = 0.0762 \times 10^{-12}\ \text{m}^2$$

$$= \frac{0.0762 \times 10^{-12}}{9.869 \times 10^{-13}} D$$

$$= 0.0772 D$$

$$A = \pi D^2 / 4 = 25\pi / 4\ \text{cm}^2$$

$$L = 30\ \text{cm}$$

$$q = (100/3600)\ \text{cm}^3/\text{s}$$

Substituting these values into Eq.(3.3.1) gives

$$\Delta P = \frac{(100/3600)(2)(30)}{(0.0772)(25\pi/4)} = 1.0995\ \text{atm} = 1.0995 \times 14.696 = 16.16\ \text{psi}$$

PROBLEM 3.4

3.4a

Darcy's law:

$$q = -\frac{kA}{\mu}\frac{dP}{dx} \quad (3.4.1)$$

$$A = \pi r^2 \quad (3.4.2)$$

$$r = r_1 + \left(\frac{r_2 - r_1}{L}\right)x = r_1 + \beta x \quad (3.4.3)$$

where

$$\beta = \frac{r_2 - r_1}{L} \quad (3.4.4)$$

Substituting Eqs.(3.4.2) and (3.4.3) into (3.4.1) gives

$$q = -\frac{k\pi(r_1+\beta x)^2}{\mu}\frac{dP}{dx} \quad (3.4.5)$$

Separating variables gives

$$-\int_{P_1}^{P_2} dP = \frac{q\mu}{k\pi}\int_0^L \frac{dx}{(r_1+\beta x)^2} \quad (3.4.6)$$

Performing the integrations in Eq.(3.4.6) gives

$$P_1 - P_2 = -\frac{q\mu}{k\pi}\left[\frac{1}{(r_1+\beta x)}\frac{1}{\beta}\right]_0^L = \frac{q\mu}{k\pi}\frac{L}{r_1 r_2} \quad (3.4.7)$$

Thus,

$$\Delta P = \frac{\mu L}{\pi k r_1 r_2} q \tag{3.4.8}$$

3.4b

A graph of Δp versus q is linear with the slope given by

$$m = \frac{\mu L}{\pi k r_1 r_2} \tag{3.4.9}$$

The permeability of the core is calculated as

$$k = \frac{\mu L}{m \pi r_1 r_2} \tag{3.4.10}$$

FIGURE 3.4.1 shows the graph of Δp

versus q.

$$m = 16 \frac{\text{atm}}{\text{cm}^3/\text{s}}$$

$$r_1 = 1 \text{ cm}$$

$$r_2 = 2 \text{ cm}$$

$$L = 10 \text{ cm}$$

$$\mu = 1 \text{ cp}$$

Substituting numerical values into Eq. (3.4.10) gives the permeability as

$$k = \frac{\mu L}{m \pi r_1 r_2} = \frac{(1)(10)}{(16)(\pi)(1)(2)} = 0.0995 D$$

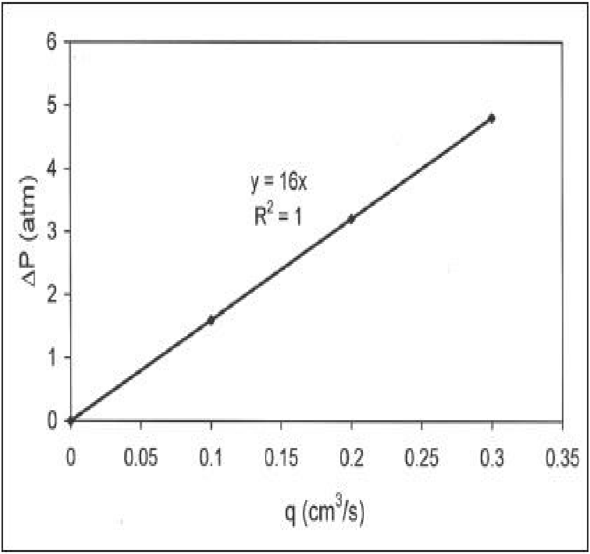

FIGURE 3.4.1 Graph of ΔP versus q.

PROBLEM 3.5

Darcy's law for inclined flow takes the form:

$$q = -\frac{kA}{\mu}\left(\frac{dp}{ds} - \frac{\rho g}{1.0133\times10^{6}}\frac{dz}{ds}\right) \quad (3.5.1)$$

Required to show that in oilfield units, the law is of the form:

$$q = -0.001127\frac{kA}{\mu B}\left(\frac{dp}{ds} - 0.433\gamma\frac{dz}{ds}\right) \quad (3.5.2)$$

To show that (3.5.1) is Eq.(3.5.2) in field units, it is pertinent to state the units of measurement for the various parameters in both equations.

In Darcy units

q [cm^3/s]
k [D]
A [cm^2]
μ [cp]
P [atm]
z [cm]
s [cm]

In oilfield units

q [STB/day]
k [mD]
A [ft^2]
μ [cp]
P [psi]

z [ft]
s [ft]

Convert all the variables in field units into Darcy units and substitute into Eq. (3.5.1).

$$qB\left[\frac{BBL}{\mathrm{D}}\right]=qB\left[\frac{BBL}{\mathrm{D}}\right]\left[\frac{5.615\ \mathrm{ft}^3}{BBL}\right]\left[\frac{30.48^3\ \mathrm{cm}^3}{\mathrm{ft}^3}\right]\left[\frac{\mathrm{D}}{86400s}\right]$$

$$=\left(\frac{5.615\times 30.48^3}{86400}\right)q\left[\frac{\mathrm{cm}^3}{\mathrm{s}}\right]$$

$$k[\mathrm{mD}]=k[\mathrm{mD}]\left[\frac{\mathrm{D}}{1000\ \mathrm{mD}}\right]=\left(\frac{k}{1000}\right)\mathrm{D}$$

$$A\left[\mathrm{ft}^2\right]=A\left[\mathrm{ft}^2\right]\left[\frac{30.48^2\ \mathrm{cm}^2}{\mathrm{ft}^2}\right]=30.48^2\ \mathrm{A\ cm}^2$$

$$\frac{dP}{ds}\left[\frac{\mathrm{psi}}{\mathrm{ft}}\right]=\frac{dP}{ds}\left[\frac{\mathrm{psi}}{\mathrm{ft}}\right]\left[\frac{\mathrm{atm}}{14.696\ \mathrm{psi}}\right]\left[\frac{\mathrm{ft}}{30.48\ \mathrm{cm}}\right]$$

$$=\left(\frac{1}{14.696\times 30.48}\right)\frac{dP}{ds}\left[\frac{\mathrm{atm}}{\mathrm{cm}}\right]$$

$$\rho\left[\frac{\text{lb}}{\text{ft}^3}\right]=\gamma\rho_w\left[\frac{\text{lb}}{\text{ft}^3}\right]\left[\frac{453.6\text{ g}}{\text{lb}}\right]\left[\frac{\text{ft}^3}{30.48^3\text{ cm}^3}\right]$$

$$=\gamma(62.368)\left(\frac{453.6}{30.48^3}\right)\left[\frac{\text{g}}{\text{cm}^3}\right]$$

Substituting into Eq.(3.5.1) and rearranging gives

$$q=-\frac{kA}{\mu B}\left(\frac{86400}{5.615\times 30.48^3}\right)\left(\frac{30.48^2}{1000}\right)\left(\frac{1}{14.696\times 30.48}\right)$$
$$\times\left[\frac{dP}{ds}-(14.696\times 30.48)\left(\frac{62.368\times 453.6}{30.48^3}\right)\left(\frac{981}{1.0133\times 10^6}\right)\gamma\frac{dz}{ds}\right]$$

Simplifying gives

$$q=-0.001127\frac{kA}{\mu B}\left(\frac{dp}{ds}-0.433\gamma\frac{dz}{ds}\right)\text{ as required.}$$

PROBLEM 3.6

$q = 70\ \text{cm}^3 / \text{hr} = (70/3600)\text{cm}^3/\text{s}$
$h = 100$ cm
$L = 10$ cm
$r_1 = 2$ cm
$r^2 = 1$ cm
$\rho = 1.05\ \text{g/cm}^3$
$\mu = 1$ cp
$g = 981\ \text{cm/s}^2$
$1\ \text{atm} = 1.0133 \times 10^6\ \text{dynes/cm}^2$
$1\ \text{atm} = 14.696$ psia

FIGURE 3.6.1 shows the flow configuration.

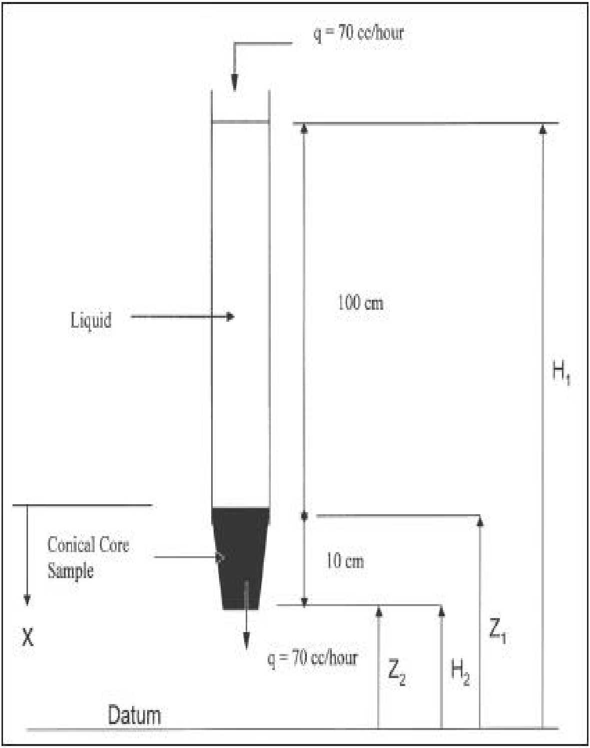

FIGURE 3.6.1 Constant head liquid permeameter.

Apply Darcy's Law in terms of hydraulic head and hydraulic conductivity to obtain

$$q=-KA\frac{dH}{dx} \tag{3.6.1}$$

where H is the hydraulic head and K is the hydraulic conductivity. But $A = f(\times)$. Let the radius along the cone be given by

$$r=a-bx \tag{3.6.2}$$

where

$$a=r_1 \tag{3.6.3}$$

and b is given by

$$b=\frac{r_1-r_2}{L} \tag{3.6.4}$$

Now

$$A(x) = \pi r^2 = \pi(a - bx)^2 \tag{3.6.5}$$

Substituting Eq.(3.6.5) into Eq.(3.6.1) gives

$$q = -K\pi(a - bx)^2 \frac{dH}{dx} \tag{3.6.6}$$

Separating variables gives

$$\frac{dx}{(a - bx)^2} = -\frac{K\pi}{q} dH \tag{3.6.7}$$

$$\int_0^L \frac{dx}{(a - bx)^2} = -\frac{K\pi}{q} \int_{H_1}^{H_2} dH \tag{3.6.8}$$

$$\frac{1}{b}\left[\frac{1}{(a-bx)}\right]_0^L=\frac{K\pi(H_1-H_2)}{q} \qquad (3.6.9)$$

$$\frac{1}{b}\left[\frac{1}{(a-bL)}-\frac{1}{a}\right]=\frac{K\pi(H_1-H_2)}{q} \qquad (3.6.10)$$

Eq.(3.6.10) can be simplified and rearranged as

$$q=\frac{a(a-bL)K\pi(H_1-H_2)}{L} \qquad (3.6.11)$$

From the FIGURE,

$$H_1-H_2=h+L \qquad (3.6.12)$$

Substituting Eqs.(3.6.3), (3.6.4), and (3.6.12) into Eq.(3.6.11) and simplifying gives

$$q = \frac{r_1 r_2 K \pi (h+L)}{L} \tag{3.6.13}$$

The hydraulic conductivity can be written in Darcy units as

$$K = \frac{k \rho g}{1.0133 \times 10^6 \mu} \tag{3.6.14}$$

Substituting Eq.(3.6.14) into Eq.(3.6.13) and solving for the permeability gives

$$k = \frac{1.0133 \times 10^6 q \mu L}{r_1 r_2 \rho g \pi (h+L)} \tag{3.6.15}$$

Substituting numerical values into Eq.(3.6.15) gives

$$k = \frac{1.0133 \times 10^{6}(70/3600)(1)(10)}{(2)(1)(1.05)(981)(\pi)(100+10)} = 0.277 \text{ D}$$

PROBLEM 3.7

$k = 2$ D
$A = 100$ cm^2
$\rho = 1.024$ g/cm^3
$\mu = 1.5$ cp
$g = 981$ cm/s^2

3.7a
To determine if there is flow, we look at the hydraulic heads (or the flow potentials) at the ends of the porous medium.

$$h_A = +100\text{cm}$$

h_B=-25cm

Since $h_A < h_B$, there is flow from A to B.

3.7b

$$q = KA\frac{\Delta h}{L} = \frac{k\rho g}{1.0133\times10^6\mu}A\frac{\Delta h}{L}$$

$$= \frac{(2)(1.024)(981)}{\left(1.0133\times10^6\right)(1.5)}(100)\left(\frac{125}{100}\right) = 0.1652 \text{ cm}^3/\text{s}$$

3.7c

$$P_{Agauge} = \frac{(1.024)(981)(100)}{1.0133\times10^6} = 0.0991 \text{ atm}$$

$$P_{Bgauge} = \frac{(1.024)(981)(50)}{1.0133\times10^6} = 0.0496 \text{ atm}$$

3.7d

$$\mathrm{Re} = \frac{\rho v D_p}{\mu} = \frac{(1.024)(0.1652/100)(1/160)}{0.015} = 7.05\times 10^{-4}$$

Since Re 1, the flow is Darcy flow.

PROBLEM 3.8

$$L = 10 \text{ cm}$$
$$d = 5 \text{ cm}$$
$$d_{manometer} = 1 \text{ cm}$$
$$\rho = 1.02 \text{ g/cm}^3$$
$$\mu = 1 \text{ cp}$$
$$g = 981 \text{ cm/s}^2$$
$$1 \text{ atm} = 1.0133 \times 10^6 \text{ dynes/cm}^2$$

3.8a

The performance equation for the falling head permeameter is given in Darcy units by Eq.(3.192) as

$$\ln\left(\frac{h}{h_o}\right) = -\left(\frac{k\rho gA}{1.0133\times10^6\,\mu aL}\right)t \qquad (3.8.1)$$

The graph of $\ln(h/h_o)$ versus t is linear with the slope given by

$$m = -\frac{k\rho gA}{1.0133\times10^6\,\mu aL} \qquad (3.8.2)$$

$$k = -\frac{m\times1.0133\times10^6\,\mu aL}{\rho gA} \qquad (3.8.3)$$

FIGURE 3.8.1 shows the graph of $\ln(h/h_o)$ versus t. From the regression line, m = –0.0004. Substituting numerical values into Eq.(3.8.3) gives the permeability as

$$k = -\frac{(-0.004)(1.0133\times10^{6})(1)(0.7854)(10)}{(1.02)(981)(19.6350)} = 0.162\ \text{D}$$

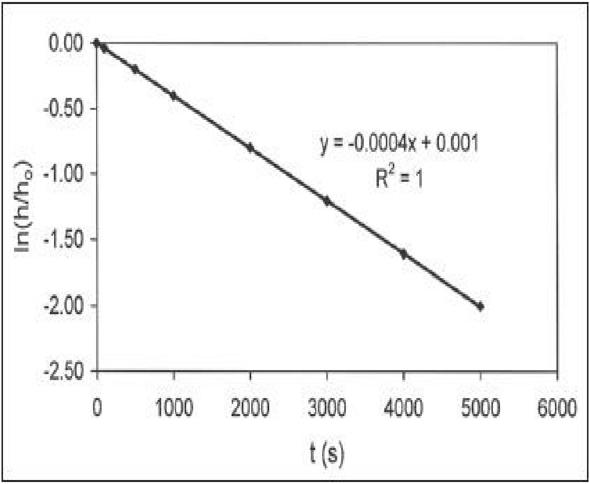

FIGURE 3.8.1 Graph of ln(h/h_o) versus t.

3.8b

The volumetric flow rate is given by Eq. (3.188) in Darcy units as

$$q = \left(\frac{k\rho g A}{1.0133 \times 10^6 \mu a L} \right) A \frac{h}{L} \quad (3.8.4)$$

FIGURE 3.8.2 shows the graph of q versus t. The equation for the rate in cm^3/s is

$$q = 0.3145 e^{-0.0004t} \quad (3.8.5)$$

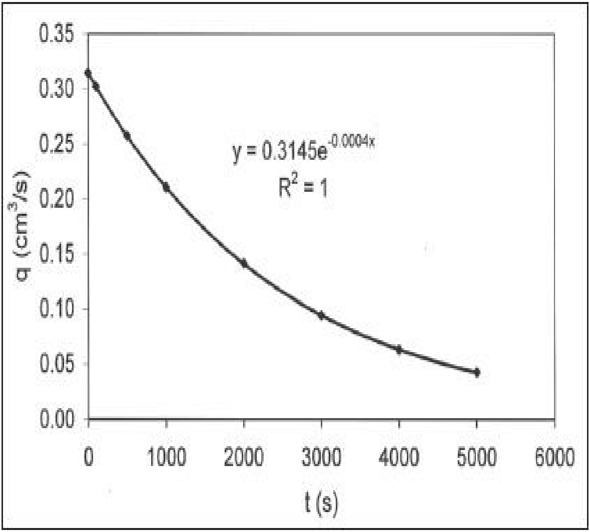

FIGURE 3.8.2 Graph of *q* versus *t*.

PROBLEM 3.9

3.9a

FIGURE 3.9.1 shows the hydraulic heads for the flow.

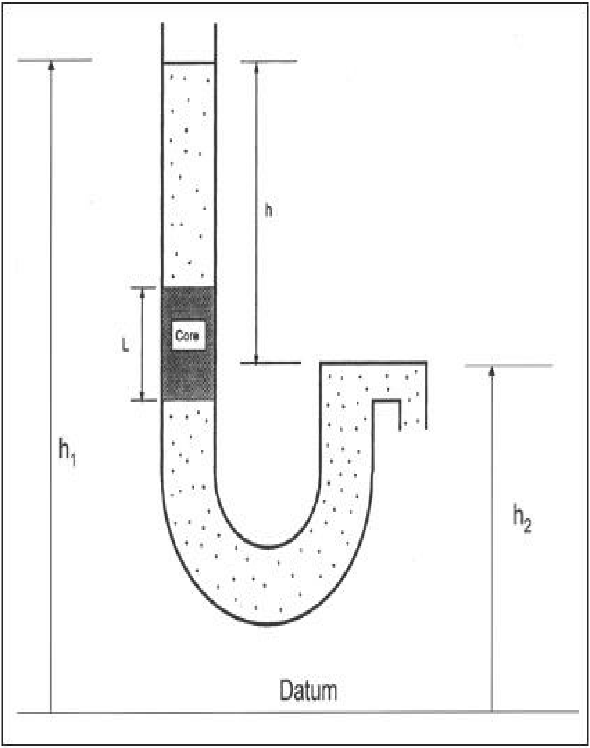

FIGURE 3.9.1 Hydraulic heads.

Darcy's law:

$$q = -KA\frac{h_2 - h_1}{L} = KA\frac{h}{L} \quad (3.9.1)$$

Volumetric balance gives

$$q = -A\frac{dh_1}{dt} = -A\frac{d(h_1 - h_2)}{dt} = -A\frac{dh}{dt} \quad (3.9.2)$$

Thus,

$$-A\frac{dh}{dt} = KA\frac{h}{L} \quad (3.9.3)$$

$$\frac{dh}{dt} = -K\frac{h}{L} = -\left(\frac{k\rho g}{1.0133\times10^6\mu}\right)\frac{h}{L} \quad (3.9.3)$$

3.9b

Separating variables gives

$$\frac{dh}{h} = -\left(\frac{k\rho g}{1.0133\times10^6 \mu L}\right) dt \tag{3.9.4}$$

Integration and application of the initial condition gives

$$\ln\left(\frac{h}{h_o}\right) = -\left(\frac{k\rho g}{1.0133\times10^6 \mu L}\right) t \tag{3.9.5}$$

3.9c

$L = 2$ cm

$\rho = 1.02$, g/cm^3

$\mu = 1$ cp

$g = 981$ cm/s^2

1 atm $= 1.0133\times10^6$ dynes/cm^2

The graph of In(h/h_o) versus t is linear with the slope given by

$$m=-\left(\frac{k\rho g}{1.0133\times10^{6}\mu L}\right) \tag{3.9.6}$$

$$k=-\frac{m\times1.0133\times10^{6}\mu L}{\rho g} \tag{3.9.7}$$

FIGURE 3.9.2 shows the graph of In(h/h_o) versus t. From the regression line, m = –0.0004. Substituting numerical values into Eq.(3.9.7) gives the permeability as

$$k=-\frac{(-0.004)\left(1.0133\times10^{6}\right)(1)(2)}{(1.02)(981)}=0.814\text{ D}$$

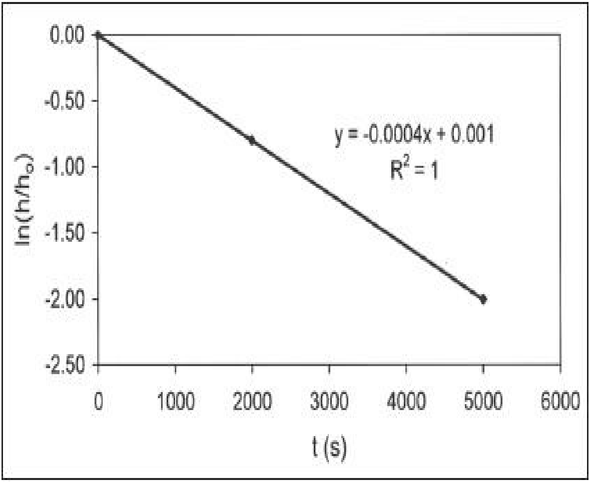

FIGURE 3.9.2 Graph of $\ln(h/h_o)$ versus t.

3.9d

FIGURE 3.9.3 shows the graph of the flow rate versus time. The flow rate decays exponentially toward zero with time.

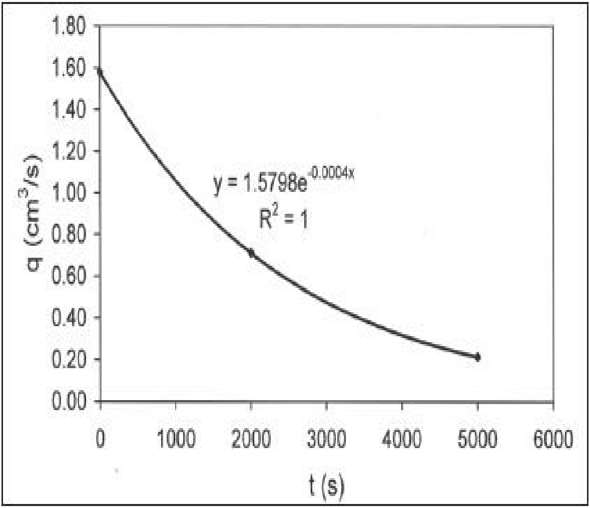

FIGURE 3.9.3 Graph of *q* versus *t*.

PROBLEM 3.10

3.10a

FIGURE 3.10.1 shows the flow configurations. Flow is vertical downward.

Subscripts: inlet = 1, outlet = 2. Choose a datum at the outlet and compute the hydraulic heads as follows:

$$h_1 = z_1 + \psi_1 = L + 0 = L \quad (3.10.1)$$

$$h_2 = z_2 + \psi_2 = 0 \quad (3.10.2)$$

Darcy's law:

$$q = KA\frac{h_1 - h_2}{L} = KA\frac{L - 0}{L} = KA = \frac{k\rho g}{1.0133 \times 10^6 \mu}A \qquad \textbf{(3.10.3)}$$

$$k = \frac{1.0133 \times 10^6 q\mu}{\rho g A} \qquad \textbf{(3.10.4)}$$

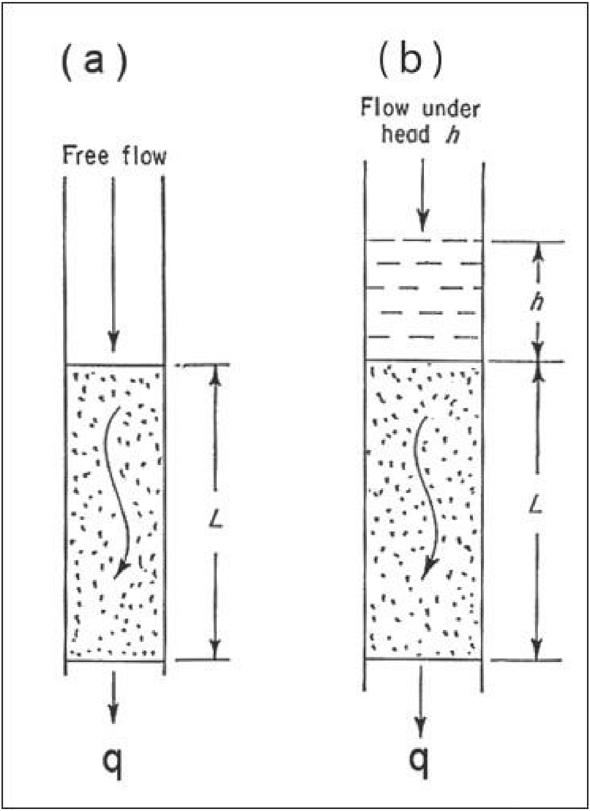

FIGURE 3.10.1 Vertical flow.

3.10b

$$h_1 = z_1 + \psi_1 = L + h \qquad (3.10.5)$$

$$h_2 = z_2 + \psi_2 = 0 \qquad (3.10.6)$$

Darcy's law:

$$q = KA\frac{h_1 - h_2}{L} = KA \ \frac{L+h}{L} \ = \frac{k\rho g}{1.0133\times 10^6} A \ 1 + \frac{h}{L} \qquad (3.10.7)$$

$$k = \frac{1.0133\times 10^6 q}{\rho g A \ 1 + \dfrac{h}{L}} \qquad (3.10.8)$$

PROBLEM 3.11

FIGURE 3.11.1 shows the hydraulic heads for the flow. Darcy's law gives

$$q = -KA\left(\frac{h_2 - h_1}{s_2 - s_1}\right) = \frac{k\rho g}{1.0133\times 10^6 \mu} A \frac{h}{L} \qquad (3.11.1)$$

$$k = \frac{1.0133\times 10^6 q\mu L}{\rho g A h} \qquad (3.11.2)$$

$L = 2$ cm
$d - 1$ cm
$L = 1.02$ g/cm^3
$\mu = 1$ cp

$$q = 0.012 \text{ cm}^3/\text{s}$$

Substituting numerical values into Eq. (3.11.2) gives the permeability as

$$k = \frac{\left(1.0133 \times 10^6\right)(0.01)(1)(2)}{(1.02)(981)(\pi/4)(52)} = 0.496 \text{ D}$$

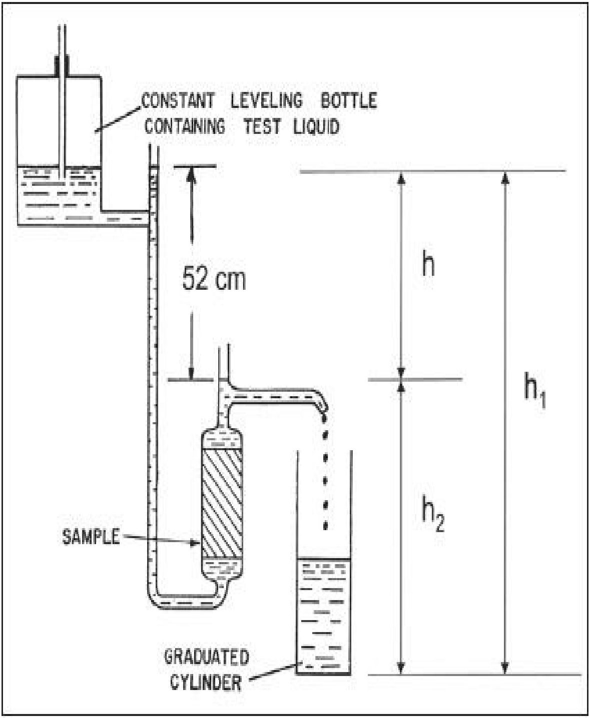

FIGURE 3.11.1 Hydraulic heads.

PROBLEM 3.12

3.12a, b

FIGURE 3.12.1 defines the hydraulic head at a point in the porous medium.

$$h = z + \psi \tag{3.12.1}$$

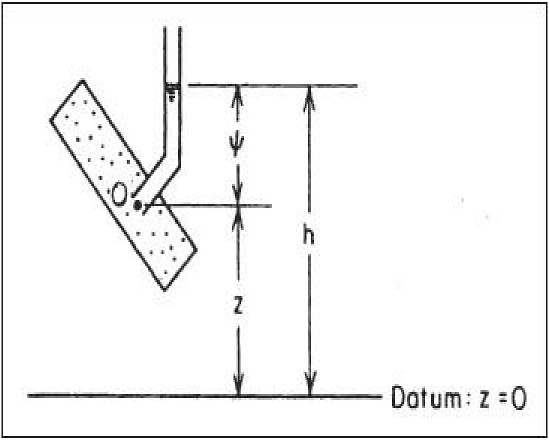

FIGURE 3.12.1 Hydraulic head at a point in the porous medium.

This problem can easily be solved by inspection as follows as shown in TABLE 3.12.1.

TABLE 3.12.1

z ft	ψ ft	h ft
0	0	0
3	1	4
6	0	6
9	1	10

FIGURE 3.12.2 shows the graphs of gauge pressure and hydraulic head.

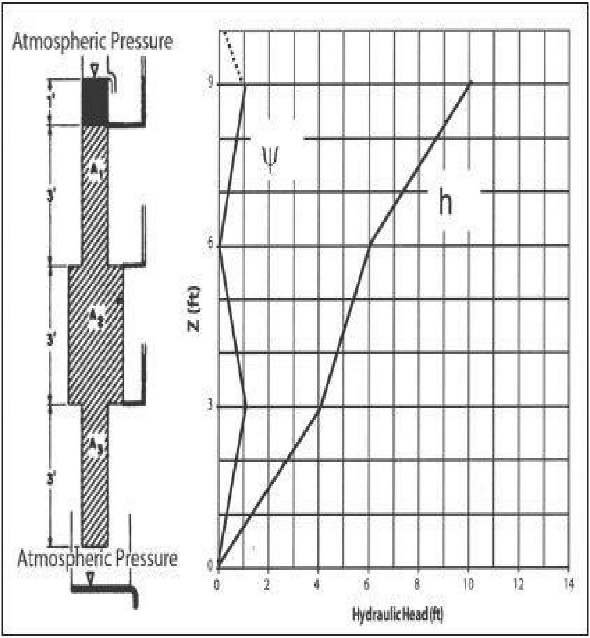

FIGURE 3.12.2 Variation of gauge pressure and hydraulic head.

3.12c

Darcy's law:

$$q = -KA\frac{dh}{dx} = KA\frac{dh}{dz} \quad (3.12.2)$$

$$dh = \frac{q}{KA}dz \quad (3.12.3)$$

Integration of Eq.(3.12.3) from z =0 to z = 3ft gives

$$\int_{h_o}^{h_3} dh = \frac{q}{KA_3}\int_{z_o}^{z_3} dz \quad (3.12.4)$$

$$h_3 - h_o = \frac{q}{KA_3}\left(z_3 - z_o\right) \quad (3.12.5)$$

$$\frac{q}{KA_3} = \frac{h_3 - h_o}{z_3 - z_o} \qquad (3.12.6)$$

$$z_o = 0,\ z_3 = 3,\ h_o = 0,\ h_3 = 4$$

Substituting numerical values into Eq. (3.12.6) gives

$$\frac{q}{KA_3} = \frac{4-0}{3-0} = \frac{4}{3}$$

PROBLEM 3.13

3.13a

FIGURE 3.13.1 shows the hydraulic heads for the flow.

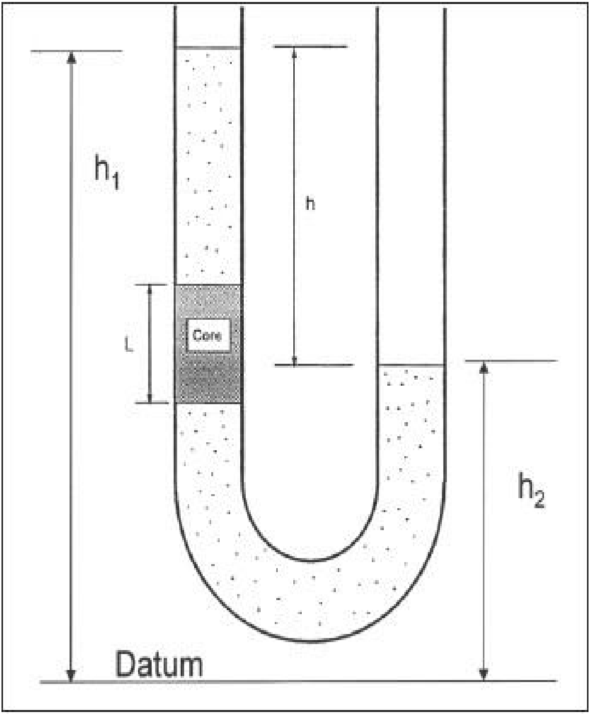

FIGURE 3.13.1 Hydraulic heads for flow.

Darcy's law:

$$q = KA\frac{h}{L} \tag{3.13.1}$$

Volumetric balance gives

$$q = -A\frac{dh_1}{dt} \tag{3.13.2}$$

$$q = A\frac{dh_2}{dt} \tag{3.13.3}$$

Adding Eqs.(3.13.2) and (3.13.3) gives

$$2q = -A\left(\frac{dh_1}{dt} - \frac{dh_2}{dt}\right) = -A\frac{dh}{dt} \tag{3.13.4}$$

$$q = -\frac{A}{2}\frac{dh}{dt} \tag{3.13.5}$$

Substituting Eq.(3.13.5) into (3.13.1) gives

$$-\frac{A}{2}\frac{dh}{dt} = KA\frac{h}{L} \tag{3.13.6}$$

The differential equation is

$$\frac{dh}{dt} = -\frac{2K}{L}h \tag{3.13.7}$$

3.13b

Separation of variables gives

$$\frac{dh}{h} = -\frac{2K}{L}dt \tag{3.13.8}$$

Integration and substitution of the initial condition gives

$$\ln\left(\frac{h}{h_o}\right)=-\frac{2K}{L}t=-\frac{2}{L}\left(\frac{k\rho g}{1.0133\times10^6\mu}\right)t \quad (3.13.9)$$

3.13c

The graph of $\ln(h/h_o)$ versus t is linear with the slope given by

$$m=-\frac{2}{L}\left(\frac{k\rho g}{1.0133\times10^6\mu L}\right) \quad (3.13.10)$$

$$k=-\frac{m\times1.0133\times10^6\mu L^2}{2\rho g} \quad (3.13.11)$$

FIGURE 3.13.2 shows the graph of

$\ln(h/h_o)$ versus t. From the regression line, $m = -0.0004$. Substituting numerical values into Eq.(3.13.11) gives the permeability as

$$k = -\frac{(-0.004)\left(1.0133\times10^{6}\right)(1)\left(2^{2}\right)}{(2)(1.02)(981)} = 2.028\,\mathrm{D}$$

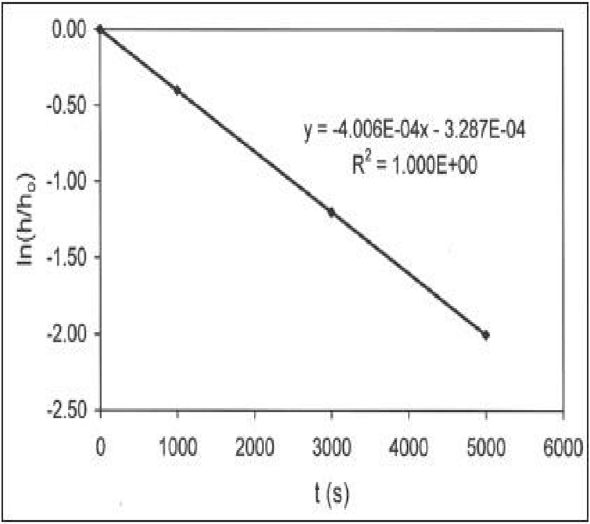

FIGURE 3.13.2 Graph of $\ln(h/h_o)$ versus t.

3.13d

Eq.(3.13.9) can be written as

$$h = h_o e^{-\frac{2}{L}\left(\frac{k\rho g}{1.0133\times 10^6 \mu}\right)t} \quad (3.13.12)$$

Substituting Eq.(3.13.12) into (3.13.1) gives the flow rate as

$$q=\left(\frac{k\rho g}{1.0133\times10^{6}\mu}\right)\left(\frac{A}{L}\right)h_{o}e^{-\frac{2}{L}\left(\frac{k\rho g}{1.0133\times10^{6}\mu}\right)t} \quad (3.13.13)$$

$L = 10$ cm
$D = 2$ cm
$h_o = 100$ cm
$\rho = 1.02$ g/cm^3
$\mu = 1$ cp
$g = 981$ cm/s^2

Substituting numerical values into Eq. (3.13.13) gives the rate as

$$q = 0.062961 e^{-0.0004t} \qquad (3.13.14)$$

FIGURE 3.13.3 shows the graph of q versus t.

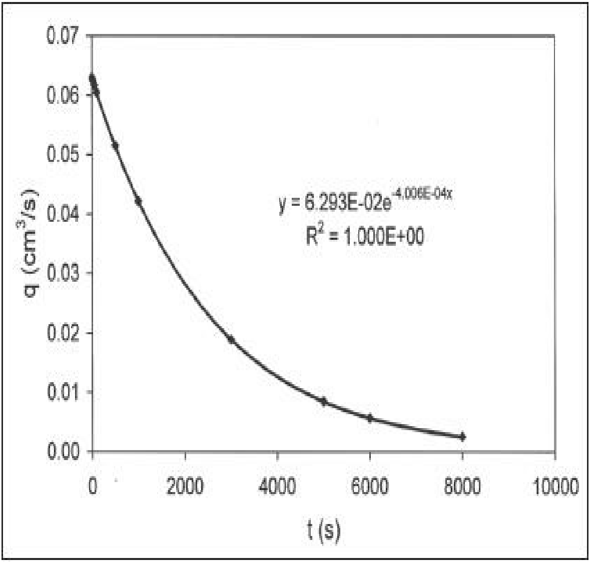

FIGURE 3.13.3 Graph of q versus t.

PROBLEM 3.14

3.14a

Darcy's law:

$$q = KA\frac{\Delta h}{L} \tag{3.14.1}$$

The graph of q versus Δh is linear with slope given by

$$m = \frac{KA}{L} \tag{3.14.2}$$

$$K = \frac{mL}{A} \tag{3.14.3}$$

FIGURE 3.14.1 shows the graph of q

versus Δh. From the regression line, m = 0.0061. Substituting numerical values into Eq.(3.14.3) gives the hydraulic conductivity as

$$K = \frac{(0.0061)(15.2)}{\pi(4.8/2)^2} = 0.005124 \text{ cm/s}$$

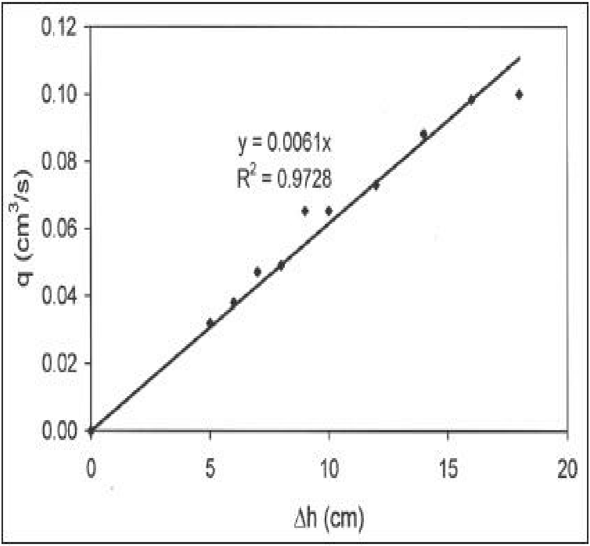

FIGURE 3.14.1 Graph of q versus Δh.

3.14b

In Darcy units

$$K = \frac{k \rho g}{1.0133 \times 10^6 \mu} \tag{3.14.4}$$

Therefore,

$$k = \frac{1.0133 \times 10^6 \mu K}{\rho g} \tag{3.14.5}$$

Substituting numerical values into Eq. (3.14.5) gives the permeability as

$$k = \frac{\left(1.0133 \times 10^6\right)(1)(0.005124)}{(1)(981)} = 5.29 \text{ D}$$

PROBLEM 3.15

This is an inclined flow problem that can be solved in a variety of ways.

Method 1.
Apply Darcy's law for inclined flow. Using the coordinate system shown in **FIGURE 3.15.1**. Darcy's law for inclined flow in oilfield units is given by Eq.(3.166) in the text as

$$qB = -0.001127\frac{kA}{\mu}\left(\frac{dP}{ds} - 0.433\gamma\frac{dz}{ds}\right) \quad \textbf{(3.15.1)}$$

Differentiation gives

$$qB = -0.001127\frac{kA}{\mu}\left(\frac{P_2 - P_1}{s_2 - s_1} - 0.433\gamma\frac{z_2 - z_1}{s_2 - s_1}\right) \quad (3.15.2)$$

$P_1 = P_a + 0.433y(250) = 14.7 + (0.433)(1.038)(250) = 127.06$ psia

$z_1 = 0$

$P_2 = 1450$ psia

$z_2 = 5000$ ft $S_2 - s_1$ 10×5280 ft

k = 850 mD

μ = 1 cp

$A = 3000 \times 65$ ft^2

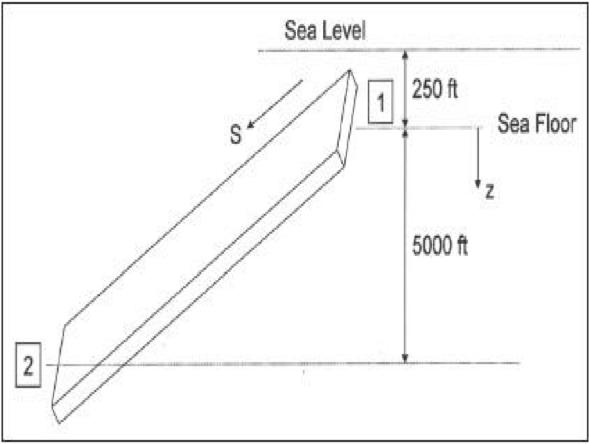

FIGURE 3.15.1 Coordinate system for inclined flow. Figure not to scale.

Substituting the numerical values into Eq.(3.16.2) gives

$$qB = -0.001127\frac{(850)(3000\times 65)}{1}$$

$$\times\left(\frac{1450-127.06}{10\times 5280}-0.433(1.038)\frac{5000-0}{10\times 5280}\right)=3270\ RB/D$$

Method 2.

The problem also can be solved in terms of hydraulic or piezometric head and hydraulic conductivity (see **FIGURE 3.15.2**).

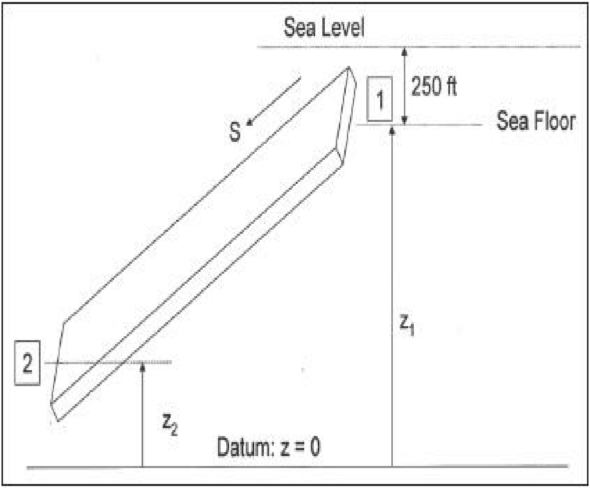

FIGURE 3.15.2 Hydraulic heads for inclined flow. Not to scale.

The components of the hydraulic head are shown in Figure 3.42 in the text. The hydraulic head at any point in the porous medium is given by

$$h = \psi + z \quad (3.15.3)$$

where

h = hydraulic head
ψ = pressure head
z = elevation of the point above the datum

The hydraulic heads in ft are computed as follows.

$$h_1 = 250 + z_1 \quad (3.15.4)$$

$$h_2 = \frac{P_2}{0.433\gamma} + z_2 = \frac{1450 - 14.7}{(0.433)(1.038)} + z_2 = 3193.43 + z_2 \quad (3.15.5)$$

The hydraulic conductivity in ft/day is given by

$$K = 0.001127\frac{k(0.433\gamma)}{\mu} \quad (3.15.6)$$

Darcy's law in terms of hydraulic head and hydraulic conductivity is given by Eq.(3.181) in the text as

$$qB = -KA\left(\frac{h_2 - h_1}{s_2 - s_1}\right) \quad (3.16.7)$$

Substituting Eqs.(3.16.2), (3.16.5), and (3.16.6) into Eq.(3.16.7) gives

$$qB = -0.001127\frac{k(0.433\gamma)A}{\mu}\left(\frac{3193.43 + z_2 - 250 - z_1}{s_2 - s_1}\right) \quad (3.15.8)$$

$k = 850$ mD
$\gamma = 1.038$

$z_2 - Z_1 = -5000$ ft

$s_2 - s_1 = 10 \times 5280$ ft

$\mu = 1$ cp

A = 3000×65 ft^2

Substituting the numerical values into Eq.(3.16.8) gives

$$qB = -0.001127 \frac{(850)(0.433 \times 1.038)(3000 \times 65)}{1} \times \left(\frac{3193.43 - 250 - 5000}{10 \times 5280} \right) = 3270 \text{ RB/D}$$

Method 3.

Compute the velocity potentials for the inlet and the outlet of the porous medium at any convenient datum and apply the oilfield version of Eq.(3.167) in the text to calculate the flow rate. **FIGURE 3.15.3** shows the reference datum used in this computation. The oilfield version of Eq.(3.167) is given by

$$qB = -0.001127 \frac{kA}{\mu} \frac{d\Phi}{ds} \tag{3.16.9}$$

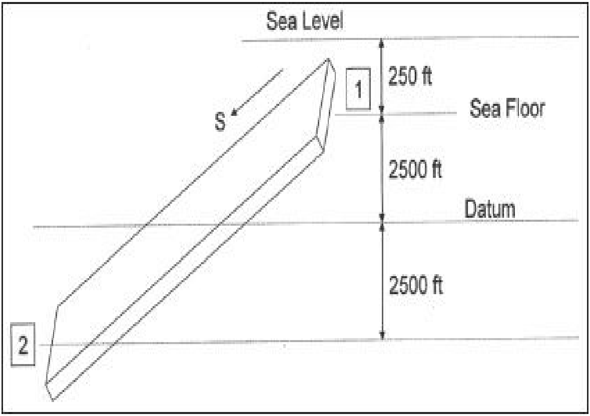

FIGURE 3.15.3 Reference datum for inclined flow. Not to scale.

Differentiation gives

$$qB = -0.001127\frac{kA}{\mu}\left(\frac{\Phi_2 - \Phi_1}{s_2 - s_1}\right) \qquad \textbf{(3.16.10)}$$

Eq.(3.169) gives the velocity potential

in oilfield units as

$$\Phi_i = P_i \pm 0.433\gamma z_i \tag{3.16.11}$$

where z_i is the elevation of point i above or below the reference datum. If point i is above the reference datum, then

$$\Phi_i = P_i + 0.433\gamma z_i \tag{3.16.12}$$

If point i is below the reference datum, then

$$\Phi_i = P_i - 0.433\gamma z_i \tag{3.16.13}$$

For this problem,

$$\Phi_1 = P_1 + 0.433\gamma(250) = 127.06 + (0.433)(1.038)(2500)$$

$$= 1250.70 \text{ psia}$$

$$\Phi_2 = P_2 - 0.433\gamma(2500) = 1450 - (0.433)(1.038)(2500)$$

$$= 326.37 \text{ psia}$$

Substituting the numerical values into Eq.(3.16.10) gives

$$qB = -0.001127 \frac{(850)(3000 \times 65)}{1} \left(\frac{326.37 - 1250.70}{10 \times 5280} \right)$$

$$= 3270 \text{ RB/D}$$

PROBLEM 3.16

q = 600 STB/D

P_i=5000 psia

A = 200 acres

r_w = 0.28 ft

h = 80ft

$Ø$ = 0.20

k = 200 mD

c_t=30×10^{-6} psi^{-1}

B_o = 1.20 RB/STB

μ = 1.5 cp

3.16a

$$r_e = \sqrt{\frac{A}{\pi}} = \sqrt{\frac{200 \times 43560}{\pi}} = 1665.3\,\text{ft}$$

$$r = r_w e^{\left[\frac{n}{N}\ln\left(\frac{r_e}{r_w}\right)\right]} \text{ for } n = 0,1,2,\ldots,N\left(N=9\right) \quad \textbf{(3.16.1)}$$

$$P(r,t) = P_i - \frac{141.2 q\mu B}{kh}\left[-\frac{1}{2}Ei\left(-\frac{948\phi\mu c_t r^2}{kt}\right)\right] \quad \textbf{(3.16.2)}$$

Let

$$x_i = \frac{948\phi\mu c_t r_i^2}{kt} \quad \textbf{(3.16.3)}$$

For $\times \leq 0.01$, the *Ei* function is given by

$$Ei(-x) = \ln x + 0.5772 \quad \textbf{(3.16.4)}$$

For $x > 0.01$, the Ei function is read from the Ei function TABLE.

FIGURE 3.16.1 shows the calculated pressure profiles.

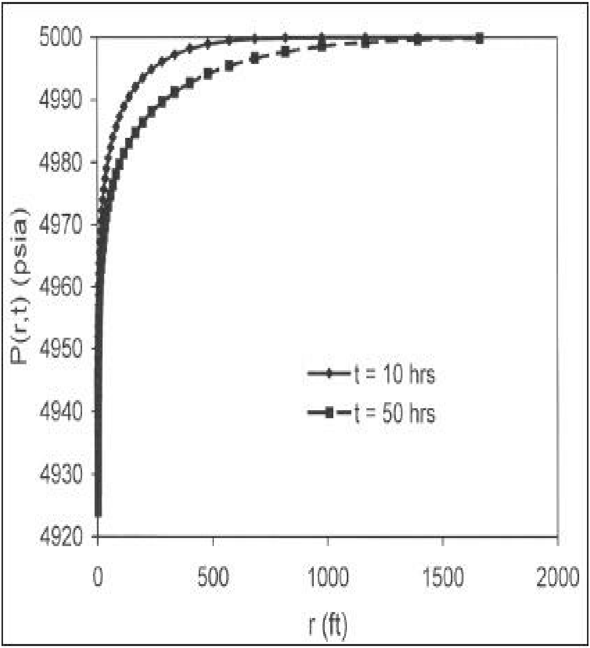

FIGURE 3.16.1 Pressure profiles at t = 10 and 50 hours.

3.16b

$$P_{wf}(t) = P_i - \frac{162.6q\mu B}{kh}\left[\log t + \log\frac{k}{\phi\mu c_t r_w^2} - 3.23\right] \quad (3.16.4)$$

The calculated wellbore pressures are shown in TABLE 3.16.1.

TABLE 3.16.1 Calculated Wellbore Pressures.

t (hr)	P_{wf} (psia)
0.25	4949.29
1	4942.68
10	4931.71
30	4926.47
50	4924.03
60	4923.16

3.17c

FIGURE 3.16.2 shows the semilog plot of the flowing wellbore pressures of

TABLE 3.16.1. The slope is given by

$$m = -\frac{162.6 q \mu B}{kh} \tag{3.16.5}$$

$$k = -\frac{162.6 q \mu B}{mh} \tag{3.16.6}$$

Substituting numerical values into Eq. (3.16.6) gives the permeability as

$$k = -\frac{(162.6)(600)(1.5)(1.2)}{(-4.7655 \times \ln 10)(80)} = 200\,\text{mD}$$

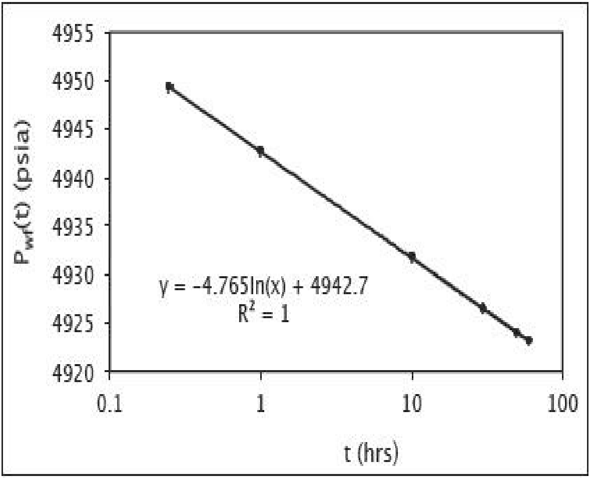

FIGURE 3.16.2 Semilog plot of wellbore pressures.

3.17d

At log$t$ = 0, the wellbore pressure is given by

$$4942.7 = P_i - \frac{162.6 q\mu B}{kh}\left[\log\left(\frac{k}{\phi\mu c_t r_w^2}\right) - 3.23\right] \quad \textbf{(3.17.7)}$$

$$P_i = 4942.7 + \frac{162.6 q\mu B}{kh}\left[\log\left(\frac{k}{\phi\mu c_t r_w^2}\right) - 3.23\right] \quad \textbf{(3.17.8)}$$

Substituting numerical values into Eq. (3.16.8) gives the initial pressure as

$$P_i = 4942.7 + 10.987(8.45 - 3.23) = 5000 \text{ psia}$$

PROBLEM 3.17

$q = 2500$ STB/D
$h = 23$ ft
$\mu = 0.92$ cp
$B = 1.21$ RB/STB
$r_w = 0.401$ ft
$Ø = 0.21$
$c_t = 8.72 \times 10^{-6}$ psi^{-1}
$P_i = 6009$ psia

3.17a

FIGURE 3.17.1 shows the diagnostic plots. The test is affected by wellbore storage. However, the late time data can be subjected to a semilog analysis.

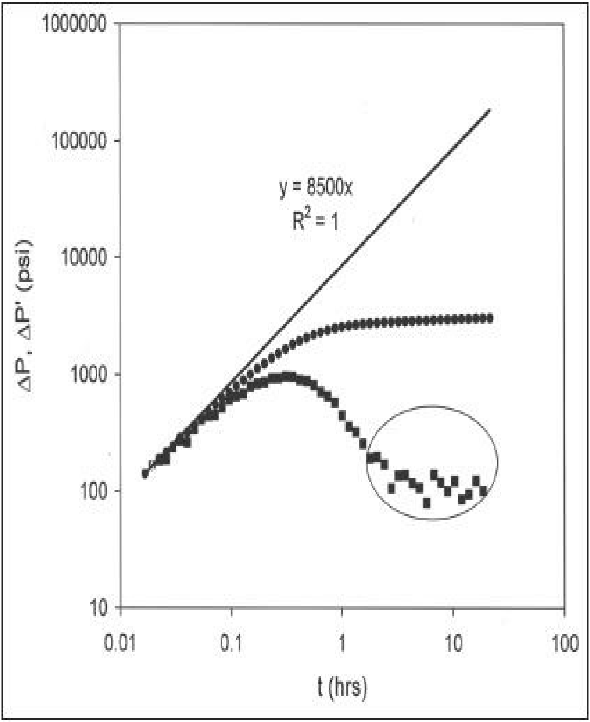

FIGURE 3.17.1 Log-log diagnostic plots.

3.17b

FIGURE 3.17.2 shows the semilog plot. The slope of the semilog line is given by

$$m = -\frac{162.6 q \mu B}{kh} \tag{3.17.1}$$

$$k = -\frac{162.6 q \mu B}{mh} \tag{3.17.2}$$

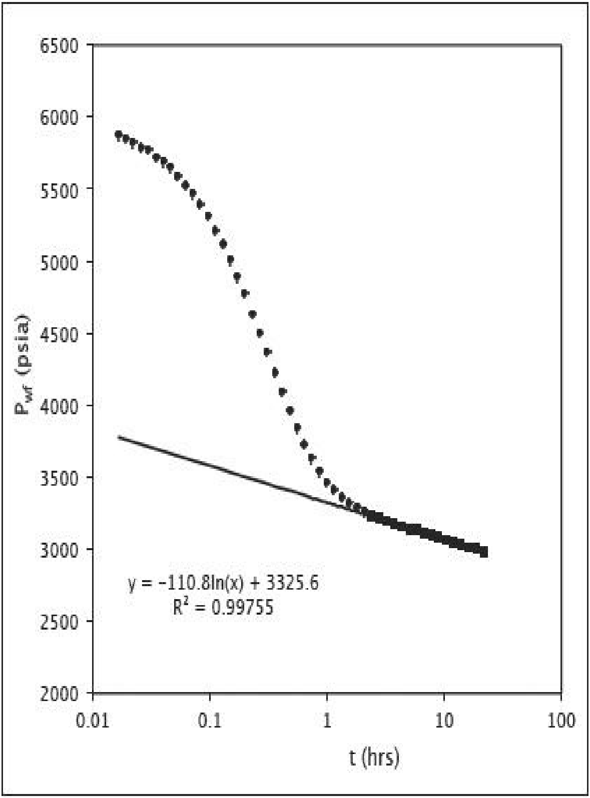

FIGURE 3.17.2 Semilog plot.

From the regression line, m = –110.83ln10 = –255.196psi/log cycle.

Substituting numerical values into Eq. (3.17.2) gives the permeability as

$$k = -\frac{(162.6)(2500)(0.92)(1.21)}{(-255.196)(23)} = 77.10 \text{ mD}$$

$$P_{wf}(1 \text{ hr}) = 3325.60 \text{ psia}$$

The skin factor is given by

$$S = 1.1513\left[\frac{P_{wf}(1hr) - P_i}{-\left(\frac{162.6q\mu B}{kh}\right)} - \log\left(\frac{k}{\phi\mu c_t r_w^2}\right) - 3.23\right] \quad (3.17.3)$$

Substituting numerical values into Eq.

(3.17.3) gives the skin factor as

$$S = 1.1513\left[\frac{3325.60 - 6009}{-255.196} - \log\left(\frac{77.10}{0.21 \times 0.92 \times 8.72 \times 10^{-6} \times (0.401)^2}\right) - 3.23\right]$$

$$= 1.1513(10.52 - 8.45 - 3.23)$$

$$= 6.09$$

PROBLEM 3.18

$q = 519$ STB/D
$h = 13.0$ ft
$\mu = 0.92$ cp
$B = 1.06$ RB/STB
$r_w = 0.27$ ft
$\O = 0.223$
$S_{wi}=0.32$
$c_t = 13.0\times10^{-6}$ psi^{-1}

3.18a

FIGURE 3.18.1 shows the overview plot of the test.

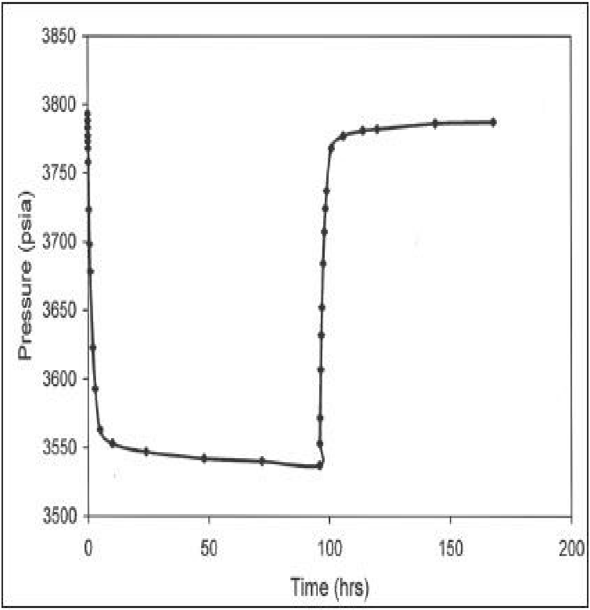

FIGURE 3.18.1 Pressure versus time.

3.18b

FIGURE 3.18.2 shows the diagnostic plots for the drawdown test. The wellbore storage coefficient is calculated from the unit slope line as

$$C=\left(\frac{qB}{24}\right)\left(\frac{t}{\Delta P}\right)_{unit\ slope\ line} \tag{3.18.1}$$

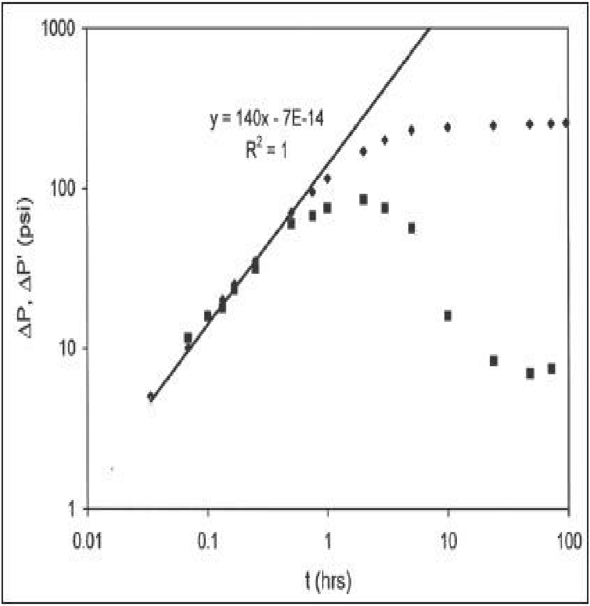

FIGURE 3.18.2 Diagnostic plots for drawdown.

Substituting numerical values into Eq. (3.18.1) gives the wellbore storage coefficient as

$$C=\left(\frac{519\times1.06}{34}\right)\left(\frac{1}{140}\right)=0.1545\,\text{RB/psi}$$

The dimensionless wellbore storage coefficient is given by

$$C_D=\frac{5.615C}{2\pi\phi c_t h r_w^2} \tag{3.18.2}$$

Substituting numerical values into Eq. (3.18.2) gives the dimensionless wellbore storage coefficient as

$$C_D=\frac{(5.615)(0.1545)}{2\pi(0.223)\left(13.0\times10^{-6}\right)(13.0)(0.27)^2}=50243$$

FIGURE 3.18.3 shows the diagnostic plots for the buildup test.

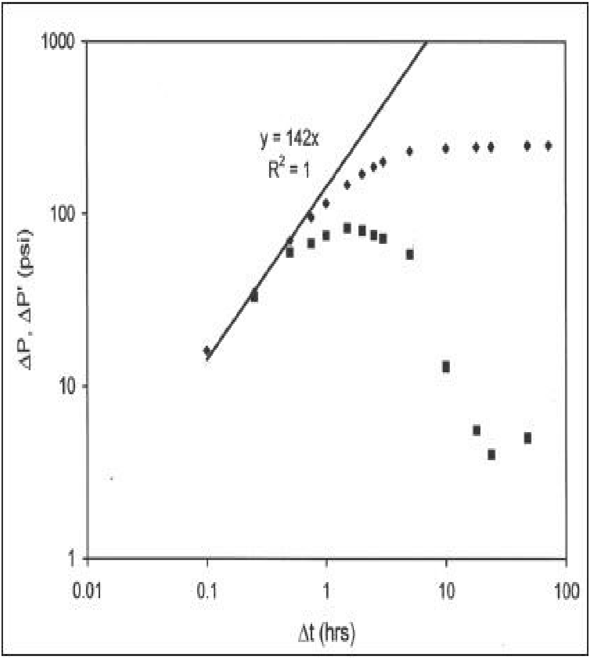

FIGURE 3.18.3 Diagnostic plots for buildup.

The wellbore storage coefficient is calculated from the unit slope line as

$$C=\left(\frac{519\times1.06}{34}\right)\left(\frac{1}{142}\right)=0.1523\ \text{RB/psi}$$

Substituting numerical values into Eq. (3.18.2) gives the dimensionless wellbore storage coefficient as

$$C_D=\frac{(5.615)(0.1523)}{2\pi(0.223)\left(13.0\times10^{-6}\right)(13.0)(0.27)^2}=49536$$

3.18c

The slope of the semilog line for drawdown and buildup is given by

$$m=-\frac{162.6q\mu B}{kh} \tag{3.18.3}$$

$$k=-\frac{162.6q\mu B}{mh} \tag{3.18.4}$$

FIGURE 3.18.4 shows the semilog plot for the drawdown. From the regression line, m = –6.9085ln10 = –15.91 psi/log cycle.

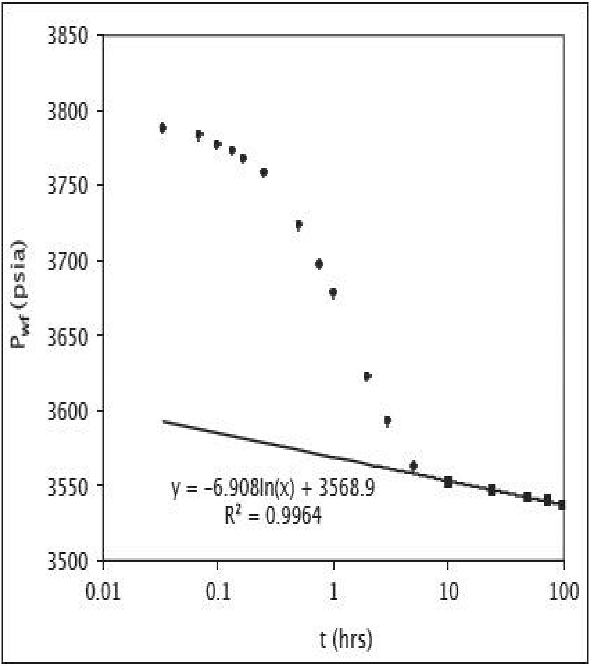

FIGURE 3.18.4 Semilog plot for drawdown.

Substituting numerical values into Eq. (3.18.4) gives the permeability as

$$k = -\frac{(162.6)(519)(0.92)(1.06)}{(-15.91)(13)} = 397.96 \text{ mD}$$

For the drawdown, the skin factor is given by

$$S = 1.1513\left[\frac{P_{wf}(1\text{ hr}) - P_i}{-\left(\frac{162.6 q\mu B}{kh}\right)} - \log\left(\frac{k}{\phi\mu c_t r_w^2}\right) - 3.23\right] \quad \textbf{(3.18.5)}$$

$$P_{wf}(1\text{ hr}) = 3568.9 \text{ psia}$$

Substituting numerical values into Eq. (3.18.5) gives the skin factor as

$$S = 1.1513\left[\frac{3568.9-3793}{-15.91} - \log\left(\frac{397.96}{0.223\times0.92\times13.0\times10^{-6}\times(0.27)^2}\right) - 3.23\right]$$

$$= 1.1513(14.09 - 9.31 - 3.23)$$

$$= 9.22$$

FIGURE 3.18.5 shows the Horner plot for the buildup. From the regression line, $m = -6.6916\ln 10 = -15.41$ psi/log cycle.

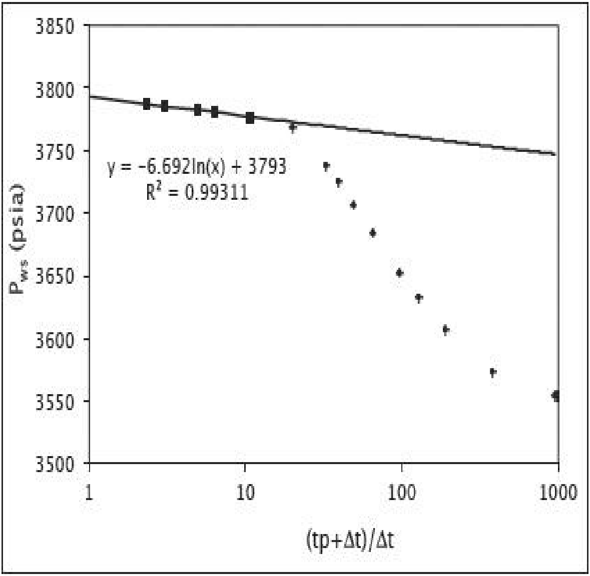

FIGURE 3.18.5 Horner plot.

Substituting numerical values into Eq. (3.18.4) gives the permeability as

$$k = -\frac{(162.6)(519)(0.92)(1.06)}{(-15.41)(13)} = 410.86 \text{ mD}$$

For the buildup, the skin factor is given by

$$S = 1.1513\left[\frac{P_{wf}(t_p) - P_{ws}(1\text{ hr})}{-\left(\frac{162.6 q\mu B}{kh}\right)} - \log\left(\frac{k}{\phi \mu c_t r_w^2}\right) - 3.23\right] \quad \textbf{(3.18.6)}$$

$$P_{ws}(1\text{ hr}) = 3762.39 \text{ psia}$$

$$P_{ws}(t_p) = 3537 \text{ psia}$$

Substituting numerical values into Eq. (3.18.6) gives the skin factor as

$$S = 1.1513\left[\frac{3537 - 3762.39}{-15.41}\right.$$

$$\left. -\log\left(\frac{410.86}{0.223 \times 0.92 \times 13.0 \times 10^{-6} \times (0.27)^2}\right) - 3.23\right]$$

$$= 1.1513(14.63 - 9.32 - 3.23)$$
$$= 9.82$$

3.19d

The positive skin factor indicates that the well is damaged.

PROBLEM 3.19

3.19a

The initial-boundary value problem to be solved consists of the following equations. The partial differential equation is

$$\frac{\partial^2 P}{\partial x^2} = \frac{\varphi \mu c_t}{k} \frac{\partial P}{\partial t} \tag{3.19.1}$$

The initial condition is

$$P(x,0) = P_i \tag{3.19.2}$$

The internal boundary condition is

$$P(0,t) = P_w \tag{3.19.3}$$

The external no flow boundary condition is

$$\frac{\partial P(x,t)}{\partial x}=0,\ x=L \tag{3.19.4}$$

3.19b

We can recast the initial-boundary value problem in dimensionless form as follows. Let

$$P_D=\frac{P_i-P(x,t)}{P_i-P_w} \tag{3.19.5}$$

$$x_D=\frac{x}{L} \tag{3.19.6}$$

$$t_D = \frac{kt}{\phi \mu c_t L^2} \tag{3.19.7}$$

Substituting Eqs.(3.19.5), (3.19.6), and (3.19.7) into Eqs. (3.19.1), (3.19.2), (3.19.3), and (3.19.4) gives

$$\frac{\partial^2 P_D}{\partial x_D^2} = \frac{\partial P_D}{\partial t_D} \tag{3.19.8}$$

$$P_D(x_D, 0) = 0 \tag{3.19.9}$$

$$P_D(0, t_D) = 1 \tag{3.19.10}$$

$$\frac{\partial P_D}{\partial x_D} = 0,\ x_D = 1 \tag{3.19.11}$$

3.19b

The initial-boundary value problem can be solved by the separation of variables. Let

$$P_D(x_D, t_D) = X(x_D)T(t_D) \tag{3.19.12}$$

Substituting Eq.(3.19.13) into (3.19.8) and separating variables gives

$$\frac{1}{X}\frac{d^2X}{dx_D^2} = \frac{1}{T}\frac{dT}{dt_D} \tag{3.19.13}$$

The left side of Eq.(3.19.13) is a function of x_D only and the right side is a function of t_D only. Both sides will be equal only if each is separately equal to some constant. Thus,

$$\frac{1}{X}\frac{d^2X}{dx_D^2}=-\lambda^2,\ \lambda\neq 0 \qquad (3.19.14)$$

$$\frac{1}{T}\frac{dT}{dt_D}=-\lambda^2,\ \lambda\neq 0 \qquad (3.19.15)$$

The solution of Eq.(3.19.14) gives

$$X=C'\sin(\lambda x_D)+E'\cos(\lambda x_D) \qquad (3.19.16)$$

The solution of Eq.(3.19.15) gives

$$T=Fe^{-\lambda^2 t_D} \qquad (3.19.17)$$

Thus, for $\lambda \neq 0$, the solution is

$$P_D(x_D,t_D)=\left[C'F\sin(\lambda x_D)+E'F\cos(\lambda x_D)\right]e^{-\lambda^2 t_D} \quad (3.19.18)$$

which can be written as

$$P_D(x_D,t_D)=\left[C\sin(\lambda x_D)+E\cos(\lambda x_D)\right]e^{-\lambda^2 t_D} \quad (3.19.19)$$

For λ = 0, the solution of Eq.(3.20.14) gives

$$X=A'x_D+B' \quad (3.19.20)$$

For λ = 0, the solution of Eq.(3.20.15) gives

$$T=D \quad (3.20.21)$$

Thus, for λ = 0,

$$P_D(x_D,t_D)=DA'x_D+DB'=Ax_D+B \quad (3.19.22)$$

The general solution to the initial-boundary value problem is

$$P_D(x_D,t_D)=Ax_D+B+\left[C\sin(\lambda x_D)+E\cos(\lambda x_D)\right]e^{-\lambda^2 t_D} \quad (3.19.23)$$

The solution contains five constants (A,B,C,E,λ) to be determined from the three initial and boundary conditions. It appears some of these constants can be chosen arbitrarily. Application of Eq. (3.19.11) gives

$$\frac{\partial P_D}{\partial x_D}=A+\left[\lambda C\cos\lambda-\lambda E\sin\lambda\right]e^{-\lambda^2 t_D}=0,\ x_D=1 \quad (3.19.24)$$

To satisfy Eq.(3.19.24), A must be zero and

$$C\cos\lambda - E\sin\lambda = 0 \tag{3.19.25}$$

Since λ≠0. By choosing E= 0, then

$$C\cos\lambda = 0 \tag{3.19.26}$$

Since C≠O, then

$$\cos\lambda = 0 \tag{3.19.27}$$

The solution of Eq.(3.19.27) gives

$$\lambda = \frac{\pi}{2}, \frac{3\pi}{2}, \frac{5\pi}{2}, \ldots, \frac{(2n+1)\pi}{2}, \text{ for } n = 0,1,2,\ldots,\infty \tag{3.19.28}$$

Eq.(3.19.23) can now be written as

$$P_D(x_D, t_D) = B + \sum_{n=0}^{n=\infty} C_n \sin\left[\left(\frac{2n+1}{2}\right)\pi x_D\right] e^{-\left(\frac{2n+1}{2}\right)^2 \pi^2 t_D} \tag{3.19.29}$$

Substituting Eq.(3.19.29) into (3.19.10) gives $B = 1$. Eq.(3.19.29) becomes

$$P_D(x_D,t_D)=1+\sum_{n=0}^{n=\infty} C_n \sin\left[\left(\frac{2n+1}{2}\right)\pi x_D\right] e^{-\left(\frac{2n+1}{2}\right)^2 \pi^2 t_D} \quad (3.19.30)$$

Substituting Eq.(3.19.30) into (3.19.9) gives

$$-1=\sum_{n=0}^{n=\infty} C_n \sin\left[\left(\frac{2n+1}{2}\right)\pi x_D\right] \quad (3.19.31)$$

Thus, we need an infinite sine series that converges to –1 for *0D* 1. The required series is the half interval Fourier sine series. Taking advantage of the orthogonal property of the trigonometric function gives

$$C_n = -2\int_0^1 \sin\left(\frac{2n+1}{2}\pi x_D\right)dx_D = \frac{4}{(2n+1)\pi}\left[\cos\left(\frac{2n+1}{2}\pi x_D\right)\right]_0^1$$

$$= -\frac{4}{(2n+1)\pi} \tag{3.19.32}$$

Substituting Eq.(3.19.32) into (3.19.30) gives the general solution to the initial-boundary value problem as

$$P_D(x_D, t_D) = 1 - \frac{4}{\pi}\sum_{n=0}^{n=\infty}\left(\frac{1}{2n+1}\right)\sin\left(\frac{2n+1}{2}\pi x_D\right)e^{-\left(\frac{2n+1}{2}\right)^2 \pi^2 t_D} \tag{3.19.34}$$

3.19c

FIGURE 3.19.1 shows a sketch of the pressure profiles.

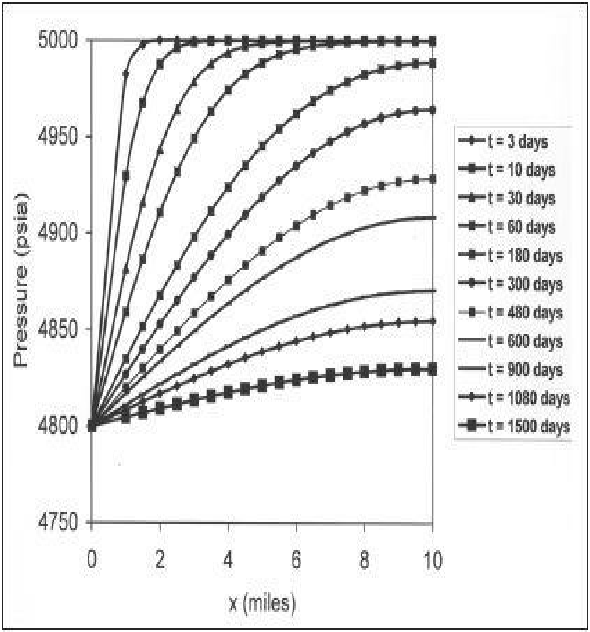

FIGURE 3.19.1 Sketch of pressure profiles.

3.19d

The cumulative water influx is given by

$$W_e = \int_0^T q\,dt \tag{3.19.35}$$

Darcy's law in modified oilfield units with q in reservoir barrels per hour gives

$$q(t) = \frac{0.001127}{24} \frac{kA}{\mu} \frac{\partial P}{\partial x}, \; x = 0 \tag{3.19.36}$$

Substituting Eqs.(3.19.5) and (3.19.6) into (3.19.36) gives

$$q(t) = -\frac{0.001127}{24} \frac{kA\left(P_i - P_w\right)}{\mu L} \frac{\partial P_D}{\partial x_D}, \; x_D = 0 \tag{3.19.37}$$

Substituting Eq.(3.19.37) into (3.19.35) gives

$$W_e = -\frac{0.001127}{24}\frac{kA(P_i - P_w)}{\mu L}\int_0^T -\frac{\partial P_D}{\partial x_D}dt,\ x_D = 0 \qquad (3.19.38)$$

The dimensionless time in oilfield units is given by

$$t_D = \frac{0.0002637kt}{\phi\mu c_t L^2} \qquad (3.19.39)$$

Differentiation of Eq.(3.19.39) gives

$$dt_D = \frac{0.0002637k}{\phi\mu c_t L^2}dt \qquad (3.19.40)$$

Substituting Eq.(3.19.40) into (3.19.38) gives

$$W_e = -\frac{0.001127}{24}\frac{kA\left(P_i - P_w\right)}{\mu L}\left(\frac{\phi\mu c_t L^2}{0.0002637k}\right)\int_0^{T_D} -\frac{\partial P_D}{\partial x_D} dt_D,\ x_D = 0$$

(3.19.41)

Differentiation of Eq.(3.19.34) at $x_D = 0$ gives

$$\frac{\partial P_D}{\partial x_D} = -2\sum_{n=0}^{n=\infty} e^{-\left(\frac{2n+1}{2}\right)^2 \pi^2 t_D} \tag{3.19.42}$$

Substituting Eq.(3.19.42) into (3.19.38) and performing the integration gives

$$W_e = 0.1781 wh\phi c_t L\left(P_i - P_w\right)\sum_{n=0}^{n=\infty}\frac{8}{\pi^2}\frac{1}{(2n+1)^2}\left[1 - e^{-\left(\frac{2n+1}{2}\right)^2 \pi^2 t_D}\right]$$

(3.19.43)

Eq.(3.19.43) can be simplified by noting that

$$\sum_{n=0}^{n=\infty} \frac{1}{(2n+)^2} = \frac{\pi^2}{8} \tag{3.19.44}$$

Substituting Eq.(3.19.44) into (3.19.43) gives

$$W_e = 0.1781 wh\phi c_t L\left(P_i - P_w\right)\left[1 - \frac{8}{\pi^2}\sum_{n=0}^{n=\infty}\frac{1}{(2n+1)^2} e^{-\left(\frac{2n+1}{2}\right)^2 \pi^2 t_D}\right] \tag{3.19.43}$$

3.19e

P_i=5000 psia

P_w = 4800 psia

$c_f = 4\times10^{-6}$ psi^{-1}

$C_W = 4\times10^{-6}$ psi^{-1}

$w = 5000$ ft

L = 10 miles = 10×5280 = 52800 ft

$h = 100$ ft

$k = 800$ mD

$\mu = 1$ cp

Ø = 0.35

$t = 3$ years = 3 × 365 × 24 = 26280 hrs

$$c_t = 4\times10^{-6} + 5\times10^{-6} = 9\times10^{-6}\ \text{psi}^{-1}$$

$$t_D = \frac{(0.0002637)(800)(26280)}{(0.35)(1)\left(9\times10^{-6}\right)(52800)^2} = 0.6313$$

Substituting numerical values into Eq. (3.19.43) gives

$$W_e = (0.1781)(5000)(100)(0.35)\left(9\times10^{-6}\right)(52800)(5000-4800)$$

$$\times\left[1-\frac{8}{\pi^2}\left(0.210618+9.06\times10^{-8}\right)\right] = 2.456\times10^6 \text{ reservoir barrels}$$

PROBLEM 3.20

3.20a

The initial-boundary value problem to be solved consists of the following equations. The partial differential equation is

$$\frac{\partial^2 P}{\partial x^2} = \frac{\varphi \mu c_t}{k} \frac{\partial P}{\partial t} \tag{3.20.1}$$

The initial condition is

$$P(x,0) = P_i \tag{3.20.2}$$

The internal boundary condition is

$$P(0,t) = P_w \tag{3.20.3}$$

The external no flow boundary condition is

$$\lim_{x \to \infty} P(x,t) = P_i \qquad (3.20.4)$$

3.20b

It is convenient to define a new dependent variable as

$$p(x,t) = P_i - P(x,t) \qquad (3.20.5)$$

Let

$$\alpha = \frac{k}{\phi \mu c_t} \qquad (3.20.6)$$

Substituting Eqs.(3.20.5) and (3.20.6) into Eqs(3.20.1), (3.20.2), (3.20.3), and

(3.20.4) gives

$$\frac{\partial^2 p}{\partial x^2}=\frac{1}{\alpha}\frac{\partial p}{\partial t} \tag{3.20.7}$$

$$p(x,0)=0 \tag{3.20.8}$$

$$p(0,t)=P_i-P_w \tag{3.20.9}$$

$$\lim_{x\to\infty} p(x,t)=0 \tag{3.20.10}$$

The initial-boundary value problem can be solved by Laplace transform. Taking the Laplace transform of Eq.(3.20.7) gives

$$\frac{d^2\bar{p}}{dx^2} = -\frac{1}{\alpha} p(x,0) + \frac{s}{\alpha}\bar{p} \qquad (3.20.11)$$

Substituting Eq.(3.20.8) into (3.20.11) and rearranging gives

$$\frac{d^2\bar{p}}{dx^2} - \frac{s}{\alpha}\bar{p} = 0 \qquad (3.20.12)$$

The solution of Eq.(3.20.12) is

$$\bar{p}(x;s) = Ae^{-x\sqrt{\frac{s}{\alpha}}} + Be^{x\sqrt{\frac{s}{\alpha}}} \qquad (3.20.13)$$

To satisfy Eq.(3.20.10) requires that $B = 0$. Eq.(3.20.13) becomes

$$\bar{p}(x;s) = Ae^{-x\sqrt{\frac{s}{\alpha}}} \qquad (3.20.14)$$

Taking the Laplace transform of Eq. (3.20.15) gives

$$\overline{p}(0;s)=\frac{P_i-P_w}{s} \tag{3.20.15}$$

Substituting Eq.(3.20.15) into Eq. (3.20.14) gives

$$A=\frac{P_i-P_w}{s} \tag{3.20.16}$$

Substituting Eq.(3.20.16) into (3.20.14) gives the solution as

$$\overline{p}(x;s)=\left(P_i-P_w\right)\frac{1}{s}e^{-x\sqrt{\frac{s}{\alpha}}} \tag{3.20.17}$$

Taking the inverse Laplace transform of Eq.(3.20.17) gives

$$p(x,t)=(P_i-P_w)erfc\left(\frac{x}{\sqrt{4\alpha t}}\right) \quad (3.20.18)$$

Substituting Eq.(3.20.5) into (3.20.18) gives the solution as

$$P(x,t)=P_i-(P_i-P_w)erfc\left(\frac{x}{\sqrt{4\alpha t}}\right) \quad (3.20.19)$$

Substituting Eq.(3.20.6) into (3.20.19) gives the solution as

$$P(x,t)=P_i-(P_i-P_w)erfc\left(\sqrt{\frac{\phi\mu c_t x^2}{4kt}}\right) \quad (3.20.20)$$

Eq.(3.20.20) can be written in oilfield units as

$$P(x,t) = P_i - (P_i - P_w)\,erfc\left(\sqrt{\frac{948\phi\mu c_t x^2}{kt}}\right) \quad (3.20.21)$$

3.20c

FIGURE 3.20.1 shows a sketch of the pressure profiles.

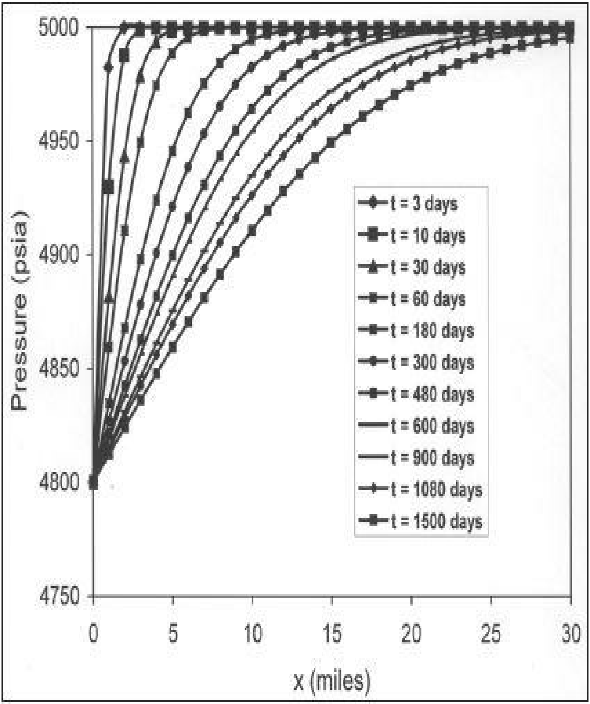

FIGURE 3.20.1 Sketch of pressure profiles.

3.20d

The cumulative water influx is given by

$$W_e = \int_0^T q\,dt \tag{3.20.22}$$

Darcy's law in Darcy units gives

$$q(t) = \frac{kA}{\mu}\frac{\partial P}{\partial x}, \ x = 0 \tag{3.20.23}$$

Differentiation of Eq.(3.20.19) gives

$$\frac{\partial P}{\partial x} = \left(P_i - P_w\right)\frac{2}{\sqrt{\pi}}\frac{d}{dx}\left(\frac{x}{2\sqrt{\alpha t}}\right)e^{-\frac{x^2}{4\alpha t}} \tag{3.20.24}$$

Substituting $x = 0$ into Eq.(3.20.24) gives

$$\frac{\partial P}{\partial x} = \frac{1}{\sqrt{\pi}}\frac{P_i - P_w}{\sqrt{\alpha t}} \tag{3.20.25}$$

Substituting Eq.(3.20.25) into (3.20.23) gives

$$q(t)=\frac{kA}{\mu}\frac{1}{\sqrt{\pi}}\frac{P_i-P_w}{\sqrt{\alpha t}}, x=0 \quad (3.20.26)$$

Substituting Eq.(3.20.26) into (3.20.22) and performing the integration gives

$$W_e=2\frac{kwh}{\mu}\left(P_i-P_w\right)\sqrt{\frac{t}{\pi\alpha}} \quad (3.20.27)$$

Substituting Eq.(3.20.6) into Eq.(3.20.27) gives the cumulative water influx in Darcy units as

$$W_e=2wh\frac{\left(P_i-P_w\right)}{\sqrt{\pi}}\left(\frac{\phi c_t k}{\mu}\right)^{1/2}\sqrt{t} \quad (3.20.28)$$

Eq.(3.20.28) can be written in oilfield units with t in hours as

$$W_e = 3.263\times10^{-3}\, wh\left(P_i - P_w\right)\left(\frac{\phi c_t k}{\mu}\right)^{1/2}\sqrt{t} \quad (3.20.29)$$

3.20e

P_i=5000 psia

P_w = 4800 psia

$c_f = 4\times10^{-6}$ psi^{-1}

$c_w = 4\times10^{-6}$ psi^{-1}

w = 5000 ft

h = 100 ft

k = 800 mD

μ = 1 cp

$\O$ = 0.35

t = 3 years = 3 × 365 × 24 = 26280 hrs

$C_t = 4\times10^{-6} + 5\times10^{-6} = 9\times10^{-6}$ psi^{-1}

Substituting numerical values into Eq. (3.20.29) gives

$$W_e = \left(3.263\times10^{-3}\right)(5000)(100)(5000-4800)\left(\frac{0.35\times9\times10^{-6}\times800}{1}\right)^{1/2}\times$$

$$\sqrt{3\times365\times24} = 2.655\times10^{6} \text{ reservoir barrels}$$

PROBLEM 3.21

The Navier-Stokes equation in Cartesian coordinates is given by

$$\rho\left(\frac{\partial v_x}{\partial t}+v_x\frac{\partial v_x}{\partial x}+v_y\frac{\partial v_y}{\partial y}+v_z\frac{\partial v_z}{\partial z}\right)=-\frac{\partial P}{\partial x}+\mu\left[\frac{\partial^2 v_x}{\partial x^2}+\frac{\partial^2 v_x}{\partial y^2}+\frac{\partial^2 v_x}{\partial z^2}\right]+\rho g_x \tag{3.21.1}$$

For 1D flow in the x direction and negligible gravity effect, Eq.(3.21.1) simplifies to

$$\frac{dP}{dx}=\mu\frac{\partial^2 v_x}{\partial z^2}=\text{constant} \tag{3.21.2}$$

The no-slip boundary conditions at the walls are

$$v_x = 0, \text{ at } x = 0 \tag{3.21.3}$$

$$v_x = 0, \text{ at } x = w \tag{3.21.4}$$

Integration of Eq.(3.21.2) gives

$$v_x = \frac{1}{2\mu}\left(\frac{dp}{dx}\right)z^2 + c_1 z + c_2 \tag{3.21.5}$$

Application of the boundary conditions gives

$$c_2 = 0 \text{ and } c_1 = -\frac{w}{2\mu}\frac{dP}{dx} \tag{3.21.6}$$

Substituting Eq.(3.21.6) into (3.21.5) gives

$$v_x = \frac{1}{2\mu}\frac{dP}{dx}\left(z^2 - wz\right) \qquad (3.21.7)$$

The volumetric flow rate is given by

$$q = B\int_0^w v_x dz \qquad (3.21.8)$$

Substituting Eq.(3.21.7) into (3.21.8) gives

$$q = \frac{B}{2\mu}\left(\frac{dP}{dx}\right)\int_0^w \left(z^2 - wz\right)dz \qquad (3.21.9)$$

Integration of Eq.(2.21.9) gives

$$q = \frac{B}{2\mu}\left(\frac{dP}{dx}\right)\left[\frac{z^3}{3} - \frac{wz^2}{2}\right]_0^w = \frac{B}{2\mu}\left(\frac{dP}{dx}\right)\left[\frac{w^3}{3} - \frac{w^3}{2}\right] = -\frac{Bw^3}{12\mu}\frac{dP}{dx}$$

$$(3.21.10)$$

Eq.(3.21.10) can be written as

$$q = -\frac{w^2 A}{12\mu}\frac{dP}{dx} \tag{3.21.11}$$

where A is the area normal to flow. Darcy's law is

$$q = -\frac{kA}{\mu}\frac{dP}{dx} \tag{3.21.12}$$

A comparison of Eqs.(3.21.11) and (3.21.12) gives the permeability as

$$k = \frac{w^2}{12} \tag{3.21.13}$$

PROBLEM 3.22

3.22a

FIGURE 3.22.1 shows the fractured medium. For flow in the x direction, we have linear systems in parallel. The average permeability in the x direction is given by

$$k_x = \frac{\sum k_i A_i}{\sum A_i} = \frac{\sum k_m A_m + \sum k_f A_f}{A_m + A_f} \qquad (3.22.1)$$

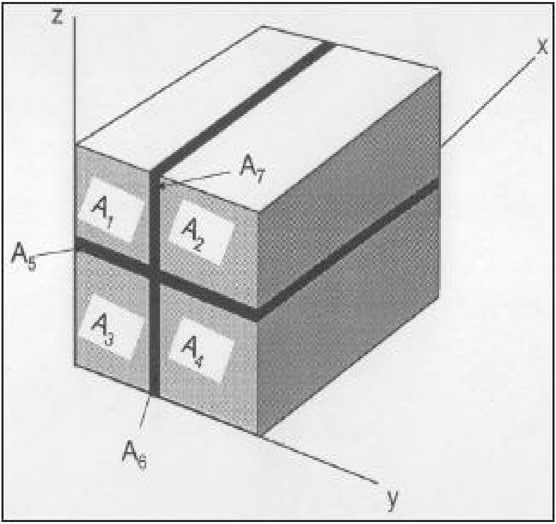

FIGURE 3.22.1 Fractured dolomite (not to scale).

For the matrix,

$$k_m = 20\times10^{-3}\times9.869\times10^{-9} = 1.974\times10^{-10}\ \text{cm}^2$$

$$A_1 = A_2 = A_3 = A_4 = \left(\frac{100-0.20}{2}\right)^2 = 2.490\times10^3\ \text{cm}^2$$

$$A_m = A_1 + A_2 + A_3 + A_4 = 4\times2.490\times10^3 = 9.960\times10^3\ \text{cm}^2$$

$$\sum k_m A_m = \left(1.974\times10^{-10}\right)\left(9.96\times10^{-3}\right) = 1.966\times10^{-6}\ \text{cm}^4$$

For the fracture,

$$w = 2 \text{ mm}$$

$$k_f = \frac{w^2}{12} = \frac{(0.20)^2}{12} = 3.333 \times 10^{-3} \text{ cm}^2$$

$$A_5 = (100)(0.20) = 20 \text{ cm}^2$$

$$A_6 = A_7 = \left(\frac{100 - 0.20}{2}\right)(0.20) = 9.980 \text{ cm}^2$$

$$A_f = A_5 + A_6 + A_7 = 20 + 9.98 + 9.98 = 39.96 \text{ cm}^2$$

$$\sum k_f A_f = \left(3.333 \times 10^{-3}\right)(39.96) = 0.1332 \text{ cm}^4$$

Substituting numerical values into Eq. (3.22.1) gives

$$k_x = \frac{1.96\times10^{-6}+0.1332}{9.96\times10^{3}+39.96} = 1.332\times10^{-5}\ \text{cm}^2$$

$$= \frac{1.332\times10^{-5}}{9.869\times10^{-9}} = 1349.7\ \text{D}$$

From symmetry, $k_y = k_z$. Examination of the FIGURE shows that in the y direction, we have linear media in series and in parallel. The media above and below the fracture are in series. These series media are then in parallel with the horizontal fracture. Thus, we will calculate k_y in two steps. First, we calculate the segments in series and then combine them in parallel with the horizontal fracture to calculate k_y. The average permeability of the linear media in series above and below the horizontal fracture is given by

$$k_a = \frac{L}{\sum \frac{L_i}{k_i}} = \frac{L}{\frac{L_{m1}}{k_{m1}} + \frac{L_f}{k_f} + \frac{L_{m2}}{k_{m2}}} \tag{3.22.2}$$

Substituting numerical values into Eq. (3.22.2) gives

$$k_a = \frac{100}{\frac{49.90}{1.974 \times 10^{-10}} + \frac{0.20}{3.333 \times 10^{-3}} + \frac{49.90}{1.974 \times 10^{-10}}} = 1.978 \times 10^{-10}\ \text{cm}^2$$

The series media above and below the horizontal fracture can be combined in parallel with the horizontal fracture to obtain k_y as

$$k_y = \frac{k_a A_a + k_f A_f + k_a A_a}{A_a + A_f + A_a} \qquad (3.22.3)$$

Substituting numerical values into Eq. (3.22.3) gives

$$k_y = \frac{\left(1.978\times10^{-10}\right)(4990)+\left(3.333\times10^{-3}\right)(20)+\left(1.978\times10^{-10}\right)(4990)}{4990+20+4990}$$

$$= 6.666\times10^{-6}\ \text{cm}^2 = \frac{6.666\times10^{-6}}{9.869\times10^{-9}} = 675.5\ \text{D}$$

$$k_z = k_y = 675.5\ \text{D}$$

3.22b

Before fracturing, the porous medium was homogeneous and isotropic with respect to permeability. After fracturing, porous has become heterogeneous. Because there are more fractures in the *x* direction than in the y and z directions, the porous medium also is anisotropic with respect to permeability.

PROBLEM 3.23

3.23a

$$\bar{k}(x,y) = \begin{bmatrix} 100 & 100 \\ 100 & 100 \end{bmatrix} \text{mD}$$

Examine the permeability tensor in the principal axes of the anisotropy.

$$k_{x'y'} = k_{y'x'} = 0$$

$$\theta = \frac{1}{2}\tan^{-1}\left(\frac{2k_{xy}}{k_{xx} - k_{yy}}\right) = \frac{1}{2}\tan^{-1}\left(\frac{2\times 100}{100-100}\right) = \frac{1}{2}\left(90^{\circ}\right) = 45^{\circ}$$

$$k_{x'x'} = \frac{k_{xx} + k_{yy}}{2} + \frac{k_{xx} - k_{yy}}{2}\cos 2\theta + k_{xy}\sin 2\theta$$

$$= \frac{100+100}{2} + \frac{100-100}{2}\cos 90^{\circ} + 100\sin 90^{\circ}$$

$$= 100 + 0 + 100$$

$$= 200 \text{ mD}$$

$$k_{y'y'} = \frac{k_{xx} + k_{yy}}{2} - \frac{k_{xx} - k_{yy}}{2}\cos 2\theta - k_{xy}\sin 2\theta$$

$$= \frac{100+100}{2} - \frac{100-100}{2}\cos 90^{\circ} - 100\sin 90^{\circ}$$

$$= 100 - 0 - 100$$

$$= 0 \text{ mD}$$

When viewed in the axes of the permeability anisotropy, the permeability tensor is given by

$$\bar{k}(x',y') = \begin{bmatrix} 200 & 0 \\ 0 & 0 \end{bmatrix} \text{mD}$$

No. The reservoir is not isotropic with respect to permeability. It is anisotropic because $k_{x'x'} \neq k_{y'y'}$. FIGURE 3.23.1 shows the porous medium in the principal axes of the anisotropy.

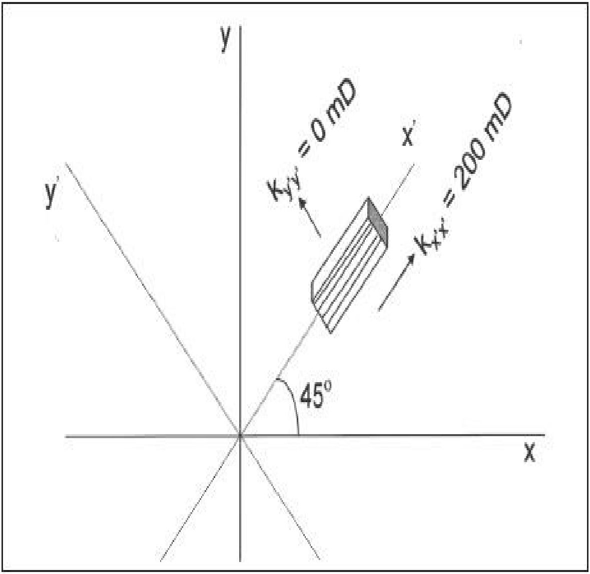

FIGURE 3.23.1 Porous medium in the axes of anisotropy.

3.23b

The permeability along the bedding plane is $k_{x \cdot x}$= 200 mD.

PROBLEM 3.24

$$\bar{k}(x,y)=\begin{bmatrix} 100 & 0 \\ 0 & 100 \end{bmatrix} \text{mD}$$

The directional permeability along the direction of flow can be determined graphically with the equation

$$\frac{x^2}{\left(\sqrt{100}\right)^2}+\frac{y^2}{\left(\sqrt{100}\right)^2}=1 \qquad (3.24.1)$$

or

$$x^2+y^2=10^2 \qquad (3.25.2)$$

Eq.(3.24.2) is the equation of a circle of radius 10 units. **FIGURE 3.24.1** shows the permeability ellipse which in this case is a circle.

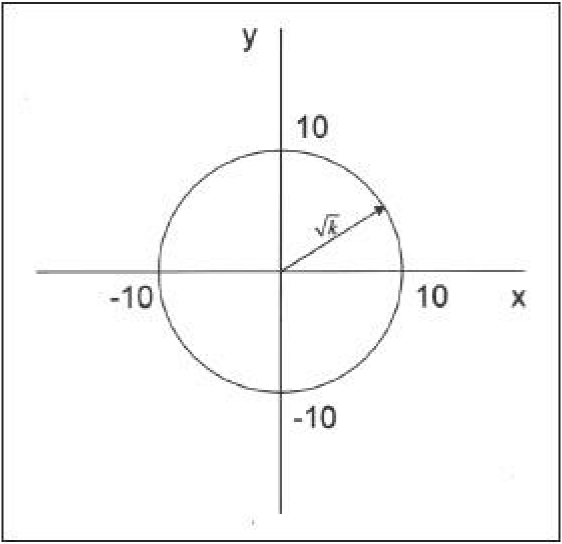

FIGURE 3.24.1 Permeability ellipse.

The reservoir is isotropic with respect to permeability. All orthogonal axes are principal axes of the permeability tensor. The permeability ellipse degenerates into a circle for an isotropic reservoir.

PROBLEM 3.25

3.25a

The hydraulic conductivity tensor for the aquifer is given by

$$\overline{K}(x,y)=\begin{bmatrix} 20 & 6 \\ 6 & 10 \end{bmatrix} \text{meters/day} \qquad (3.25.1)$$

Darcy's law is

$$\vec{v}=-\overline{K}\cdot\nabla h \qquad (3.25.2)$$

$$\nabla h=\begin{bmatrix} (11.5-10)/(300-0) \\ (8.4-10)/(200-0) \end{bmatrix}=\begin{bmatrix} 0.005 \\ -0.008 \end{bmatrix} \qquad (3.25.3)$$

$$|\nabla h| = \sqrt{(0.005)^2 + (-0.008)^2} = 0.0094 \text{ m} \qquad (3.25.4)$$

Substituting Eqs.(3.25.1) and (3.25.3) into (3.25.2) gives

$$\vec{v} = -\begin{bmatrix} 20 & 6 \\ 6 & 10 \end{bmatrix}\begin{bmatrix} 0.005 \\ -0.008 \end{bmatrix} = -0.005\begin{bmatrix} 20 \\ 6 \end{bmatrix} + 0.008\begin{bmatrix} 6 \\ 10 \end{bmatrix}$$

$$= \begin{bmatrix} -0.052 \\ 0.050 \end{bmatrix} \text{m/day} \qquad (3.25.5)$$

The Darcy velocity vector lies in the second quadrant and makes an angle α with negative x-axis given by

$$\alpha = \tan^{-1}\left(\frac{0.050}{0.052}\right) = \tan^{-1}(0.9615) = 43.88^\circ$$

It makes an angle θ with positive x-axis

given by

$$\theta = 180 - 43.88 = 136.12^\circ$$

3.25b

The hydraulic gradient vector lies in the fourth quadrant and makes an angle θ with the positive x-axis given by

$$\beta = \tan^{-1}\left(\frac{0.008}{0.005}\right) = \tan^{-1}(1.60) = 57.99^\circ$$

The directional hydraulic conductivity in the direction of flow is given by

$$K_{df} = \frac{|\vec{v}|}{|\nabla h|\cos(\beta - \alpha)} = \frac{0.07214}{(0.00943)\cos 14.11^\circ} = 7.88 \text{ m/d}$$

3.25c

Let one of the principal axes make an angle θ with the positive x-axis given by

$$\theta=\frac{1}{2}\tan^{-1}\left(\frac{2K_{xy}}{K_{xx}-K_{yy}}\right)=\frac{1}{2}\tan^{-1}\left(\frac{2\times 6}{20-10}\right)=\frac{1}{2}\left(50.19^{\circ}\right)=25.10^{\circ}$$

The other axis is 90° away.

3.26d

$$K_{uu} = \frac{K_{xx} + K_{yy}}{2} + \frac{K_{xx} - K_{yy}}{2} \cos 2\theta + K_{xy} \sin 2\theta$$

$$= \frac{20+10}{2} + \frac{20-10}{2} \cos 50.19^\circ + 6 \sin 50.19^\circ$$

$$= 15 + 3.20 + 4.61$$

$$= 22.81 \text{ m/d}$$

$$K_{vv} = \frac{K_{xx} + K_{yy}}{2} - \frac{K_{xx} - K_{yy}}{2} \cos 2\theta - K_{xy} \sin 2\theta$$

$$= \frac{20+10}{2} - \frac{20-10}{2} \cos 50.19^\circ - 6 \sin 50.19^\circ$$

$$= 15 - 3.20 - 4.61$$

$$= 7.19 \text{ m/d}$$

PROBLEM 3.26

3.26a

$$\bar{k}(x,y)=\begin{bmatrix} 100 & 50 \\ 50 & 200 \end{bmatrix} \text{mD}$$

Darcy's law:

$$\begin{bmatrix} v_x \\ v_y \end{bmatrix} = -\frac{1}{\mu}\begin{bmatrix} k_{xx} & k_{xy} \\ k_{yx} & k_{yy} \end{bmatrix}\begin{bmatrix} \frac{\partial \Phi}{\partial x} \\ \frac{\partial \Phi}{\partial y} \end{bmatrix} \tag{3.26.1}$$

Substituting numerical values into Eq. (3.26.1) gives

$$\begin{bmatrix} v_x \\ v_y \end{bmatrix} = -\frac{1}{1.5}\begin{bmatrix} 0.1 & 0.05 \\ 0.05 & 0.2 \end{bmatrix}\begin{bmatrix} -0.154 \\ 0.005 \end{bmatrix} = \begin{bmatrix} 1.010\times10^{-2} \\ 4.467\times10^{-3} \end{bmatrix} \text{cm/s}$$

$$|\vec{v}| = \sqrt{v_x^2 + v_y^2} = \sqrt{\left(1.010\times10^{-2}\right)^2 + \left(4.467\times10^{-3}\right)^2} = 1.104\times10^{-2} \text{ cm/s}$$

3.26b

The angle between the flow direction and the positive x-axis is given by

$$\alpha = \tan^{-1}\left(\frac{v_y}{v_x}\right) = \tan^{-1}\left(\frac{4.467\times10^{-3}}{1.010\times10^{-2}}\right) = \tan^{-1}(0.4422) = 23.86^\circ$$

3.26c

The angle between the flow direction and the direction of the potential gradient is given by

$$\cos\beta = \frac{\vec{v}.\nabla\Phi}{|\vec{v}||\nabla\Phi|} = \frac{\left(1.010\times10^{-2}i + 4.467\times10^{-3}j\right)\cdot\left(-0.154i + 0.005j\right)}{\left(1.104\times10^{-2}\right)(0.1541)}$$

$$= -0.9010$$

$$\beta = 154.28^{\circ}$$

3.26d

The angle θ that one of the principal axes (u) makes with the positive x-axis is given by

$$\theta = \frac{1}{2}\tan^{-1}\left(\frac{2k_{xy}}{k_{xx}-k_{yy}}\right) = \frac{1}{2}\tan^{-1}\left(\frac{2(50)}{100-200}\right) = \frac{1}{2}\tan^{-1}(-0.7854)$$

$$= -22.5^{\circ}$$

The other principal axis (v) is 90° away and makes an angle of 67.5° with the positive x-axis.

3.26e

The principal values of the permeability anisotropy are given by

$$k_{uu} = \frac{k_{xx}+k_{yy}}{2} + \frac{k_{xx}-k_{yy}}{2}\cos 2\theta + K_{xy}\sin 2\theta$$

$$= \frac{100+200}{2} + \frac{100-200}{2}\cos\left(-45^\circ\right) + 50\sin\left(-45^\circ\right)$$

$$= 150 - 35.36 - 35.55$$

$$= 79.29 \text{ mD}$$

$$k_{uu} = \frac{k_{xx}+k_{yy}}{2} - \frac{k_{xx}-k_{yy}}{2}\cos 2\theta - K_{xy}\sin 2\theta$$

$$= \frac{100+200}{2} - \frac{100-200}{2}\cos\left(-45^\circ\right) - 50\sin\left(-45^\circ\right)$$

$$= 150 + 35.36 + 35.55$$

$$= 220.71 \text{ mD}$$

Parts (e) and (d) also can be solved by

linear algebra as follows:

$$\overline{k} = \begin{bmatrix} 100 & 50 \\ 50 & 200 \end{bmatrix}$$

The eigenvalues are given by

$$\det\begin{bmatrix} 100-\lambda & 50 \\ 50 & 200-\lambda \end{bmatrix} = 0$$

$$(\lambda - 100)(\lambda - 200) - 50^2 = 0$$

$$\lambda^2 - 300\lambda + 17500 = 0$$

$$\lambda = \frac{300 \pm \sqrt{300^2 - (4)(1)(17500)}}{2}$$

$$\lambda_1 = k_{uu} = 79.29\,\text{mD}$$

$$\lambda_2 = k_{vv} = 220.71\,\text{mD}$$

The principal axes of the permeability anisotropy are given by the eigenvectors of the permeability tensor.

$$\begin{bmatrix} 100-\lambda & 50 \\ 50 & 200-\lambda \end{bmatrix}\begin{bmatrix} x \\ y \end{bmatrix}=\begin{bmatrix} 0 \\ 0 \end{bmatrix}$$

For $\lambda_1 = 79.29$ mD

$$\begin{bmatrix} 20.71 & 50 \\ 50 & 120.71 \end{bmatrix}\begin{bmatrix} x \\ y \end{bmatrix}=\begin{bmatrix} 0 \\ 0 \end{bmatrix}$$

$$20.71x + 50y = 0$$

$$50x + 120.71y = 0$$

The eigenvector is given by

$$\vec{u}=\begin{bmatrix} -50/20.71 \\ 1 \end{bmatrix}=\begin{bmatrix} -2.4143 \\ 1 \end{bmatrix}$$

This eigenvector makes an angle θu with the positive x-axis given by,

$$\tan\theta=\frac{1}{-2.4143}=-0.4142$$
$$\theta=-22.5°$$

For $\lambda_2 = 220.71$ mD

$$\begin{bmatrix} -120.71 & 50 \\ 50 & -20.71 \end{bmatrix}\begin{bmatrix} x \\ y \end{bmatrix}=\begin{bmatrix} 0 \\ 0 \end{bmatrix}$$
$$-120.71x+50y=0$$
$$50x-20.71y=0$$

The eigenvector is given by

$$\vec{v} = \begin{bmatrix} 50/120.71 \\ 1 \end{bmatrix} = \begin{bmatrix} 0.4142 \\ 1 \end{bmatrix}$$

This eigenvector makes an angle θv with the positive x-axis given by,

$$\tan\theta = \frac{1}{0.4142} = 2.4142$$
$$\theta_v = 67.5°$$

3.26f

$$\gamma = 180 - \alpha = 180 - 154.28 = 25.72^{\circ}$$

The directional permeability in the flow direction is given by

$$k_{df} = \frac{\mu|\vec{v}|}{|\nabla\phi|\cos\gamma} = \frac{(1.5)\left(1.104\times10^{-2}\right)}{(0.1541)\cos\left(25.72^{\circ}\right)} = 0.1193\text{ D}$$

The directional permeability in the direction of potential gradient is given by

$$k_{dp} = \frac{\mu|\vec{v}|\cos\beta}{|\nabla\phi|} = \frac{(1.5)\left(1.104\times10^{-2}\right)\cos\left(25.72^{\circ}\right)}{0.1541} = 0.0969 \text{ D}$$

The directional permeabilities also can be calculated as follows. The directional permeability in the flow direction is also given by

$$\frac{1}{k_{df}} = \frac{\cos^2\theta}{k_u} + \frac{\sin^2\theta}{k_v}$$

$$= \frac{\cos^2(23.86^\circ + 22.5^\circ)}{79.29} + \frac{\sin^2(23.86^\circ + 22.5^\circ)}{220.71} = 0.00838$$

$$k_{df} = 1/0.00838 = 119.33 \text{ mD}$$

The directional permeability in the direction of the potential gradient is given by

$$\begin{aligned} k_{dp} &= k_u \cos^2\theta + k_v \sin^2\theta \\ &= 79.29\cos^2(46.36^\circ + 154.28^\circ) + 220.71\sin^2(46.36^\circ + 154.28^\circ) \\ &= 96.86 \text{ mD} \end{aligned}$$

The permeability ellipse in the flow direction is given by

$$k_u = 79.29 \text{ mD}; k_v = 220.71 \text{ mD}$$

$$\frac{u^2}{79.29} + \frac{v^2}{220.71} = 1 \quad (3.26.2)$$

The permeability ellipse in the flow direction is shown in **FIGURE 3.26.1**.

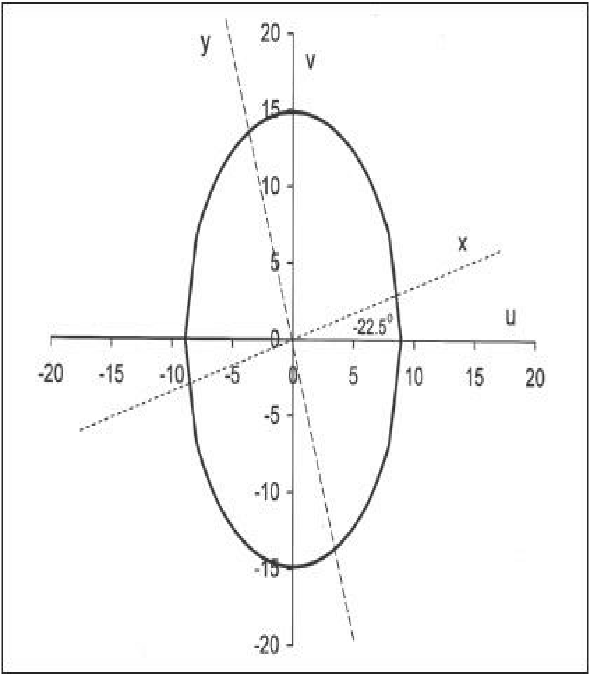

FIGURE 3.26.1 Permeability ellipse in the flow direction.

The permeability ellipse in the direction of potential gradient is given by

$$\frac{u^2}{1/79.29}+\frac{v^2}{1/220.71}=1 \tag{3.26.3}$$

The permeability ellipse in the direction of the potential gradient is shown in **FIGURE 3.26.2**.

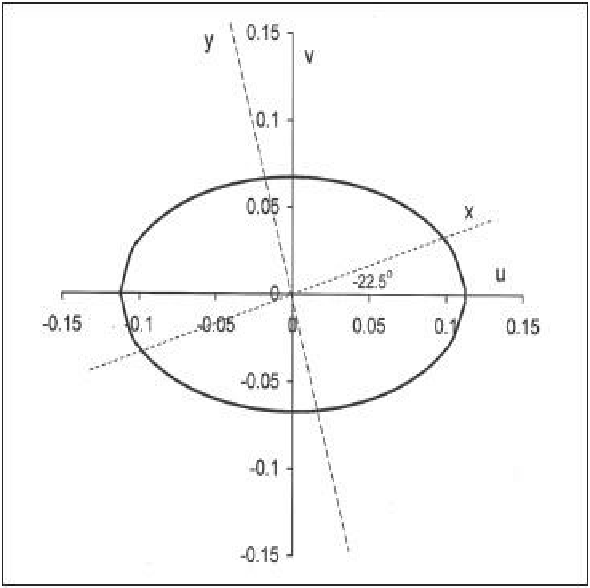

FIGURE 3.26.2 Permeability ellipse in the direction of the potential gradient.

PROBLEM 3.27

Method 1.
Based on Darcy's Law for Homogeneous and Anisotropic Porous Media.
Given:

$$\bar{k}(x,y)=\begin{bmatrix} 179 & 54 \\ 54 & 61 \end{bmatrix} \text{mD} \tag{3.27.1}$$

3.27a
One of the principal axes of the permeability anisotropy makes an angle *?* with the positive *x*-axis, where *?* is given by Eq.(3.257) in the text as

$$2\theta = \tan^{-1}\left(\frac{2k_{xy}}{k_{xx} - k_{yy}}\right) = \tan^{-1}\left(\frac{2\times 54}{179-61}\right) = \tan^{-1}(0.9153)$$

(3.27.2)

The other principal axis makes an angle *?* with the positive *x*-axis given by

$$2\theta = 42.47^{\circ}$$

$$\theta = 21.23^{\circ}$$

3.27b

One of the principal values of the permeability anisotropy is given by Eq. (3.249) in the textbook as

$$\beta = 21.23 + 90 = 111.23^{\circ}$$

Substituting the numerical values into Eq.(3.27.3) gives

$$k_u = \frac{k_{xx} + k_{yy}}{2} + \frac{k_{xx} - k_{yy}}{2}\cos 2\theta + k_{yx}\sin 2\theta \quad (3.27.3)$$

The other principal value is given by Eq. (3.253) in the text as

$$k_u = \frac{179+61}{2} + \frac{179-61}{2}\cos 42.47^\circ + 54\sin 42.47^\circ$$
$$= 120 + 43.5217 + 36.4596$$
$$= 199.98 \text{ mD}$$

Substituting the numerical values into Eq.(3.27.4) gives

$$k_v = \frac{k_{xx} + k_{yy}}{2} - \left(\frac{k_{xx} - k_{yy}}{2}\right)\cos 2\theta - k_{yx}\sin 2\theta \quad (3.27.4)$$

The permeability tensor when viewed in the principal axes of the anisotropy is

given by

$$k_u = \frac{179+61}{2} - \left(\frac{179-61}{2}\right)\cos 42.47^\circ - 54\sin 42.47^\circ$$
$$= 120 - 43.5217 - 36.4596$$
$$= 40.02 \text{ mD}$$

3.27c

The flow direction makes an angle of +45° with the positive x-axis where anticlockwise rotation is positive and clockwise rotation is negative. The flow direction makes an angle of 45° –21.23° = 23.77° with the positive u-axis. The directional permeability in the direction of flow is given by Eq.(3.272) in the text as

$$\bar{k}(u,v)=\begin{bmatrix} 199.98 & 0 \\ 0 & 40.02 \end{bmatrix} \text{mD} \qquad (3.27.5)$$

Method 2.
Based on Linear Algebra.

$$\frac{1}{k_{df}}=\frac{\cos^2 23.77^\circ}{199.98}+\frac{\sin^2 23.77^\circ}{40.02}=0.0042+0.0041=0.0082$$

$$k_{df}=\frac{1}{0.0082}=121.27 \text{ mD}$$

3.27b
The principal values of the permeability tensor are given by the eigenvalues of the tensor. The characteristic equation is

$$\det\begin{bmatrix} 179-\lambda & 54 \\ 54 & 61-\lambda \end{bmatrix}=\lambda^2-240\lambda+8003=0 \qquad (3.27.6)$$

$$\lambda = \frac{240 \pm \sqrt{240^2 - (4)(1)(8003)}}{2}$$

$$\lambda_1 = 199.98 \text{ mD}$$

$$\lambda_2 = 40.02 \text{ mD}$$

3.27a

The principal axes of the permeability anisotropy are given by the eigenvectors of the permeability tensor. For $\lambda_1 =$ 199.98 mD, the homogeneous equation to be solved for the eigenvector is

$$\begin{bmatrix} -20.98 & 54 \\ 54 & -138.98 \end{bmatrix} \begin{pmatrix} x \\ y \end{pmatrix} = \begin{pmatrix} 0 \\ 0 \end{pmatrix}$$

This gives the eigenvector associated with λ_1 =199.98 mDas

$$\vec{u} = \begin{pmatrix} 2.5739 \\ 1 \end{pmatrix}$$

$$\tan\theta = \frac{1}{2.5739} = 0.3885$$

$$\theta = 21.23^{\circ}$$

For λ_2 = 40.02 mD, the homogeneous equation to be solved for the eigenvector is

$$\begin{bmatrix} 138.98 & 54 \\ 54 & 20.98 \end{bmatrix} \begin{pmatrix} x \\ y \end{pmatrix} = \begin{pmatrix} 0 \\ 0 \end{pmatrix}$$

This gives the eigenvector associated

with λ_2= 40.02 mD as

$$\vec{v} = \begin{pmatrix} -0.3885 \\ 1 \end{pmatrix}$$

$$\tan\alpha = \frac{1}{-0.3885} = -2.5739$$

$$\alpha = -68.77^\circ$$

where α is the angle the second principal axis makes with the positive *x*-axis. It can be shown that both eigenvectors are orthogonal as they should be.

3.27c

The square root of the directional permeability in the direction of flow is is given by the intersection of the line in the direction of flow with the permeability ellipse. The equation of the line along the direction of flow is

$$v = \tan 21.23^{\circ} u \tag{3.27.7}$$

The equation of the permeability ellipse is

$$\frac{u^2}{199.98} + \frac{v^2}{40.02} = 1 \tag{3.27.8}$$

Solving Eqs.(3.27.7) and (3.27.8) simultaneously gives

$$u^2 = 101.57$$

$$v^2 = 19.69$$

$$\sqrt{k_{df}} = \sqrt{u^2 + v^2} = \sqrt{101.57 + 19.69} = \sqrt{121.26}$$

$$k_{df} = 121.26 \text{ mD}$$

PROBLEM 3.28

3.28a

Given:

$$\begin{bmatrix} v_x \\ v_y \end{bmatrix} = \begin{bmatrix} 2.0\times10^{-5} \\ 1.0\times10^{-5} \end{bmatrix} \text{cm / s} \qquad (3.28.1)$$

$$\begin{bmatrix} \frac{\partial P}{\partial x} \\ \frac{\partial P}{\partial y} \end{bmatrix} = \begin{bmatrix} -0.001 \\ -0.002 \end{bmatrix} \text{atm / cm} \qquad (3.28.2)$$

Apply Darcy's law to obtain

$$\begin{bmatrix} v_x \\ v_y \end{bmatrix} = -\frac{1}{\mu}\begin{bmatrix} k_{xx} & 0 \\ 0 & k_{yy} \end{bmatrix}\begin{bmatrix} \dfrac{\partial P}{\partial x} \\ \dfrac{\partial P}{\partial y} \end{bmatrix} \quad (3.28.3)$$

Substituting the numerical values into Eq.(3.28.3) gives

$$\begin{bmatrix} 2.0\times10^{-5} \\ 1.0\times10^{-5} \end{bmatrix} = -\frac{1}{1}\begin{bmatrix} k_{xx} & 0 \\ 0 & k_{yy} \end{bmatrix}\begin{bmatrix} -0.001 \\ -0.002 \end{bmatrix} \quad (3.29.4)$$

$$1.0\times10^{-5}=0.002k_{yy}$$

$$k_{xx}=2.0\times10^{-5}/0.001=0.020D=20\text{ mD}$$

$$2.0\times10^{-5}=0.001k_{xx}$$

$$k_{yy}=1.0\times10^{-5}/0.002=0.005D=5\text{ mD}$$

The permeability tensor is given by

$$\overline{k}(x,y)=\begin{bmatrix} 20 & 0 \\ 0 & 5 \end{bmatrix}\text{mD}$$

3.28b

The Darcy velocity vector makes and angle *a* with the positive *x*-axis given by

$$\alpha=\tan^{-1}\left(\frac{v_y}{v_x}\right)=\tan^{-1}\left(\frac{1\times10^{-5}}{2\times10^{-5}}\right)=\tan^{-1}(0.50)=26.565^{\circ}$$

3.28c

The directional permeability in the flow direction is given by

$$\frac{1}{k_{df}} = \frac{\cos^2\left(26.565^\circ\right)}{20} + \frac{\sin^2\left(26.565^\circ\right)}{5} = 0.04 + 0.04 = 0.08$$

$$k_{df} = 1/0.08 = 12.5 \text{ mD}$$

The pressure gradient vector lies in the third quadrant and makes an angle γ with the negative x-axis given by

$$\gamma = \tan^{-1}\left(\frac{-0.002}{-0.001}\right) = \tan^{-1}\left(2.0\right) = 63.435^\circ$$

The directional permeability in the direction of the pressure gradient is

given by

$$k_{dp} = 20\cos^2\left(63.435^\circ + 180^\circ\right) + 5\sin^2\left(63.435^\circ + 180^\circ\right)$$

$$= 4.0 + 4.0 = 8 \text{ mD}$$

3.28d

$$
\begin{aligned}
k_{x'x'} &= \frac{k_{xx}+k_{yy}}{2} + \frac{k_{xx}-k_{yy}}{2}\cos 2\theta + K_{xy}\sin 2\theta \\
&= \frac{20+5}{2} + \frac{20-5}{2}\cos\left(60^\circ\right) + 0 \\
&= 12.50 - 3.75 \\
&= 16.25 \text{ mD}
\end{aligned}
$$

$$
\begin{aligned}
k_{y'y'} &= \frac{k_{xx}+k_{yy}}{2} - \frac{k_{xx}-k_{yy}}{2}\cos 2\theta - K_{xy}\sin 2\theta \\
&= \frac{20+5}{2} - \frac{20-5}{2}\cos\left(60^\circ\right) - 0 \\
&= 12.50 - 3.75 \\
&= 8.75 \text{ mD}
\end{aligned}
$$

$$
\begin{aligned}
k_{x'y'} = k_{y'x'} &= -\left(\frac{k_{xx}-k_{yy}}{2}\right)\sin 2\theta + k_{xy}\cos 2\theta \\
&= -\left(\frac{20-5}{2}\right)\sin\left(60^\circ\right) + 0 \\
&= -6.50
\end{aligned}
$$

The permeability tensor in the new coordinate system is given by

$$\bar{k}(x'y') = \begin{bmatrix} 16.25 & -6.50 \\ -6.50 & 8.75 \end{bmatrix} \text{mD}$$

PROBLEM 3.29

3.29a

Darcy's law gives

$$\begin{bmatrix} V_x \\ V_y \\ V_z \end{bmatrix} = -\frac{1}{\mu} \begin{bmatrix} k_{xx} & k_{xy} & k_{xz} \\ k_{yx} & k_{yy} & k_{yz} \\ k_{zx} & k_{zy} & k_{zz} \end{bmatrix} \begin{bmatrix} \frac{\partial \Phi}{\partial x} \\ \frac{\partial \Phi}{\partial y} \\ \frac{\partial \Phi}{\partial z} \end{bmatrix} \qquad (3.29.1)$$

Substituting the numerical values into Eq.(3.29.1) gives

$$\begin{bmatrix} V_x \\ V_y \\ V_z \end{bmatrix} = -\frac{1}{1.5}\begin{bmatrix} 0.20 & 0.05 & 0.04 \\ 0.05 & 0.15 & 0.03 \\ 0.04 & 0.03 & 0.10 \end{bmatrix}\begin{bmatrix} -0.15 \\ 0.05 \\ 0.40 \end{bmatrix}$$

$$= \begin{bmatrix} 7.667\times10^{-3} \\ -8.000\times10^{-3} \\ -2.367\times10^{-2} \end{bmatrix} \text{cm/s}$$

$$\left|\vec{V}\right| = \sqrt{V_x^2 + V_y^2 + V_z^2}$$

$$= \sqrt{\left(7.667\times10^{-3}\right)^2 + \left(-8.000\times10^{-3}\right)^2 + \left(-2.367\times10^{-2}\right)^2}$$

$$= 2.613\times10^{-2} \text{ cm/s}$$

3.29b

The angles that V makes with the x, y, and z axes are

$$\varphi_x = \cos^{-1}\left(\frac{|V_x|}{|V|}\right) = \cos^{-1}\left(\frac{7.667\times10^{-3}}{2.613\times10^{-2}}\right) = 72.9^\circ$$

$$\varphi_y = 180^\circ - \cos^{-1}\left(\frac{|V_y|}{|V|}\right) = 180^\circ - \cos^{-1}\left(\frac{-8.000\times10^{-3}}{2.613\times10^{-2}}\right) = 107.8^\circ$$

$$\varphi_z = 180^\circ - \cos^{-1}\left(\frac{|V_z|}{|V|}\right) = 180^\circ - \cos^{-1}\left(\frac{-2.367\times10^{-2}}{2.613\times10^{-2}}\right) = 154.9^\circ$$

3.29c

The principal values of the permeability tensor are given by the eigenvalues of the tensor. The characteristic equation is

$$\det\begin{bmatrix} 200-\lambda & 50 & 40 \\ 50 & 150-\lambda & 30 \\ 40 & 30 & 100-\lambda \end{bmatrix}$$

$$= \lambda^3 - 450\lambda^2 + 60{,}000\lambda - 2{,}450{,}000 = 0 \qquad \textbf{(3.29.2)}$$

The solution of Eq.(3.29.2) gives

$$\lambda_1 = 82.7117 \text{ mD}$$

$$\lambda_2 = 119.5800 \text{ mD}$$

$$\lambda_3 = 247.7083 \text{ mD}$$

3.29d

The principal axes of the permeability anisotropy are given by the eigenvectors of the permeability tensor. For ?$_1$ =82.7117 mD, the homogeneous equation to be solved for the eigenvector is

$$\begin{bmatrix} 117.2883 & 50 & 40 \\ 50 & 67.2883 & 30 \\ 40 & 30 & 17.2883 \end{bmatrix} \begin{bmatrix} x \\ y \\ z \end{bmatrix} = \begin{bmatrix} 0 \\ 0 \\ 0 \end{bmatrix}$$

This gives the eigenvector associated with λ_1= 82.7117 mD as

$$\vec{u} = \begin{bmatrix} -0.2210 \\ -0.2816 \\ 1 \end{bmatrix}$$

$$|\vec{u}| = \sqrt{(-0.2210)^2 + (-0.2816)^2 + 1^2} = 1.0621$$

For λ_2 =119.5800 mD, the homogeneous equation to be solved for the eigenvector is

$$\begin{bmatrix} 80.4200 & 50 & 40 \\ 50 & 30.4200 & 30 \\ 40 & 30 & -19.5800 \end{bmatrix} \begin{bmatrix} x \\ y \\ z \end{bmatrix} = \begin{bmatrix} 0 \\ 0 \\ 0 \end{bmatrix}$$

This gives the eigenvector associated with λ_2 =119.5800 mD as

$$|\vec{v}| = \begin{bmatrix} -5.2811 \\ 7.6942 \\ 1 \end{bmatrix}$$

$$|\vec{u}| = \sqrt{(-0.2210)^2 + (-0.2816)^2 + 1^2} = 1.0621$$

$$|\vec{v}| = \sqrt{(-5.2811)^2 + (7.6942)^2 + 1^2} = 9.3857$$

For λ_3 = 247.7083 mD, the homogeneous equation to be solved for the eigenvector is

$$\begin{bmatrix} -47.7083 & 50 & 40 \\ 50 & -97.7083 & 30 \\ 40 & 30 & -147.7083 \end{bmatrix} \begin{bmatrix} x \\ y \\ z \end{bmatrix} = \begin{bmatrix} 0 \\ 0 \\ 0 \end{bmatrix}$$

This gives the eigenvector associated with $\lambda_3 = 247.7083$ mD as

$$|\vec{w}| = \begin{bmatrix} 2.5021 \\ 1.5874 \\ 1 \end{bmatrix}$$

$$|\vec{w}| = \sqrt{(2.5021)^2 + (1.5874)^2 + 1^2} = 3.1274$$

3.29e

The directional permeability in the direction of flow is given by

$$\frac{1}{k_{df}} = \frac{\cos^2 \alpha}{k_u} + \frac{\cos^2 \beta}{k_v} + \frac{\cos^2 \gamma}{k_w} \tag{2.29.1}$$

$$\cos\alpha = \frac{\vec{V}\cdot\vec{u}}{|\vec{V}||\vec{u}|}$$

$$= \frac{(7.667\times10^{-3})(-0.2210)+(-8.000\times10^{-3})(-0.2816)+(-2.367\times10^{-2})(1)}{(2.613\times10^{-2})(1.0621)}$$

$$= -0.8325$$

$$\cos\beta = \frac{\vec{V}\cdot\vec{v}}{|\vec{V}||\vec{v}|}$$

$$= \frac{(7.667\times10^{-3})(-5.2811)+(-8.000\times10^{-3})(7.6942)+(-2.367\times10^{-2})(1)}{(2.613\times10^{-2})(9.3857)}$$

$$= -0.5125$$

$$\cos\gamma = \frac{\vec{V}\cdot\vec{w}}{|\vec{V}||\vec{w}|}$$

$$= \frac{(7.667\times10^{-3})(2.5021)+(-8.000\times10^{-3})(1.5874)+(-2.367\times10^{-2})(1)}{(2.613\times10^{-2})(3.1274)}$$

$$= -0.2103$$

$$\frac{1}{k_{df}} = \frac{\cos^2\alpha}{k_u} + \frac{\cos^2\beta}{k_v} + \frac{\cos^2\gamma}{k_w}$$

$$= \frac{(-0.8325)^2}{82.7117} + \frac{(-0.5125)^2}{119.7083} + \frac{(-0.2103)^2}{247.7083} = 0.0108$$

$$k_{df} = 1/0.0108 = 93 \text{ mD}$$

PROBLEM 3.30

3.30a

The porosity of the porous medium is given by

$$\phi = \frac{A_c}{A_T} \qquad (3.30.1)$$

where A_c is cross sectional area of the porous medium occupied by all the capillary tubes and *At* is the total cross-sectional area of the porous medium. The cross-sectional area of a typical capillary tube is given by

$$A_i = \frac{\pi\delta_i^2}{4} \qquad (3.30.2)$$

There are five capillary tubes with diameters δ_1, δ_2, δ_3, δ_4, and δ_5. From the given data, $\delta_2 = \delta_3 = \delta_4 = \delta_5$. Thus the cross-sectional areas of the capillary tubes are given by

$$A_1 = \frac{\pi\delta_1^2}{4} \qquad (3.30.3)$$

$$A_2 = A_3 = A_4 = A_5 = \frac{\pi\delta_2^2}{4} \qquad (3.30.4)$$

The cross-sectional area occupied by the all the capillary tubes is given by

$$A_c = A_1 + A_2 + A_3 + A_4 + A_5 = \frac{\pi\delta_1^2}{4} + 4\left(\frac{\pi\delta_2^2}{4}\right) \quad (3.30.5)$$

The total cross-sectional area of the porous medium is given by

$$A_T = \frac{\pi\delta_T^2}{4} \quad (3.30.6)$$

where $?_T$ is the diameter of the porous medium. Substituting Eqs.(3.30.5) and (3.30.6) into (3.30.1) gives

$$\phi = \frac{\delta_1^2 + 4\delta_2^2}{\delta_T^2} \quad (3.30.7)$$

Substituting numerical values into Eq. (3.30.7) gives

$$\phi = \frac{\delta_1^2 + 4\delta_2^2}{\delta_T^2} = \frac{6^2 + (4 \times 3^2)}{50^2} = 0.0288$$

3.30b

Darcy's law applied to the porous medium gives

$$q_T = \frac{kA_T}{\mu} \frac{\Delta P}{L} \tag{3.30.8}$$

Eq.(3.30.8) can be solved for the permeability as

$$k = \frac{q_T \mu L}{A_T \Delta P} \tag{3.30.9}$$

Hagen-Poiseuillie's law for a typical capillary tube is

$$q_i = \frac{\pi \delta_i^4}{128\mu} \frac{\Delta P}{L} \quad (3.30.10)$$

The contribution to flow by each capillary tube is given by

$$q_1 = \frac{\pi \delta_1^4}{128\mu} \frac{\Delta P}{L} \quad (3.30.11)$$

$$q_2 = q_3 = q_4 = q_5 = \frac{\pi \delta_2^4}{128\mu} \frac{\Delta P}{L} \quad (3.30.12)$$

The total flow rate is given by

$$q_T = q_1 + q_2 + q_3 + q_4 + q_5 = \frac{\pi \left(\delta_1^4 + 4\delta_2^4 \right)}{128\mu} \frac{\Delta P}{L} \quad (3.30.13)$$

Substituting Eqs.(3.30.6) and (3.30.13)

into (3.30.9) gives the permeability of the porous medium as

$$k = \frac{1}{32}\left(\frac{\delta_1^4 + 4\delta_2^4}{\delta_T^2}\right) \quad (3.30.14)$$

Substituting numerical values for the capillary tube diameters in cm into Eq. (3.30.14) gives the permeability as

$$k = \frac{1}{32}\left[\frac{(0.6)^4 + 4\times(0.3)^4}{5^2}\right]$$

$$= 2.025\times10^{-4}\ \text{cm}^2 = 2.025\times10^{-4} / 9.869\times10^{-9} = 2.052\times10^{4}\ \text{D}$$

3.30c

The specific surface area is given by

$$S = \frac{A_s}{V_b} \quad (3.30.15)$$

where A_s is the surface area of all the capillary tubes and Vb is the bulk volume of the porous medium. The surface area of a typical capillary tube is given by

$$A_{si} = \pi\delta_i L \qquad (3.30.16)$$

where L is the length of the porous medium. The surface area of each capillary tube is given by

$$A_{s1} = \pi\delta_1 L \qquad (3.30.17)$$

$$A_{s2} = A_{s3} = A_{s4} = A_{s5} = \pi\delta_2 L \qquad (3.31.18)$$

The total surface area of all the capillary tubes is given by

$$A_s = A_{s1} + A_{s2} + A_{s3} + A_{s4} + A_{s5} = \pi\left(\delta_1 + 4\delta_2\right)L \qquad (3.30.19)$$

The bulk volume of the porous medium is given by

$$V_b = \frac{\pi \delta_T^2 L}{4} \qquad (3.30.20)$$

Substituting Eqs.(3.30.19) and (3.30.20) into (3.30.15) gives the specific surface area as

$$S = \frac{4\left(\delta_1 + 4\delta_2\right)}{\delta_T^2} \qquad (3.30.21)$$

Substituting numerical values into Eq. (3.30.21) gives the specific surface area as

$$S = \frac{4(0.60 + 4 \times 0.30)}{5^2} = 0.288\ \text{cm}^2/\text{cm}^3$$

PROBLEM 3.31

3.31a

The porosity of the porous medium is given by

$$\phi = \frac{A_c}{A_T} = 0.20$$

3.31b

Eq.(3.153) in the textbook gives the equation for calculating the permeability of a porous medium from the probability density function of the pore throat size distribution as

$$k = \frac{\phi}{32\tau}\left[\frac{\int_0^\infty f(\delta)\delta^4\,d\delta}{\int_0^\infty f(\delta)\delta^2\,d\delta}\right] \quad (3.31.1)$$

For the triangular probability density function,

$$f(\delta) = \begin{cases} \dfrac{\delta}{75}, & 0 \le \delta \le 10\ \mu\text{m} \\ \dfrac{30-2\delta}{75}, & 10 \le \delta \le 15\ \mu\text{m} \end{cases} \quad (3.31.2)$$

Now

$$\int_0^{15} f(\delta)\delta^4 d\delta = \int_0^{10} f(\delta)\delta^4 d\delta + \int_{10}^{15} f(\delta)\delta^4 d\delta$$

$$= \int_0^{10}\left(\frac{\delta}{75}\right)\delta^4 d\delta + \int_{10}^{15}\left(\frac{30-2\delta}{75}\right)\delta^4 d\delta$$

$$= \frac{1}{75}\left[\frac{\delta^6}{6}\right]_0^{10} + \frac{30}{75}\left[\frac{\delta^5}{5}\right]_{10}^{15} - \frac{2}{75}\left[\frac{\delta^6}{6}\right]_{10}^{15} \quad \textbf{(3.31.3)}$$

$$= 2222.22 + 52750 - 46180.56$$

$$= 8791.66\ \mu\text{m}^2$$

$$\int_0^{15} f(\delta)\delta^2 d\delta = \int_0^{10} f(\delta)\delta^2 d\delta + \int_{10}^{15} f(\delta)\delta^2 d\delta$$

$$= \int_0^{10}\left(\frac{\delta}{75}\right)\delta^2 d\delta + \int_{10}^{15}\left(\frac{30-2\delta}{75}\right)\delta^2 d\delta$$

$$= \frac{1}{75}\left[\frac{\delta^4}{4}\right]_0^{10} + \frac{30}{75}\left[\frac{\delta^3}{3}\right]_{10}^{15} - \frac{2}{75}\left[\frac{\delta^4}{4}\right]_{10}^{15} \quad \textbf{(3.31.4)}$$

$$= 33.33 + 316.67 - 270.833$$

$$= 79.167\ \mu\text{m}^2$$

Substituting Eqs.(3.32.3) and (3.31.4) into (3.31.1) gives

$$k = \frac{(0.20)(8791.66)}{(32)(76.167)}$$

$$= 0.694\ \mu\text{m}^2 = 6.94 \times 10^{-13}\ \text{m}^2 = 6.94 \times 10^{-13} / 9.869 \times 10^{-13}$$

$$= 0.7032\ \text{D}$$

PROBLEM 3.32

Eq.(3.153) in the textbook gives the equation for calculating the absolute permeability of a porous medium from the probability density function of the pore throat size distribution as

$$k = \frac{\phi}{32\tau}\left[\frac{\int_0^\infty f(\delta)\delta^4\,d\delta}{\int_0^\infty f(\delta)\delta^2\,d\delta}\right] \quad (3.32.1)$$

Eq.(3.154) in Example 3.4 in the textbook shows how this equation can be used to calculate the permeability in the case of a triangular probability density function. This worked example can easily be adapted to solve the problem at hand. For the right triangular probability density function,

$$\delta_3 = \delta_2$$
$$\delta_1 = 0$$

$$f(\delta) = f_1(\delta) = \frac{2\delta}{\delta_2^2} \tag{3.32.2}$$

Substituting Eq.(3.32.2) into (3.32.1) and simplifying gives the permeability as

$$k = \frac{\phi}{32\tau}\left[\frac{\int_0^{\delta_2} \delta^5\, d\delta}{\int_0^{\delta_2} \delta^3\, d\delta}\right] \tag{3.32.3}$$

Performing the integrations in Eq.

(3.32.3) and simplifying gives

$$k = \frac{\phi}{32\tau} \frac{\left[\frac{1}{6}\delta^6\right]_0^{\delta_2}}{\left[\frac{1}{4}\delta^4\right]_0^{\delta_2}} = \frac{\phi\delta_2^2}{48\tau} \quad (3.32.4)$$

For this problem,

$\varnothing = 0.05$
$\tau = l$ because the capillary tubes are straight.
$\delta_2 = 8\times10^{-6}\text{m}$

Substituting the numerical values into Eq.(3.32.4) gives the permeability as

$$k = \frac{(0.05)(8\times10^{-6})^2}{(48)(1)} = 6.667\times10^{-14}\ \text{m}^2 = \frac{6.667\times10^{-14}}{9.869\times10^{-13}} = 0.0676\ \text{D}$$

The function $f_1(?)$ also can be derived as follows.

$$f_1(\delta) = m\delta \qquad (3.32.5)$$

where m is the slope of the line.

$$m = \frac{h}{\delta_2} \qquad (3.32.6)$$

where h is the height of the right triangle at $\delta = \delta_2$. Because the area of the triangle is 1.0 since $f(\delta)$ is a probability density function,

$$\frac{1}{2}h\delta_2 = 1 \tag{3.32.7}$$

$$h = \frac{2}{\delta_2} \tag{3.32.8}$$

$$m = \frac{2}{\delta_2^2} \tag{3.32.9}$$

$$f_1(\delta) = \frac{2\delta}{\delta_2^2} \tag{3.32.10}$$

PROBLEM 3.33

3.33a

Given

$$\Delta P = f\left(\pi, \mu, r, r_1, r_2, L_c, k\right) \quad (3.33.1)$$

$$G_1 = \pi \quad (3.33.2)$$

The dimensional matrix can be derived by inspection and shown in **TABLE 3.33.1**.

TABLE 3.33.1 Dimensional Matrix

	μ	q	r_1	r_2	L_c	k	ΔP
	x_1	x_2	x_3	x_4	x_5	x_6	x_7
M	1	0	0	0	0	0	1
L	-1	3	1	1	1	2	-1
T	-1	-1	0	0	0	0	-2

3.33b

The determinant of the following 3×3 submatrix is

$$\det\begin{vmatrix} 1 & 0 & 0 \\ -1 & 3 & 1 \\ -1 & -1 & 0 \end{vmatrix} = 1 \neq 0$$

Thus, the rank of the dimensional matrix is 3. The number of independent dimensionless groups is 7–3 = 4.

3.33c

The homogeneous linear equations can be solved by row operations as follows.

$$\begin{array}{l} \text{row1} \\ \text{row2} \\ \text{row3} \end{array} \begin{bmatrix} 1 & 0 & 0 & 0 & 0 & 0 & 1 \\ -1 & 3 & 1 & 1 & 1 & 2 & -1 \\ -1 & -1 & 0 & 0 & 0 & 0 & -2 \end{bmatrix}$$

$$\begin{array}{l} \\ \text{row1} + \text{row2} \\ \text{row2} - \text{row3} \end{array} \begin{bmatrix} 1 & 0 & 0 & 0 & 0 & 0 & 1 \\ 0 & 3 & 1 & 1 & 1 & 2 & 0 \\ 0 & 4 & 1 & 1 & 1 & 2 & 1 \end{bmatrix}$$

$$\begin{array}{l} \\ \text{row3} - \text{row2} \\ 4\text{row2} - 3\text{row3} \end{array} \begin{bmatrix} 1 & 0 & 0 & 0 & 0 & 0 & 1 \\ 0 & 1 & 0 & 0 & 0 & 0 & 1 \\ 0 & 0 & 1 & 1 & 1 & 2 & -3 \end{bmatrix}$$

The solution is

$$
\begin{aligned}
x_1 &= -x_7 \\
x_2 &= -x_7 \\
x_3 &= -x_4 - x_5 - 2x_6 + 3x_7 \\
x_4 &= x_4 \\
x_5 &= x_5 \\
x_6 &= x_6 \\
x_7 &= x_7
\end{aligned}
\tag{3.33.3}
$$

Eq.(3.33.3) can be written as

$$
\begin{pmatrix} \mu \\ q \\ r_1 \\ r_2 \\ L_c \\ k \\ \Delta P \end{pmatrix}
\begin{pmatrix} x_1 \\ x_2 \\ x_3 \\ x_4 \\ x_5 \\ x_6 \\ x_7 \end{pmatrix}
=
\begin{pmatrix} 0 \\ 0 \\ -1 \\ 1 \\ 0 \\ 0 \\ 0 \end{pmatrix} x_4 +
\begin{pmatrix} 0 \\ 0 \\ -1 \\ 0 \\ 1 \\ 0 \\ 0 \end{pmatrix} x_5 +
\begin{pmatrix} 0 \\ 0 \\ -2 \\ 0 \\ 0 \\ 1 \\ 0 \end{pmatrix} x_6 +
\begin{pmatrix} -1 \\ -1 \\ 3 \\ 0 \\ 0 \\ 0 \\ 1 \end{pmatrix} x_7
\tag{3.33.4}
$$

3.33d

The dimensionless groups can be derived from Eq.(3.33.4) by inspection to obtain

$$G_2 = \frac{r_2}{r_1} \qquad (3.33.5)$$

$$G_3 = \frac{L}{r_1} \qquad (3.33.6)$$

$$G_4 = \frac{k}{r_1^2} \qquad (3.33.7)$$

$$G_5 = \frac{r_1^3 \Delta P}{q\mu} \qquad (3.33.8)$$

3.33e

From Darcy's law,

$$\Delta P = \frac{q\mu L_c}{\pi k r_1 r_2} \tag{3.33.9}$$

Eq.(3.33.9) can be derived from the dimensional analysis as

$$G_5 = \frac{G_3}{G_2 G_2 G_4} \tag{3.33.10}$$

PROBLEM 3.34

Let *Vb* be the bulk volume.

Before acidization,

$$\phi_o = 0.26$$
$$k_o = 100 \text{ mD}$$
$$V_s = (1-\phi)V_b = (1-0.26)V_b = 0.74V_b$$

The volume of the solid is distributed among the minerals as follows:

Calcium carbonate = (0.05) $(0.74V_b) = 0.0370V_b$

Orthoclase feldspar = (0.04) $(0.74V_b) = 0.0296_b$

Kaolinite (clay) = $(0.09)(0.74V_b) =$

$0.0666V_b$

Quartz = $(0.82)(0.74V_b) = 0.6068V_b$

After acidization, the new solid volume is distributed among the minerals as follows:

Calcium carbonate=0

Orthoclase feldspar = $(1 - 0.45)(0.0296V_b) = 0.0163V_b$

Kaolinite (clay) = $(1 - 0.78)(0.0666V_b) = 0.0147V_b$

Quartz = $(1 - 0.07)(0.6068V_b) = 0.5643V_b$

$V_s = (0+0.0163 + 0.0147+0.5643)V_b = 0.5953V_b =(1-0.4047)\ V_b$

? = 0.4047

$$\frac{k}{100} = \left(\frac{0.4047}{0.26}\right)^3 = 3.7724$$

$$k = 377 \text{ mD}$$

PROBLEM 3.35

3.35a

FIGURE 3.35.1 shows a sketch of the flow arrangement.

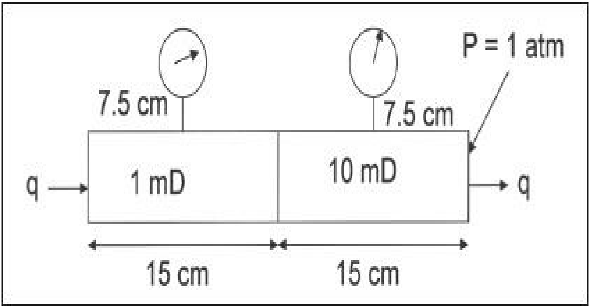

FIGURE 3.35.1 Single-phase steady state flow experiment in a composite core.

3.35b

Darcy's law gives

$$q=-\frac{kA}{\mu}\frac{dP}{dx} \tag{3.35.1}$$

$$\frac{dP}{dx}=-\frac{q\mu}{kA} \tag{3.35.2}$$

Integration of Eq.(3.35.2) for the 10 mD core gives

$$P=-\frac{q\mu}{kA}x+C_1 \tag{3.35.3}$$

where C_1 is an integration constant. Application of the boundary condition at the end of the 10 mD core gives

$$1 = -\frac{q\mu}{kA}(15) + C_1 \tag{3.35.4}$$

$$C_1 = 1 + \frac{q\mu}{kA}(15) \tag{3.35.5}$$

Substituting Eq.(3.35.5) into (3.35.3) gives

$$P(x) = 1 + \frac{q\mu}{kA}(15 - x) \tag{3.35.6}$$

Given:

$$k = 10 \text{ mD} = 0.010 \text{ D}$$
$$A = 20 \text{ cm}^2$$
$$q = 5 \text{ cm}^3/\text{hr} = \left(\frac{5}{3600}\right) \text{cm}^3/\text{s}$$
$$\mu = 1 \text{ cp}$$

Substituting numerical values into Eq. (3.35.6) gives

$$P(x)=1+\frac{(5/3600)(1)}{(0.010)(20)}(15-x)=1+6.944\times10^{-3}(15-x)L \tag{3.35.6}$$

At x = 7.5 cm,

$$P(7.5)=1+6.944\times10^{-3}(15-7.5)=1.0521\text{ atm}$$

$$P(7.5)_{gauge}=0.0521\text{ atm}$$

At x = 0, the pressure at the junction of the two cores is given by

$$P(0)=1+6.944\times10^{-3}(15-0)=1.1042\text{ atm}$$

Application of Darcy's law to the 1 mD

core and integration gives

$$P=-\frac{q\mu}{kA}x+C_2 \qquad (3.35.7)$$

where C_2 is an integration constant. Application of the boundary condition at the end of the 1 mD core gives

$$1.1042=-\frac{q\mu}{kA}(15)+C_2 \qquad (3.35.8)$$

$$C_2=1.1042+\frac{q\mu}{kA}(15) \qquad (3.35.9)$$

Substituting Eq.(3.36.9) into (3.35.7) gives **(3.35.10)**

$$P(x)=1.1042+\frac{q\mu}{kA}(15-x) \qquad (3.35.10)$$

$$k = 1 \text{ mD} = 0.001 \text{ D}$$

Substituting numerical values into Eq. (3.35.10) gives

$$P(x) = 1 + \frac{(5/3600)(1)}{(0.001)(20)}(15 - x) = 1 + 6.944 \times 10^{-2}(15 - x) \tag{3.35.11}$$

At x = 7.5 cm,

$$P(7.5) = 1.1042 + 6.944 \times 10^{-2}(15 - 7.5) = 1.6250 \text{ atm}$$

$$P(7.5)_{gauge} = 0.6250 \text{ atm}$$

PROBLEM 3.36

3.36a

The transformation equations are as follows:

$$k^{*} = \sqrt{k_x k_y} = \sqrt{20 \times 5} = 10 \text{ mD}$$

$$X = x\sqrt{\frac{k^{*}}{k_x}} = x\sqrt{\frac{10}{20}} = \frac{x}{\sqrt{2}}$$

$$L_x^{*} = \frac{L_x}{\sqrt{2}} = \frac{2000}{\sqrt{2}} = 1414.2 \text{ ft}$$

$$L_f^* = \frac{L_f}{\sqrt{2}} = \frac{100}{\sqrt{2}} = 70.7 \text{ ft}$$

$$Y = y\sqrt{\frac{k^*}{k_x}} = y\sqrt{\frac{10}{5}} = y\sqrt{2}$$

$$L_y^* = L_y\sqrt{2} = 2000\sqrt{2} = 2828.4 \text{ ft}$$

3.36b

The transformed 5-spot pattern is shown in **FIGURE 3.36.1**.

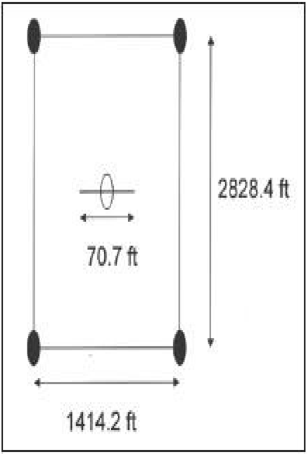

FIGURE 3.36.1 Plan view of transformed 5-spot waterflood pattern.

3.36c

The circular wells are transformed into ellipses as

$$\frac{X^2}{\left(r_w\sqrt{\frac{k^*}{k_x}}\right)^2}+\frac{Y^2}{\left(r_w\sqrt{\frac{k^*}{k_y}}\right)^2}=1 \quad (3.36.1)$$

Substituting numerical values into Eq. (3.36.1) gives

$$\frac{X^2}{(0.18)^2}+\frac{Y^2}{(0.35)^2}=1$$

PROBLEM 3.37

3.37 a and b

In general, pereability is proportional to the square of the pore size.

$k_A > k_B$ because B has smaller pore size than A due to tighter packing.

$k_A > k_c$ because C has smaller pore size than A due to smaller grain size.

$k_A > k_D$ because D has smaller pore size than A due to poor sorting.

$k_A > k_E$ because E has smaller pore size than A due to very poor sorting.

$k_A > k_p$ because F has smaller pore size than A due to compaction.

CHAPTER 4 SOLUTIONS

PROBLEM 4.1

4.1a

FIGURE 4.1.1 shows the graphs of permeability, porosity, and water saturation plotted as logs. The increase in water saturation with a decrease in permeability can easily be observed.

4.1b

FIGURES 4.1.2 and 4.1.3 show the histograms of permeability and porosity. The permeability distribution is highly skewed with most of the data concentrated at low values of permeability. This observation is consistent with the fact that permeability tends to be log-normally distributed. The porosity data are more evenly distributed than the permeability data although there is a tendency toward high porosities in this case.

4.1c

FIGURE 4.1.4 shows the histogram of natural log of permeability. The distribution is more symmetric than that of permeability confirming the log-normal nature of the permeability distribution.

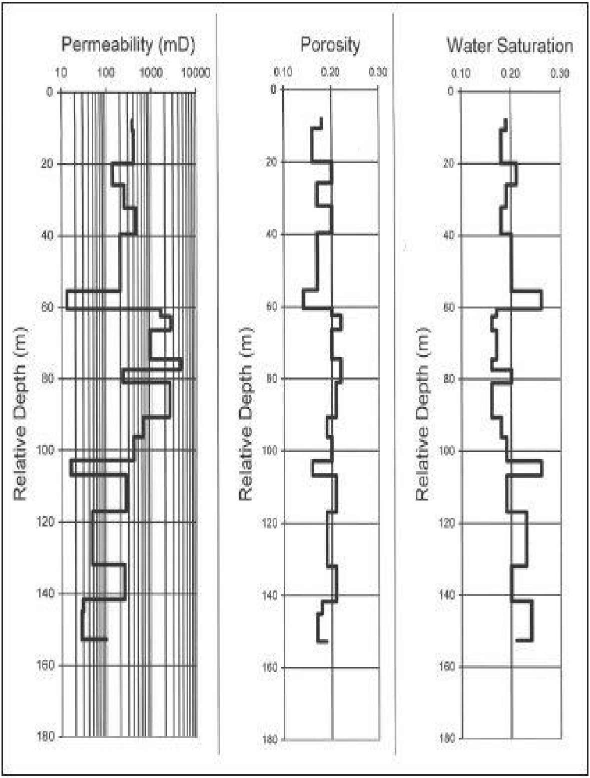

FIGURE 4.1.1 Graphs of permeability, porosity, and water saturation versus depth.

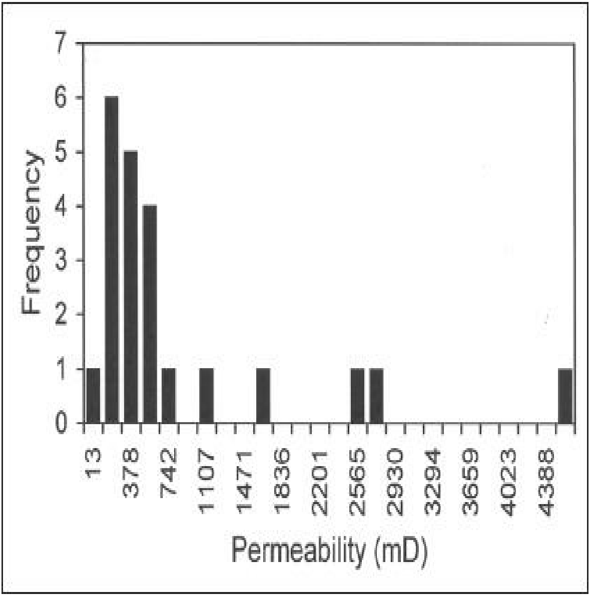

FIGURE 4.1.2 Permeability histogram.

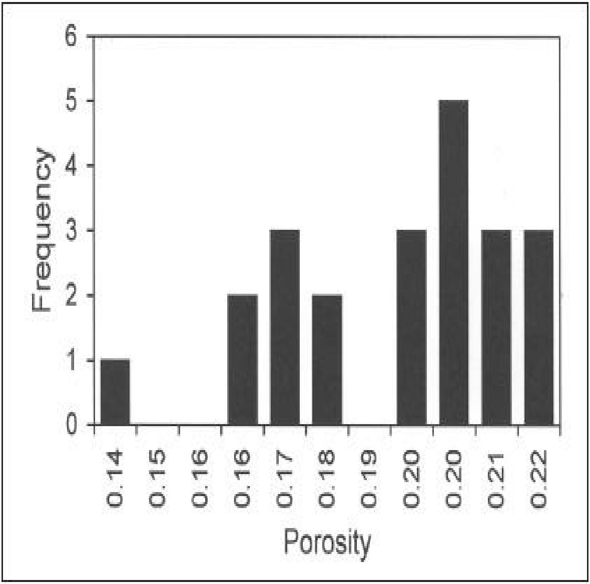

FIGURE 4.1.3 Porosity histogram.

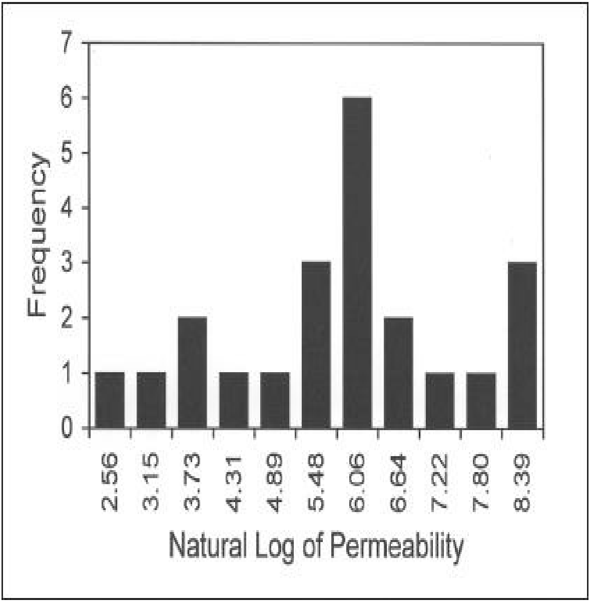

4.1d

Figure 4.1.5 shows the scatter plot of the natural log of permeability versus porosity. The correlation coefficient for the scatter plot can be calculated as follows.

$$\overline{\phi} = \frac{\sum \phi_i}{N} = 0.1905$$

$$\sum\left(\phi_i - \overline{\phi}\right)^2 = 0.0101$$

$$s_\phi = \sqrt{\frac{\sum\left(\phi_i - \overline{\phi}\right)^2}{N-1}} = 0.0219$$

$$\ln \overline{k} = \frac{\sum \ln k_i}{N} = 5.5275$$

$$\sum\left(\ln k_i - \ln \overline{k}\right)^2 = 55.8443$$

$$s_{\ln k} = \sqrt{\frac{\sum\left(\ln k_i - \ln \overline{k}\right)^2}{N-1}} = 1.6307$$

$$\sum\left(\phi_i - \overline{\phi}\right)\left(\ln k_i - \ln \overline{k}\right) = 0.5194$$

$$C(\ln k, \phi) = \frac{\sum\left(\phi_i - \overline{\phi}\right)\left(\ln k_i - \ln \overline{k}\right)}{N-1} = 0.0247$$

$$\rho(\ln k, \phi) = \frac{C(\ln k, \phi)}{s_\phi s_{\ln k}} = 0.6917$$

$$R^2 = \rho^2 = 0.4785$$

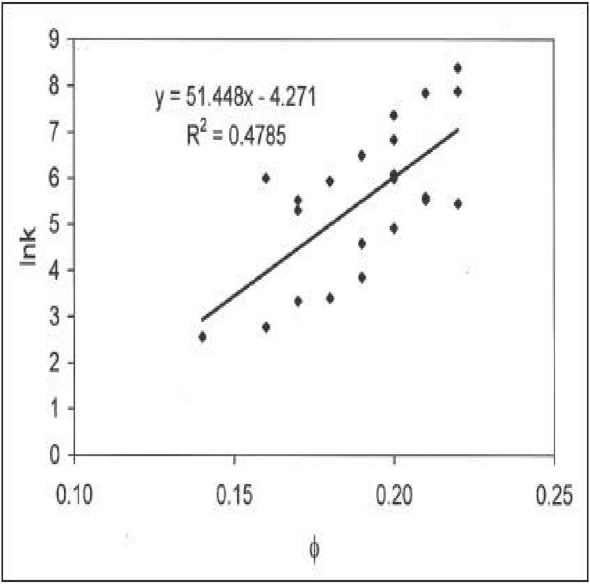

FIGURE 4.1.5 Scatter plot of permeability versus porosity.

The correlation coefficient of 0.6917 indicates a strong linear relationship between the natural log of permeability and the porosity.

4.1e

FIGURE 4.1.6 shows the graph for determining the Dykstra-Parsons coefficient of permeability variation. From the regression line,

$$\bar{k} = 251.52 \text{ mD}$$

$$k_{84.1} = 251.52e^{-1.7926} = 41.88 \text{ mD}$$

$$V = \frac{\bar{k} - k_{84.1}}{\bar{k}} = \frac{251.52 - 41.88}{251.52} = 0.83$$

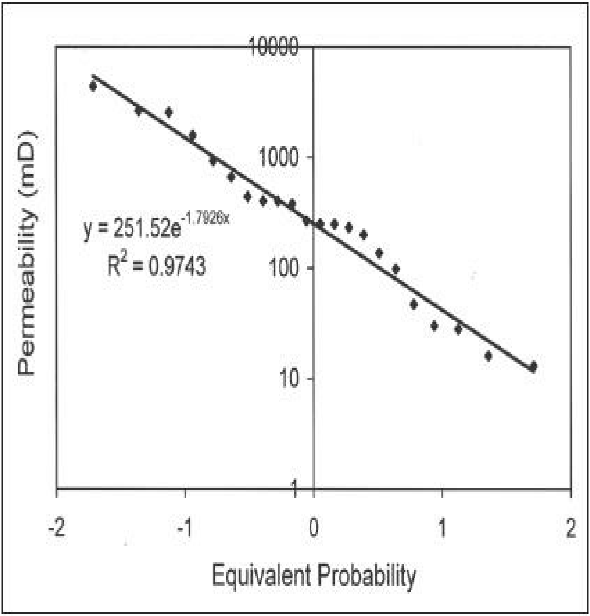

FIGURE 4.1.6 Graph for determination of Dykstra-Parsons coefficient of permeability variation.

4.1f

FIGURE 4.1.7 shows the graph for determining the Lorenz coefficient of variation. The area under the curve can be obtained by integrating the polynomial curve fit to the data to obtain

$$Area = 0.8382$$

$$Lorenz\ Coefficient = \frac{Area - 0.50}{Area} = \frac{0.8382 - 0.50}{0.50} = 0.68$$

Both the Dykstra-Parson's coefficient of variation and the Lorenz coefficient indicate a high degree of heterogeneity. However, there is no numerical relationship between the two measures of heterogeneity.

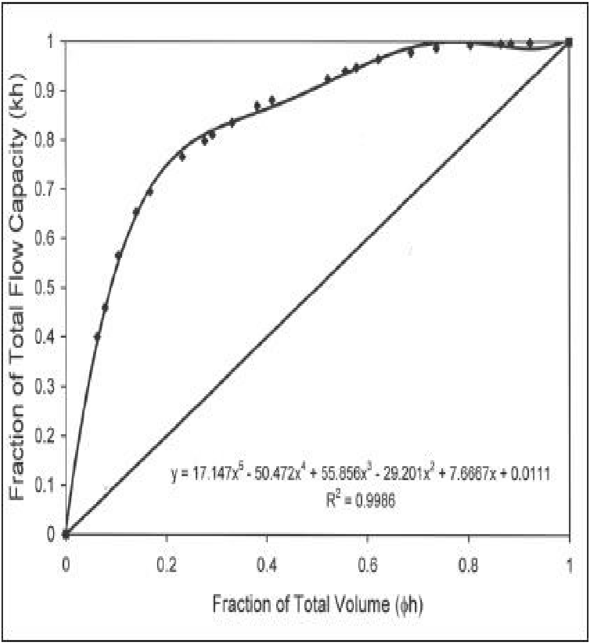

FIGURE 4.1.7 Graph for determination of Lorenz coefficient of variation.

4.1g

FIGURE 4.1.8 shows the scatter plot for determining the variogram for nonuniformly distributed data obtained using the algorithm outlined in the textbook. The experimental variogram shown in the FIGURE was obtained with a bin size of 10 meters.

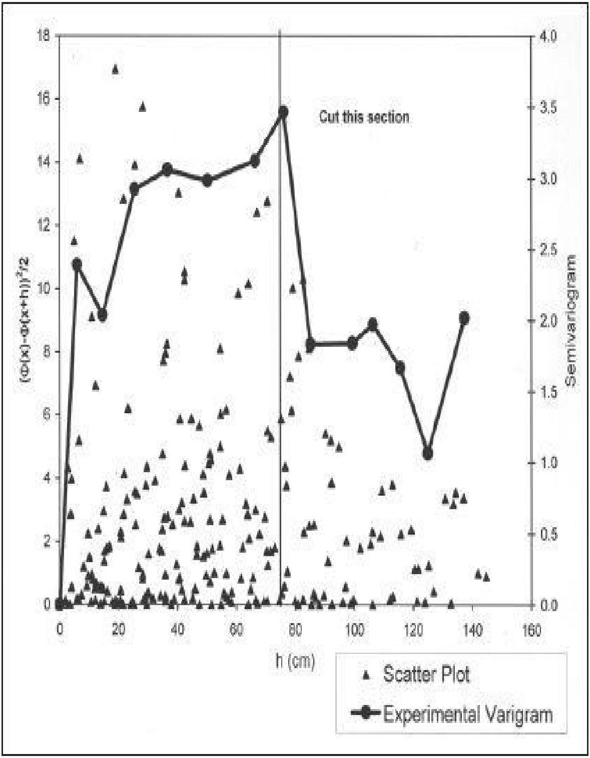

FIGURE 4.1.8 Scatter plot for determination of experimental variogram for nonuniformly distributed data.

4.1h

FIGURE 4.1.9 shows a satisfactory fit of the following exponential model to the experimental variogram:

$$\gamma(h) = 3\left(1 - e^{-\frac{h}{5}}\right)$$

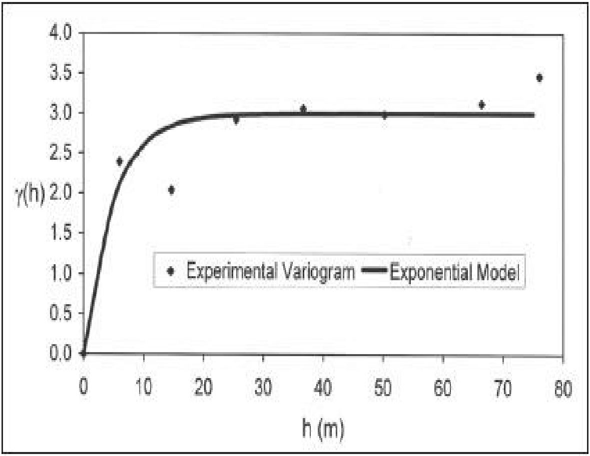

FIGURE 4.1.9 Theoretical variogram fit.

4.1i

FIGURE 4.1.10 shows the scatter plot for determining the covariance function for nonuniformly distributed data obtained using the algorithm outlined in the textbook. The experimental covariance function shown in the FIGURE was obtained with a bin size of 10 meters.

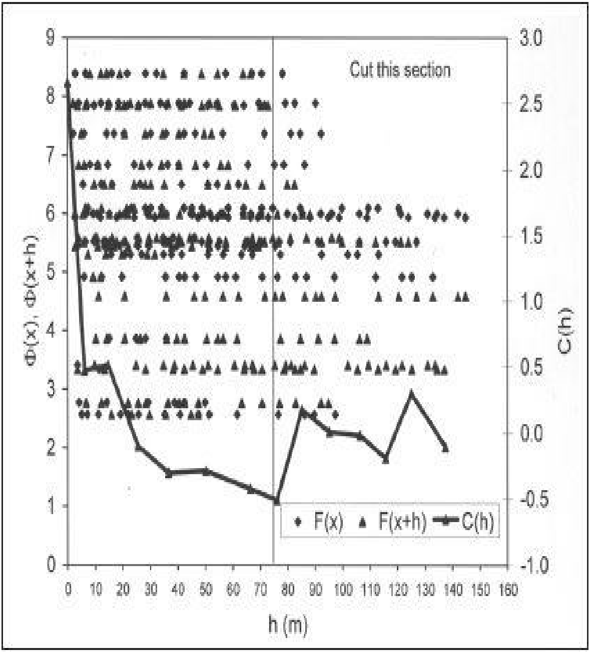

FIGURE 4.1.10 Scatter plot for determination of experimental covariance function for nonuniformly distributed data.

4.1j

FIGURE 4.1.11 shows the correlation coefficient function, which is a dimensionless version of the covariance function.

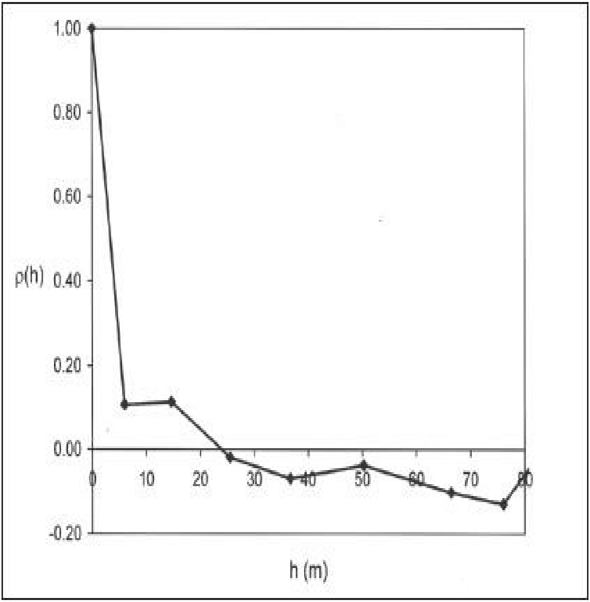

FIGURE 4.1.11 Experimental correlation coefficient function.

problem 4.2

4.2a

FIGURE 4.2.1 shows the graphs of permeability, porosity, and water saturation plotted as logs. The permeability, porosity, and water saturation are fairly uniform except at the bottom. It may expected that the various indicators of heterogeneity (Dykstra-Parsons coefficient, Lorenz coefficient, the magnitude of the sill of the variogram) for this reservoir show be lower than for the reservoir of Problem 4.1.

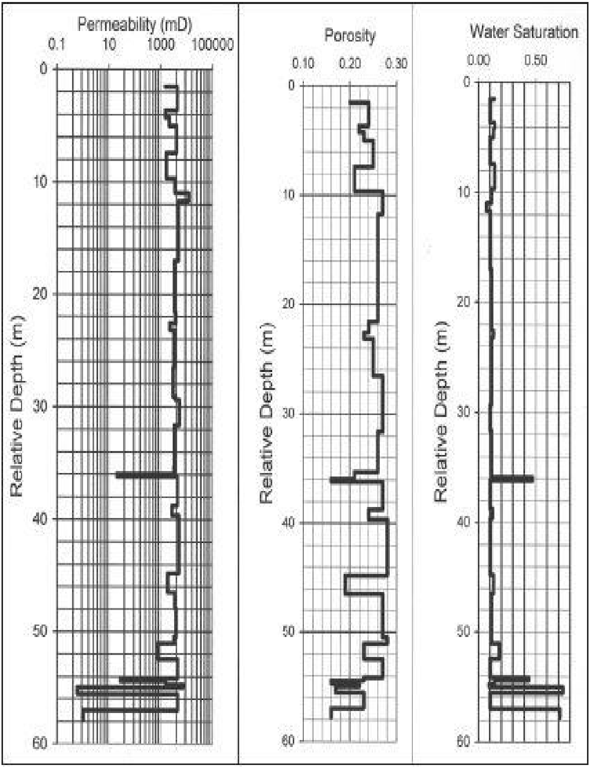

FIGURE 4.2.1 Graphs of permeability, porosity, and water saturation versus depth.

4.2b

figures 4.2.2 and 4.2.3 show the histograms of permeability and porosity. The permeability distribution is highly skewed with most of the data concentrated at low values of permeability. This observation is consistent with the fact that permeability tends to be log-normally distributed. The porosity data are more evenly distributed than the permeability data although there is a tendency toward high porosities in this case.

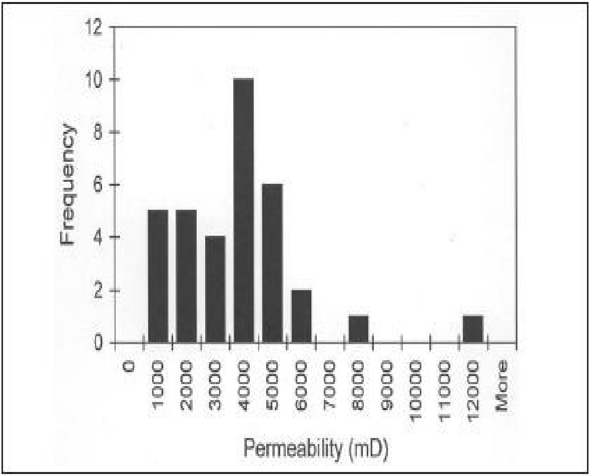

FIGURE 4.2.2 Permeability histogram.

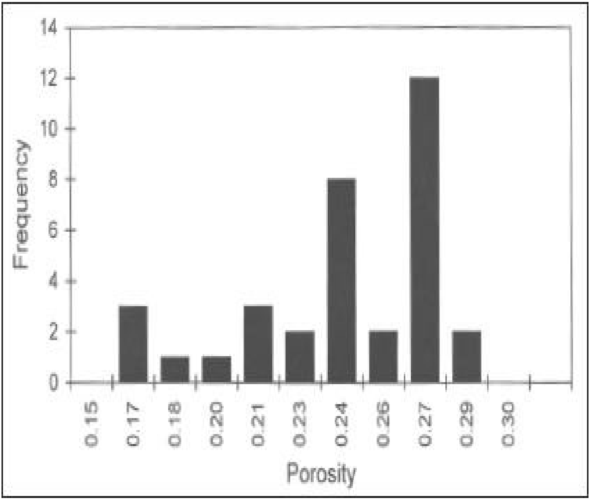

FIGURE 4.2.3 Porosity histogram.

4.2c

FIGURE 4.2.4 shows the histogram of natural log of permeability. The distribution is more symmetric than that of permeability confirming the log-normal nature of the permeability distribution.

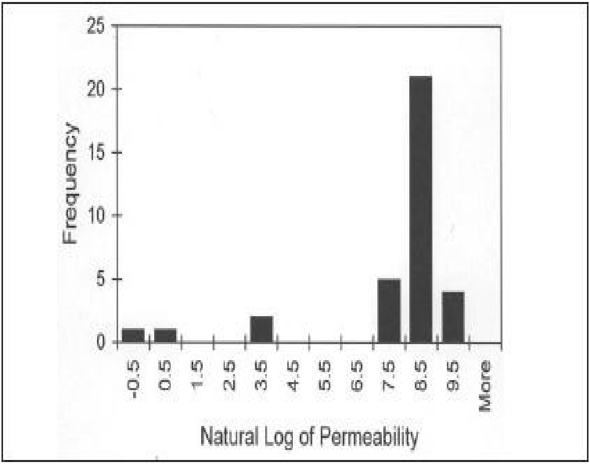

FIGURE 4.2.4 Histogram of natural log of permeability.

4.2d

FIGURE 4.2.5 shows the scatter plot of the natural log of permeability versus porosity. The correlation coefficient for the scatter plot can be calculated as follows.

$$\overline{\phi}=\frac{\sum \phi_i}{N}=0.2365$$

$$\sum\left(\phi_i-\overline{\phi}\right)^2=0.0436$$

$$s_\phi=\sqrt{\frac{\sum\left(\phi_i-\overline{\phi}\right)^2}{N-1}}=0.0363$$

$$\ln\overline{k}=\frac{\sum \ln k_i}{N}=7.3011$$

$$\sum\left(\ln k_i-\ln\overline{k}\right)^2=175.0354$$

$$s_{\ln k}=\sqrt{\frac{\sum\left(\ln k_i-\ln\overline{k}\right)^2}{N-1}}=2.3031$$

$$\sum\left(\phi_i-\overline{\phi}\right)\left(\ln k_i-\ln\overline{k}\right)=1.8760$$

$$C(\ln k,\phi)=\frac{\sum\left(\phi_i-\overline{\phi}\right)\left(\ln k_i-\ln\overline{k}\right)}{N-1}=0.0568$$

$$\rho(\ln k,\phi)=\frac{C(\ln k,\phi)}{s_\phi s_{\ln k}}=0.6793$$

$$R^2=\rho^2=0.4614$$

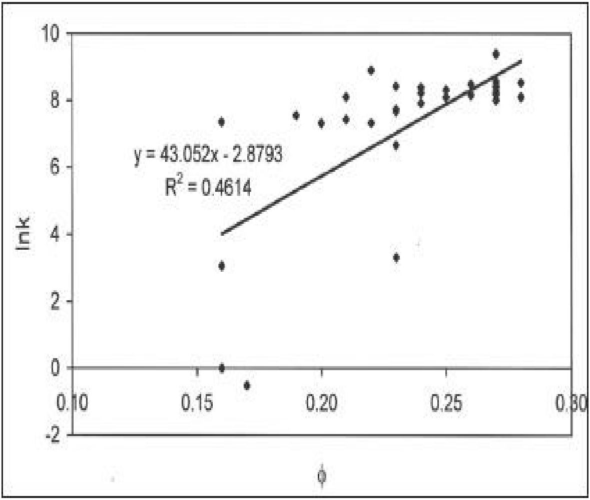

FIGURE 4.2.5 Scatter plot of permeability versus porosity.

The correlation coefficient of 0.4614 indicates a strong linear relationship between the natural log of permeability and the porosity.

4.2e

FIGURE 4.2.6 shows the graph for determining the Dykstra-Parsons coefficient of permeability variation. From the regression line,

$$\bar{k} = 3230.25 \text{ mD}$$

$$k_{84.1} = 3230.2e^{-0.5630} = 1839.62 \text{ mD}$$

$$V = \frac{\bar{k} - k_{84.1}}{\bar{k}} = \frac{3230.25 - 1839.62}{3230.25} = 0.43$$

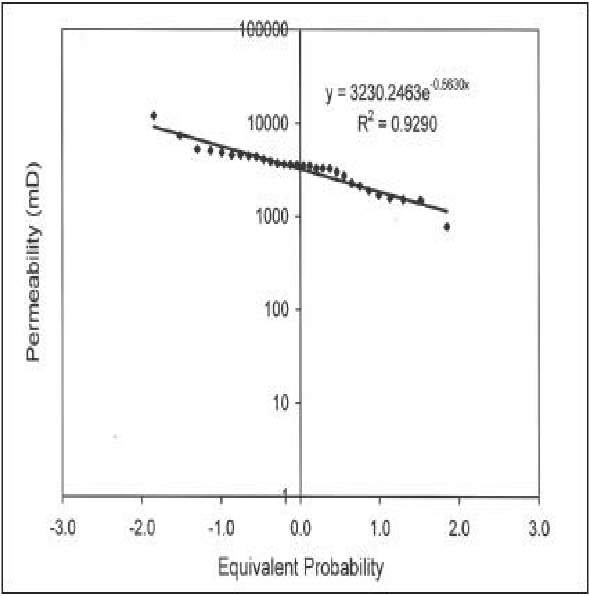

FIGURE 4.2.6 Graph for determination of Dykstra-Parsons coefficient of permeability variation.

4.2f

FIGURE 4.2.7 shows the graph for determining the Lorenz coefficient of variation. The area under the curve can be obtained by integrating the polynomial curve fit to the data to obtain

$$Area = 0.8382$$

$$Lorenz\ Coefficient = \frac{Area - 0.50}{Area} = \frac{0.5921 - 0.50}{0.50} = 0.18$$

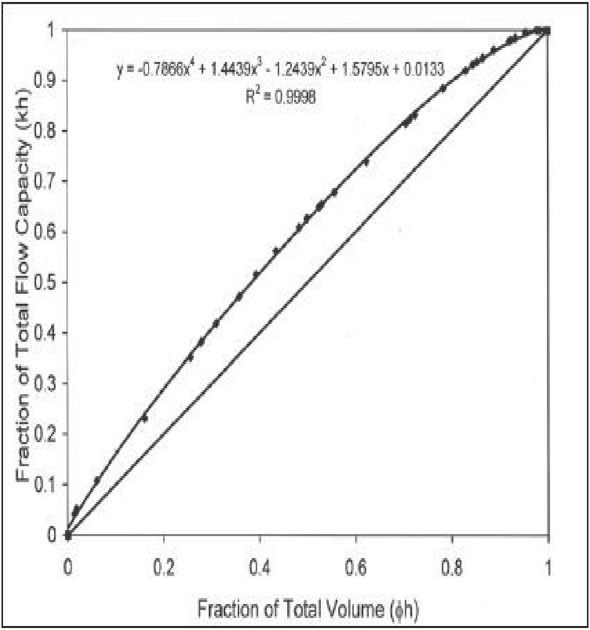

FIGURE 4.2.7 Graph for determination of Lorenz coefficient of variation.

Both the Dykstra-Parson's coefficient of variation and the Lorenz coefficient indicated a low degree of heterogeneity. However, there is no numerical relationship between the two measures of heterogeneity.

4.2g

FIGURE 4.2.8 shows the scatter plot for determining the variogram for nonuniformly distributed data obtained using the algorithm outlined in the textbook. The experimental variogram shown in the FIGURE was obtained with a bin size of 10 meters.

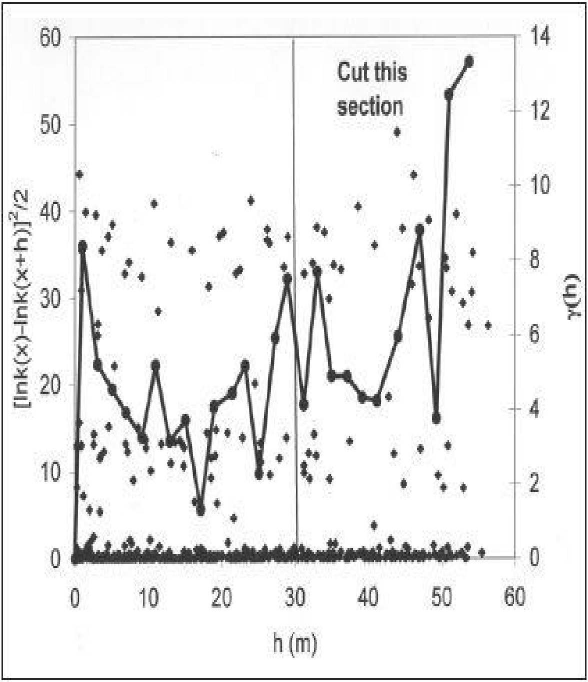

FIGURE 4.2.8 Scatter plot for determination of experimental variogram for nonuniformly distributed data.

4.2h

FIGURE 4.2.9 shows a satisfactory fit of the following exponential model to the experimental variogram:

$$\gamma(h)=3\left(1-e^{-\frac{h}{5}}\right)$$

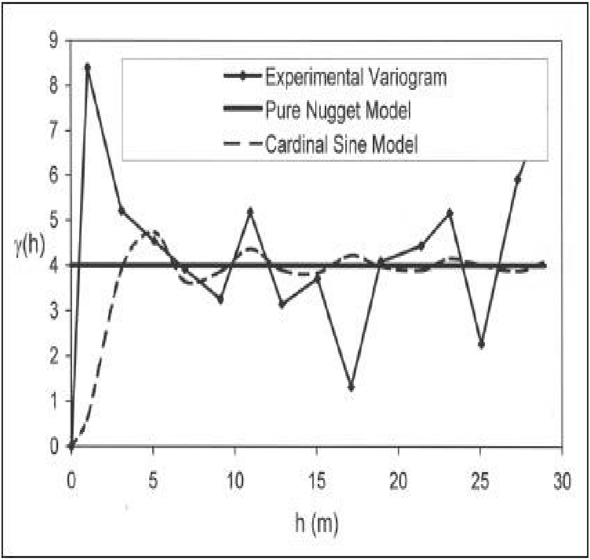

FIGURE 4.2.9 Theoretical variogram fit.

4.2i

[FIGURE 4.2.10](#) shows the scatter plot for determining the covariance function for nonuniformly distributed data obtained using the algorithm outlined in the textbook. The experimental experimental covariance function shown in the FIGURE was obtained with a bin size of 10 meters.

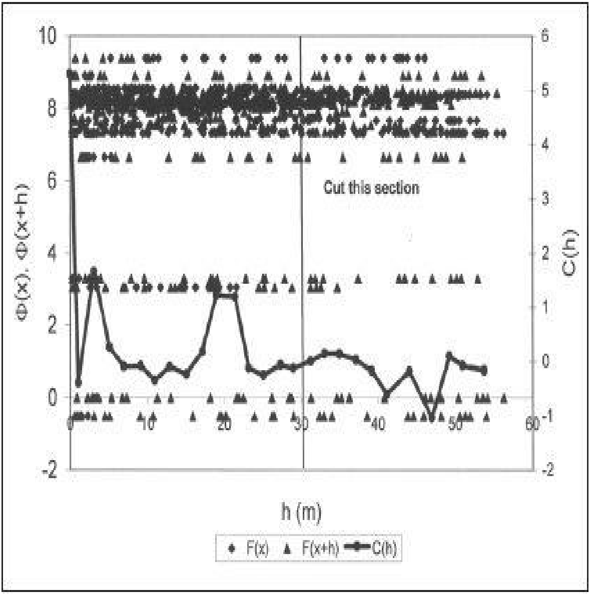

FIGURE 4.2.10 Scatter plot for determination of experimental covariance function for nonuniformly distributed data.

4.2j

FIGURE 4.2.11 shows the correlation coefficient function, which is a dimensionless version of the covariance function.

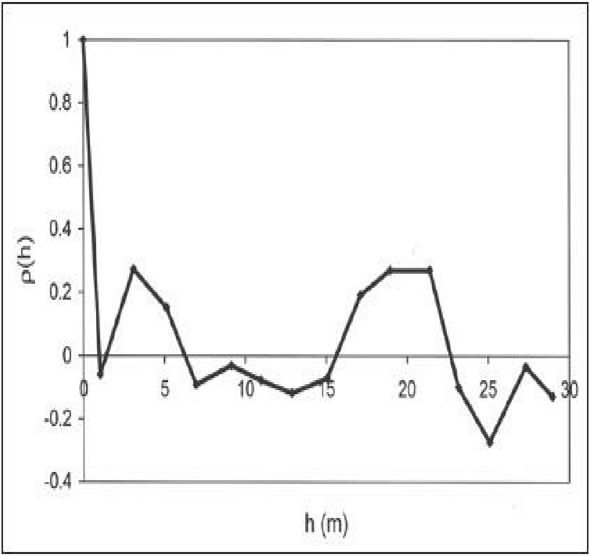

FIGURE 4.2.11 Experimental correlation coefficient function.

PROBLEM 4.3

4.3a

One version of the Carman-Kozeny equation is

$$k = \frac{\phi^3}{5S^2} \quad (4.3.1)$$

where S in the surface area per unit bulk volume of the sample. Assuming spherical grains,

$$S = \frac{3(1-\phi)}{r} = \frac{6(1-\phi)}{D_p} \text{ cm}^2/\text{cm}^3 \quad (4.3.2)$$

where D_p is the grain diameter.

Substituting Eq.(4.3.2) into (4.3.1) and rearranging gives the grain diameter as

$$D_p = \sqrt{\frac{5 \times 36 \times (1-\phi)^2 k}{\phi^3}} \qquad \textbf{(4.3.3)}$$

For Sample 10,

$$\phi = 0.233$$

$$k = 30 \text{ mD} = 0.030 \times 9.869 \times 10^{-9} \text{ cm}^2$$

Substituting the numerical values into Eq.(4.3.3) gives the grain diameter as

$$D_p = \sqrt{\frac{5 \times 36 \times (1-0.233)^2 \times 0.030 \times 9.869 \times 10^{-9}}{(0.233)^3}}$$

$$= 15.74 \times 10^{-4} \text{ cm} = 15.74 \ \mu\text{m}$$

4.3b

FIGURE 4.3.1 shows the graph for determining the Dykstra-Parsons coefficient of permeability variation. From the regression line,

$$\bar{k} = 104.79 \text{ mD}$$

$$k_{84.1} = 104.79e^{-0.902} = 42.52 \text{ mD}$$

$$V = \frac{\bar{k} - k_{84.1}}{\bar{k}} = \frac{104.79 - 42.52}{104.79} = 0.59$$

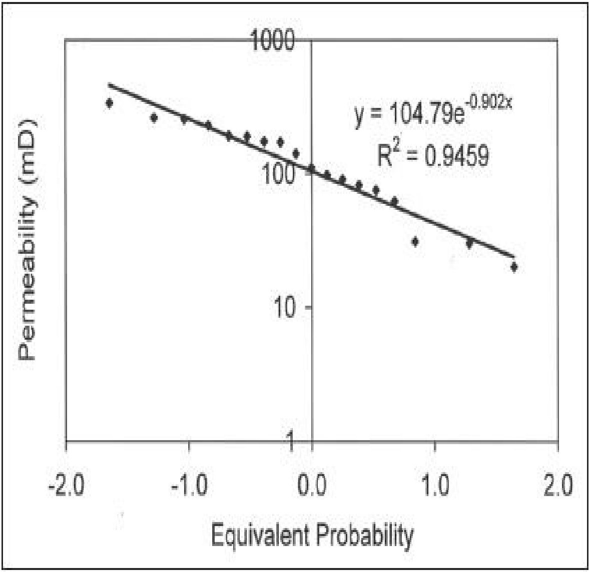

FIGURE 4.3.1 Graph for determination of Dykstra-Parsons coefficient of permeability variation.

4.3c

TABLE 4.3.1 shows the data used to calculate the semivariance at a lag distance of 3 ft.

$$\Sigma\left[k(x)-k(x+3)\right]^2=311117$$

$$N_h=16$$

$$\gamma(3)=\frac{311117}{2\times16}=9722.41$$

TABLE 4.3.1 Data for Calculating Semivariance at a Lag Distance of 3ft.

k(x)	**k(x+3)**
75	62
20	31
142	98
62	231

31	111
98	82
231	30
111	258
82	191
30	339
258	263
191	193
339	91
263	173
193	30
91	175

PROBLEM 4.4

4.4a

FIGURE 4.4.1 shows the graph for determining the Dykstra-Parsons coefficient of permeability variation. From the regression line,

$$\bar{k} = 122.95 \text{ mD}$$

$$k_{84.1} = 122.95e^{-2.2816} = 12.56 \text{ mD}$$

$$V = \frac{\bar{k} - k_{84.1}}{\bar{k}} = \frac{122.95 - 12.56}{122.95} = 0.90$$

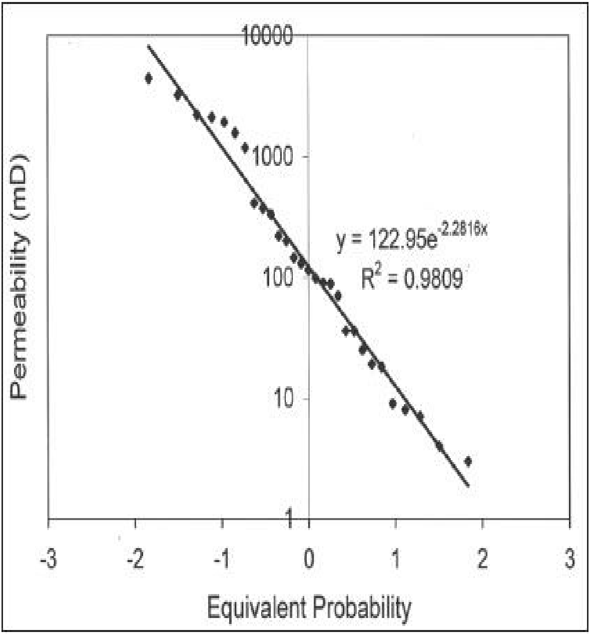

FIGURE 4.4.1 Graph for determination of Dykstra-Parsons coefficient of permeability variation.

4.4b

The numerical coefficient that indicates the strength of the linear relationship is the correlation coefficient.

$$\bar{\phi} = \frac{\Sigma\phi_i}{N} = 0.2081$$

$$\Sigma\left(\phi_i - \bar{\phi}\right)^2 = 0.0964$$

$$s_\phi = \sqrt{\frac{\Sigma\left(\phi_i - \bar{\phi}\right)^2}{N-1}} = 0.0587$$

$$\ln\bar{F} = \frac{\Sigma\ln F_i}{N} = 2.8993$$

$$\Sigma\left(\ln k_i - \ln\bar{k}\right)^2 = 9.6534$$

$$s_{\ln k} = \sqrt{\frac{\sum\left(\ln k_i - \ln \overline{k}\right)^2}{N-1}} = 0.5872$$

$$\sum\left(\phi_i - \overline{\phi}\right)\left(\ln k_i - \ln \overline{k}\right) = -0.9030$$

$$C(\ln k, \phi) = \frac{\sum\left(\phi_i - \overline{\phi}\right)\left(\ln k_i - \ln \overline{k}\right)}{N-1} = -0.0323$$

$$\rho(\ln k, \phi) = \frac{C(\ln k, \phi)}{s_\phi s_{\ln k}} = -0.9356$$

$$R^2 = \rho^2 = 0.8754$$

Yes. There is a strong linear relation between the natural log of the formation resistivity factor and the porosity.

PROBLEM 4.5

TABLE 4.5.1 shows the data for calculating the semivariance at a lag distance of 5 meters.

$$\Sigma[Z(x+5)-Z(x)]^2=94$$

$$N_h=10$$

$$\gamma(5)=\frac{94}{2\times 10}=4.7$$

TABLE 4.5.1 Data for h = 5 m

Z(x)	Z(x+5)	$[Z(x+5)-Z(x)]^2$
8	6	4

6	4	4
4	3	1
3	6	9
6	5	1
5	7	4
7	2	25
2	8	36
5	6	1
6	3	9
Total		94

TABLE 4.5.2 shows the data for calculating the semivariance at a lag distance of 15 meters.

$$\Sigma\left[Z(x+15)-Z(x)\right]^2=80$$

$$N_h=8$$

$$\gamma(15)=\frac{80}{2\times 8}=5.0$$

TABLE 4.5.2 Data for *h* = 15 m

Z(x)	**Z(x+15)**	**[Z(x+15)-Z(x)]^2**
8	3	25
6	6	0
4	5	1
3	7	16
6	2	16
5	8	9
2	5	9
8	6	4

Total	80

PROBLEM 4.6

4.6a

TABLE 4.6.1 and FIGURE 4.6.1 show the computed variograms in the E-W, N-S, NE-SW, and NW-SE directions.

TABLE 4.6.1 Variograms in the Various Directions.

h (m)	E-W $\gamma(h)$	N-S $\gamma(h)$	h (m)	NE-SW $\gamma(h)$	NW-SE $\gamma(h)$
0.0	0.000	0.000	0.0	0.000	0.000
100.0	0.587	0.533	141.4	0.892	0.794
200.0	0.705	0.738	282.8	0.529	0.782
300.0	0.925	0.740	424.3	0.632	0.824

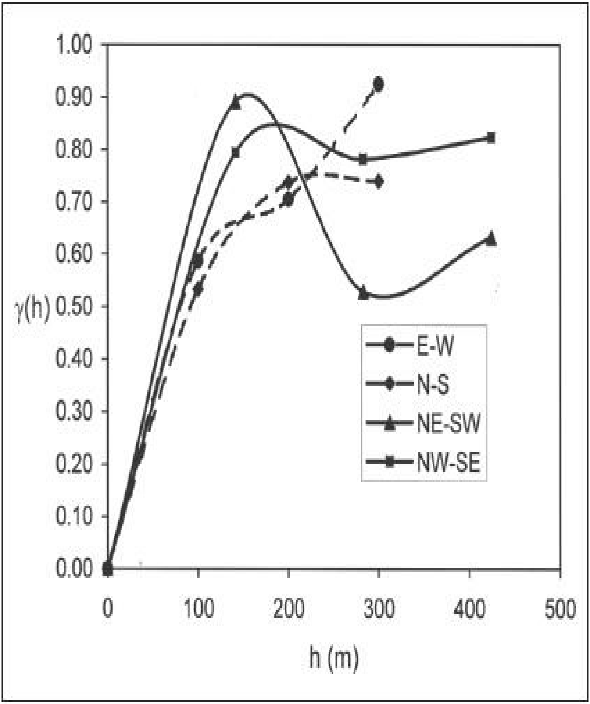

FIGURE 4.6.1 Variograms in the various directions.

4.6b

The variogram is anisotropic.

4.6c

Yes. The conclusion would have been different. The variograms in the E-W and N-S are essentially the same and would have led to a conclusion of isotropy. However, the variograms in the NE-SW and NW-SE directions clearly show anisotropy.

PROBLEM 4.7

4.7a

TABLE 4.7.1 and **FIGURE 4.7.1** show the computed semivariograms in the E-W, N-S, NE-SW, and NW-SE directions.

TABLE 4.7.1 Semivariograms in the Different Directions.

		E-W	N-S			NE-SW	NW-SE
h	N_h	γ(h)	γ(h)	h	N_h	γ(h)	γ(h)
0		0.000	0.000	0.000		0.000	0.000
1	56	6.411	4.982	1.414	49	7.459	7.806
2	48	9.490	8.750	2.828	36	13.194	13.431
3	40	10.575	10.675	4.243	25	19.280	10.680
4	32	10.547	12.953	5.657	16	18.406	12.625

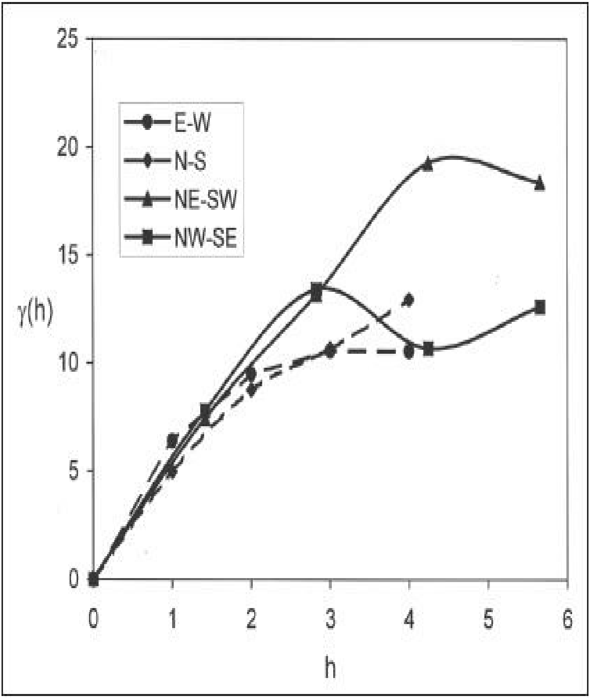

FIGURE 4.7.1 Variograms in the various directions.

4.7b

Yes. There is evidence of anisotropy in the semivariograms in the different directions. The semivariograms in the E-W and N-S directions are essentially the same. The semivariograms in the NE-SW and NW-SE directions are higher than in the other two directions at lag distances greater than 2.

4.7c

FIGURE 4.7.2 shows the average semivariograms and their model fits. Again, anisotropy is evident. The theoretical model used to fit the data from the E-W/N-S combination is the exponential model given by

$$\gamma(h) = 15.5\left(1 - e^{-h/3.5}\right) \tag{4.7.1}$$

The theoretical model used to fit the data from the NE-SW/NW-SE combination is the spherical model given by

$$\begin{aligned} \gamma(h) &= 15\left(\frac{3}{2}\frac{h}{4} - \frac{1}{2}\frac{h^3}{4^3}\right) \text{ for } h < 4 \\ &= 15 \text{ for } h \geq 4 \end{aligned} \tag{4.7.2}$$

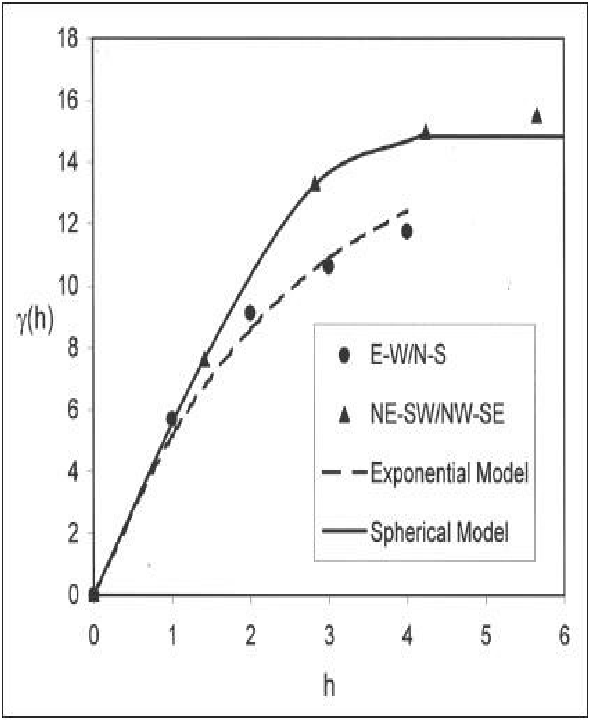

FIGURE 4.7.2 Average semivariograms.

PROBLEM 4.8

4.8a

TABLE 4.8.1 shows the data used to calculate the semivariance at a lag distance of c in the NE-SW direction.

$$\Sigma\left[k\left(x+\sqrt{2}\right)-k(x)\right]^2 = 2352846$$

$$N_h = 12$$

$$\gamma\left(\sqrt{2}\right) = \frac{2352846}{2\times 12} = 98035.25$$

TABLE 4.8.1 Data for Calculation of Semivariance.

k(x)	k(x+h)
47	137
906	1261
1261	1141
415	782
782	1385
1385	917
1365	369
369	484
484	251
413	789
789	482
91	529

4.8b

The strength of the linear relationship between natural log of permeability and the porosity for Wells 1 through 5 can be tested with correlation coefficient.

$$\bar{\phi} = \frac{\sum \phi_i}{N} = 21.8000$$

$$\sum \left(\phi_i - \bar{\phi} \right)^2 = 614.8000$$

$$s_\phi = \sqrt{\frac{\sum \left(\phi_i - \bar{\phi} \right)^2}{N-1}} = 12.3976$$

$$\ln \bar{k} = \frac{\sum \ln k_i}{N} = 5.7475$$

$$\sum \left(\ln k_i - \ln \bar{k} \right)^2 = 4.4761$$

$$s_{\ln k} = \sqrt{\frac{\sum \left(\ln k_i - \ln \bar{k} \right)^2}{N-1}} = 1.0578$$

$$\sum \left(\phi_i - \bar{\phi} \right)\left(\ln k_i - \ln \bar{k} \right) = -9.9043$$

$$C(\ln k, \phi) = \frac{\sum \left(\phi_i - \bar{\phi} \right)\left(\ln k_i - \ln \bar{k} \right)}{N-1} = -2.4761$$

$$\rho(\ln k, \phi) = \frac{C(\ln k, \phi)}{s_\phi s_{\ln k}} = -0.1888$$

$$R^2 = \rho^2 = 0.0356$$

The correlation between **In*k*** and δ is weak. The young engineer's claim is not supported by the data.

4.8c

FIGURE 4.8.1 shows the graph for calculating the Dykstra-Parsons coefficient of variation for the permeability of Wells 1 through 5.

$$\bar{k} = 313.4 \text{ mD}$$

$$k_{84.1} = 313.4e^{-1.374} = 79.3192 \text{ mD}$$

$$V = \frac{\bar{k} - k_{84.1}}{\bar{k}} = \frac{313.4 - 79.3192}{313.4} = 0.75$$

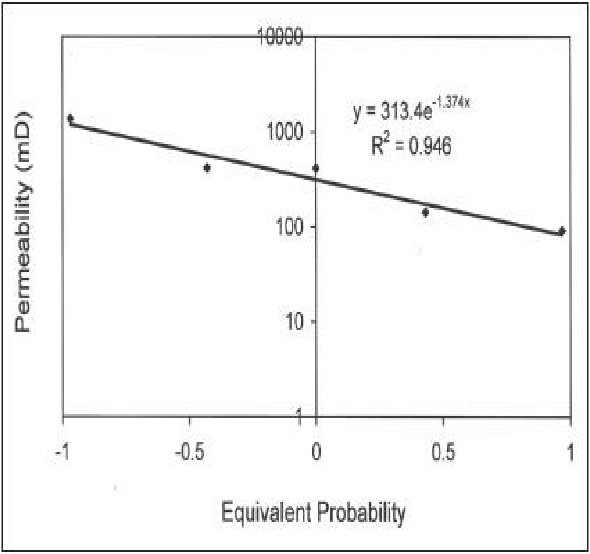

FIGURE 4.8.1. Graph for determination of Dykstra-Parsons coefficient of permeability variation.

PROBLEM 4.9

4.9a

In terms of the variogram, the kriging equations are given in matrix form as

$$\begin{bmatrix} \gamma_{11} & \gamma_{12} & \gamma_{13} & -1 \\ \gamma_{21} & \gamma_{22} & \gamma_{23} & -1 \\ \gamma_{31} & \gamma_{32} & \gamma_{33} & -1 \\ 1 & 1 & 1 & 0 \end{bmatrix} \begin{bmatrix} \lambda_1 \\ \lambda_2 \\ \lambda_3 \\ \beta \end{bmatrix} = \begin{bmatrix} \gamma_{10} \\ \gamma_{20} \\ \gamma_{30} \\ 1 \end{bmatrix} \quad (4.9.1)$$

$$h_{11} = h_{22} = h_{33} = 0; \gamma_{11} = \gamma_{22} = \gamma_{33} = 0$$

$$h_{12} = h_{21} = 1; \gamma_{12} = \gamma_{21} = 2+1 = 3$$

$$h_{13} = h_{31} = 3; \gamma_{13} = \gamma_{31} = 2+3 = 5$$

$$h_{23} = h_{32} = 2; \gamma_{23} = \gamma_{32} = 2+2 = 4$$

$$h_{10} = 2; \gamma_{10} = 2+2 = 4$$

$$h_{20} = 1; \gamma_{20} = 2+1 = 3$$

$$h_{30} = 1; \gamma_{30} = 2+1 = 3$$

Eq.(4.9.1) becomes

$$\begin{bmatrix} 0 & 3 & 5 & -1 \\ 3 & 0 & 4 & -1 \\ 5 & 4 & 0 & -1 \\ 1 & 1 & 1 & 0 \end{bmatrix} \begin{bmatrix} \lambda_1 \\ \lambda_2 \\ \lambda_3 \\ \mu \end{bmatrix} = \begin{bmatrix} 4 \\ 3 \\ 3 \\ 1 \end{bmatrix} \qquad (4.9.2)$$

The solution to Eq.(4.9.2) is

$$\lambda_1 = \frac{2}{11}, \lambda_2 = \frac{4}{11}, \lambda_3 = \frac{5}{11}, \beta = -\frac{7}{11}$$

The estimate at location 2 is given by

$$\Phi_0 = \frac{2}{11}\Phi_1 + \frac{4}{11}\Phi_2 + \frac{5}{11}\Phi_3$$

4.9b

The estimation error variance is given by

$$\sigma_0^2 = -\beta + \sum_{i=1}^{i=3} \lambda_i \gamma_{i0} = -\left(-\frac{7}{11}\right) + \frac{2}{11}(4) + \frac{4}{11}(3) + \frac{5}{11}(3) = \frac{42}{11}$$

PROBLEM 4.10

4.10a

The ordinary kriging equation to be solved is

$$\begin{bmatrix} \gamma_{BB} & \gamma_{BC} & -1 \\ \gamma_{CB} & \gamma_{CC} & -1 \\ 1 & 1 & 0 \end{bmatrix} \begin{bmatrix} \lambda_B \\ \lambda_C \\ \beta \end{bmatrix} = \begin{bmatrix} \gamma_{BA} \\ \gamma_{CA} \\ 1 \end{bmatrix} \qquad (4.10.1)$$

From the variogram,

$$\gamma_{BB} = \gamma_{CC} = 0$$

$$\gamma_{BC} = \gamma_{CB} = \gamma_{BA} = \gamma_{CA} = 60$$

Eq.(4.10.1) becomes

$$\begin{bmatrix} 0 & 60 & -1 \\ 60 & 0 & -1 \\ 1 & 1 & 0 \end{bmatrix} \begin{bmatrix} \lambda_B \\ \lambda_C \\ \beta \end{bmatrix} = \begin{bmatrix} 60 \\ 60 \\ 1 \end{bmatrix} \quad (4.10.2)$$

The solution to Eq.(4.10.2) is

$$\lambda_B = \lambda_C = \frac{1}{2}, \ \beta = -30$$

The kriged estimate at *A* is given by

$$\Phi_A^* = \lambda_B \Phi_B + \lambda_C \Phi_C = \frac{1}{2}(20) + \frac{1}{2}(50) = 35$$

It should be observed that because there is no correlation between the locations, each location is assigned the same weight and the estimated value becomes the arithmetic mean of the measured values.

4.10b

The minimum error variance is given by

$$\sigma^2_{e\min} = -\beta + \sum_{i=1}^{i=2} \lambda_i \gamma_{iA} = -(-30) + \frac{1}{2}(60) + \frac{1}{2}(60) = 90$$

$$\sigma_{e\min} = \sqrt{90} = 9.4868$$

4.10c

The simulated value at *A* is given by

$$\Phi_{sA} = \Phi^*_A + z_A \sigma_{eA} = 35 + (-1.1679)(9.4868) = 23.92$$

Alternatively, this problem can be solved with the covariance function. In this case, the matrix equation to be solved is

$$\begin{bmatrix} 60 & 0 & 1 \\ 0 & 60 & 1 \\ 1 & 1 & 0 \end{bmatrix} \begin{bmatrix} \lambda_B \\ \lambda_C \\ \beta \end{bmatrix} = \begin{bmatrix} 0 \\ 0 \\ 1 \end{bmatrix} \qquad (4.10.3)$$

The solution to Eq.(4.10.3) is

$$\lambda_B = \lambda_C = \frac{1}{2}, \ \beta = -30$$

The kriged estimate at *A* is given by

$$\Phi_A^* = \lambda_B \Phi_B + \lambda_C \Phi_C = \frac{1}{2}(20) + \frac{1}{2}(50) = 35$$

The minimum error variance is given by

$$\sigma_{e\min}^2 = \sigma^2 - \beta - \sum_{i=1}^{i=2} \lambda_i C_{iA} = 60 - (-30) - 0 - 0 = 90$$

$$\sigma_{e\min} = \sqrt{90} = 9.4868$$

The simulated value at *A* is given by

$$\Phi_{sA} = \Phi_A^* + z_A \sigma_{eA} = 35 + (-1.1679)(9.4868) = 23.92$$

PROBLEM 4.11

4.11a

The kriging equation to be solved is

$$\begin{bmatrix} C_{AA} & C_{AC} & 1 \\ C_{cA} & C_{CC} & 1 \\ 1 & 1 & 0 \end{bmatrix} \begin{bmatrix} \lambda_A \\ \lambda_C \\ \beta \end{bmatrix} = \begin{bmatrix} C_{A0} \\ C_{C0} \\ 1 \end{bmatrix} \tag{4.11.1}$$

$$h_{AA}=0,\ C_{AA}=0$$

$$h_{AC}=h_{CA}=\sqrt{100^2+200^2}$$

$$=223.6068,\ C_{AC}=C_{CA}=20e^{-(0.01\times 223.6068)}=2.1376$$

$$h_{CC}=0,\ C_{CC}=20$$

$$h_{A0}=200\,ft,\ C_{A0}=20e^{-(0.01\times 200)}=2.7067$$

$$h_{C0}=100\,ft,\ C_{C0}=20e^{-(0.01\times 100)}=7.3576$$

Eq(4.11.1) becomes

$$\begin{bmatrix} 20 & 2.1376 & 1 \\ 2.1376 & 20 & 1 \\ 1 & 1 & 0 \end{bmatrix}\begin{bmatrix} \lambda_A \\ \lambda_C \\ \beta \end{bmatrix}=\begin{bmatrix} 2.7067 \\ 7.3576 \\ 1 \end{bmatrix} \qquad (4.11.2)$$

The solution to Eq.(4.11.2) is

$$\lambda_A = 0.3698,\ \lambda_C = 0.6302,\ \beta = -6.0366$$

The kriged estimate at *A* is given by

$$k_B^* = \lambda_A k_A + \lambda_C k_C = (0.3698)(500) + (0.6302)(80) = 235.32 mD$$

4.11b

The minimum error variance is given by

$$\sigma_{e\min}^2 = \sigma^2 - \beta - \sum_{i=1}^{i=2} \lambda_i C_{iA}$$

$$= 20 - (-6.0366) - \left[(0.3698)(2.7067) + (0.6302)(7.3576)\right]$$

$$= 20.3990$$

$$\sigma_{e\min} = \sqrt{20.3990} = 4.5165$$

PROBLEM 4.12

$$Z^{*} = Z(x_1) + Z(x_2) \tag{4.12.1}$$

$$\begin{aligned} Var\left[Z^{*}\right] &= Cov\left[Z(x_1)Z(x_1)\right] + Cov\left[Z(x_1)Z(x_2)\right] + Cov\left[Z(x_2)Z(x_2)\right] \\ &= C(0) + C(100) + C(0) \end{aligned} \tag{4.12.2}$$

The variogram is given by the spherical model

$$\begin{aligned} \gamma(h) &= 3\left(\frac{3}{2}\frac{h}{250} - \frac{1}{2}\frac{h^3}{250^3}\right) \text{ for } h < 250 \\ &= 3 \text{ for } h \geq 250 \end{aligned} \tag{4.12.3}$$

From the variogram,

$$C(0)=\sigma^2=3$$

For a stationary random function,

$$C(h)=C(0)-\gamma(h) \qquad \textbf{(4.12.4)}$$

$$\gamma(100)=3\left(\frac{3}{2}\frac{100}{250}-\frac{1}{2}\frac{100^3}{250^3}\right)=1.704$$

$$C(100)=3-1.704=1.296$$

$$Var\left[Z^*\right]=C(0)+C(100)+C(0)=3+1.296+3=7.296$$

For a pure nugget effect variogram, there is no correlation between $Z(\times_1)$ and $Z(x_2)$ and as a result, C(100) is zero.

$$Var\left[Z^*\right]=3+0+3=6$$

If the range of influence is 25 m, there is no correlation between $\boldsymbol{Z(x_1)}$ and $\boldsymbol{Z(x_2)}$ beyond 25 m and as a result, C(100) is zero. The variance of Z* is given by

$$Var\left[Z^*\right]=3+0+3=6$$

which is the same as for the pure nugget effect variogram.

PROBLEM 4.13

The covariance function is given by

$$C(h) = 100e^{-0.2h} \tag{4.13.1}$$

Kriging and simulation at Location 5. The matrix equation is given by

$$\begin{pmatrix} 100 & 43.8 & 56.8 & 36.1 & 21.0 & 1 \\ 43.8 & 100 & 63.9 & 27.8 & 36.1 & 1 \\ 56.8 & 63.9 & 100 & 42.8 & 36.8 & 1 \\ 36.1 & 27.8 & 42.8 & 100 & 29.6 & 1 \\ 21.0 & 36.1 & 36.8 & 29.6 & 100 & 1 \\ 1 & 1 & 1 & 1 & 1 & 0 \end{pmatrix} \begin{pmatrix} \lambda_1 \\ \lambda_2 \\ \lambda_3 \\ \lambda_4 \\ \lambda_5 \\ \beta \end{pmatrix} = \begin{pmatrix} 36.78 \\ 67.03 \\ 63.94 \\ 34.06 \\ 53.13 \\ 1 \end{pmatrix} \tag{4.13.2}$$

The solution is given by

$$\begin{pmatrix} \lambda_1 \\ \lambda_2 \\ \lambda_3 \\ \lambda_4 \\ \lambda_5 \\ \beta \end{pmatrix} = \begin{pmatrix} -0.0333 \\ 0.3964 \\ 0.2964 \\ 0.0490 \\ 0.2915 \\ -1.9754 \end{pmatrix} \qquad (4.13.3)$$

The kriged value is

$$Z_{o5}^{*} = \sum_{i=1}^{N} \lambda_i Z_i = 38.16$$

The minimum error variance is

$$\sigma^2_{e_{\min}} = \sigma^2 - \beta - \sum_{i=1}^{N} \lambda_i C_{io} = 40.521$$

$$\sigma_{e\min} = \sqrt{40.521} = 6.306$$

The 95% confidence interval is

$$Z_5 = 40.52 \pm 12.36$$

$$z_5 = -0.1411$$

The simulated value is

$$Z^*_{s5} = Z^*_5 + z_5 \sigma_{e\min} = 39.63$$

Kriging and simulation at Location 2. The matrix equation is given by

$$\begin{pmatrix} 100 & 43.84 & 56.8 & 36.8 & 36.1 & 20.97 & 1 \\ 43.84 & 100 & 63.94 & 67.03 & 27.79 & 36.07 & 1 \\ 56.8 & 63.94 & 100 & 63.94 & 42.80 & 36.79 & 1 \\ 36.8 & 67.03 & 63.94 & 100 & 34.06 & 53.13 & 1 \\ 36.1 & 27.79 & 42.80 & 34.06 & 100 & 29.62 & 1 \\ 20.97 & 36.07 & 36.79 & 53.13 & 29.62 & 100 & 1 \\ 1 & 1 & 1 & 1 & 1 & 1 & 0 \end{pmatrix} \begin{pmatrix} \lambda_1 \\ \lambda_2 \\ \lambda_3 \\ \lambda_4 \\ \lambda_5 \\ \lambda_6 \\ \beta \end{pmatrix} = \begin{pmatrix} 75.36 \\ 54.88 \\ 75.36 \\ 48.62 \\ 40.88 \\ 27.79 \\ 1 \end{pmatrix} \tag{4.13.4}$$

The solution is

$$\begin{pmatrix} \lambda_1 \\ \lambda_2 \\ \lambda_3 \\ \lambda_4 \\ \lambda_5 \\ \lambda_6 \\ \beta \end{pmatrix} = \begin{pmatrix} 0.4689 \\ 0.0692 \\ 0.4480 \\ -0.0269 \\ 0.0444 \\ -0.0037 \\ -0.5444 \end{pmatrix} \tag{4.13.5}$$

The kriged value is

$$Z_{o2}^{*} = \sum_{i=1}^{N} \lambda_i Z_i = 41.14$$

The minimum error variance is

$$\sigma^2_{e_{\min}} = \sigma^2 - \beta - \sum_{i=1}^{N} \lambda_i C_{io} = 27.24$$

$$\sigma_{e\min} = \sqrt{27.24} = 5.22$$

The 95% confidence interval is

$$Z_2 = 41.14 \pm 10.23$$

$$z_2 = 1.6092$$

The simulated value is

$$Z^*_{s2} = Z^*_2 + z_2 \sigma_{e\min} = 49.54$$

Kriging and simulation at Location 6. The matrix equation is given by

$$\begin{pmatrix} 100 & 75.36 & 43.84 & 56.8 & 36.79 & 36.07 & 20.97 & 1 \\ 75.36 & 100 & 54.88 & 75.36 & 48.62 & 40.88 & 27.79 & 1 \\ 43.84 & 54.88 & 100 & 63.94 & 67.03 & 27.79 & 36.07 & 1 \\ 56.8 & 75.36 & 63.94 & 100 & 63.94 & 42.8 & 36.79 & 1 \\ 36.79 & 48.62 & 67.03 & 63.94 & 100 & 34.06 & 53.13 & 1 \\ 36.07 & 40.88 & 27.79 & 42.8 & 34.06 & 100 & 29.62 & 1 \\ 20.97 & 27.79 & 36.07 & 36.79 & 53.13 & 29.62 & 100 & 1 \\ 1 & 1 & 1 & 1 & 1 & 1 & 1 & 0 \end{pmatrix} \begin{pmatrix} \lambda_1 \\ \lambda_2 \\ \lambda_3 \\ \lambda_4 \\ \lambda_5 \\ \lambda_6 \\ \lambda_7 \\ \beta \end{pmatrix} = \begin{pmatrix} 40.88 \\ 53.13 \\ 48.62 \\ 67.03 \\ 63.94 \\ 53.13 \\ 48.62 \\ 1 \end{pmatrix} \tag{4.13.6}$$

The solution is

$$\begin{pmatrix} \lambda_1 \\ \lambda_2 \\ \lambda_3 \\ \lambda_4 \\ \lambda_5 \\ \lambda_6 \\ \lambda_7 \\ \beta \end{pmatrix} = \begin{pmatrix} -0.0057 \\ 0.0236 \\ -0.0597 \\ 0.3553 \\ 0.2810 \\ 0.2526 \\ 0.1530 \\ -0.5395 \end{pmatrix} \tag{4.13.7}$$

The kriged value is

$$Z_{o6}^{*} = \sum_{i=1}^{N} \lambda_i Z_i = 38.43$$

The minimum error variance is

$$\sigma^2_{e_{\min}} = \sigma^2 - \beta - \sum_{i=1}^{N} \lambda_i C_{io} = 39.783$$

$$\sigma_{e\min} = \sqrt{39.783} = 6.307$$

The 95% confidence interval is

$$Z_6 = 38.43 \pm 12.36$$

$$z_6 = 0.2029$$

The simulated value is

$$Z^*_{s6} = Z^*_6 + z_6 \sigma_{e\min} = 39.71$$

TABLE 4.13.1 Kriged and Simulated Values.

Location	Coordinates (x,y)	Measured Value	Kriged Value	Estimation Variance	Standard Deviation	Simulated Value
1	1, 2	25				
2	2, 3		41.14	27.235	5.219	49.54
3	2,6	40				
4	3, 4	60				
5	4, 6		38.16	40.521	6.306	39.63
6	5, 4		38.43	39.783	6.307	39.71
7	6,1	20				
8	7, 7	15				

PROBLEM 4.14

TABLE 4.14.1 h_x

	1	2	3	4	5	6	7
1	0						
2	1	0					
3	1	0	0				
4	3	2	2	0			
5	3	2	2	0	0		
6	4	3	3	1	1	0	
7	5	4	4	2	2	1	0

TABLE 4.14.2 h_y

	1	2	3	4	5	6	7
1	0						
2	2	0					
3	4	2	0				
4	5	3	1	0			
5	1	1	3	4	0		
6	2	0	2	3	1	0	
7	6	4	2	1	5	4	0

TABLE 4.14.3 h_{ij}

	1	2	3	4	5	6	7
1	0.0000						
2	4.1231	0.0000					
3	8.0623	4.0000	0.0000				
4	10.4403	6.3246	2.8284	0.0000			
5	3.6056	2.8284	6.3246	8.0000	0.0000		
6	5.6569	3.0000	5.0000	6.0828	2.2361	0.0000	
7	13.0000	8.9443	5.6569	2.8284	10.1980	8.0623	0.0000

TABLE 4.14.4 γ_{ij}

	1	2	3	4	5	6	7
1	0.0000						
2	42.2779	0.0000					
3	60.0000	41.2500	0.0000				
4	60.0000	56.3281	30.4940	0.0000			
5	37.8160	30.4940	56.3281	60.0000	0.0000		
6	53.0330	32.1680	48.9258	55.2438	24.5007	0.0000	
7	60.0000	60.0000	60.0000	30.4940	60.0000	60.0000	0.0000

$$\gamma(h)=\gamma_x(h) \quad (4.14.1)$$

$$h=\sqrt{h_x^2+\left(\frac{8}{4}\right)^2 h_y^2} \quad (4.14.2)$$

$$\gamma_x(h) = 60\left(\frac{3}{2}\frac{h}{8} - \frac{1}{2}\frac{h^3}{8^3}\right) \text{ for } h < 8 \tag{4.14.3}$$

$$= 60 \text{ for } h \geq 8$$

Kriging and simulation at Location 4. The matrix equation is given by

$$\begin{bmatrix} 0.0 & 60.0 & 37.8160 & 53.0330 & 60.0 & -1.0 \\ 60.0 & 0.0 & 56.3281 & 48.9258 & 60.0 & -1.0 \\ 37.8160 & 56.3281 & 0.0 & 24.5007 & 60.0 & -1.0 \\ 53.0330 & 48.9258 & 24.5007 & 0.0 & 60.0 & -1.0 \\ 60.0 & 60.0 & 60.0 & 60.0 & 0.0 & -1.0 \\ 1.0 & 1.0 & 1.0 & 1.0 & 1.0 & 0.0 \end{bmatrix} \begin{bmatrix} \lambda_1 \\ \lambda_3 \\ \lambda_5 \\ \lambda_6 \\ \lambda_7 \\ \beta \end{bmatrix}$$

$$
= \begin{bmatrix} 60.0 \\ 30.4940 \\ 60.0 \\ 55.2438 \\ 30.4940 \\ 1.0 \end{bmatrix} \qquad (4.14.4)
$$

The solution is

$$
\begin{bmatrix} \lambda_1 \\ \lambda_3 \\ \lambda_5 \\ \lambda_6 \\ \lambda_7 \\ \beta \end{bmatrix} = \begin{bmatrix} 0.0217 \\ 0.5001 \\ -0.0396 \\ 0.0169 \\ 0.5008 \\ -0.5433 \end{bmatrix} \qquad (4.14.5)
$$

The kriged value is

$$\phi_4^* = \sum \lambda_i \phi_i = 29.6690$$

The minimum error variance is

$$\sigma_{e\min}^2 = -\beta + \sum \lambda_i \gamma_{4i} = 30.9289$$

$$\sigma_{e\min} = \sqrt{30.9289} = 5.5614$$

The 95% confidence interval is

$$\phi_4 = 29.67 \pm 10.90$$

$$z_4 = 0.9333$$

The simulated value is

$$\phi_{s4}^* = \phi_4^* + z_4 \sigma_{e\min} = 34.8595$$

Kriging and simulation at Location 2. The matrix equation is given by

$$
\begin{bmatrix}
0.0 & 60.0 & 60.0000 & 37.8160 & 53.0330 & 60.0 & -1.0 \\
60.0 & 0.0 & 30.4940 & 56.3281 & 48.9258 & 60.0 & -1.0 \\
60.0 & 30.4940 & 0.0 & 60.0 & 55.2438 & 30.4940 & -1.0 \\
37.8160 & 56.3281 & 60.0 & 0.0 & 24.5007 & 60.0 & -1.0 \\
53.0330 & 48.9258 & 55.2438 & 24.5007 & 0.0 & 60.0 & -1.0 \\
60.0 & 60.0 & 30.4940 & 60.0 & 60.0 & 0.0 & -1.0 \\
1.0 & 1.0 & 1.0 & 1.0 & 1.0 & 1.0 & 0.0
\end{bmatrix}
$$

$$
\begin{bmatrix} \lambda_1 \\ \lambda_3 \\ \lambda_4 \\ \lambda_5 \\ \lambda_6 \\ \lambda_7 \\ \beta \end{bmatrix} = \begin{bmatrix} 42.2779 \\ 41.2500 \\ 56.3281 \\ 30.4940 \\ 32.1680 \\ 60.0 \\ 1.0 \end{bmatrix} \tag{4.14.6}
$$

The solution is

$$\begin{bmatrix} \lambda_1 \\ \lambda_3 \\ \lambda_4 \\ \lambda_5 \\ \lambda_6 \\ \lambda_7 \\ \beta \end{bmatrix} = \begin{bmatrix} 0.1857 \\ 0.3482 \\ -0.1568 \\ 0.2761 \\ 0.2484 \\ 0.0984 \\ -1.2775 \end{bmatrix} \tag{4.14.7}$$

The kriged value is

$$\phi_2^* = \sum \lambda_i \phi_i = 20.3500$$

The minimum error variance is

$$\sigma_{e\min}^2 = -\beta + \sum \lambda_i \gamma_{2i} = 36.9734$$

$$\sigma_{e\min} = \sqrt{36.9734} = 6.0806$$

The 95% confidence interval is

$$\phi_2 = 20.35 \pm 11.92$$

$$z_2 = 0.7598$$

The simulated value is

$$\phi_{s2}^* = \phi_2^* + z_2 \sigma_{emin} = 24.9698$$

TABLE 4.14.5 Kriged and Simulated Results.

Location	Coordinates x	y	Measured Porosity (%)	Kriged Value (%)	Estimation Variance	Standard Deviation (%)	95% Confidence Interval Low (%)	High (%)	Simulated Value (%)
1	1	1	15						
2	2	3		20.35	36.97	6.08	8.43	32.27	24.97
3	2	5	30						
4	4	6		29.67	30.93	5.56	18.77	40.57	34.86
5	4	2	25						
6	5	3	18						
7	6	7	30						

CHAPTER 5 SOLUTIONS

PROBLEM 5.1

This problem can be solved using either of the following two equations:

$$D_L = uL\left(\frac{J_{0.90} - J_{0.10}}{3.625}\right)^2 \tag{5.1.1}$$

$$D_L = \frac{uL}{8}\left(J_{0.84} - J_{0.16}\right)^2 \tag{5.1.2}$$

Here the problem is solved using both equations. Let $C_D = C/C_o$ and $J = \frac{1-t_D}{\sqrt{t_D}}$. The graph of C_D versus J on a probability-linear scale is a straight line as shown in **FIGURE 5.1.1**. In this FIGURE, C_D has been converted into a standard normal variate z using Excel's NORMSINV function and plotted against J instead of using a normal probability graph paper. The regression line is

$$z = -11.645J - 0.0077 \tag{5.1.3}$$

On the standard normal scale, C_D=**0.10** corresponds to **Z = –1.2816** and C_D=**0.90** corresponds to Z = 1.2816. From the regression line,

$$J_{0.10} = 0.1094$$

$$J_{0.90} = -0.1107$$

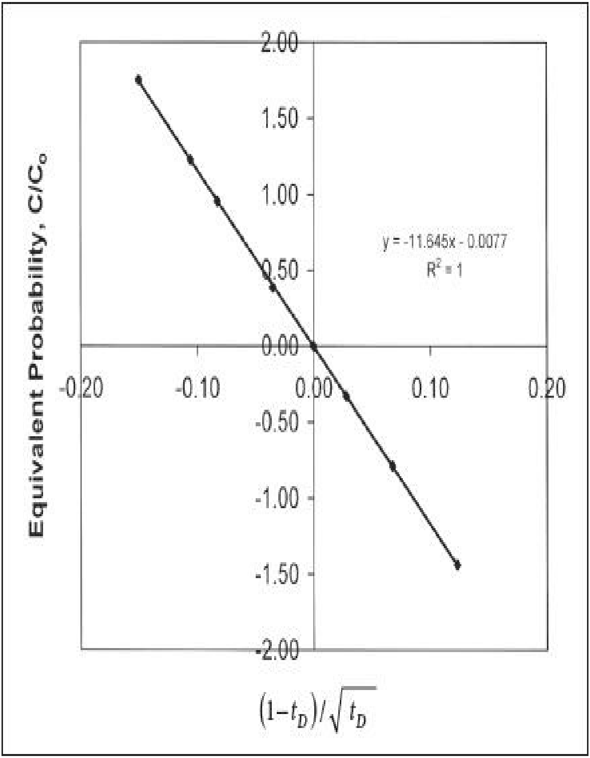

FIGURE 5.1.1 Graph of *z* verus *J* for Problem 5.1.

Also,

$$q = 1000\ \text{cm}^3/\text{hr} = 0.2778\ \text{cm}^3/\text{s}$$

$$d = 6\ \text{cm}$$

$$A = \pi\left(\frac{d}{2}\right)^2 = 28.2743\ \text{cm}^2$$

$$\phi = 0.35$$

$$u = \frac{q}{\phi A} = 2.807 \times 10^{-2}\ \text{cm/s}$$

$$L = 40\ \text{cm}$$

Substituting the numerical values into Eq.(5.1.1) gives

$$D_L = \left(2.807\times10^{-2}\right)(40)\left(\frac{-0.1107-0.1094}{3.625}\right)^2 = 4.139\times10^{-3}\,\mathrm{cm}^2/\mathrm{s}$$

$$\alpha_L = \frac{D_L}{u} = \frac{4.139\times10^{-3}}{2.807\times10^{-2}} = 0.1475\,\mathrm{cm}$$

$$N_{Pe} = \frac{uL}{D_L} = \frac{2.807\times10^{-2}\times40}{4.139\times10^{-3}} = 271$$

On the standard normal scale, C_D=0.16 corresponds to Z = –1.0 and C_D=0.84 corresponds to Z = 1.0. From the regression line,

$$J_{0.16} = 0.0852$$

$$J_{0.84} = -0.0865$$

Substituting the numerical values into

Eq.(5.1.2) gives

$$D_L = \frac{\left(2.807\times10^{-2}\right)(40)}{8}\left(-0.0865-0.0852\right)^2 = 4.140\times10^{-3}\,\text{cm}^2/\text{s}$$

$$\alpha_L = \frac{D_L}{u} = \frac{4.140\times10^{-3}}{2.807\times10^{-2}} = 0.1475\,\text{cm}$$

$$N_{Pe} = \frac{uL}{D_L} = \frac{2.807\times10^{-2}\times40}{4.140\times10^{-3}} = 271$$

PROBLEM 5.2

This problem can be solved using either of the following two equations:

$$N_{Pe} = \left(\frac{3.625}{J_{0.90} - J_{0.10}} \right)^2 \tag{5.2.1}$$

$$N_{Pe} = \frac{8}{\left(J_{0.84} - J_{0.16} \right)^2} \tag{5.2.2}$$

Here, the problem is solved using both equations. **FIGURE 5.2.1** shows the graph of z versus J. The regression line is

$$z = -5.1312J - 0.0362 \tag{5.2.3}$$

From the regression line,

$$J_{0.10} = 0.2427$$

$$J_{0.90} = -0.2568$$

$$J_{0.16} = 0.1878$$

$$J_{0.84} = -0.2019$$

Substituting the numerical values into Eq.(5.2.1) gives

$$N_{Pe} = \left(\frac{3.625}{-0.2568 - 0.2427} \right)^2 = 53$$

Substituting the numerical values into Eq.(5.2.2) gives

$$N_{Pe}=\frac{8}{\left(-0.2019-0.1878\right)^{2}}=53$$

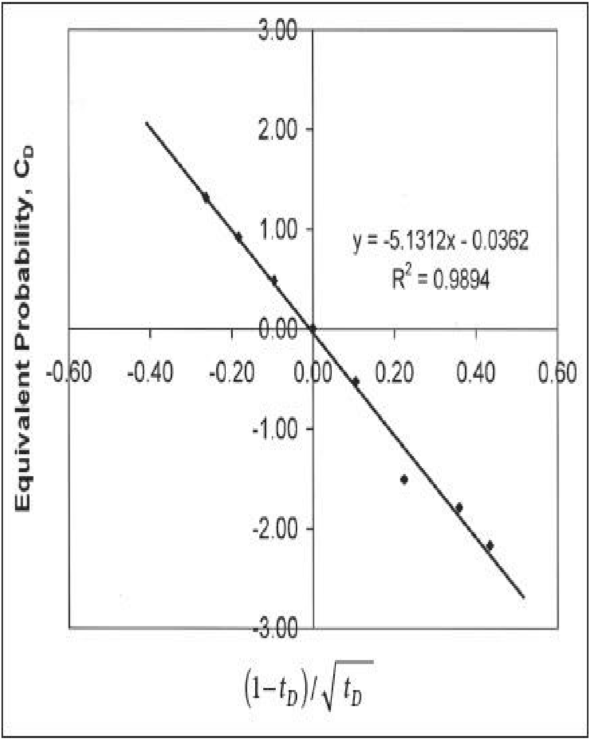

FIGURE 5.2.1 Graph of *z* verus *J* for Problem 5.2.

PROBLEM 5.3

5.3a

FIGURE 5.3.1 shows the solvent concentration profile at the instant of the measurement. $C/C_o=50\%$ travels at the average speed u. At the instant of measurement,

$$x_{50\%} = 57.1 \text{ cm}$$

$$u = 1.6 \text{ cm/hr} = 2.667 \times 10^{-2} \text{ cm/s}$$

$$t = \frac{x_{50\%}}{u} = \frac{57.1}{1.6} = 35.7 \text{ minutes or } 2141.3 \text{ seconds.}$$

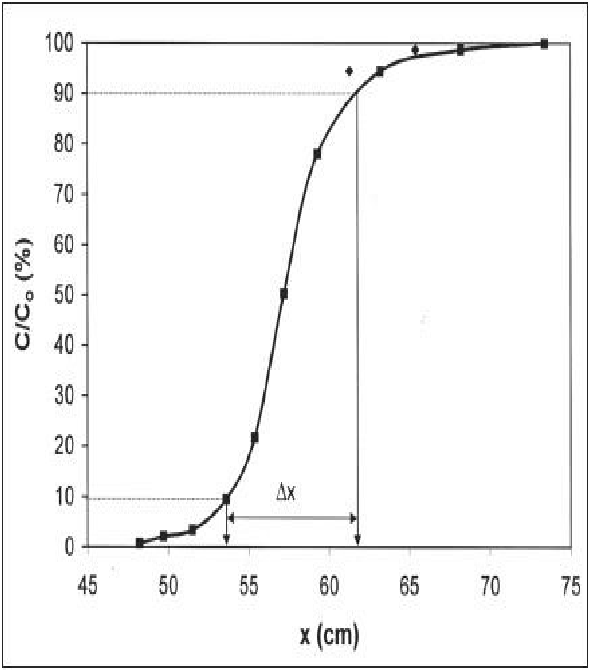

FIGURE 5.3.1 Graph of C/C_o verus x for Problem 5.3.

5.3b

The mixing zone length is given by

$$\Delta x = x_{90\%} - x_{10\%} = 3.625\sqrt{D_L t} \tag{5.3.1}$$

$$D_L = \frac{\Delta x^2}{3.625^2 t} = \frac{\left(x_{90\%} - x_{10\%}\right)^2}{3.625^2 t} \tag{5.3.2}$$

From **FIGURE 5.3.1**,

$$x_{90\%} = 61.8 \text{ cm}$$

$$x_{10\%} = 53.6 \text{ cm}$$

Substituting the numerical values into Eq.(5.3.2) gives the longitudinal dispersion coefficient as

$$D_L = \frac{(61.8 - 53.8)^2}{3.625^2 \times 2141.3} = 2.390 \times 10^{-3} \text{ cm}^2/\text{s}$$

$$D_L = \alpha_L u \tag{5.3.3}$$

$$\alpha_L = \frac{D_L}{u} = \frac{2.390 \times 10^{-3}}{2.667 \times 10^{-2}} = 0.0896 \text{ cm}$$

PROBLEM 5.4

Let $C_D = C/C_0$. The initial-boundary value problem for diffusion is

$$\frac{\partial C_D}{\partial t} - D_L \frac{\partial^2 C_L}{\partial x^2} = 0 \quad (5.4.1)$$

$$C_D(x,0) = 0 \quad (5.4.2)$$

$$C_D(0,t) = 1 \quad (5.4.3)$$

$$\lim_{x \to \infty} C_D(x,t) = 0 \quad (5.4.4)$$

The initial-boundary value problem can

be solved by Laplace transformation as was done in Problem 3.21 to obtain

$$C_D = erfc\left(\frac{x}{\sqrt{4D_L t}}\right) \tag{5.4.5}$$

$$x = 5 \text{ m}$$

$$D_L = 5\times 10^{-10} \text{ m}^2/\text{s}$$

$$t = 100 \text{ yrs}\times 365\frac{\text{D}}{\text{yr}}\times 86400\frac{\text{s}}{\text{D}} = 3.154\times 10^9 \text{ s}$$

Substituting the numerical values into Eq.(5.4.5) gives

$$C_D = erfc\left(\frac{5}{\sqrt{4\times 5\times 10^{-10}\times 3.154\times 10^9}}\right) = erfc(1.99091) = 0.004869$$

After 100 years of diffusion, the relative solvent concentration 5 meters away is only 0.005. It can be concluded that molecular diffusion is not a very effective mass transport mechanism in porous media.

PROBLEM 5.5

$$L = 30 \text{ cm}$$

$$d = 10 \text{ cm}$$

$$A = \pi\left(\frac{d}{2}\right)^2 = \pi\left(\frac{10}{2}\right)^2 = 78.5398 \text{ cm}^2$$

$$q = 1000 \text{ cm}^3/\text{hr} = 0.2778 \text{ cm}^3/\text{s}$$

$$u = \frac{q}{A\phi} = \frac{0.2778}{78.5398 \times 0.35} = 1.011 \times 10^{-2} \text{ cm/s}$$

$$\phi = 0.35$$

$$\nabla h = 0.1$$

$$\mu = 1.0 \text{ cp}$$

$$\rho = 1.0 \text{ g/cm}^3$$

$$g = 981 \text{ cm/s}^2$$

5.5a

$$C_D = \frac{1}{2} erfc\left[\sqrt{N_{Pe}}\left(\frac{x_D - t_D}{2\sqrt{t_D}}\right)\right] \tag{5.5.1}$$

$$t = 0.90\text{ hr} = 3.240 \times 10^3\text{ s}$$

$$t_D = \frac{qt}{A\phi L} = \frac{0.2778 \times 3.240 \times 10^3}{78.5398 \times 0.35 \times 30} = 1.0914$$

$$x_D = 1.0$$

$$C_D = 0.75$$

$$\frac{x_D - t_D}{2\sqrt{t_D}} = \frac{1 - 1.0914}{2\sqrt{1.0914}} = -0.0438$$

Substituting the numerical values into Eq.(5.5.1) gives

$$0.75 = \frac{1}{2} erfc\left(-0.0438\sqrt{N_{Pe}}\right)$$

$$erfc\left(-0.0438\sqrt{N_{Pe}}\right) = 1.50$$

$$erfc\left(-0.0438\sqrt{N_{Pe}}\right) = 1 + erf\left(0.0438\sqrt{N_{Pe}}\right) = 1.50$$

$$erf\left(0.0438\sqrt{N_{Pe}}\right) = 0.50$$

From linear interpolation,

$$0.0438\sqrt{N_{Pe}} = 0.45 + \left(\frac{0.520500 - 0.475482}{0.50 - 0.45}\right)(0.50 - 0.475482)$$

$$= 0.4721$$

$$N_{Pe} = \left(\frac{0.4721}{0.0438}\right)^2 = 116.3843$$

$$N_{Pe} = \frac{qL}{A\phi D_L} \tag{5.5.2}$$

$$D_L = \frac{qL}{A\phi N_{Pe}} = \frac{0.2778 \times 30}{78.5398 \times 0.35 \times 116.3843} = 2.605 \times 10^{-3}\ \text{cm}^2/\text{s}$$

$$\alpha_L = \frac{D_L}{u} = \frac{2.605 \times 10^{-3}}{1.011 \times 10^{-2}} = 0.2578\ \text{cm}$$

Also,

$$\alpha_L = \frac{L}{N_{Pe}} = \frac{30}{116.3843} = 0.2578 \text{ cm}$$

5.5b

From Darcy's law,

$$k = \frac{1.0133 \times 10^6 q\mu}{\rho g A \nabla h} \tag{5.5.3}$$

Substituting numerical values into Eq. (5.5.3) gives

$$k = \frac{\left(1.0133 \times 10^6\right)(0.2778)(1)}{(1)(981)(78.5398)(0.1)} = 36.53 \text{ D}$$

PROBLEM 5.6

5.6a

$$\Delta x = 3.625\sqrt{D_L t} \tag{5.6.1}$$

$$D_L = \frac{\Delta x^2}{3.625^2 t} \tag{5.6.2}$$

$$\Delta x = 8 \text{ cm}$$

$$t = 50 \text{ minutes } = 50 \times 60 = 3000 \text{ s}$$

Substituting the numerical values into Eq.(5.6.2) gives

$$D_L = \frac{8^2}{3.625^2 \times 3000} = 1.623 \times 10^{-3} \text{cm}^2/\text{s}$$

$$u = 1.6 \text{ cm/minute} = 1.6/60 = 2.667 \times 10^{-2} \text{ cm/s}$$

$$\alpha_L = \frac{D_L}{u} = \frac{1.623 \times 10^{-3}}{2.667 \times 10^{-2}} = 0.0609 \text{ cm}$$

5.6b

No. The core is heterogeneous. Since the fluid densities and viscosities are equal, the distortion in the concentration contours is caused by permeability heterogeneity of the core and not by gravity segregation. The lower half of the core is more permeable than the upper half.

5.6c

The dispersivity from the breakthrough curve will be larger than that computed in part (a) because the distortion in the concentration contours will cause the breakthrough curve to be more stretched out. This stretching out will result in a higher dispersivity from the breakthrough curve than from the mixing zone length in the core.

PROBLEM 5.7

5.7a

FIGURE 5.7.1 shows the expected solvent concentration profile at t_D = 0.50 pore volume injected. Note that C_D = 0.50 is located at x = L/2.

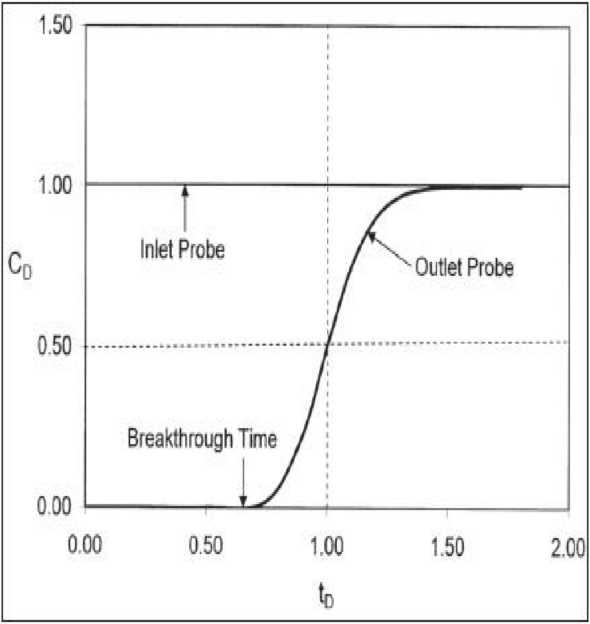

FIGURE 5.7.1 Solvent concentration profile at $t_D = 0.50$.

5.7b

FIGURE 5.7.2 shows the expected

solvent concentrations versus time at the inlet and outlet ends of the core.

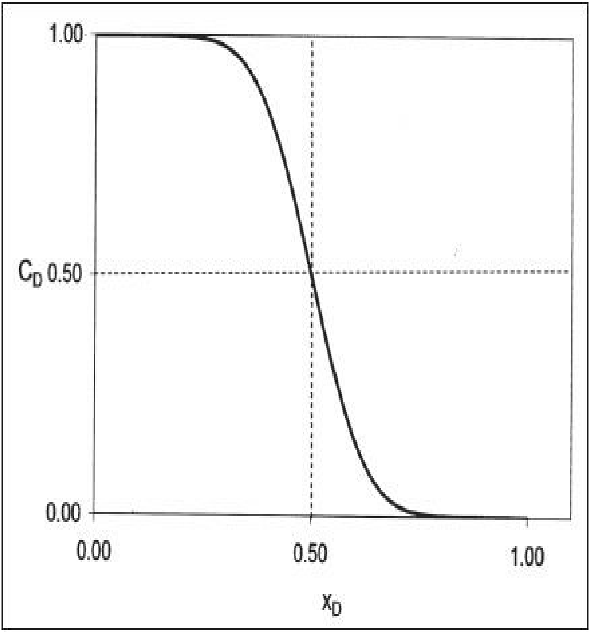

FIGURE 5.7.2 Solvent concentration versus time at the inlet and outlet of the core.

5.7c

Longitudinal dispersion coefficient and longitudinal dispersivity of the core can be determined from the experiment.

4.7d

$$L = 30 \text{ cm}$$

$$A = 20 \text{ cm}^2$$

$$q = 50 \text{ cm}^3/\text{hr} = 1.389 \times 10^{-2} \text{ cm}^3/\text{s}$$

$$\phi = 0.15$$

$$u = \frac{q}{A\phi} = \frac{1.389 \times 10^{-2}}{20 \times 0.15} = 4.630 \times 10^{-3} \text{ cm/s}$$

$$D_L = 400 \times 10^{-5} \, cm^2/s$$

$$C_D(1,t_D)=\frac{1}{2}erfc\left[\sqrt{N_{Pe}}\left(\frac{1-t_D}{2\sqrt{t_D}}\right)\right] \quad (5.7.1)$$

$$t = 108 \text{ minutes} = 108\times 60 = 6480 \text{ s}$$

$$t_D=\frac{qt}{A\phi L}=\frac{1.389\times 10^{-2}\times 6480}{20\times 0.15\times 30}=1.0$$

$$N_{Pe}=\frac{qL}{A\phi D_L}=\frac{1.389\times 10^{-2}\times 30}{20\times 0.15\times 400\times 10^{-5}}=34.7250$$

Substituting numerical values into Eq. (5.7.1) gives

$$C_D(1,t_D)=\frac{1}{2}erfc\left[\sqrt{34.7250}\left(\frac{1-1}{2\sqrt{1}}\right)\right]=\frac{1}{2}erfc(0)=0.50$$

PROBLEM 5.8

$$L = 30 \text{ cm}$$

$$u = 0.01 \text{ cm/s}$$

$$t = 46.6 \text{ minutes } = 46.6 \times 60 = 2796 \text{ s}$$

$$t_D = \frac{ut}{L} = \frac{(0.01)(2796)}{30} = 0.9320$$

$$x_D = 1.0$$

$$C_D = 0.42$$

$$C_D = \frac{1}{2} erfc\left[\sqrt{N_{Pe}}\left(\frac{x_D - t_D}{2\sqrt{t_D}}\right)\right] \qquad (5.8.1)$$

$$\frac{x_D - t_D}{2\sqrt{t_D}} = \frac{1-0.9320}{2\sqrt{0.9320}} = 0.0352$$

Substituting the numerical values into Eq.(5.8.1) gives

$$0.42 = \frac{1}{2} erfc\left(0.0352\sqrt{N_{Pe}}\right)$$

$$erfc\left(0.0352\sqrt{N_{Pe}}\right) = 0.84$$

$$0.0352\sqrt{N_{Pe}} = 0.14276$$

$$N_{Pe} = \left(\frac{0.14276}{0.0352}\right)^2 = 16.4313$$

$$\alpha_L = \frac{L}{N_{Pe}} = \frac{30}{16.4313} = 1.8258 \text{ cm}$$

PROBLEM 5.9

This problem can be solved using either of the following two equations:

$$\alpha_L = \frac{D_L}{u} = L\left(\frac{J_{0.90} - J_{0.10}}{3.625}\right)^2 \tag{5.9.1}$$

$$\alpha_L = \frac{D_L}{u} = \frac{L}{8}\left(J_{0.84} - J_{0.16}\right)^2 \tag{5.9.2}$$

Here, the problem is solved using both equations. **FIGURE 5.9.1** shows the graph of z versus J. The regression line is

$$z = -3.8643J - 0.0006 \tag{5.9.3}$$

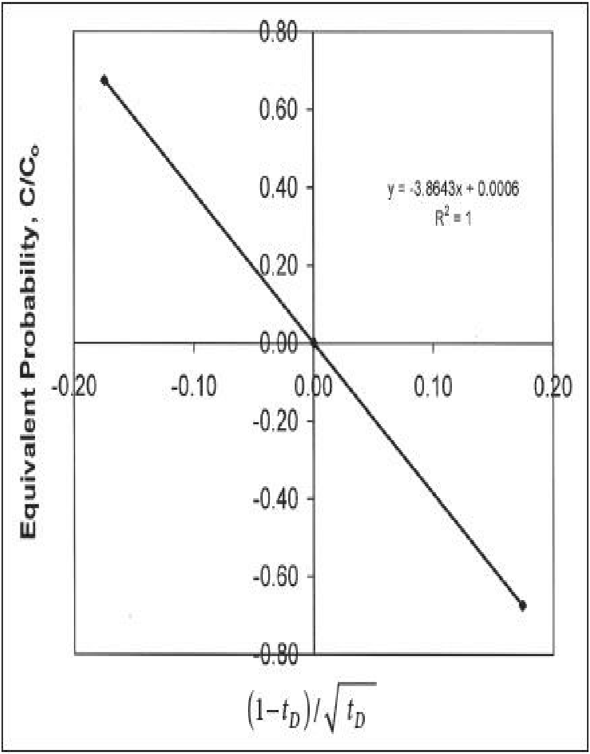

FIGURE 5.9.1 Graph of *z* verus *J* for Problem 5.9.

From the regression line,

$$J_{0.10} = 0.3318$$

$$J_{0.90} = -0.3315$$

$$J_{0.16} = 0.2589$$

$$J_{0.84} = -0.2586$$

Substituting the numerical values into Eq.(5.9.1) gives

$$\alpha_L = \frac{D_L}{u} = 30\left(\frac{-0.3315 - 0.3318}{3.625}\right)^2 = 1.0044 \text{ cm}$$

Substituting the numerical values into Eq.(5.9.2) gives

$$\alpha_L = \frac{D_L}{u} = \frac{30}{8}\left(-0.2586 - 0.2589\right)^2 = 1.0043 \text{ cm}$$

CHAPTER 6 SOLUTIONS

PROBLEM 6.1

$$\sigma = \left[\Lambda \left(\frac{\rho_L - \rho_g}{M} \right) \right]^4 \tag{6.1.1}$$

$$\Lambda = 351.5$$

$$\rho_L = 0.70 \text{ g/cm}^3$$

$$\rho_g = 0.0 \text{ g/cm}^3$$

$$M = 114.231 \text{ g/g} - \text{mol}$$

Substituting numerical values into Eq. (6.1.1) gives

$$\sigma = \left[351.5\left(\frac{0.70-0.0}{114.231}\right)\right]^4 = 21.52 \text{ dynes/cm}$$

Experimental value from TABLE 6.3 = 21.8 dynes/cm

$$\text{Error\%} = \frac{(21.8-21.52)}{21.8}\times 100 = 1.28\%$$

PROBLEM 6.2

The parachor for n-octane (C_8H_{18}) is given by

$$\Lambda = 8 \times 4.8 + 18 \times 17.1 = 346.2$$

Value from TABLE 6.2 = 351.5

$$\text{Error\%} = \frac{(351.5 - 346.3)}{351.5} \times 100 = 1.48\%$$

PROBLEM 6.3

For one drop, $m = 2.2/100 = 0.022$ g.

$$\rho = 0.773 \text{ g/cm}^3$$

$$V = \frac{m}{\rho} = \frac{0.022}{0.773} = 2.846 \times 10^{-2} \text{ cm}^3$$

$$r = 0.20 \text{ cm}$$

$$\frac{r}{V^{1/3}} = \frac{0.20}{\left(2.846 \times 10^{-2}\right)^{1/3}} = 0.6551$$

From linear interpolation,

$$f = 0.6171 + \left(\frac{0.6551 - 0.65}{0.70 - 0.65}\right)(0.6093 - 0.6171) = 0.6163$$

$$\sigma = \frac{mg}{2\pi rf} = \frac{0.022 \times 981}{2 \times \pi \times 0.20 \times 0.6163} = 27.87 \text{ dynes/cm}$$

Note that without the correction for the dynamics of the drop, the estimated surface tension would have been 17.17 dynes/cm, which is too low. Tabulated value in a TABLE of physical constants = 27.1 dynes/cm.

$$\text{Error\%} = \frac{(27.1 - 27.87)}{27.1} \times 100 = -2.84\%$$

PROBLEM 6.4

For horizontal equilibrium before the addition of Super XX,

$$\sigma_{so} = \sigma_{sw} + \sigma_{ow} \cos\theta \quad (6.4.1)$$

Let the addition of x ppm of Super XX be required to cause the changes indicated. At equilibrium,

$$\sigma_{so} = \sigma^*_{sw} + \sigma^*_{ow} \cos 0^\circ \quad (6.4.2)$$

$$\sigma^*_{sw} = \sigma_{sw} - 2x \quad (6.4.3)$$

$$\sigma^*_{ow} = \sigma_{ow} - 4x \quad (6.4.4)$$

Substituting Eqs.(6.4.3) and (6.4.4) into (6.4.2) and rearranging gives

$$x = \frac{\sigma_{sw} + \sigma_{ow} - \sigma_{so}}{6} \tag{6.4.5}$$

$$\sigma_{so} = 45 \text{ dynes/cm}$$

$$\sigma_{sw} = 30 \text{ dynes/cm}$$

$$\sigma_{ow} = 30 \text{ dynes/cm}$$

Substituting the numerical values into Eq.(6.4.5) gives

$$x = \frac{30 + 30 - 45}{6} = 2.50 \text{ ppm}$$

PROBLEM 6.5

The Amott wettability indices for water and oil are given by

$$WI_w = \frac{V_{oi}}{V_{oi} + V_{od}} \tag{6.5.1}$$

$$WI_o = \frac{V_{wi}}{V_{wi} + V_{wd}} \tag{6.5.2}$$

$$V_{oi} = 1.0 \text{ cm}^3$$

$$V_{od} = 1.8 \text{ cm}^3$$

$$V_{wi} = 0.2 \text{ cm}^3$$

$$V_{wd} = 1.95 \text{ cm}^3$$

Substituting the numerical values into Eqs.(6.5.1) and (6.5.2) gives

$$WI_w = \frac{1.0}{1.0+1.8} = 0.3571$$

$$WI_o = \frac{0.2}{0.2+1.95} = 0.0930$$

$$WI_w - WI_o = 0.3571 - 0.0930 = 0.2641 > 0.0$$

Therefore, the porous medium is water wet.

PROBLEM 6.6

6.6a

Let the radius of the circular cross-section be r, the length of each side of the square cross-section be l and the length of the shorter side of the 2×1 rectangular cross-section be x. Since the cross-sectional areas are equal,

$$\pi r^2 = l^2 = 2x^2 \qquad (6.6.1)$$

The perimeters for the circle, square and rectangle are $2\pi r,\ 41$, and 6x. We perform a force balance to determine the equilibrium capillary rise for each shape. For the circular cross-section, For the circular cross-section,

$$2\pi\sigma\cos\theta = (\rho_L - \rho_{air})gh_A\pi r^2 \quad (6.6.2)$$

$$h_A = \frac{2\pi r\sigma\cos\theta}{\Delta\rho g\pi r^2} = \frac{2\sigma\cos\theta}{r\Delta\rho g} \quad (6.6.3)$$

where

$$\Delta\rho = \rho_L - \rho_{air} \quad (6.6.4)$$

For the square cross-section,

$$4l\sigma\cos\theta = (\rho_L - \rho_{air})gh_B l^2 \quad (6.6.5)$$

$$h_B = \frac{4l\sigma\cos\theta}{\Delta\rho g l^2} = \frac{4\sigma\cos\theta}{l\Delta\rho g} \quad (6.6.6)$$

From Eq.(6.6.1),

$$l = r\sqrt{\pi} \tag{6.6.7}$$

Substituting Eq.(6.6.7) into (6.6.6) gives

$$h_B = \frac{4l\sigma\cos\theta}{\Delta\rho g r\sqrt{\pi}} = \frac{2.2568\sigma\cos\theta}{r\Delta\rho g} \tag{6.6.8}$$

For the rectangular cross-section,

$$6x\sigma\cos\theta = \left(\rho_L - \rho_{air}\right) g h_C 2x^2 \tag{6.6.9}$$

$$h_C = \frac{6x\sigma\cos\theta}{\Delta\rho g 2x^2} = \frac{3\sigma\cos\theta}{x\Delta\rho g} \tag{6.6.10}$$

From Eq.(6.6.1),

$$x = r\sqrt{\frac{\pi}{2}} \tag{6.6.11}$$

Substituting Eq.(6.6.11) into (6.6.10) gives

$$h_C = \frac{6r\sqrt{\pi/2}\sigma\cos\theta}{\Delta\rho g 2r^2\pi/2} = \frac{2.3937\sigma\cos\theta}{r\Delta\rho g} \tag{6.6.12}$$

A comparison of Eqs.(6.6.3), (6.6.8), and (6.6.12) shows that the highest capillary rise will occur in the tube with the rectangular cross-section.

6.6b

$$\frac{h_B}{h_A} = \frac{2.2568}{2} = 1.1284$$

$$\frac{h_C}{h_A} = \frac{2.3937}{2} = 1.1969$$

PROBLEM 6.7

$L = 60$ cm
$r = 50\ \mu m = 50 \times 10^{-4}$ cm
? = 72 dynes/cm
$\lambda = 0°$
$p_w = 1.0\ g/cm^3$

$$\rho_{nw} = 0.0\ g/cm^3$$
$$\Delta\rho = \rho_w - \rho_{nw} = 1 - 0 = 1\ g/cm^3$$
$$g = 981\ cm/s^2$$

6.7a

$$h = \frac{2\sigma\cos\theta}{r\Delta\rho g} = \frac{2 \times 72 \times \cos 0^{\circ}}{50 \times 10^{-4} \times 1 \times 981} = 29.3578\ \text{cm}$$

6.7b

Let α be the angle of inclination of the capillary tube with the vertical.

$$h\sin(90-\alpha)=\frac{2\sigma\cos\theta}{r\Delta\rho g} \qquad (6.7.1)$$

$$\alpha=45^{\circ}$$

$$h=\frac{2\sigma\cos\theta}{r\Delta\rho g\sin(90-\alpha)}=\frac{2\times72\times\cos0^{\circ}}{50\times10^{-4}\times1\times981\times\sin(90^{\circ}-45^{\circ})}$$

$$=41.5182\text{ cm}$$

6.7c

Let

P_{nw} = pressure of the trapped gas at equilibrium

P_w = pressure in the water just

below the gas water interface
P_a = atmospheric pressure

From Boyle's law,

$$P_a L = P_{nw}(L - h) \tag{6.7.2}$$

$$P_{nw} = \frac{P_a L}{L - h} \tag{6.7.3}$$

$$P_w = P_a - \rho g h \tag{6.7.4}$$

At equilibrium,

$$P_c = P_{nw} - P_w = \frac{2\sigma \cos\theta}{r} \tag{6.7.5}$$

Substituting Eqs.(6.7.3) and (6.7.4) into

(6.7.5) and rearranging gives

$$h^2 - \left(\frac{P_a + \rho g L + 2\sigma \cos\theta / r}{\rho g} \right) h + \frac{2\sigma L \cos\theta}{r \rho g} = 0 \tag{6.7.6}$$

$$P_a = 1.0133 \times 10^6 \text{ dynes/cm}^2$$

Substituting the numerical values into Eq.(6.7.6) gives

$$h^2 - \left(\frac{1.0133 \times 10^6 + 1 \times 981 \times 60 + 2 \times 72 \times 1 / 50 \times 10^{-4}}{1 \times 981} \right) h$$

$$+ \frac{2 \times 72 \times 60 \times 1}{50 \times 10^{-4} \times 1 \times 981} = 0 \tag{6.7.7}$$

$$h^2 - 1122.2834 h + 1761.4679 = 0 \tag{6.7.8}$$

Eq.(6.7.8) can be solved as

$$h = \frac{1122.2834 \pm \sqrt{1122.2834^2 - (4)(1)(1761.4679)}}{2}$$

$$h = \frac{1122.2834 \pm 1119.1399}{2}$$

h = 1.5717 cm or 1120.7116 cm, which is non-physical.

The impact of the trapped air in the equilibrium capillary rise is surprisingly high. The trapped gas has reduced the equilibrium height from 29.3578 cm to 1.5717 cm. This is a significant impact.

PROBLEM 6.8

$$\text{Force up} = 2\pi R\sigma\cos\theta + 2\pi r\sigma\cos\theta = 2\pi(R+r)\sigma\cos\theta \quad (6.8.1)$$

$$\text{Force down} = \pi\left(R^2 - r^2\right)\Delta\rho gh \quad (6.8.2)$$

At equilibrium, force up equals force down.

$$2\pi(R+r)\sigma\cos\theta = \pi\left(R^2 - r^2\right)\Delta\rho gh \quad (6.8.3)$$

$$h = \frac{2(R+r)\sigma\cos\theta}{\left(R^2 - r^2\right)\Delta\rho g} = \frac{2\sigma\cos\theta}{(R-r)\Delta\rho g} \quad (6.8.4)$$

The problem also can be solved by application of the Young-Laplace equation.

$$\Delta P = \sigma\left(\frac{1}{r_1}+\frac{1}{r_2}\right) = \Delta\rho g h \quad (6.8.5)$$

$$r_1 = \frac{(R-r)/2}{\cos\theta} = \frac{(R-r)}{2\cos\theta} \quad (6.8.6)$$

$$r_2 = \infty \quad (6.8.7)$$

Substituting Eqs.(6.8.6) and (6.8.7) into (6.8.5) gives

$$\Delta P = \sigma\left(\frac{2\cos\theta}{R-r}+0\right) = \Delta\rho g h \quad (6.8.8)$$

$$h = \frac{2\sigma \cos\theta}{(R - r)\Delta\rho g} \tag{6.8.9}$$

PROBLEM 6.9

When the experiment is repeated with the shorter capillary tube, the liquid will rise to the top and stop. It will not flow out of the top of the tube as one would intuitively expect.

Before the cut, application of Young-Laplace equation gives

$$\Delta P = \frac{2\sigma\cos\theta_1}{r} = \Delta\rho g h_1 \tag{6.9.1}$$

After the cut, application of Young-Laplace equation gives

$$\Delta P = \frac{2\sigma\cos\theta_2}{r} = \Delta\rho g h_2 \tag{6.9.2}$$

Dividing Eq.(6.9.2) by (6.9.1) and rearranging gives

$$h_2 = \frac{\cos\theta_2}{\cos\theta_1} h_1 \tag{6.9.3}$$

In the limit, as $h_2 \rightarrow 0$, $\lambda_2 \rightarrow 90°$. The liquid will never overflow no matter how small h_2 is.

PROBLEM 6.10

$$r_1 = 1 \text{ cm}$$

$$r_2 = 2 \text{ cm}$$

$$\sigma = 25 \text{ dynes/cm}$$

$$W = -\sigma(dA) \qquad (6.10.1)$$

$$dA = 2 \times 4\pi\left(r_2^2 - r_1^2\right) \qquad (6.10.2)$$

where the factor of 2 accounts for the fact that the soap bubble has two air-liquid interfaces. Substituting Eq. (6.10.2) into (6.10.1) gives

$$W = -\sigma \times 2 \times 4\pi \left(r_2^2 - r_1^2 \right) \tag{6.10.3}$$

Substituting the numerical values into Eq.(6.10.3) gives

$$W = -25 \times 2 \times 4\pi \left(2^2 - 1^2 \right) = -672,427 \text{ ergs}$$

The negative sign indicates that work is done on the system.

PROBLEM 6.11

$p_w = 1\ g/cm^3$

$p_{air} \approx 0 g/cm^3$

$\sigma = 72$ dynes/cm

$\Theta = 0°$

$g = 981\ cm/s^2$

$r = 50 \times 10^{-6} m = 50 \times 10^{-4} cm$

6.11a

In order for the water to drain from the overhanging portion of the capillary tube into container B, the gravity driving force must exceed the capillary retention force preventing drainage. In other words, the hydrostatic pressure exerted by the column of water must exceed the capillary pressure at the end of the tube. This condition can be expressed mathematically based on our knowledge of capillarity as

$$(\rho_w - \rho_{air})gh > \frac{2\sigma\cos\theta}{r} \tag{6.11.1}$$

or

$$h > \frac{2\sigma\cos\theta}{(\rho_w - \rho_{air})gr} \tag{6.11.2}$$

Substituting the numerical values into Eq.(6.11.2) gives the requirement for successful siphoning of the water as

$$h > \frac{(2)(72)(1)}{(1-9)(981)\left(50\times10^{-4}\right)} = 29.36 \text{ cm}$$

In the current design, h = 20 cm, which is not sufficient for the gravity driving force to exceed the capillary retention force. Therefore, as currently designed, the experiment will not be successful in siphoning water spontaneously from container A to container B. The water will imbibe and then stop at the end of the capillary tube. We can calculate the equilibrium contact angle from the equation:

$$\frac{2\sigma\cos\theta}{r} = \left(\rho_w - \rho_{air}\right)gh$$

Or

$$\cos\theta = \frac{(\rho_w - \rho_{air})ghr}{2\sigma} = \frac{(1-0)(981)(20)(50x10^{-4})}{(2)(72)} = 0.6813$$

$$\theta = 47^\circ$$

6.11b

Make the length of the overhanging portion of the capillary tube (h) greater than 29.36 cm.

CHAPTER 7 SOLUTIONS

PROBLEM 7.1

The total work done by the pressure and capillary forces is given by

$$\delta W = -P_o \Delta V_o - P_w \Delta V_w + \sigma_{ow} \Delta A \tag{7.1.1}$$

Before displacement,

$$V_{o1} = \frac{4}{3}\pi R^3 \tag{7.1.2}$$

After displacement,

$$V_{o2} = \frac{4}{3}\pi (R+dR)^3 = \frac{4}{3}\pi \left[R^3 + 3R^2 dR + 3R(dR)^2 + (dR)^3 \right] \tag{7.1.3}$$

If the terms $(dR)^2$ and $(dR)^3$ are neglected in comparison to the other terms, Eq.(7.1.3) becomes

$$V_{o2} = \frac{4}{3}\pi(R+dR)^3 = \frac{4}{3}\pi\left(R^3 + 3R^2 dR\right) \quad (7.1.4)$$

$$\Delta V_o = V_{o2} - V_{o1} = \frac{4}{3}\pi\left(R^3 + 3R^2 dR - R^3\right) = 4\pi R^2 dR \quad (7.1.5)$$

$$\Delta V_w = -\Delta V_o = -4\pi R^2 dR \quad (7.1.6)$$

Before displacement,

$$A_1 = 4\pi R^2 \quad (7.1.7)$$

After displacement,

$$A_2 = 4\pi(R+dR)^2 = 4\pi\left[R^2 + 2RdR + (dR)^2\right] \quad (7.1.8)$$

If the term $(dR)^2$ is neglected in comparison to the other terms, Eq. (7.1.8) becomes

$$A_2 = 4\pi(R+dR)^2 = 4\pi\left(R^2 + 2RdR\right) \quad (7.1.9)$$

$$\Delta A = A_2 - A_1 = 4\pi\left(R^2 + 2RdR\right) - 4\pi R^2 = 8\pi RdR \quad (7.1.10)$$

Substituting Eqs.(7.1.5), (7.1.6), and (7.1.10) into Eq.(7.1.1) gives

$$\delta W = -P_o\left(4\pi R^2 dR\right) + P_w\left(4\pi R^2 dR\right)_w + \sigma_{ow}\left(8\pi RdR\right) \quad (7.1.11)$$

At equilibrium, $\delta W = 0$ and Eq.(7.1.11) becomes upon rearrangement

$$P_o - P_w = \frac{2\sigma_{ow}}{R} \quad (7.1.12)$$

Eq.(7.1.12) is the special form of the Young-Laplace equation for a spherical liquid drop.

PROBLEM 7.2

7.2a

Young-Laplace equation gives

$$\Delta P = \sigma\left(\frac{1}{r_1}+\frac{1}{r_2}\right) \tag{7.2.1}$$

For the meniscus,

$$r_1 = -\frac{H/2}{\cos\theta} = -\frac{H}{2\cos\theta} \tag{7.2.2}$$

$$r_2 = R \tag{7.2.3}$$

Substituting Eqs.(7.2.2) and (7.2.3) into (7.2.1) gives

$$\Delta P = P_{film} - P_{air} = \sigma\left(-\frac{2\cos\theta}{H} + \frac{1}{R}\right) = \sigma\left(\frac{1}{R} - \frac{2\cos\theta}{H}\right) \quad (7.2.4)$$

7.2b

The pressure in the film is obtained from Eq.(7.2.4) as

$$P_{film} = P_{air} + \sigma\left(\frac{1}{R} - \frac{2\cos\theta}{H}\right) \quad (7.2.5)$$

Given:

$\sigma = 72$ dynes/cm
$\theta = 0^{\circ}$
$R = 1$ cm
$H = 5\ \mu\text{m} = 5\times10^{-6} = 5\times10^{-4}$ cm

$$P_{film} = 1 + \frac{72\left(\frac{1}{1} - \frac{2\cos 0^{\circ}}{5\times10^{-4}}\right)}{1.0133\times10^{6}} = 1 - \frac{287{,}928}{1.0133\times10^{6}}$$

$$= 1 - 0.2841 = 0.7159 \text{ atm}$$

Notice that the pressure in the film is less than the atmospheric pressure. The adhesive force is caused by the pressure difference between the film and the outside air. This is an attractive force that glues the plates together. The force is given by

$$F = \Delta P \times Area = \Delta P \times \pi R^2 \tag{7.2.6}$$

$$F = -287{,}928 \frac{\text{dynes}}{\text{cm}^2} \times \pi (1)^2 \text{ cm}^2 = -904{,}552 \text{ dynes}$$

$$= -9.046 \text{ Newtons}$$

The negative sign indicates an attractive force.

PROBLEM 7.3

FIGURE 7.3.1 shows the pressure profile in the capillary tube.

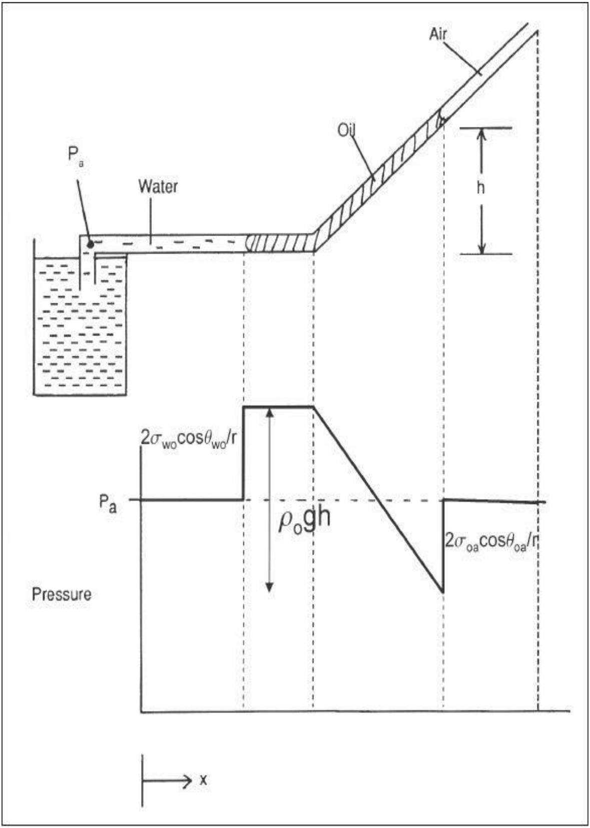

FIGURE 7.3.1 Pressure profile in the capillary tube.

PROBLEM 7.4

7.4a

Young-Laplace equation applied to bubble A gives

$$P_A - P_a = \frac{4\sigma}{r_A} = \frac{4\sigma}{4R} = \frac{\sigma}{R} \qquad (7.4.1)$$

$$P_A = P_a + \frac{\sigma}{R} \qquad (7.4.2)$$

For bubble B,

$$P_B - P_a = \frac{4\sigma}{r_B} = \frac{4\sigma}{R} \qquad (7.4.3)$$

$$P_B = P_a + \frac{4\sigma}{R} \tag{7.4.4}$$

7.4b

It is apparent that $P_b P_a$. Therefore, when valve 1 is opened, air will flow from B to A until pressure equilibrium is achieved. Bubble B will "shrink" while bubble A will be enlarged.

7.4c

FIGURE 7.4.1 shows the sketch of the final equilibrium configurations of the two bubbles.

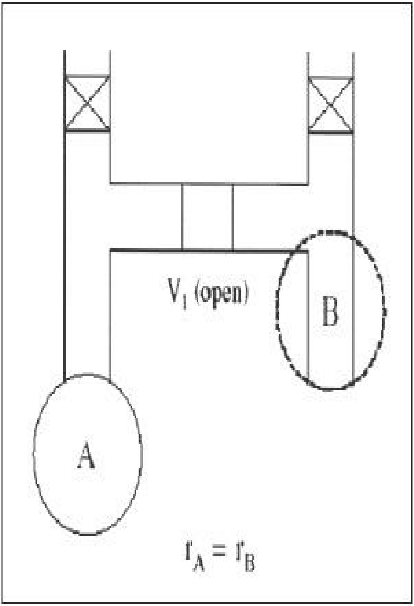

FIGURE 7.4.1 Sketch of final equilibrium configurations of A and B.

7.4d

At equilibrium, to satisfy the Young-

Laplace equation, the radii of the two bubbles must be equal. However, only a small piece of B remains and lies on an imaginary sphere with the same radius as A.

PROBLEM 7.5

7.5a

From Pythagoras Theorem,

$$R^2+(r_1+r_2)^2=(R+r_1)^2 \tag{7.5.1}$$

Expansion of the terms in Eq.(7.5.1) gives

$$R^2+r_1^2+2r_1r_2+r_2^2=R^2+2Rr_1+r_1^2 \tag{7.5.2}$$

Simplification of Eq.(7.5.2) gives

$$r_2^2+2r_1r_2-2Rr_1=0 \tag{7.5.3}$$

Solving Eq.(7.5.3) for r_1 gives

$$r_1 = \frac{r_2^2}{2(R - r_2)} \tag{7.5.4}$$

Eq.(7.5.3) also can be solved for r_2 in terms of r_1 to obtain

$$r_2 = r_1\left[\left(1 + \frac{2R}{r_1}\right)^{1/2} - 1\right] \tag{7.5.5}$$

Although it may not be obvious, $r_1 r_2$.

7.5b

Application of the Young-Laplace equation gives

$$\Delta P = P_w - P_{nw} = -P_c = \sigma\left(\frac{1}{r_2} - \frac{1}{r_1}\right) \qquad (7.5.6)$$

$$r_2 = 10\ \mu\text{m} = 10\times10^{-4}\ \text{cm}$$

$$R = 80\ \mu\text{m} = 80\times10^{-4}\ \text{cm}$$

$$\sigma = 72\ \text{dynes/cm}$$

$$r_1 = \frac{r_2^2}{2(R-r_2)} = \frac{\left(10\times10^{-4}\right)^2}{2\left(80\times10^{-4} - 10\times10^{-4}\right)} = 0.71429\times10^{-4}\ \text{cm}$$

Substituting the numerical values into Eq.(7.5.6) gives

$$\Delta P = P_w - P_{nw} = -P_c = 72\left(\frac{1}{10\times10^{-4}} - \frac{1}{0.71429\times10^{-4}}\right)$$

$$= -935{,}993.9520 \text{ dynes/cm}^2$$

$$= -\frac{935{,}993.9520}{1.0133\times10^{6}}\times14.696 = -13.57 \text{ psi}$$

$$P_c = P_{nw} - P_w = 13.57 \text{ psi}$$

7.5c

The force of adhesion binding the grains together is given by

$$F = \Delta P\times\pi r_2^2 = -935{,}993.9520\times\pi\times\left(10\times10^{-4}\right)^2 = -2.9405 \text{ dynes}$$

$$= -2.9405\times10^{-5} \text{ Newton}$$

The negative sign indicates an attractive force.

PROBLEM 7.6

7.6a

FIGURE 7.6.1 shows the pressure profiles in the capillary tubes.

7.6b

Application of Hagen-Possueille's equation to capillary tube *i* gives

$$u_i = \frac{dx_i}{dt} = \frac{r_i^2}{8\mu}\frac{\Delta P}{x_i} \tag{7.6.1}$$

For the forced imbibition,

$$\Delta P = P_a + \rho g h - P_w \tag{7.6.2}$$

At the water-air interface,

$$P_a - P_w = \frac{2\rho\cos\theta}{r_i} \tag{7.6.3}$$

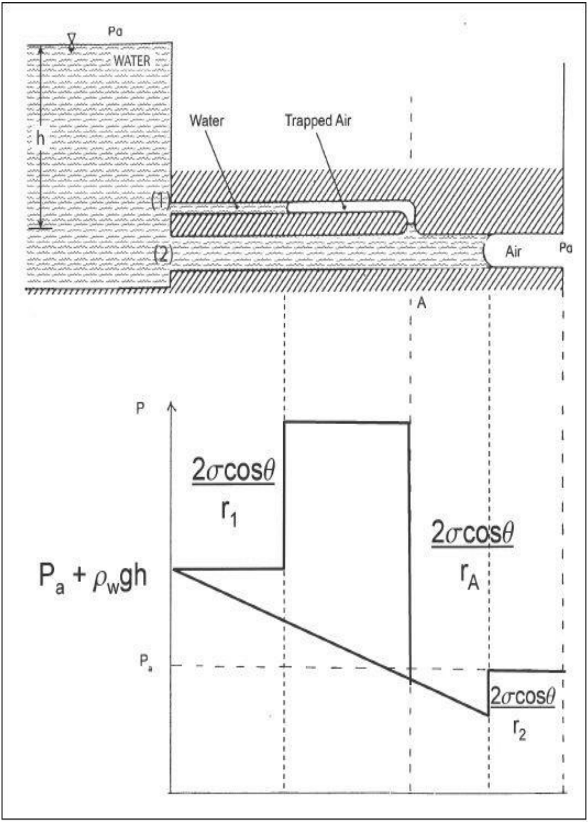

FIGURE 7.6.1 Pressure profiles in the capillary tubes for forced imbition.

Substituting Eq.(7.6.3) into (7.6.2) gives

$$\Delta P = \frac{2\sigma\cos\theta}{r_i} + \rho g h \tag{7.6.4}$$

Substituting Eq.(7.6.4) into (7.6.1) and rearranging gives

$$x_i \frac{dx_i}{dt} = \frac{r_i^2}{8\mu}\left(\frac{2\sigma\cos\theta}{r_i} + \rho g h\right) \tag{7.6.5}$$

Integration of Eq.(7.6.5) gives

$$\frac{1}{2}x_i^2 = \frac{r_i^2}{8\mu}\left(\frac{2\sigma\cos\theta}{r_i} + \rho g h\right)t + C \tag{7.6.6}$$

where C is the integration constant.

Applying the initial condition $x_i = 0$ at $t = 0$ gives $C = 0$. Rearranging Eq.(7.6.6) gives

$$x_i = \sqrt{\frac{r_i^2}{4\mu}\left(\frac{2\sigma\cos\theta}{r_i} + \rho g h\right)t} \tag{7.6.7}$$

PROBLEM 7.7

7.7a

FIGURE 7.7.1 shows the pressure profiles in the capillary tubes.

7.7b

Application of Hagen-Possueille's equation to capillary tube *i* gives

$$u_i = \frac{dx_i}{dt} = \frac{r_i^2}{8\mu}\frac{\Delta P}{x_i} \tag{7.7.1}$$

For the spontaneous imbibition,

$$\Delta P = P_a - P_w \tag{7.7.2}$$

At the water-air interface,

$$P_a - P_w = \frac{2\rho\cos\theta}{r_i} \tag{7.7.3}$$

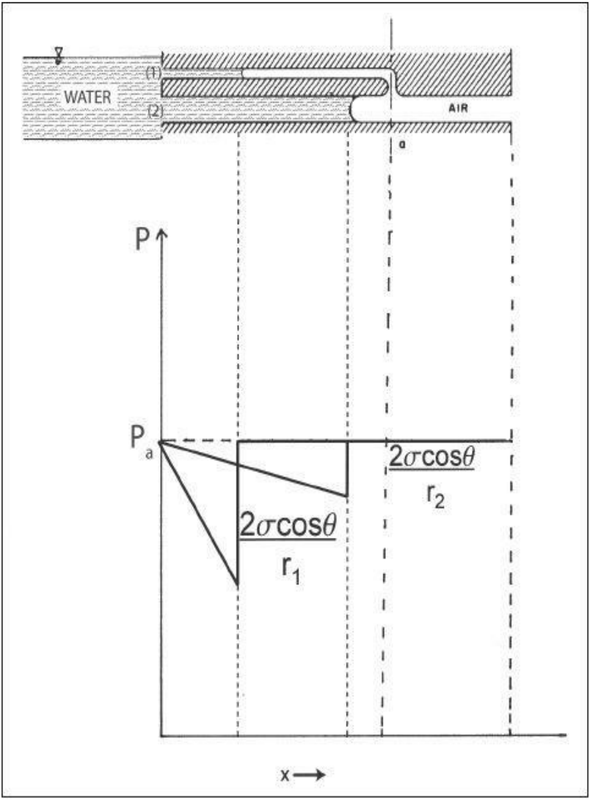

FIGURE 7.7.1 Pressure profiles in the capillary tubes for spontaneous imbibition.

Substituting Eq.(7.7.3) into (7.7.2) gives

$$\Delta P = \frac{2\sigma \cos\theta}{r_i} \tag{7.7.4}$$

Substituting Eq.(7.7.4) into (7.7.1) and rearranging gives

$$x_i \frac{dx_i}{dt} = \frac{r_i \sigma \cos\theta}{4\mu} \tag{7.7.5}$$

Integration of Eq.(7.7.5) gives

$$\frac{1}{2} x_i^2 = \frac{\sigma r_i \cos\theta}{4\mu} t + C \tag{7.7.6}$$

where C is the integration constant. Applying the initial condition $x_i = 0$ at t

= 0 gives $C = 0$. Rearranging Eq.(7.7.6) gives

$$x_i = \sqrt{\frac{r_i \sigma \cos\theta}{2\mu} t} \tag{7.7.7}$$

PROBLEM 7.8

7.8a

FIGURE 7.8.1 shows the pressure profiles in the capillary tubes.

7.8b

The distance L traveled by the meniscus in capillary tube 2 is given by

$$L = \sqrt{\frac{r_2 \sigma \cos\theta}{2\mu} t} \qquad (7.8.1)$$

The time at which air is trapped in capillarity tube 1 is obtained from Eq. (7.8.1) as

$$t = \frac{2\mu L^2}{r_2 \sigma \cos\theta} \tag{7.8.2}$$

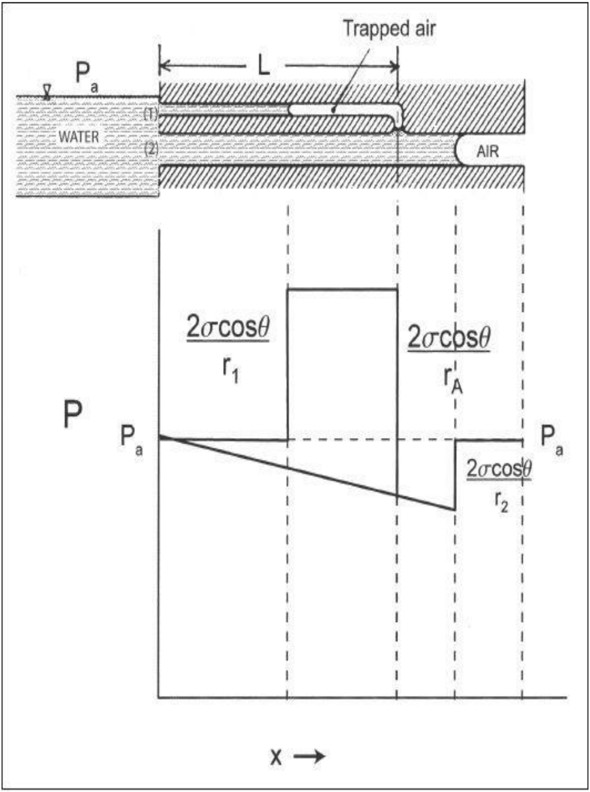

FIGURE 7.8.1 Pressure profiles in the capillary tubes for spontaneous imbibition with trapping.

PROBLEM 7.9

7.9a

Before imbibition,

$$S_w = S_{wirr} = 20\%$$

$$P_c = 20\,psi$$

FIGURE 7.9.1 shows a sketch of the capillary pressure profile before imbibition.

7.9b

Before imbibition,

$$\frac{\partial P_c}{\partial x} = 0 \text{ for } 0 \leq x < x_{inlet}$$

$$\frac{\partial P_c}{\partial x} = +\infty \text{ for } x = x_{inlet}$$

This positive capillary pressure gradient causes spontaneous imbibition of water into the core.

$$\frac{\partial P_c}{\partial x} = 0 \text{ for } x_{inlet} < x < x_{outlet}$$

$$\frac{\partial P_c}{\partial x} = -\infty \text{ for } x = x_{outlet}$$

This negative capillary pressure gradient causes capillary end effect at the outlet of the core and prevents water production from the outlet end of the core.

$$\frac{\partial P_c}{\partial x} = 0 \text{ for } x_{outlet} < x \leq L$$

FIGURE 7.9.1 shows a sketch of the capillary pressure gradient before imbibition.

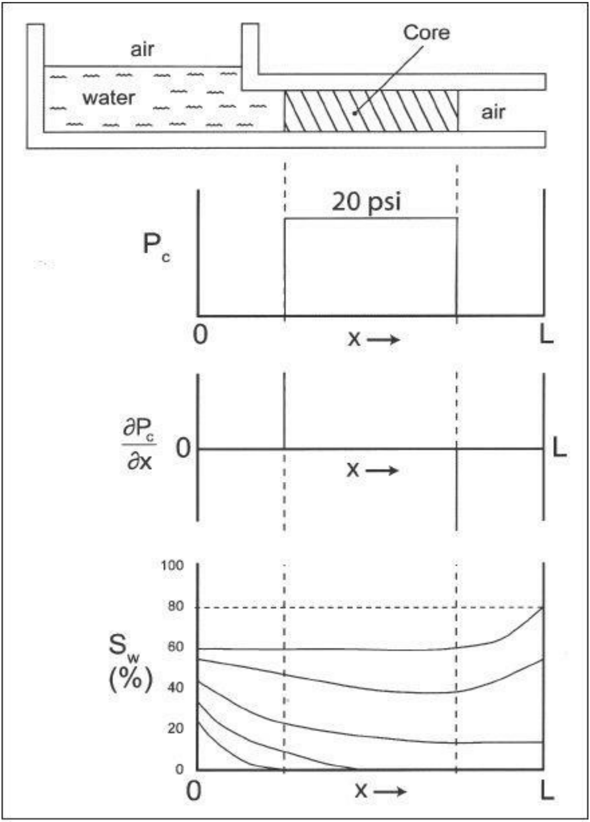

FIGURE 7.9.1 Spontaneous imbibition experiment.

7.9c

Figure 7.9.1 shows a sketch of the water saturation profiles during imbibition. Note the presence of capillary end effect.

7.9d

No. Water will not be produced from the core because of capillary end effect. The displacement is capillary driven with a very low flow rate that is not high enough to overcome the capillary end effect. After the water saturation at the outlet builds up to 0.80, the imbibition will stop. Note that capillary driven displacement will not have a Buckley-Leverett displacement front. The front is smeared by capillarity.

PROBLEM 7.10

7.10a

FIGURE 7.10.1 shows the pressure profile in the capillary tube.

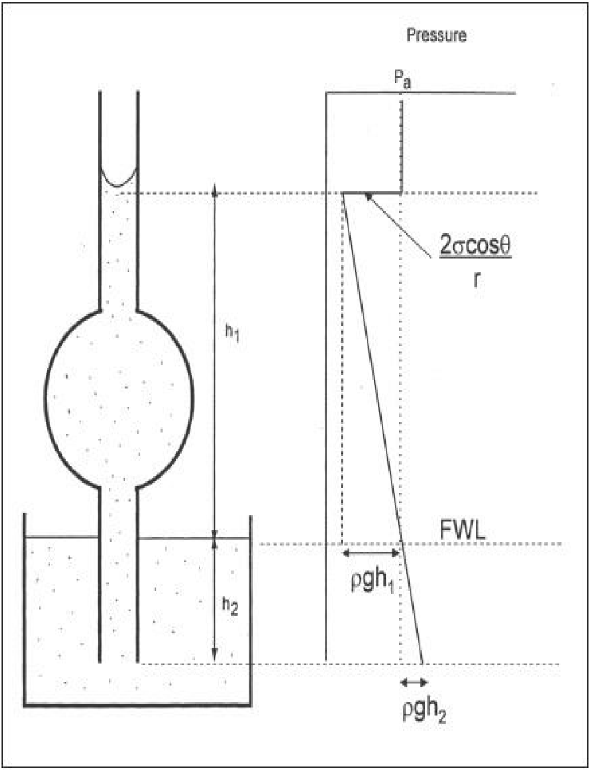

FIGURE 7.10.1 Pressure profile in the capillary tube with an enlargement.

7.10b

Dip the dry capillary tube into the water and suck the water to the top of the capillary tube. Allow the water in the capillary tube to drain to the equilibrium height h_1.

PROBLEM 7.11

7.11a

FIGURE 7.11.1 shows the air and water pressures in Core #1 for the spontaneous imbibition experiment. Because the core is long, water is imbibed to a maximum height lower than point C. The water pressure terminates at this height. The air pressure extends from A to C because there is air in the entire column in the imbibition experiment.

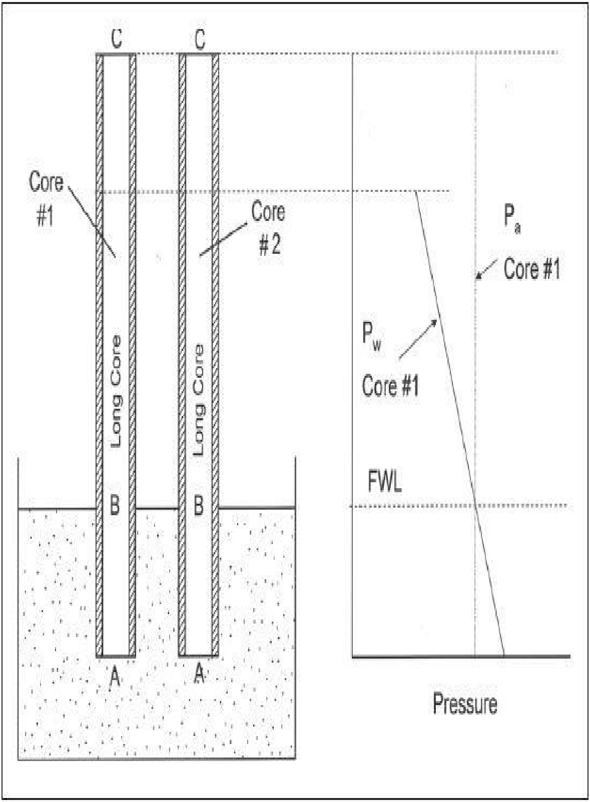

FIGURE 7.11.1 Water and air pressures in Core #1 (imbibition).

FIGURE 7.11.2 shows the air and water pressures in Core #2 for the drainage experiment. In this case, the water pressure extends from A to C because there is water in the entire column. There is a water-air contact (WAC) above the free water level (FWL). The air pressure terminates at the water-air contact because there is no air below this level. The capillary pressure at the water-air contact is equal to the displacement pressure of the core.

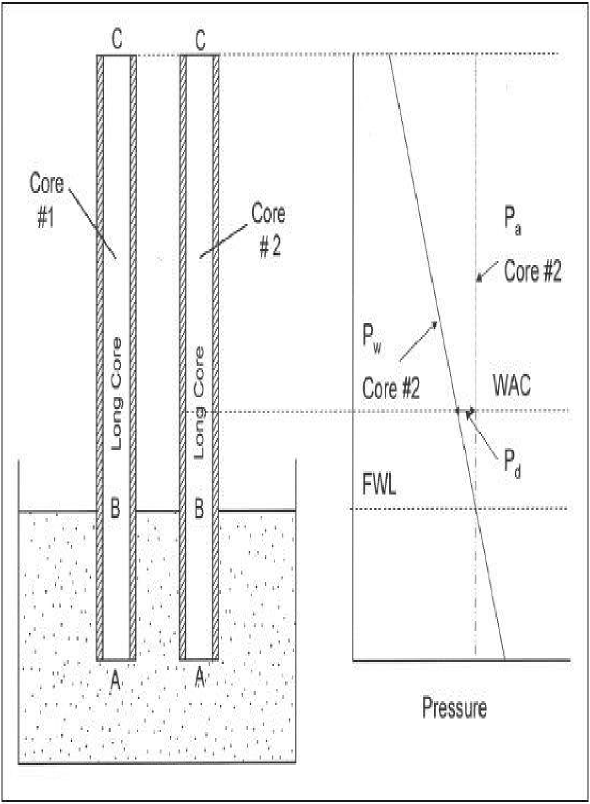

FIGURE 7.11.2 Water and air pressures in Core #2 (drainage).

7.11b

In general,

$$P_c = P_a - P_w = \pm\Delta\rho g z \tag{7.11.1}$$

where z is the height above or below the free water level. For the imbibition experiment (Core #1),

$$z_A = -h_{AB} = -100 \text{ cm}$$

$$P_{cA1} = 1.02 \times 981 \times (-100) = -100{,}062 \text{ dynes/cm}^2$$

$$= \frac{-100{,}062}{1.0133 \times 10^6} = -0.0987 \text{ atm}$$

$P_{cB1} = 0$ because B is at the free water level.

$P_{cC1} = 0$ because there is only single phase air at C.

For the drainage experiment (Core #2),

$$P_{cA2} = 0 \text{ because there is only single phase water at A.}$$

$$P_{cB2} = 0 \text{ because B is at the free water level.}$$

$$z_C = h_{BC} = 350 \text{ cm}$$

$$P_{cC2} = 1.02 \times 981 \times 350 = 350{,}217 \text{ dynes/cm}^2$$

$$= \frac{350{,}217}{1.0133 \times 10^6} = 0.3456 \text{ atm}$$

7.11c

FIGURE 7.11.3 shows the water saturation distributions in Core #1 and Core #2. In Core #1, the water saturation below the free water level is less than 1.0 because some air is trapped below this level. It could be argued that over a long period, this trapped air will dissolve in the water as water has some solubility for air. However, the sketch in Figure 7.11.3 does not reflect this possibility. In Core #2, the water saturation is 1.0 from A to the water=air contact. There is also irreducible water saturation at the top.

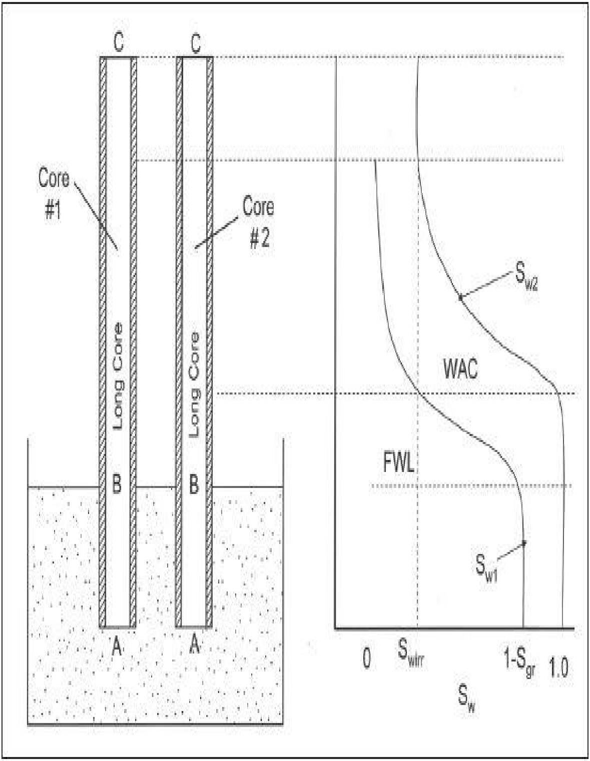

FIGURE 7.11.3 Water saturation distributions for the imbibition and drainage experiments.

PROBLEM 7.12

7.12a

In general,

$$P_c = P_a - P_w = \pm\Delta\rho g z \quad (7.12.1)$$

where *z* is the height above or below the free water level.

$$z_A = -h_{AB} = -100cm \text{ cm}$$

$$P_{cA} = 1.02 \times 981 \times (-100) = -100{,}062 \text{ dynes/cm}^2$$

$$= \frac{-100{,}062}{1.0133 \times 10^6} = -0.0987 \text{ atm}$$

$P_{cB} = 0$ because B is at the free water level.

$$z_C = h_{BC} = 200 \text{ cm}$$

$$P_{cC} = 1.02 \times 981 \times 200 = 200{,}124 \text{ dynes/cm}^2$$

$$= \frac{200{,}124}{1.0133 \times 10^6} = 0.1975 \text{ atm}$$

7.12 b

FIGURE 7.12.1 shows the sketch of the permeability profile of the core.

7.12c

We need to relate permeability to height along the core. Assume the core has the same pore structure from the bottom to the top. Therefore, it will have the same Leverett *J*-funtion.

$$J(S_w = 0.50) = \frac{P_c}{\sigma \cos\theta}\sqrt{\frac{k}{\phi}} \qquad (7.12.2)$$

$$P_c = \Delta \rho g h \qquad (7.12.3)$$

Substituting Eq.(7.12.3) into (7.12.2) and solving for *k* gives

$$k = \left[\frac{J(S_w = 0.50)\sigma \cos\theta}{\Delta \rho g}\right]^2 \frac{\phi}{h^2} = \frac{C_1}{h^2} \qquad (7.12.4)$$

where C_1 is a constant. Permeability decreases with height along the core in the manner indicated by Eq.(7.12.4). This is the justification for the sketch in Figure 7.12.1.

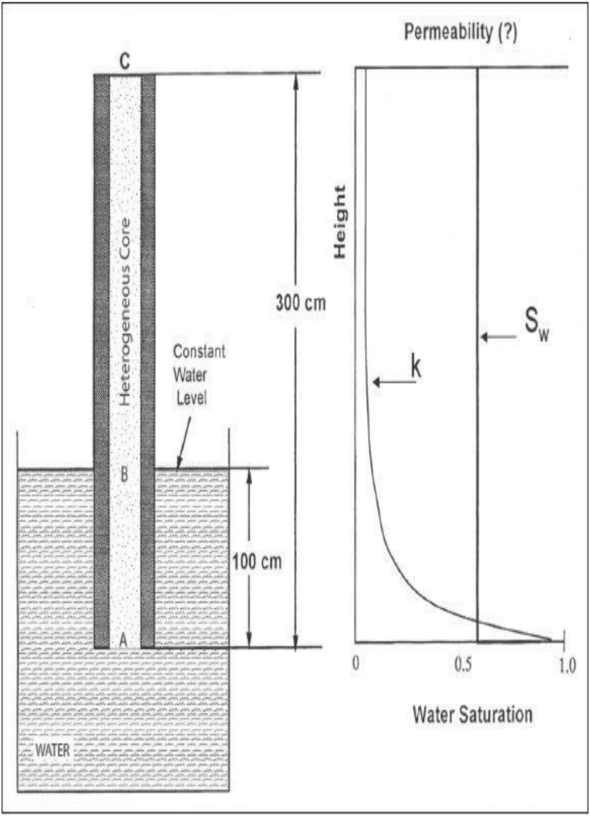

FIGURE 7.12.1 Sketch of permeability versus height along the core.

7.12c

Permeability is proportional to the square of the grain size.

$$k = C_2 D_p^2 \qquad (7.12.5)$$

where C_2 is a constant of proportionality and D_p is the grain size. Substituting Eq. (7.12.5) into (7.12.4) and solving for D_p gives

$$D_p = \frac{\sqrt{C_1 / C_2}}{h} = \frac{C_3}{h} \qquad (7.12.6)$$

Grain size decreases with height from the bottom to the top.

7.12d

FIGURE 7.12.2 shows the drainage capillary pressure curves for Samples A, B, and C. Based on the variation of permeability and grain size with height along the core, Sample A is the best quality rock and C is the least quality rock. The sketches in Figure 7.12.2 reflect these facts.

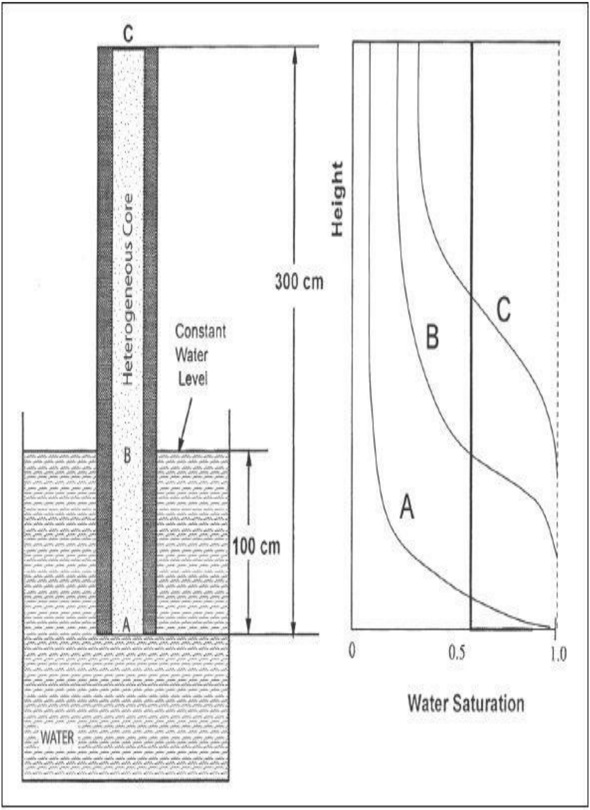

FIGURE 7.12.2 Drainage capillary pressure curves for Samples A, B, and C.

PROBLEM 7.13

7.13a

FIGURE 7.13.1 shows the mercury capillary pressure curve.

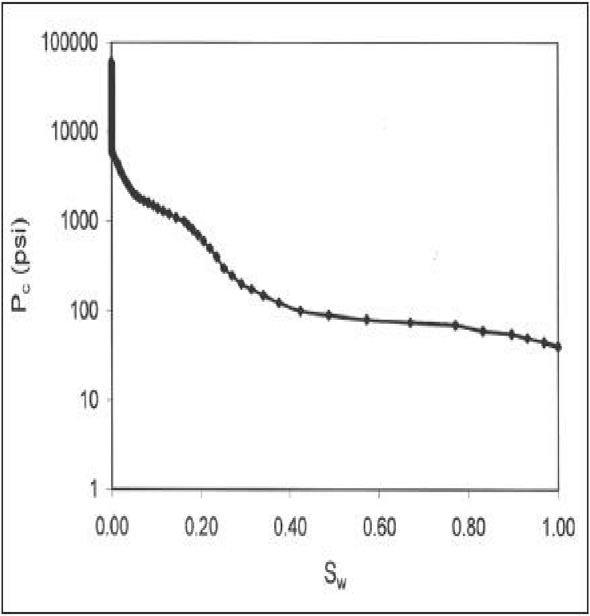

FIGURE 7.13.1 Mercury capillary pressure curve.

7.13b

The Leverett *J*-function in consistent

units is given by

$$J = \frac{P_c}{\sigma \cos\theta} \sqrt{\frac{k}{\phi}} \qquad (7.13.1)$$

Applying the required unit conversions to make / dimensionless leads to

$$J=\frac{(P_c/14.696)\times 1.0133\times 10^6}{\sigma\cos\theta}\sqrt{\frac{(k/1000)\times 9.869\times 10^{-9}}{\phi}}$$

$$=0.2166\frac{P_c}{\sigma\cos\theta}\sqrt{\frac{k}{\phi}} \quad (7.13.2)$$

$$k=3.86\text{ mD}$$

$$\phi=0.132$$

$$\sigma=480\text{ dynes/cm}$$

$$\theta=140^\circ$$

FIGURE 7.13.2 shows the Leverett *J*-function.

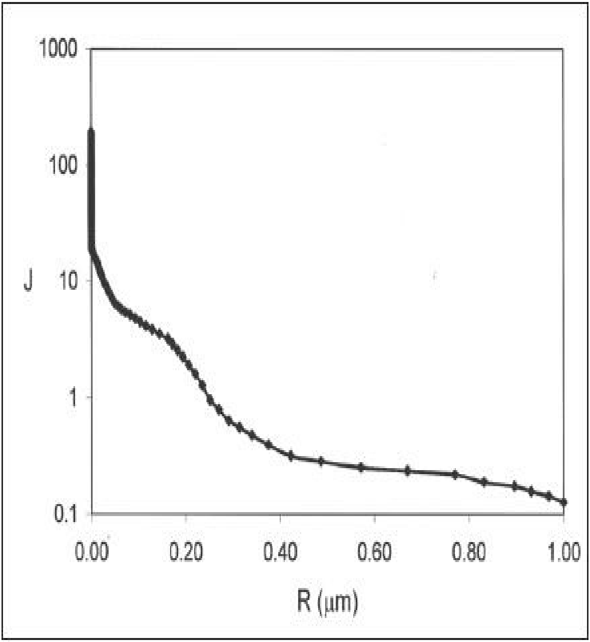

FIGURE 7.13.2 Leverett J-function.

7.13c

At reservoir conditions,

$$P_c = \frac{J \times \sigma \cos\theta}{0.2166\sqrt{k/\phi}} \quad (7.13.3)$$

$$k = 500 \text{ mD}$$

$$\phi = 0.25$$

$$\sigma = 35 \text{ dynes/cm}$$

$$\theta = 0^\circ$$

FIGURE 7.13.3 shows a comparison of the mercury and reservoir conditions' capillary pressure curves.

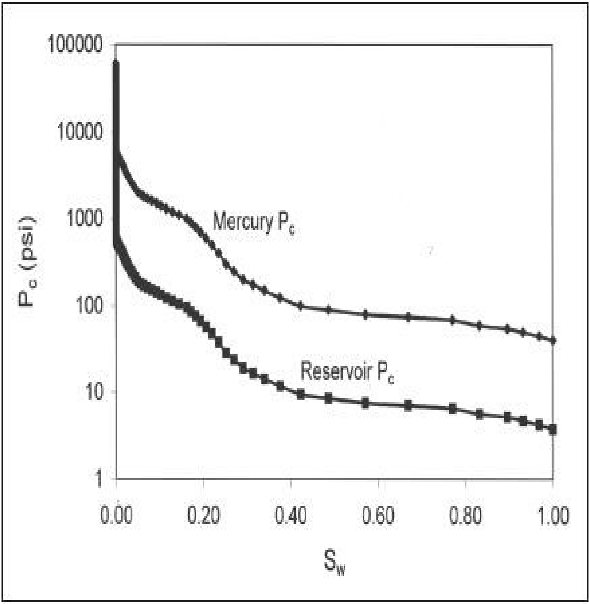

FIGURE 7.13.3 A comparison of the mercury and reservoir conditions' capillary pressure curves.

7.13d

The pore throat radius is given by

$$R = \frac{2\sigma|\cos\theta|}{P_c} \quad (7.13.4)$$

Substituting the numerical values into Eq.(7.13.4) and applying the unit conversions gives the pore throat radius in microns as

$$R = \frac{2\sigma|\cos\theta|}{P_c} = \frac{2\times 480|\cos 140^{\circ}|}{(P_c/14.696)\times 1.0133\times 10^{6}}\times 10^{4} = \frac{1.067\times 10^{-2}}{P_c} \quad (7.13.4)$$

R_{min} is read at $S_{nw} = 1.0$.

$$R_{min} = 2.424\times 10^{-3}\ \mu m$$

$$R_{max} = 2.670\ \mu m$$

7.13e

FIGURE 7.13.4 shows the graph of the incremental pore volume as a function of the pore throat size accessing the pores. The pore volume has a multi-modal distribution.

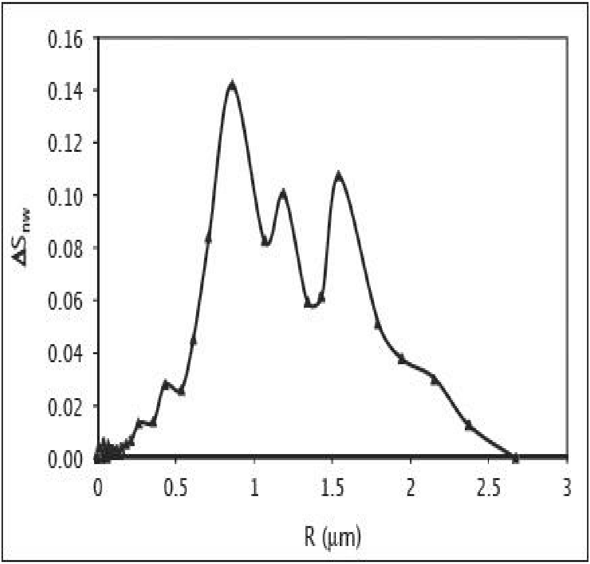

FIGURE 7.13.4 Incremental pore volume distribution.

FIGURE 7.13.4 Incremental pore volume distribution.

PROBLEM 7.14

7.14a

FIGURE 7.14.1 shows the graphs of S_w and S_{nw} versus pore throat size.

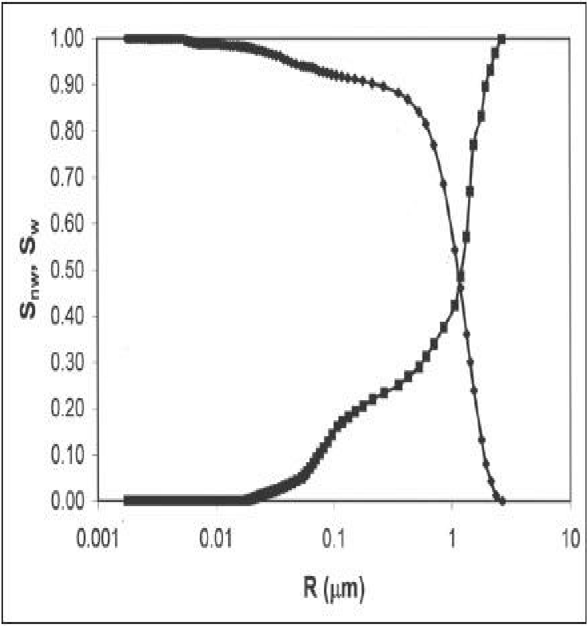

FIGURE 7.14.1 Graph of S_w and S_{nw} versus R.

7.14b

The pore volume distribution is given by

$$f(R)=\frac{dS_w}{dR} \qquad (7.14.1)$$

FIGURE 7.14.2 shows the pore volume distribution. The pore volume has a bi-modal distribution.

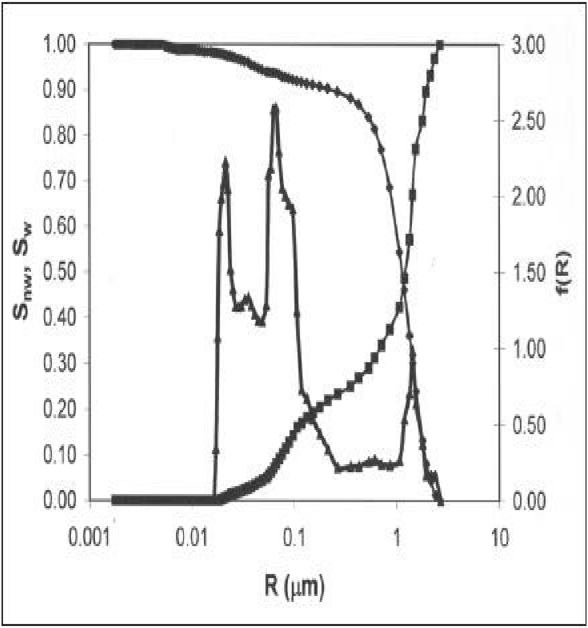

FIGURE 7.14.2 Pore volume distribution.

7.14c

The pore throat size distribution is given by

$$\delta(R) = \frac{\overline{R}^2}{R^2}\frac{dS_w}{dR} \tag{7.14.2}$$

$$\overline{R}^2 = 0.012029$$

FIGURE 7.14.3 shows a comparison of the pore volume distribution and the pore throat size distribution. The pore volume distribution is bi-modal whereas the pore throat size distribution is uni-modal and skewed to the right.

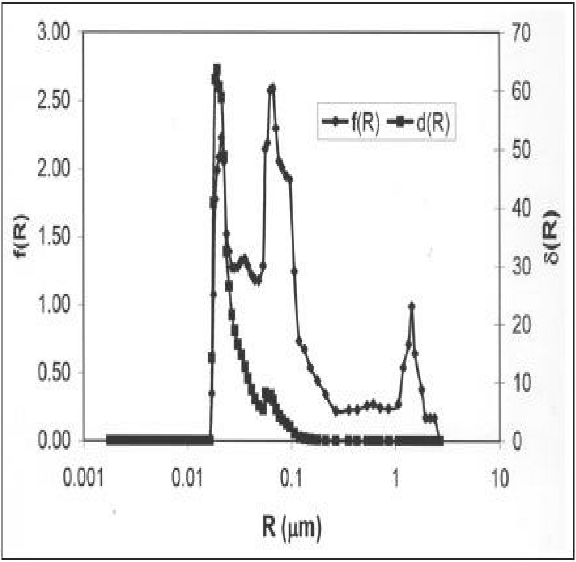

FIGURE 7.14.3 A comparison of the pore volume distribution and the pore throat size distribution.

7.14d

The permeability of the core is given by

$$k = 1.441 \times 10^6 F_1 \phi \int_0^1 \frac{dS_w}{P_c^2} \tag{7.14.3}$$

$$\int_0^1 \frac{dS_w}{P_c^2} = 1.460 \times 10^{-4}\ psi^{-2}$$

Using Purcell's average lithology factor of 0.216 gives the permeability as

$$k = 1.441 \times 10^6 F_1 \phi \int_0^1 \frac{dS_w}{P_c^2}$$

$$= 1.441 \times 10^6 \times 0.216 \times 0.132 \times 1.460 \times 10^{-4} = 6.00 \text{ mD}$$

$$Error\% = \left(\frac{3.86 - 6.00}{3.86} \right) \times 100 = -55.37\%$$

Alternatively, a better lithology factor can be estimated for the core using the following correlation between tortuosity and porosity:

$$\tau = -27.35\phi + 10.987 \tag{7.14.4}$$

$$\phi = 0.132$$

$$\tau = -27.35 \times 0.132 + 10.987 = 7.3768$$

$$F_1 = 1/\tau = 1/7.3768 = 0.1356$$

$$k = 1.441 \times 10^6 F_1 \phi \int_0^1 \frac{dS_w}{P_c^2}$$

$$= 1.441 \times 10^6 \times 0.1356 \times 0.132 \times 1.460 \times 10^{-4} = 3.76 \text{ mD}$$

$$Error\% = \left(\frac{3.86 - 3.76}{3.86} \right) \times 100 = 2.49\%$$

This method gives a better estimate of

permeability than Purcell’s method.

PROBLEM 7.15

S_w=0.32
S_0 = 0.60
S_g=0.08
Let

> $f(x)$ = the probability density function for the pore diameter distribution
> N = the total number of pores
> L = the length of the porous medium

Water, which is the wetting phase, will occupy the smallest pores. Gas, which is the most nonwetting phase, will occupy the largest pores. The balance of the pores will be occupied by oil.

$$V_p = \frac{\pi L N}{4} \int_{x_1}^{x_3} x^2 f(x) dx \tag{7.15.1}$$

$$V_w = \frac{\pi L N}{4} \int_{x_1}^{x_w} x^2 f(x) dx \tag{7.15.2}$$

$$S_w = \frac{\int_{x_1}^{x_w} x^2 f(x) dx}{\int_{x_1}^{x_3} x^2 f(x) dx} = 0.32 \tag{7.15.3}$$

For the triangular probability distribution,

$$x_1 = 10\ \mu\text{m}$$

$$x_2 = 60\ \mu\text{m}$$

$$x_3 = 110\ \mu\text{m}$$

$$f_1(x) = \frac{2(x - x_1)}{(x_3 - x_1)(x_2 - x_1)} = \frac{2(x - 10)}{(110 - 10)(60 - 10)} = \frac{x - 10}{2500} \tag{7.15.4}$$

$$f_1(x) = \frac{2(x_3 - x)}{(x_3 - x_1)(x_3 - x_2)} = \frac{2(110 - x)}{(110 - 10)(110 - 60)} = \frac{110 - x}{2500} \tag{7.15.5}$$

$$V_p = \frac{\pi LN}{4}\left[\int_{x_1}^{x_2} x^2 f_1(x)dx + \int_{x_2}^{x_3} x^2 f_2(x)dx\right]$$

$$= \frac{\pi LN}{4\times 2500}\left[\int_{10}^{60} x^2(x-10)dx + \int_{60}^{x110} x^2(110-x)dx\right]$$

(7.15.6)

Performing the integrations in Eq. (7.15.6) gives

$$V_p = \frac{\pi LN}{4\times 2500}\left\{\left[\frac{1}{4}x^4 - \frac{10}{3}x^3\right]_{10}^{60} + \left[\frac{110}{3}x^3 - \frac{1}{4}x^4\right]_{60}^{110}\right\}$$

$$= \frac{\pi LN}{4\times 2500}\left(2.521\times 10^6 + 7.521\times 10^6\right)$$

The fraction of the pore volume occupied by pores with diameter less than 60 μm is $2.521 \times 10^6/(2.521 \times 10^6 + 7.521 \times 10^6) = 0.2511$. This is less than the water saturation. Therefore, x_w >60 μm and $f_2(x)$ is needed in the integration for water saturation.

$$S_w = \frac{2.521\times10^6 + 110x_w^3/3 - x_w^4/4 - 110\times60^3/3 + 60^4/4}{2.521\times10^6 + 7.521\times10^6} = 0.32 \tag{7.15.7}$$

Eq.(7.15.7) can be solved to obtain x_w = 63.76 μm.

Proceeding in a similar manner, the gas saturation is given by

$$S_g = \frac{110\times110^3/3 - 110^4/4 - 110x_o^3/3 + x_o^4/4}{2.521\times10^6 + 7.521\times10^6} = 0.08 \tag{7.15.8}$$

Eq.(7.15.8) can be solved to obtain x_0 = 97.54 μm. The water, oil, and gas will occupy the following pore size ranges:

Water: $10\ \mu m \leq x \leq 63.76\ \mu m$
Oil: $63.76\ \mu m \leq x \leq 97.54\ \mu m$
Gas: $97.54\ \mu m \leq x \leq 110\ \mu m$

PROBLEM 7.16

$$d = 2.5 \text{ cm}$$

$$L = 7.1 \text{ cm}$$

$$k = 513 \text{ mD}$$

$$\phi = 23.4\%$$

$$V_p = 8.3 \text{ cc}$$

$$\rho_w = 1.036 \text{ g/cm}^3$$

$$\rho_o = 0.822 \text{ g/cm}^3$$

$$\Delta\rho = \rho_w - \rho_o = 1.036 - 0.822 = 0.214 \text{ g/cm}^3$$

$$\sigma_{ow} = 40 \text{ dynes/cm}$$

$$\theta = 0^\circ$$

$$r_1 = 8.5 \text{ cm}$$

$$r_2 = 15.6 \text{ cm}$$

$$\omega = \frac{2\pi N}{60} \tag{7.16.1}$$

$$P_{c1} = \frac{\Delta\rho\omega^2}{2}\left(r_2^2 - r_1^2\right) \tag{7.16.2}$$

Applying the unit conversions to Eq. (7.16.2) gives the capillary pressure in psi as

$$P_{c1} = \frac{\Delta\rho\omega^2}{2}\left(r_2^2 - r_1^2\right) \times \frac{14.696}{1.0133\times10^6} = 7.525\times10^{-6}\,\Delta\rho\omega^2\left(r_2^2 - r_1^2\right) \tag{7.16.3}$$

$$S_{wav} = \frac{V_p - V_w}{V_p} \tag{7.16.4}$$

$$S_{w1} = \frac{d\left(P_{c1} S_{wav}\right)}{dP_{c1}} \tag{7.16.5}$$

$$S_{w1} = S_{wav} + P_{c1}\left(\frac{dS_{wav}}{dP_{c1}}\right) \tag{7.16.6}$$

FIGURE 7.16.1 shows the graph of $(P_{c1}S_{wav})$ versus P_{c1}. The regression equation is

$$P_{c1}S_{wav} = 0.8951 P_{c1}^{0.5253} \tag{7.16.7}$$

In the first method, S_{w1} is calculated by substituting Eq.(7.16.7) into (7.16.5).

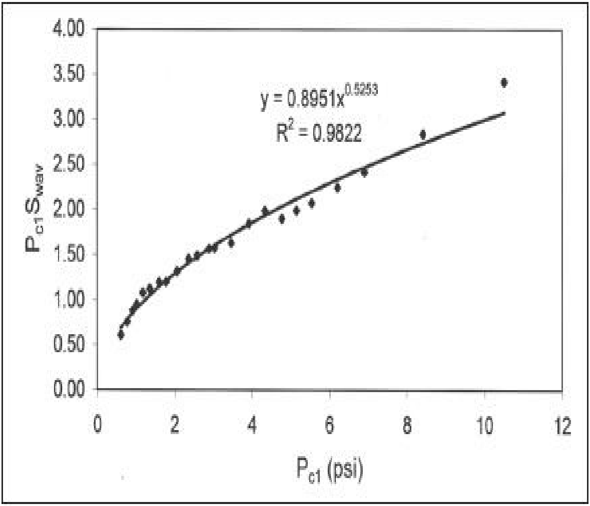

FIGURE 7.16.1 Graph of $P_{c1}S_{wav}$ versus P_{c1}.

FIGURE 7.16.2 shows the graph of S_{wav} versus P_{c1}. The regression equation is

$$P_{c1}S_{wav} = 0.8951P_{c1}^{-0.4747} \quad (7.16.8)$$

In the second method, S_{w1} is calculated by substituting Eq.(7.16.8) into (7.16.6).

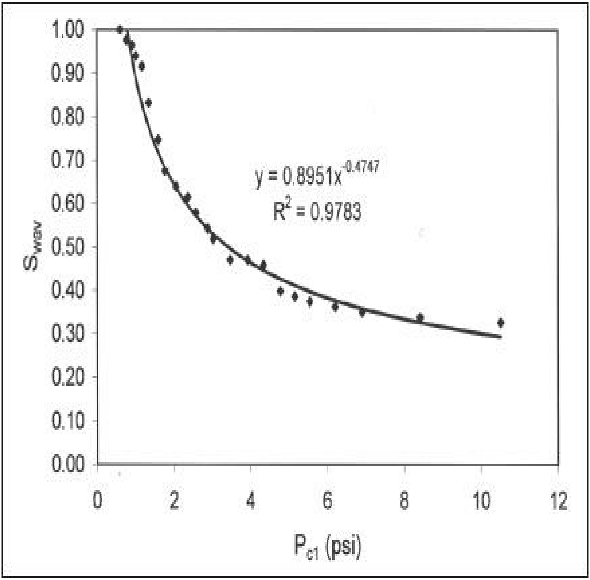

FIGURE 7.16.2 Graph of S_{wav} versus P_{c1}.

FIGURE 7.16.3 shows the capillary pressure curves from the two methods. The first method gives a smoother curve than the second method.

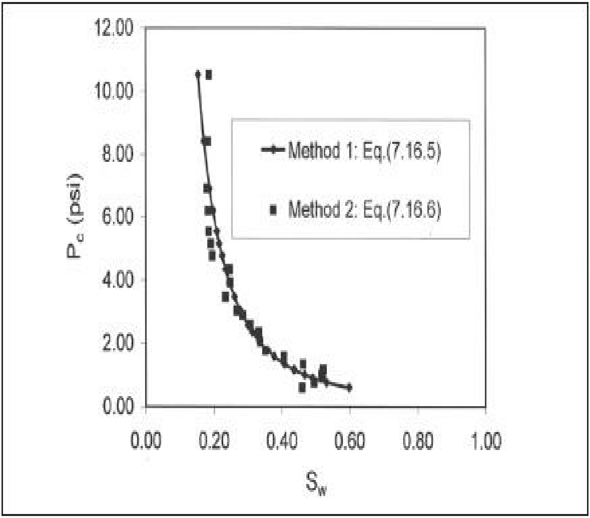

FIGURE 7.16.3 Capillary pressure curves from the two methods.

PROBLEM 7.17

7.17a

$$1 \text{ atm} = 760 \text{ mm Hg}$$

$$W_{dry} = 5.620 \text{ g}$$

$$W_w = 6.490 \text{ g}$$

$$P_c = \frac{P}{760} \times 14.696 = 0.0193P \text{ psi} \quad (7.17.1)$$

$$S_w = \frac{\left(W_{w+air} - W_{dry}\right) / \rho_w}{\left(W_w - W_{dry}\right) / \rho_w} = \frac{\left(W_{w+air} - W_{dry}\right)}{\left(W_w - W_{dry}\right)} \quad (7.17.2)$$

FIGURE 7.17.1 shows the capillary

pressure curve from the porous plate experiment.

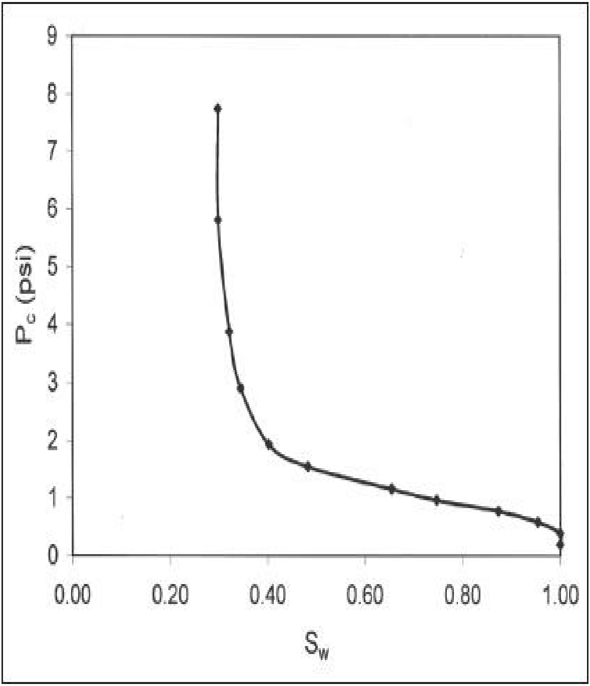

7.17b

$$P_d = 0.387 \text{ psi}$$

7.17c

$$S_{wirr}=0.299$$

7.17d

FIGURE 7.17.2 shows the Brooks-Corey model for the capillary pressure curve. The model equation is

$$\ln\left(\frac{S_w-0.255}{1-0.255}\right)=-1.3198\ln P_c+\ln(0.5488) \quad (7.17.1)$$

From the model equation,

$$\lambda = 1.3198$$

$$P_e = 0.6347 \text{ psi}$$

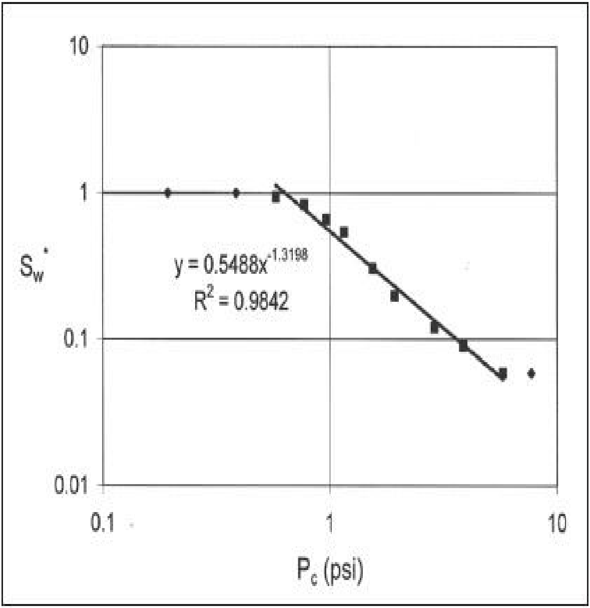

FIGURE 7.17.2 Brooks-Corey model for the capillary pressure curve from the porous plate method.

FIGURE 7.17.3 shows a comparison of the Brooks-Corey model and the experimental capillary pressure data. The fit is good.

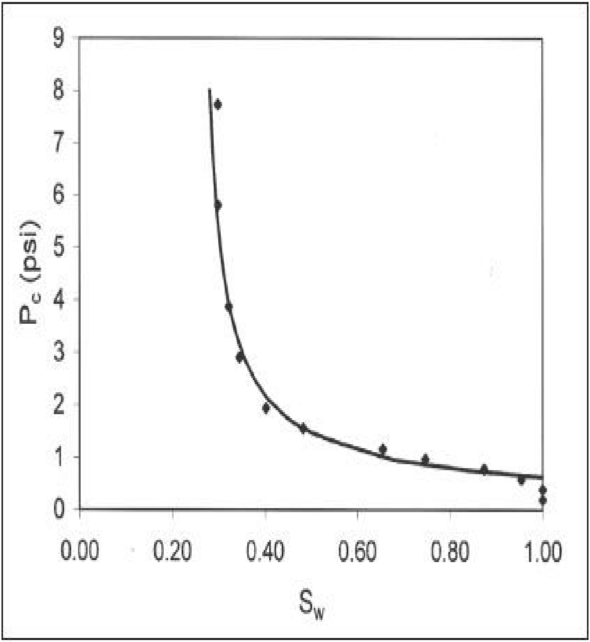

FIGURE 7.17.3 A comparison of the Brooks-Corey model and the experimental capillary pressure data.

7.17e

The van Genuchten model equation is

$$\frac{S_w - 0.310}{1 - 0.310} = \left[\frac{1}{1 + (0.18P_c)^{2.2}} \right]^{18} \quad (7.17.2)$$

FIGURE 7.17.4 shows a comparison of the van Genuchten model and the experimental capillary pressure data. The fit is very good.

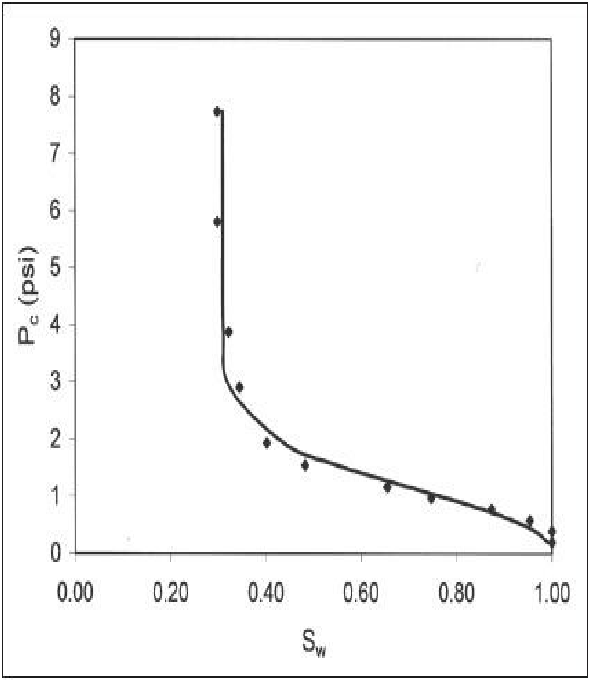

FIGURE 7.17.4 van Genuchten model for the capillary pressure curve from the porous plate method.

PROBLEM 7.18

7.18a

$$P_d = 4.4 \text{ psi}$$

$$\rho_w = 64 \text{ lb mass/ft}^3$$

$$\rho_o = 45 \text{ lb mass/ft}^3$$

$$\Delta\rho = \rho_w - \rho_o = 64 - 45 = 19 \text{ lb mass/ft}^3$$

$$d_o = \frac{144 P_d}{\Delta\rho} = \frac{144 \times 4.4}{19} = 33.35 \text{ ft}$$

At the sample point,

$$z = 33.35 + 100 = 133.35 \text{ ft}$$

$$P_c = \frac{\Delta \rho z}{144} = \frac{19 \times 133.35}{144} = 17.59 \text{ psi}$$

The expected water saturation is computed by linear interpolation as

$$S_w = 32.2 + \left(\frac{17.59 - 15.7}{35.0 - 15.7} \right) (29.8 - 32.2) = 31.96\%$$

7.18b

Assuming a constant porosity, the average water saturation is given by

$$\overline{S}_w = \frac{\int S_w \, dh}{h} \quad (7.18.1)$$

The integration can be performed using the trapezoidal rule as shown in **TABLE**

7.18.1.

TABLE 7.18.1 Calculation of Average Water Saturation.

D (ft)	z (ft)	P_c (psi)	S_w (%)	$\frac{1}{2}(S_{wi}+S_{wi+1})\Delta h$
0	208.35	27.49	30.73	
25	183.35	24.19	31.14	773.38
50	158.35	20.89	31.55	783.63
75	133.35	17.59	31.96	793.88
100	108.35	14.30	35.30	840.75
125	83.35	11.00	42.59	973.63
150	58.35	7.70	65.81	1355.00
175	33.35	4.40	100.00	2072.63
				$\sum = 7592.90$

$$h = 175 \text{ ft}$$

$$\Delta h = 25 \text{ ft}$$

$$\sum \frac{1}{2}\left(S_{wi} + S_{wi+1}\right)\Delta h = 7592.90$$

$$\overline{S}_w = \frac{\sum \frac{1}{2}\left(S_{wi} + S_{wi+1}\right)\Delta h}{h} = \frac{7592.90}{175} = 43.49\%$$

PROBLEM 7.19

$$(P_c)_{lab} = 20 \text{ psi}$$
$$(P_d)_{lab} = 2 \text{ psi}$$
$$\sigma_{lab} = 72 \text{ dynes/cm}$$
$$\sigma_{reservoir} = 24 \text{ dynes/cm}$$
$$\theta_{lab} = 0^\circ$$
$$\theta_{reservoir} = 0^\circ$$
$$\rho_w = 68 \text{ lb mass/ft}^3$$
$$\rho_w = 53 \text{ lb mass/ft}^3$$

Height of sample above the water-oil contact is given by

$$h = \frac{144(P_c - P_d)_{reservoir}}{\rho_w - \rho_o} \tag{7.19.1}$$

$$\left(P_c\right)_{reservoir} = \left(P_c\right)_{lab} \frac{\left(\sigma\cos\theta\right)_{reservoir}}{\left(\sigma\cos\theta\right)_{lab}} \qquad (7.19.2)$$

$$\left(P_c - P_d\right)_{reservoir} = \left(P_c - P_d\right)_{lab} \frac{\left(\sigma\cos\theta\right)_{reservoir}}{\left(\sigma\cos\theta\right)_{lab}} \qquad (7.19.2)$$

Substituting the numerical values into Eq.(7.19.2) gives

$$\left(P_c - P_d\right)_{reservoir} = \left(20-2\right)_{lab} \frac{\left(24\cos 0^\circ\right)_{reservoir}}{\left(72\cos 0^\circ\right)_{lab}} = 6.0 \text{ psi}$$

Substituting the numerical values into Eq.(7.19.1) gives

$$h = \frac{144\left(P_c - P_d\right)_{reservoir}}{\rho_w - \rho_o} = \frac{144\times 6.0}{68-53} = 56.7\ ft$$

PROBLEM 7.20

$$J = \frac{P_c}{\sigma \cos\theta}\sqrt{\frac{k}{\phi}} \qquad (7.20.1)$$

$$k = \frac{r^2}{8} \qquad (7.20.2)$$

$$\phi = 1 \qquad (7.20.3)$$

Substituting Eqs.(7.20.2) and (7.20.3) into (7.20.1) gives

$$J = \frac{2\sigma\cos\theta}{r} \times \frac{1}{\sigma\cos\theta}\sqrt{\frac{r^2}{(8)(1)}} = \frac{2}{\sqrt{8}} = \frac{2}{2\sqrt{2}} = \frac{1}{\sqrt{2}} = 0.7071$$

PROBLEM 7.21

7.21a

The Leverett J-function in consistent units is given by

$$J = \frac{P_c}{\sigma \cos\theta}\sqrt{\frac{k}{\phi}} \qquad (7.21.1)$$

Applying the required unit conversions to make J dimensionless leads to

$$J = \frac{(P_c / 14.696) \times 1.0133 \times 10^6}{\sigma \cos\theta}\sqrt{\frac{(k/1000) \times 9.869 \times 10^{-9}}{\phi}}$$

$$= 0.2166 \frac{P_c}{\sigma \cos\theta}\sqrt{\frac{k}{\phi}} \qquad (7.21.2)$$

In the laboratory,

$k = 150$ mD
$k = 0.22$
$\boldsymbol{\sigma cos\theta} = 72$ dynes/cm

FIGURE 7.21.1 shows the Leverett *J*-function.

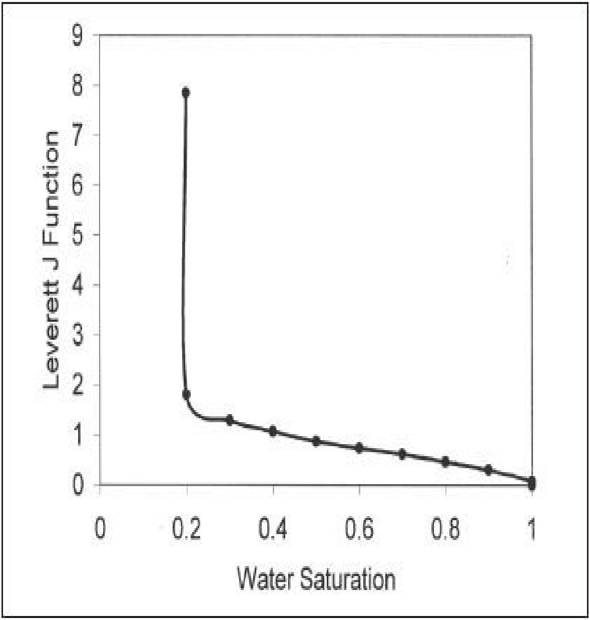

FIGURE 7.21.1 Leverett *J*-function.

7.21b

At reservoir conditions,

$$P_c = \frac{J \times \sigma \cos\theta}{0.2166\sqrt{k/\phi}} \quad (7.21.3)$$

$$k = 500 \text{ mD}$$

$$\phi = 0.25$$

$$\sigma \cos\theta = 26 \text{ dynes/cm}$$

FIGURE 7.21.2 shows a comparison of the lab and reservoir conditions capillary pressure curves.

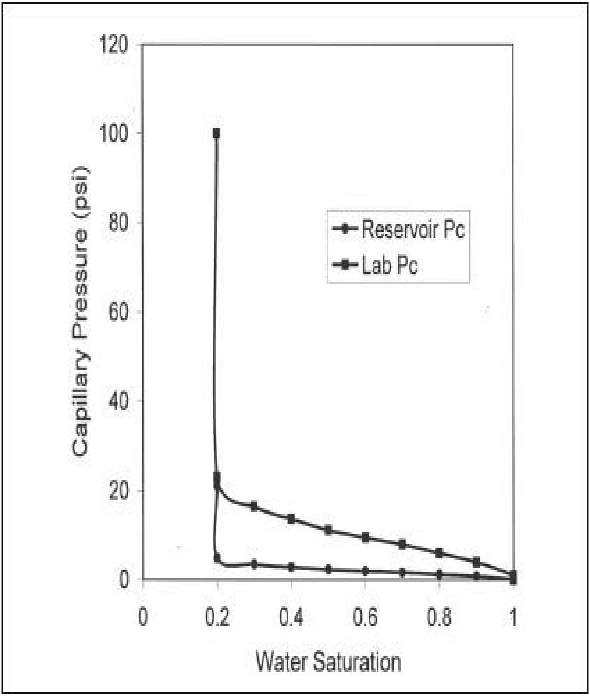

FIGURE 7.21.2 A comparison of the lab and reservoir conditions capillary pressure curves.

7.21c

At reservoir conditions, the capillary pressure at the top of the transition zone is

$$P_c = 4.850 \text{ psi}$$

The height of the top of the transition zone above the free water level is given by

$$z = \frac{144 P_c}{\rho_w - \rho_o} = \frac{144 \times 4.850}{1.026 \times 62.4 - 0.785 \times 62.4} = 46.44 \text{ ft}$$

The displacement pressure is

$$P_d = 0.211 \text{ psi}$$

The height of the top of the transition zone above the water oil contact is given by

$$z = \frac{144 P_d}{\rho_w - \rho_o} = \frac{144 \times 0.211}{1.026 \times 62.4 - 0.785 \times 62.4} = 2.02 \text{ ft}$$

PROBLEM 7.22

If Cores A and B have the same pore structure, then they must have the same Leverett *J*-function. The Leverett *J*-function in consistent units is given by

$$J = \frac{P_c}{\sigma \cos\theta} \sqrt{\frac{k}{\phi}} \qquad (7.22.1)$$

Applying the required unit conversions to make *J*-dimensionless leads to

$$J = \frac{\left(P_c/14.696\right)\times 1.0133\times 10^{6}}{\sigma\cos\theta}\sqrt{\frac{\left(k/1000\right)\times 9.869\times 10^{-9}}{\phi}}$$

$$= 0.2166\frac{P_c}{\sigma\cos\theta}\sqrt{\frac{k}{\phi}} \qquad (7.22.2)$$

$$k_A = 250 \text{ mD}$$

$$\phi_A = 0.21$$

$$k_B = 50 \text{ mD}$$

$$\phi_A = 0.18$$

$$\sigma = 72 \text{ dynes/cm}$$

$$\theta = 0^{\circ}$$

FIGURE 7.22.1 shows the capillary pressure curves for Cores A and B. **FIGURE 7.22.2** compares their Leverett *J*-functions. They are practically identical. Therefore, the two cores have the same pore structure and are likely to have come from the same reservoir.

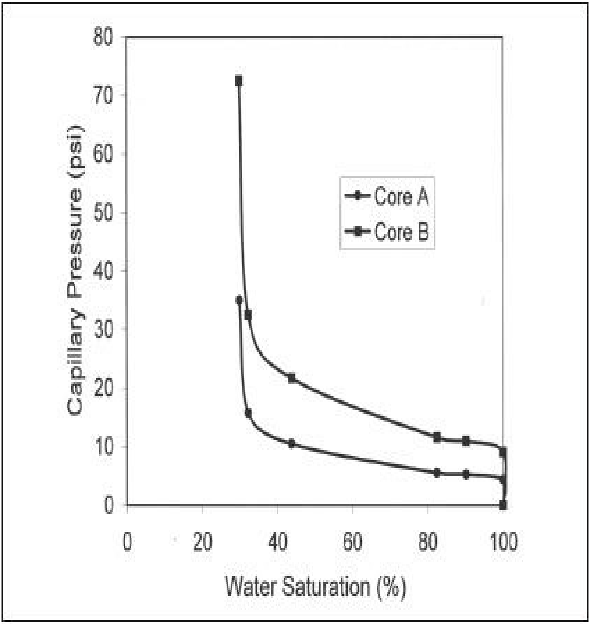

FIGURE 7.22.1 Capillary pressure curves for Cores A and B.

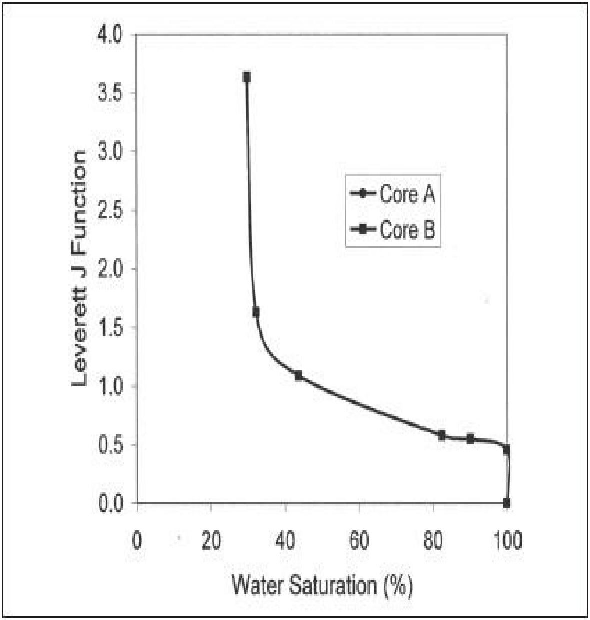

FIGURE 7.22.2 Leverett *J*-functions for Cores A and B.

PROBLEM 7.23

7.23a

FIGURE 7.23.1 shows the three capillary pressure curves. It is evident that P_{cA} belongs to the bottom layer, Layer 3, with k = 900 mD; P_{cB} belongs to the middle layer, Layer 2, with k = 50 mD; and P_{cC} belongs to the top layer, Layer 1, with k = 10 mD.

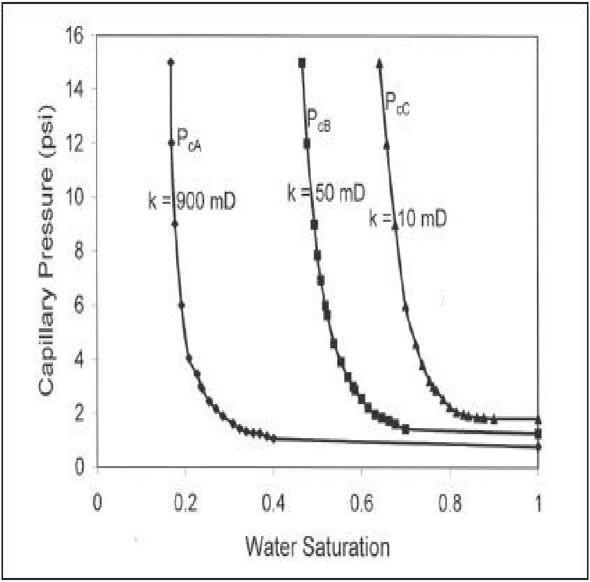

FIGURE 7.23.1 Capillary pressure curves for Problem 7.23.

7.23b

This problem can be solved by two methods. In the first method, the P_c

curves are converted into heights above the free water level and plotted together. The layers are then imposed on this plot as shown in **FIGURE 7.23.2**. The water saturation in Layer 1 is given by P_{cC}, that of Layer 2 by P_{cB},

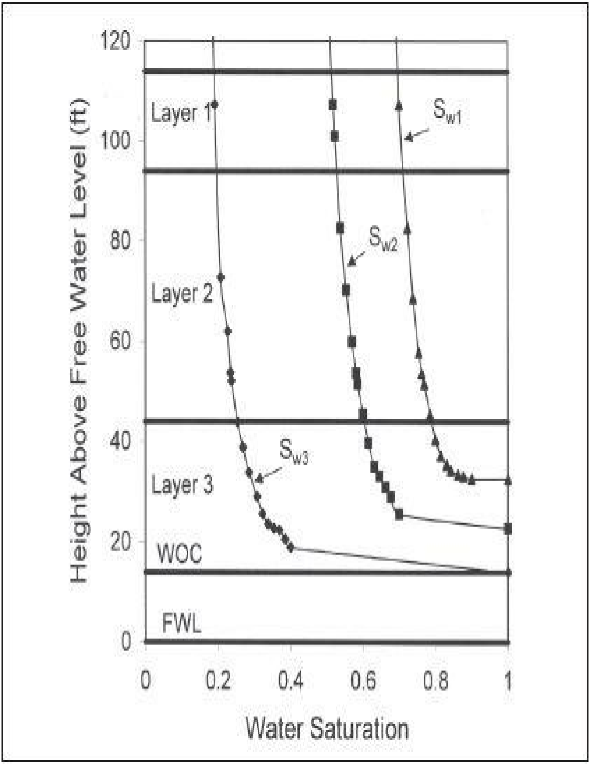

FIGURE 7.23.2 Initial water saturation distribution for the layered reservoir.

FIGURE 7.23.2 Initial water saturation distribution for the layered reservoir.

and that of Layer 3 by P_{cA}. The height above the free water level is given by

$$z = \frac{144 P_c}{\rho_w - \rho_o} = \frac{144 P_c}{62.4 - 0.871 \times 62.4} = 17.8891 P_c \qquad (7.23.1)$$

In the second method, each P_c is fitted to the Brooks-Corey model and the model equation is used to calculate the water saturation for each layer. The Brooks-Corey models are shown in **FIGURES 7.23.3** through **7.23.5**. In these figures, S^* is an adjustable curve fitting parameter. The model equations for Layers 1, 2, and 3 are as follows:

$$S_{w1} = 0.60 + 2.9018z^{-0.7213} \quad (7.23.2)$$

$$S_{w2} = 0.46 + 13.555z^{-1.1889} \quad (7.23.3)$$

$$S_{w3} = 0.16 + 15.636z^{-1.3574} \quad (7.23.4)$$

The resulting initial water saturation distribution is shown in **FIGURE 7.23.6**.

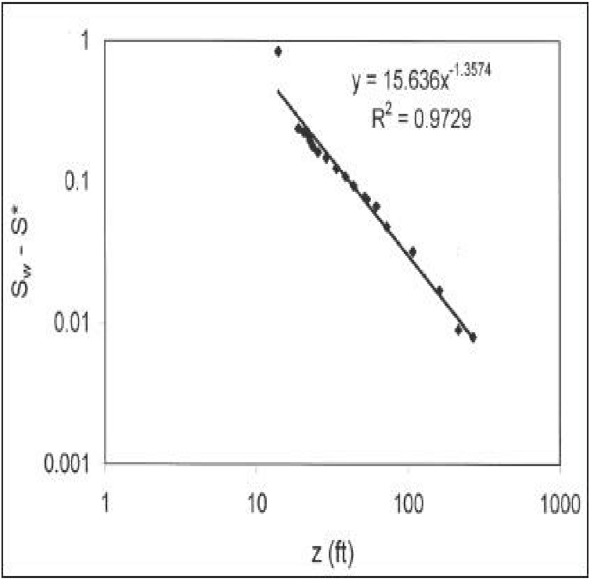

FIGURE 7.23.3 Brooks-Corey model for P_{cA} (Layer 3).

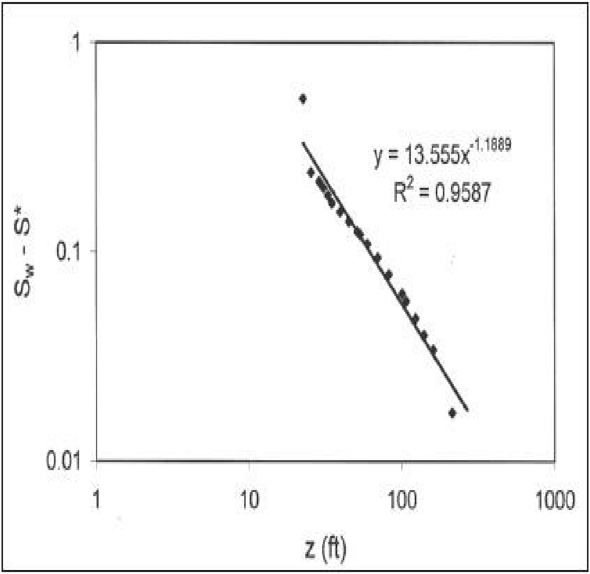

FIGURE 7.23.4 Brooks-Corey model for P_{cB} (Layer 2).

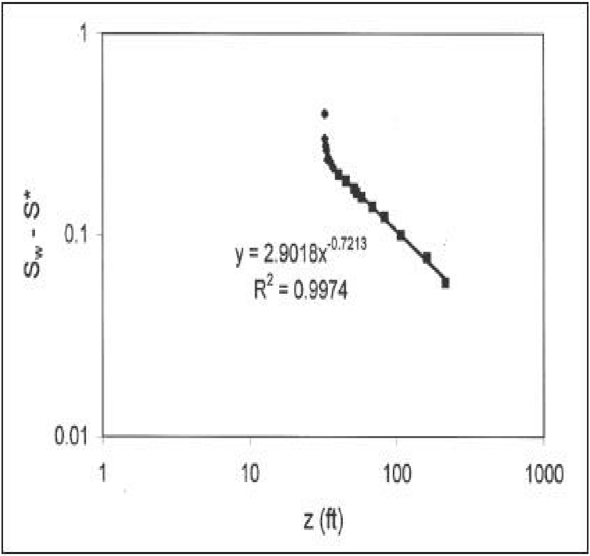

FIGURE 7.23.5 Brooks-Corey model for P_{cC} (Layer 1).

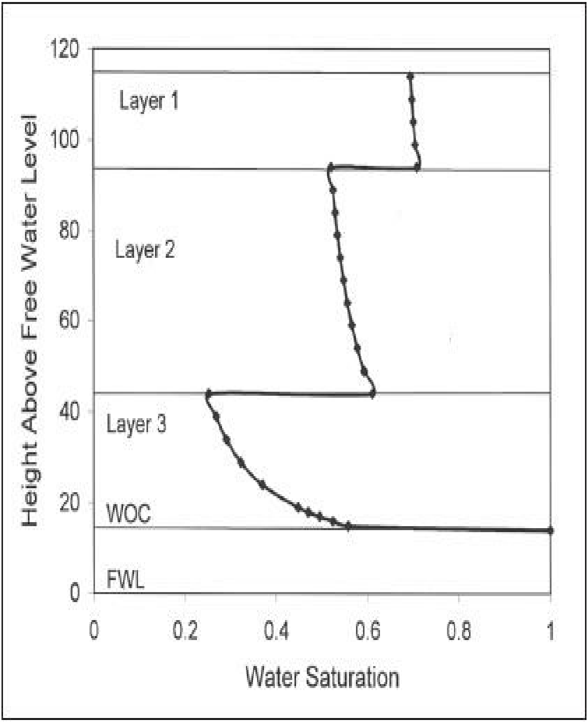

FIGURE 7.23.6 Initial water saturation distribution for layered reservoir.

7.23c

$$P_w = P_{atm} + \frac{\rho_w}{144}(113.85 - z) = 14.7 + \frac{62.4}{144}(113.95 - z)$$

$$= 14.7 + 0.433(113.95 - z) \qquad (7.23.5)$$

$$P_o = P_w + \left(\frac{\rho_w - \rho_o}{144}\right)z = P_w + \left(\frac{62.4 - 0.871 \times 62.4}{144}\right)z$$

$$= P_w + 0.0559z \qquad (7.23.6)$$

FIGURE 7.23.7 shows the water and oil pressures resulting from Eqs.(7.23.5) and (7.23.6).

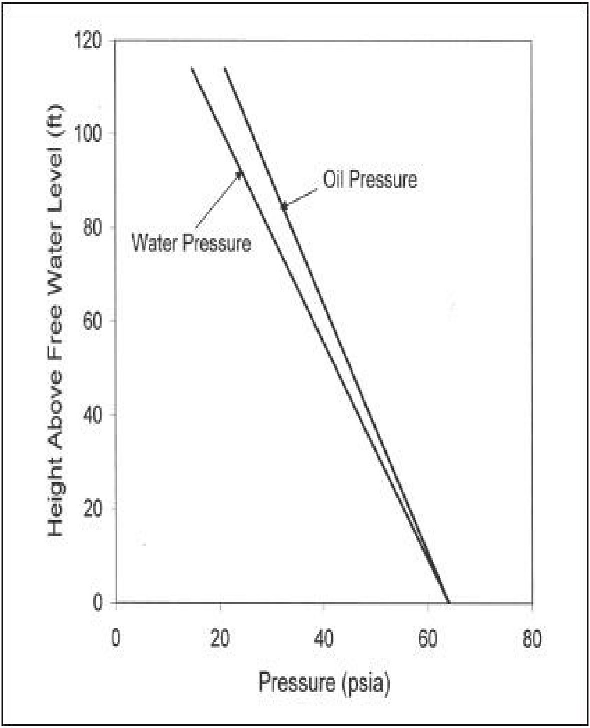

FIGURE 7.23.7 Water and oil pressure profiles.

PROBLEM 7.24

$\Delta\rho = 12.1 \text{ lb mass/ft}^3$
$P_d = 4.2 \text{ psi}$
$S_{or} = 0.30$
$S_{wirr} = 0.22$
$\lambda = 2$

7.24a

$$d_o = \frac{144 P_d}{\Delta\rho} = \frac{144 \times 4.2}{12.1} = 50 \text{ ft}$$

7.24b

At $S_w = 0.22$, $P_{cdrainage} = 26$ psi.

$$z = \frac{144 P_{cdrainage}}{\Delta\rho} = \frac{144 \times 26}{12.1} = 309.42 \text{ ft}$$

The maximum depth of water-free production is given by

$$D_{max} = 1050 - 309.42 = 741 \text{ ft}$$

7.24c

$$f_w = 1.0 \text{ for } S_w \geq 0.70.$$

$$\text{At } S_w = 0.70,\ P_{cdrainage} = 4.2\left(\frac{0.70-0.22}{1-0.22}\right)^{-1/2} = 5.35 \text{ psi.}$$

$$z = \frac{144 P_{cdrainage}}{\Delta\rho} = \frac{144 \times 5.35}{12.1} = 63.72 \text{ ft}$$

The minimum depth above which only water will be produced is given by

$$D_{min} = 1050 - 63.72 = 986 \text{ ft}$$

7.24d

$$P_{d\,\min} = \frac{\Delta\rho z_{\max}}{144} = \frac{12.1\times 1050}{144} = 88.2 \text{ psi}$$

PROBLEM 7.25

$$q = 10 \text{ cm}^3/\text{hr} = \frac{10}{3600} = 2.778 \times 10^{-3} \text{cm}^3/\text{s}$$
$$L = 500 \ \mu\text{m} = 500 \times 10^{-4} \text{ cm}$$
$$r_1 = 40 \ \mu\text{m} = 40 \times 10^{-4} \text{ cm}$$
$$r_2 = 50 \ \mu\text{m} = 50 \times 10^{-4} \text{ cm}$$
$$\beta = r_2 / r_1 = 50/40 = 1.250$$
$$\mu_w = \mu_o = 1 \text{ cp} = 0.01 \text{ Poise}$$
$$\sigma = 30 \text{ dynes/cm}$$
$$\theta = 0^\circ$$

7.25a

The critical capillary number for displacing the oil from the larger tube (and trapping some oil in the smaller tube) is given by

$$N_{ccritical} = \frac{\beta\left(\beta^2+1\right)}{4\left(\beta+1\right)} \quad \textbf{(7.25.1)}$$

Substituting the numerical values into Eq.(7.25.1) gives

$$N_{ccritical} = \frac{\beta\left(\beta^2+1\right)}{4\left(\beta+1\right)} = \frac{1.25\left(1.25^2+1\right)}{4\left(1.25+1\right)} = 0.356$$

The actual capillary number for the displacement is given by

$$N_{cactual} = \frac{q\mu L}{\pi r_1^3 \sigma \cos\theta} \quad \textbf{(7.25.2)}$$

Substituting the numerical values into Eq.(7.25.2) gives

$$N_{cactual} = \frac{q\mu L}{\pi r_1^3 \sigma \cos\theta} = \frac{2.778\times10^{-3}\times0.01\times500\times10^{-4}}{\pi\times\left(40\times10^{-4}\right)^3\times30\cos0^\circ} = 0.230$$

Since $N_{cactual} ceritical$, oil will be trapped in the larger tube.

$$\frac{v_2}{v_1} = \frac{4N_{cactual} + \left(\frac{1}{\beta}+1\right)}{\frac{4N_{cactual}}{\beta^2} - \beta^2\left(\frac{1}{\beta}-1\right)} \quad (7.25.3)$$

Substituting the numerical values into Eq.(7.25.3) gives

$$\frac{v_2}{v_1} = \frac{4N_{cactual} + \left(\frac{1}{\beta}+1\right)}{\frac{4N_{cactual}}{\beta^2} - \beta^2\left(\frac{1}{\beta}-1\right)} = \frac{4\times0.230 + \left(\frac{1}{1.25}+1\right)}{\frac{4\times0.230}{1.25^2} - 1.25^2\left(\frac{1}{1.25}-1\right)} = 0.799$$

Since v_2/v_1 is less than 1.0, the smaller tube will flood out first and oil will be trapped in the larger tube as predicted.

7.25b

The condition for displacing the oil from the larger tube and trapping some oil in the smaller tube is

$$N_{cactual} \geq N_{ccritical} \qquad (7.25.4)$$

$$\frac{q\mu L}{\pi r_1^3 \sigma \cos\theta} \geq \frac{\beta(\beta^2+1)}{4(\beta+1)} \qquad (7.25.5)$$

Solving Eq.(7.25.5) for *q* gives

$$q \geq \left[\frac{\beta\left(\beta^2+1\right)}{4(\beta+1)}\right]\frac{\pi r_1^3 \sigma \cos\theta}{\mu L} \tag{7.25.6}$$

Substituting the numerical values into Eq.(7.25.6) gives

$$q \geq 0.356 \times \frac{\pi \times \left(40 \times 10^{-4}\right)^3 \times 30 \times \cos 0^\circ}{0.01 \times 500 \times 10^{-4}} = 4.294 \times 10^{-3}\ \text{cm}^3/\text{s}$$

$$= 4.294 \times 10^{-3} \times 3600 = 15.457\ \text{cm}^3/\text{hr}$$

7.25c

$$P_A - P_B = \frac{8 q_1 \mu L}{\pi r_1^4} - \frac{2\sigma\cos\theta}{r_1} \tag{7.25.7}$$

$$q_1 = \frac{\left(\frac{8\mu L}{\pi r_2^4}\right) q - 2\sigma\cos\theta\left(\frac{1}{r_2} - \frac{1}{r_1}\right)}{\left(\frac{8\mu L}{\pi r_1^4}\right) + \left(\frac{8\mu L}{\pi r_2^4}\right)} \qquad (7.25.8)$$

Substituting the numerical values into Eq.(7.25.8) gives

$$q_1 = \frac{\left(\frac{8\times0.01\times500\times10^{-4}}{\pi\times\left(50\times10^{-4}\right)^4}\right)\times2.778\times10^{-3} - 2\times30\cos0^\circ\left(\frac{1}{50\times10^{-4}} - \frac{1}{40\times10^{-4}}\right)}{\left(\frac{8\times0.01\times500\times10^{-4}}{\pi\times\left(40\times10^{-4}\right)^4}\right) + \left(\frac{8\times0.01\times500\times10^{-4}}{\pi\times\left(50\times10^{-4}\right)^4}\right)}$$

$$= 1.235\times10^{-3}\ \text{cm}^3/\text{s} = 1.235\times10^{-3}\times3600 = 4.446\ \text{cm}^3/\text{hr}$$

Substituting the numerical values into Eq.(7.25.7) gives

$$P_A - P_B = \frac{8 \times 4.446 \times 0.01 \times 500 \times 10^{-4}}{\pi \times \left(40 \times 10^{-4}\right)^4} - \frac{2 \times 30 \cos 0^\circ}{40 \times 10^{-4}}$$

$$= 6142.766 - 15{,}000 = -8857.234 \text{ dynes/cm}^2$$

There should be no concern about the negative pressure change because the flow is dominated by capillarity which can proceed against a higher pressure because of the curvature of the meniscus.

$$t = 1.0\times10^{-3}\text{ s}$$

$$v_1 = \frac{q_1}{\pi r_1^2} = \frac{1.235\times10^{-3}}{\pi\times\left(40\times10^{-4}\right)^2} = 24.5711\text{ cm/s}$$

$$x_1 = v_1 t = 24.571\times1.0\times10^{-3} = 2.4571\times10^{-2}\text{ cm}$$

$$P_A - P_{w1} = \frac{8q_1\mu x_1}{\pi r_1^4} = \frac{8\times1.235\times10^{-3}\times0.01\times2.4571\times10^{-2}}{\pi\times\left(40\times10^{-4}\right)^4}$$

$$= 3018.69\text{ dynes/cm}^2$$
$$= 3018.69/1.0133\times10^6$$
$$= 2.979\times10^{-3}\text{ atm}$$

$$P_{w1} = P_A - 2.979\times10^{-3} = 1 - 2.979\times10^{-3} = 0.9970\text{ atm}$$

$$P_{nw1} - P_{w1} = \frac{2\sigma\cos\theta}{r_1} = \frac{2\times30\cos0^\circ}{40\times10^{-4}} = 15{,}000\text{ dynes/cm}^2$$
$$= 15{,}000/1.0133\times10^6$$
$$= 1.480\times10^{-2}\text{ atm}$$

$$P_{nw1} = P_{w1} + 1.480\times10^{-2} = 0.9970 + 1.480\times10^{-2} = 1.011824\text{ atm}$$

$$P_{nw1} - P_B = \frac{8q_1\mu\left(L - x_1\right)}{\pi r_1^4}$$

$$= \frac{8\times1.235\times10^{-3}\times0.01\times\left(500\times10^{-4} - 2.4571\times10^{-2}\right)}{\pi\times\left(40\times10^{-4}\right)^4}$$

$$= 3018.69\text{ dynes/cm}^2$$
$$= 3124.08/1.0133\times10^6$$
$$= 3.083\times10^{-3}\text{ atm}$$

$$P_B = P_{nw1} - 3.083\times10^{-3} = 1.011824 - 3.083\times10^{-3} = 1.008741\text{ atm}$$

$$v_2 = \frac{q_2}{\pi r_2^2} = \frac{1.543\times10^{-3}}{\pi\times\left(50\times10^{-4}\right)^2} = 19.6423\text{ cm/s}$$

$$x_2 = v_2 t = 19.6423\times1.0\times10^{-3} = 1.964\times10^{-2}\text{ cm}$$

$$P_A - P_{w2} = \frac{8q_2\mu x_2}{\pi r_2^4} = \frac{8\times1.543\times10^{-3}\times0.01\times1.964\times10^{-2}}{\pi\times\left(50\times10^{-4}\right)^4}$$

$$=1234.62 \text{ dynes/cm}^2$$

$$=1234.62/1.0133\times10^6$$

$$=1.218\times10^{-3} \text{ atm}$$

$$P_{w2} = P_A - 1.218\times10^{-3} = 1-1.218\times10^{-3} = 0.9988 \text{ atm}$$

$$P_{nw2} - P_{w2} = \frac{2\sigma\cos\theta}{r_1} = \frac{2\times30\cos0^\circ}{50\times10^{-4}} = 12{,}000 \text{ dynes/cm}^2$$

$$=12{,}000/1.0133\times10^6$$

$$=1.184\times10^{-2} \text{ atm}$$

$$P_{nw2} = P_{w2} + 1.184\times10^{-2} = 0.9988+1.184\times10^{-2} = 1.010624 \text{ atm}$$

$$P_{nw2} - P_B = \frac{8q_2\mu\left(L-x_2\right)}{\pi r_2^4}$$

$$= \frac{8\times1.543\times10^{-3}\times0.01\times\left(500\times10^{-4}-1.964\times10^{-2}\right)}{\pi\times\left(50\times10^{-4}\right)^4}$$

$$=1908.1436 \text{ dynes/cm}^2$$

$$=1908.1436/1.0133\times10^6$$

$$=1.883\times10^{-3} \text{ atm}$$

$$P_B = P_{nw2} - 1.883\times10^{-3} = 1.010624-1.883\times10^{-3} = 1.008741 \text{ atm}$$

FIGURE 7.25.1 shows the pressure profiles in the two tubes and visualizes the origin of the negative pressure change from A to B.

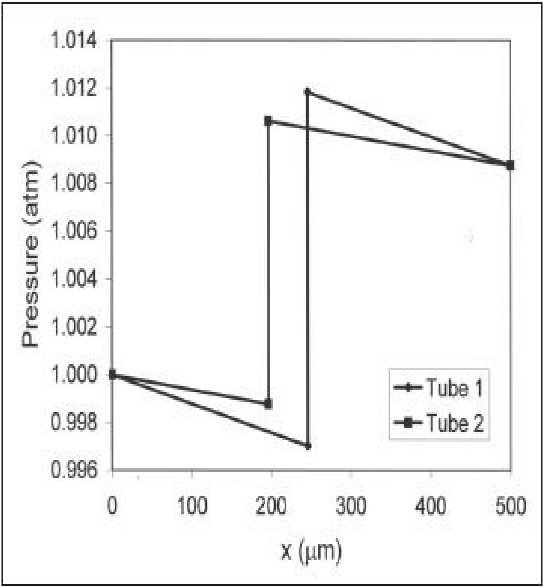

FIGURE 7.25.1 Pressure profiles for the pore doublet model at $t = 10^{-3}$ second.

7.25d

$$\%\text{Viscous Force} = \frac{6142.766}{6142.766+15{,}000} \times 100 = 29\%$$

$$\%\text{Capillary Force} = \frac{15{,}000}{6142.766+15{,}000} \times 100 = 71\%$$

From our knowledge of capillarity, there should be no surprise that the capillary force tends to dominate the viscous force for displacements at the pore scale.

7.25e

FIGURE 7.25.2 shows the variation of the critical capillary number with r_1/r_2. It is clear from the FIGURE that as r_1 approaches r_2, it becomes easier to displace the nonwetting phase from the larger tube as the critical capillary number decreases toward the limiting value of 0.25 for tubes of the same size.

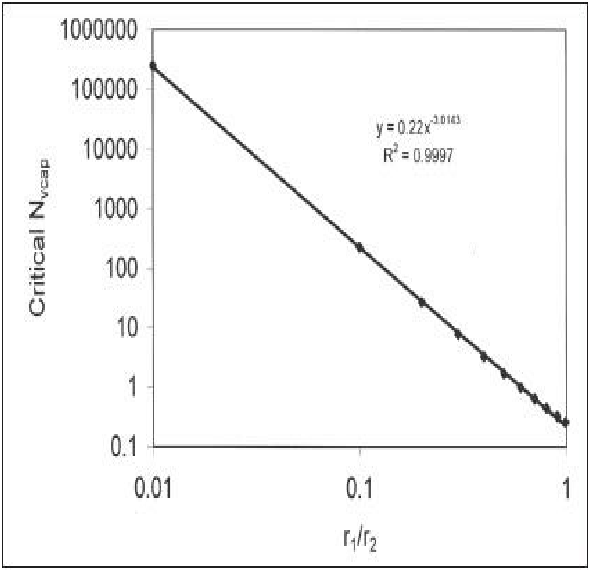

FIGURE 7.25.2 Variation of the critical capillary number with r_1/r_2.

PROBLEM 7.26

7.26a

The pressure gradient required to mobilize the oil blob is given by

$$\frac{\Delta P}{L} \geq \frac{2\sigma\cos\theta}{L}\left(\frac{1}{r}-\frac{1}{R}\right) \tag{7.26.1}$$

$$R = 5r$$

$$L = R = 5r$$

$$\sigma = 30 \text{ dynes/cm}$$

$$\theta = 0^{\circ}$$

r_1 = 50 μm = 50 × 10^{-4} cm for medium sand.

r_2 = 10 μm = 10 × 10^{-4} cm for very fine sand.

For the ordinary waterflood in the medium sand, the mobilization requirement is

$$\frac{\Delta P}{L} \geq \frac{2\sigma\cos\theta}{L}\left(\frac{1}{r}-\frac{1}{R}\right) = \frac{2\times30\times\cos0^\circ}{5\times50\times10^{-4}}\left(\frac{1}{50\times10^{-4}}-\frac{1}{5\times50\times10^{-4}}\right)$$

$$= 384{,}000 \text{ dynes/cm}^2\text{/cm}$$

$$= \frac{384{,}000\times14.696\times30.48}{1.0133\times10^6}$$

$$= 169.749 \text{ psi/ft}$$

For very fine sand,

$$\frac{\Delta P}{L} \geq \frac{2\sigma\cos\theta}{L}\left(\frac{1}{r}-\frac{1}{R}\right)=\frac{2\times 30\times\cos 0^{\circ}}{5\times 10\times 10^{-4}}\left(\frac{1}{10\times 10^{-4}}-\frac{1}{5\times 10\times 10^{-4}}\right)$$

$$=960{,}000 \text{ dynes/cm}^2\text{/cm}$$

$$=\frac{960{,}000\times 14.696\times 30.48}{1.0133\times 10^{6}}$$

$$=4243.726 \text{ psi/ft}$$

Yes. I am surprised by the extremely high pressure gradient requirements for mobilization of trapped residual oil in an ordinary waterflood.

7.26b

The pressure gradient generated in the normal waterflood is obtained from Darcy's law as

$$\frac{\Delta P}{L} = \frac{u\mu_w}{0.001127 \times 5.615 \times k_w} \quad (7.26.2)$$

$$u = 1 \text{ ft/day}$$

$$k_w = 2000 \text{ mD}$$

$$\frac{\Delta P}{L} = \frac{u\mu_w}{0.001127 \times 5.615 \times k_w} = \frac{1 \times 1}{0.001127 \times 5.615 \times 2000} = 0.079 \text{ psi/ft}$$

For very fine sand,

$$k_w = 500 \text{ mD}$$

$$\frac{\Delta P}{L} = \frac{u\mu_w}{0.001127 \times 5.615 \times k_w} = \frac{1 \times 1}{0.001127 \times 5.615 \times 500} = 0.316 \text{ psi/ft}$$

These pressure gradients are not sufficient to mobilize residual oil in these sands.

7.26c

$\sigma = 0.01$ dyne/cm

$\theta = 0°$

For the enhanced waterflood in the medium sand, the mobilization requirement is

$$\frac{\Delta P}{L} \geq \frac{2\sigma\cos\theta}{L}\left(\frac{1}{r}-\frac{1}{R}\right)=\frac{2\times0.01\times\cos0°}{5\times50\times10^{-4}}\left(\frac{1}{50\times10^{-4}}-\frac{1}{5\times50\times10^{-4}}\right)$$

$$=128 \text{ dynes/cm}^2\text{/cm}$$

$$=\frac{128\times14.696\times30.48}{1.0133\times10^{6}}$$

$$=0.057 \text{ psi/ft}$$

The pressure gradient requirement is only 0.057 psi/ft. The waterflood can generate 0.079 psi/ft. This is sufficient to mobilize residual oil in the medium sand.

For very fine sand,

$$\frac{\Delta P}{L} \geq \frac{2\sigma\cos\theta}{L}\left(\frac{1}{r}-\frac{1}{R}\right)=\frac{2\times0.01\times\cos0^{\circ}}{5\times10\times10^{-4}}\left(\frac{1}{10\times10^{-4}}-\frac{1}{5\times10\times10^{-4}}\right)$$

$$= 3200 \text{ dynes/cm}^2\text{/cm}$$

$$= \frac{3200\times14.696\times30.48}{1.0133\times10^{6}}$$

$$= 1.415 \text{ psi/ft}$$

The pressure gradient requirement is 1.415 psi/ft. The waterflood can generate 0.316 psi/ft. This is not sufficient to mobilize residual oil in the very fine sand. Therefore, the "enhanced" waterflood in this case will be unsuccessful.

7.26d

The requirement for mobilization is given by

$$\frac{u\mu_w}{\sigma\cos\theta} \geq \frac{2k_w}{L}\left(\frac{1}{r}-\frac{1}{R}\right) \quad (7.26.3)$$

The critical capillary number is deduced from Eq.(7.26.3) as

$$N_{ccritical} = \frac{2k_w}{L}\left(\frac{1}{r}-\frac{1}{R}\right) \quad (7.26.3)$$

The actual capillary number for the flood is

$$N_{cactual} = \frac{u\mu_w}{\sigma\cos\theta} \quad (7.26.4)$$

$$u = 1 \text{ ft/day} = \frac{1 \times 30.48}{86,400} = 3.528 \times 10^{-4} \text{ cm/s}$$

$$\mu_w = 1 \text{ cp} = 0.01 \text{ Poise}$$

For medium sand,

$$k_w = 2000 \text{ mD}$$

$$N_{ccritical} = \frac{2k_w}{L}\left(\frac{1}{r} - \frac{1}{R}\right)$$

$$= \frac{2 \times (2000/1000) \times 9.689 \times 10^{-9}}{5 \times 50 \times 10^{-4}}\left(\frac{1}{50 \times 10^{-4}} - \frac{1}{5 \times 50 \times 10^{-4}}\right)$$

$$= 2.526 \times 10^{-4}$$

$$N_{cactual} = \frac{u\mu_w}{\sigma \cos\theta} = \frac{3.528 \times 10^{-4} \times 0.01}{0.01 \times \cos 0^{\circ}} = 3.528 \times 10^{-4}$$

The actual capillary number in this case is greater than the critical capillary number. The conclusion from these numbers is that residual oil will be mobilized in the medium sand in the enhanced waterflood.

For very fine sand,

$$k_w = 500 \text{ mD}$$

$$N_{ccritical} = \frac{2k_w}{L}\left(\frac{1}{r} - \frac{1}{R}\right)$$

$$= \frac{2\times(500/1000)\times 9.689\times 10^{-9}}{5\times 50\times 10^{-4}}\left(\frac{1}{50\times 10^{-4}} - \frac{1}{5\times 50\times 10^{-4}}\right)$$

$$= 1.579\times 10^{-3}$$

$$N_{cactual} = \frac{u\mu_w}{\sigma\cos\theta} = \frac{3.528\times 10^{-4}\times 0.01}{0.01\times\cos 0^{\circ}} = 3.528\times 10^{-4}$$

The actual capillary number in this case is less than the critical capillary number. The conclusion from these numbers is that residual oil will not be mobilized in the very fine sand in the “enhanced” waterflood.

PROBLEM 7.27

7.27a

Capillary number is used to characterize the ability to mobilize residual oil. Capillary number is given by

$$N_c = \frac{u\mu_w}{\sigma} \qquad (7.27.1)$$

$$u = 1 \text{ ft/day} = \frac{30.48}{86{,}400} = 3.528 \times 10^{-4} \text{ cm/s}$$

$$\mu_w = 0.01 \text{ Poise}$$

For the ordinary waterflood,

$$\sigma = 35 \text{ dynes/cm}$$

$$N_c = \frac{u\mu_w}{\sigma} = \frac{3.528\times10^{-4}\times0.01}{35} = 1.008\times10^{-7}$$

From the capillary desaturation curve, S_{or}=0.35, which is consistent with the given residual oil saturation for the waterflood. For the enhanced waterflood using the chemical,

$$\sigma = 0.01 \text{ dyne/cm}$$

$$N_c = \frac{u\mu_w}{\sigma} = \frac{3.528\times10^{-4}\times0.01}{0.01} = 3.528\times10^{-4}$$

From the capillary desaturation curve,

$$S_{or} = 0.145$$

Therefore, the chemical will mobilize residual oil, reducing the residual oil saturation from 35% to 14.5%.

7.27b

The additional oil recovery to be expected is given by

$$\Delta N_p = \frac{Ah\phi \Delta S_{or}}{B_o} \tag{7.27.2}$$

$$A = 2 \text{ square miles } = 2 \times 5280^2 \text{ ft}^2$$

$$h = 200 \text{ ft}$$

$$\phi = 0.20$$

$$B_o = 1.20 \text{ RB/STB}$$

$$\Delta N_p = \frac{Ah\phi\Delta S_{or}}{B_o} = \frac{2 \times 5280^2 \times 200 \times 0.20 \times (0.35 - 0.145)}{5.615 \times 1.20}$$

$$= 6.785 \times 10^7 \text{ STB}$$

PROBLEM 7.28

FIGURE 7.28.1 shows the sketches for the capillary pressure curves for Cases B through F compared to Case A. The magnitude of the capillary pressure curve for a porous medium is inversely proportional to the pore size. The smaller the pore size, the larger is the capillary pressure. The shape of the capillary pressure depends on the sorting and pore size distribution. The sketches in Figure 2.28.1 were made to reflect these factors.

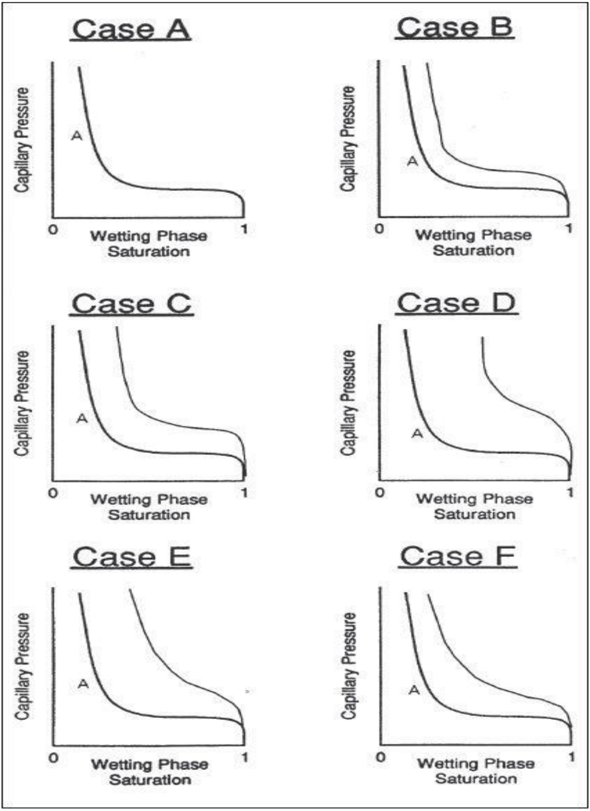

FIGURE 7.28.1 Drainage capillary pressure curves for various porous media.

Case B:

$P_{cB} > P_{cA}$ because B has smaller pore size than A as a result of the tighter packing. The shape of P_{cB} is the same as because A and B are well sorted.

Case C:

$P_{cC} > P_{cA}$ because C has smaller grain size than A. The shape of P_{cC} is the same as P_{cC} because A and C are well sorted.

Case D:

P_{cC} P_{cA} because D has smaller pore size than A as a result of poor sorting. The shape of $\boldsymbol{P_{cD}}$ is more S-shaped than $\boldsymbol{P_{cA}}$ because D is poorly sorted whereas A is well sorted.

***Case* E:**

$\boldsymbol{P_{cE} > P_{cA}}$ because E has smaller pore size than A as a result of cementation. The shape of $\boldsymbol{P_{cE}}$ is more S-shaped than $\boldsymbol{P_{cA}}$ because the cementation in E can result in a wider pore size distribution than in A, which has a uniform pore size distribution.

Case F:

$P_{cF} > P_{cA}$ because F has smaller pore size than A as a result of compaction. The shape of P_{cD} is more S-shaped than P_{cA} because the compaction in F can result in a wider pore size distribution than in A, which has a uniform pore size distribution.

CHAPTER 8 SOLUTIONS

PROBLEM 8.1

$$
\begin{aligned}
k_{rw} &= (S_w - S_{wirr})^3 \\
k_{ro} &= 2(1 - S_{or} - S_w)^2 \\
S_{wirr} &= 0.15 \\
S_{nwr} &= 0.25 \\
\mu_{nw} &= \mu_o = 10 \text{ cp} \\
\mu_w &= 1 \text{ cp} \\
B_o &= 1.20 \text{ RB/STB} \\
B_w &= 1.0 \text{ RB/STB}
\end{aligned}
$$

8.1a

FIGURE 8.1.1 shows the relative permeability curves.

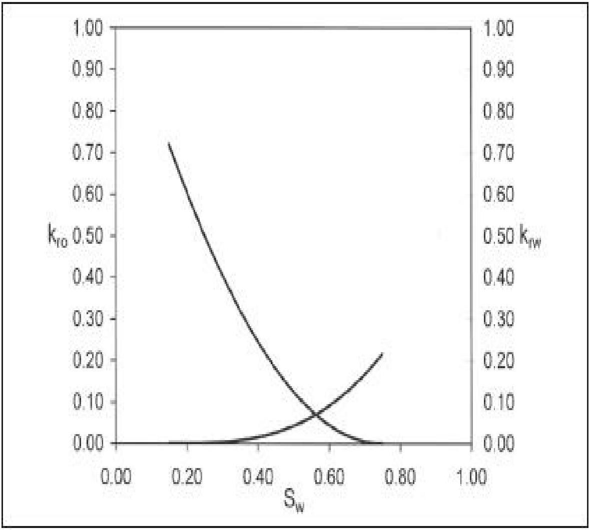

FIGURE 8.1.1 Relative permeability curves.

8.1b

FIGURE 8.1.2 shows the approximate fractional flow curve and its derivative, together with the Welge tangent construction.

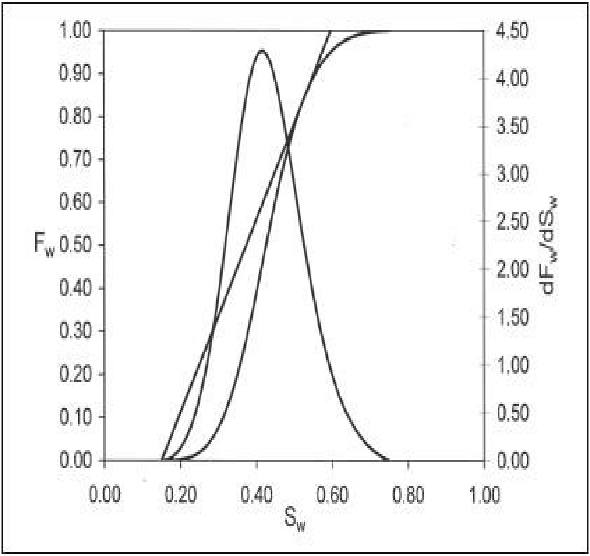

FIGURE 8.1.2 Approximate fractional flow curve and its derivative and tangent construction.

8.1c

From the Welge tangent construction,

$$S_{wf}=0.527$$

$$S_{wov}= 0.597$$

8.1d

FIGURE 8.1.3 shows the true fractional flow curve and its derivative.

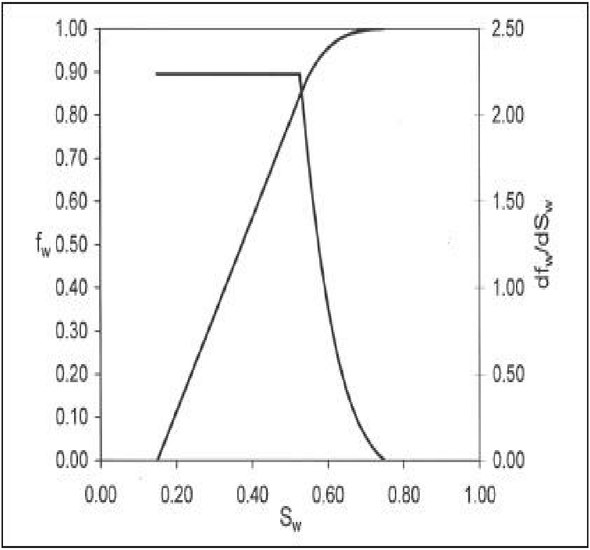

FIGURE 8.1.3 True fractional flow curve and its derivative.

8.1e

The end-point mobility ratio is given by

$$M_E = \frac{k_{wr} / \mu_w}{k_{or} / \mu_o} = \frac{0.216/1}{0.720/10} = 3$$

8.1f

From the tangent line,

$$\left(\frac{df_w}{dS_w} \right)_{S_{wf}} = 2.237$$

Before breakthrough, the distance traveled by the front is given by

$$x_D = t_D \left(\frac{df_w}{dS_w} \right)_{S_{wf}} = 2.237 t_D \tag{8.1.1}$$

$$t_D = 0.20,\ x_D = 2.237 \times 0.20 = 0.447$$

$$t_D = 0.30,\ x_D = 2.237 \times 0.30 = 0.671$$

FIGURE 8.1.4 shows the water saturation profiles at t_D = 0.20, 0.30, and 1.0.

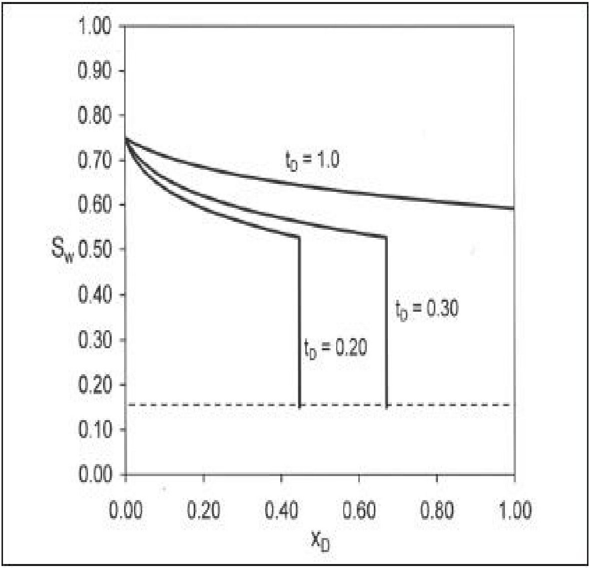

FIGURE 8.1.4 Water saturation profiles.

8.1g

At breakthrough, $x_D = 1$ and Eq.(8.1.1) gives

$$t_{DBT} = \frac{1}{2.237} = 0.447$$

8.1h

The breakthrough oil recovery as a fraction of the initial oil in place is given by

$$R_{BT} = \frac{t_{DBT}}{1 - S_{wirr}} = \frac{0.447}{1 - 0.15} = 0.526$$

8.1i

After breakthrough,

$$W_i = \frac{1}{\left(\frac{df_w}{dS_w}\right)_{S_{w2}}} \quad \text{(8.1.2)}$$

$$N_{pD} = S_{w2} - S_{wirr} + W_i\left[1 - f_w\left(S_{w2}\right)\right] \tag{8.1.3}$$

$$R = \frac{N_{pD}}{1 - S_{wirr}} \tag{8.1.4}$$

For example, for $S_{w2} = 0.580$,

$$\left(\frac{df_w}{dS_w}\right)_{S_{w2}} = 1.184$$

$$W_i = \frac{1}{\left(\frac{df_w}{dS_w}\right)_{S_{w2}}} = \frac{1}{1.184} = 0.845$$

$$f_w\left(S_{w2}\right) = 0.932$$

$$N_{pD} = S_{w2} - S_{wirr} + W_i\left[1 - f_w\left(S_{w2}\right)\right] = 0.580 - 0.15 + 0.845(1 - 0.932)$$
$$= 0.487$$

$$R = \frac{N_{pD}}{1 - S_{wirr}} = \frac{0.487}{1 - 0.15} = 0.573$$

FIGURE 8.1.5 shows the oil recovery curve.

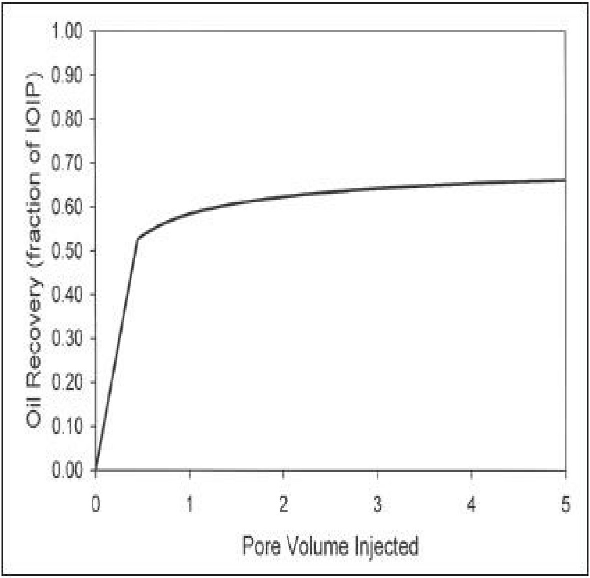

FIGURE 8.1.5 Oil recovery curve.

8.1j

After breakthrough, the oil water ratio is given by

$$WOR = \frac{B_o}{B_w}\left[\frac{f_w(S_{w2})}{1 - f_w(S_{w2})}\right] \tag{8.1.5}$$

For example, for $S_{w2} = 0.580$,

$$WOR = \frac{B_o}{B_w}\left[\frac{f_w(S_{w2})}{1 - f_w(S_{w2})}\right] = \frac{1.2}{1}\left[\frac{0.932}{1 - 0.932}\right] = 16.4$$

FIGURE 8.1.6 shows the graph of the water-oil ratio versus oil recovery. There is a dramatic increase in the water-oil ratio soon after breakthrogh.

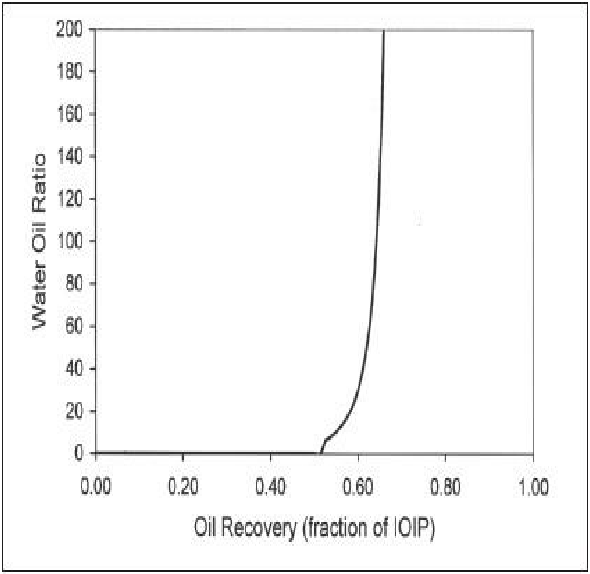

FIGURE 8.1.6 Water-oil ratio versus oil recovery.

PROBLEM 8.2

$$M_E = 60$$

$$\mu_o = 100 \text{ cp}$$

$$\left(\frac{df_w}{dS_w}\right)_{S_{wf}} = 4.275$$

Before breakthrough, the distance traveled by the front is given by

$$x_D = t_D \left(\frac{df_w}{dS_w}\right)_{S_{wf}} = 4.275 t_D \tag{8.2.1}$$

$$t_D = 0.20,\ x_D = 4.275 \times 0.20 = 0.855$$

$$t_{DBT} = \frac{1}{4.275} = 0.234$$

$$R_{BT} = \frac{t_{DBT}}{1 - S_{wirr}} = \frac{0.234}{1 - 0.15} = 0.275$$

The waterflood performance indices at the higher mobility ratio of 60 are worse than at the lower mobility ratio of 3. The frontal saturation is lower, the water breakthrough is sooner, the breakthrough oil recovery is lower as is the oil recovery after breakthrough. These differences are apparent in the comparative plots in **FIGURES 8.2.1**, **8.2.2**, and **8.2.3**.

8.2a

Figure 8.2.1 shows a comparison of the approximate fractional flow curves at the two mobility ratios. Note the shift in the curve to the left as the mobility ratio is increased from 3 to 60. The result of this shift is a lower S_{wf} and a lower S_{wav} from the tangent construction.

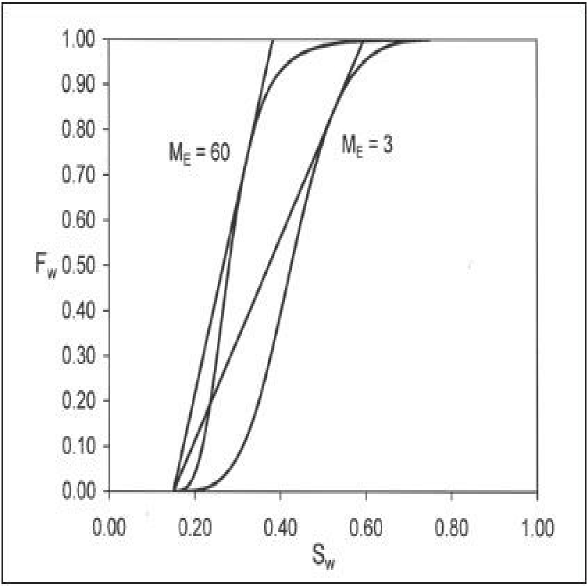

FIGURE 8.2.1 A comparison of the approximate fractional flow curves.

8.2b

Figure 8.2.2 compares the water saturation profiles at $t_D = 0.20$. Note the lower S_{wf} at the mobility ratio of 60 than at the mobility ratio of 3 and the tendency toward earlier water breakthrough.

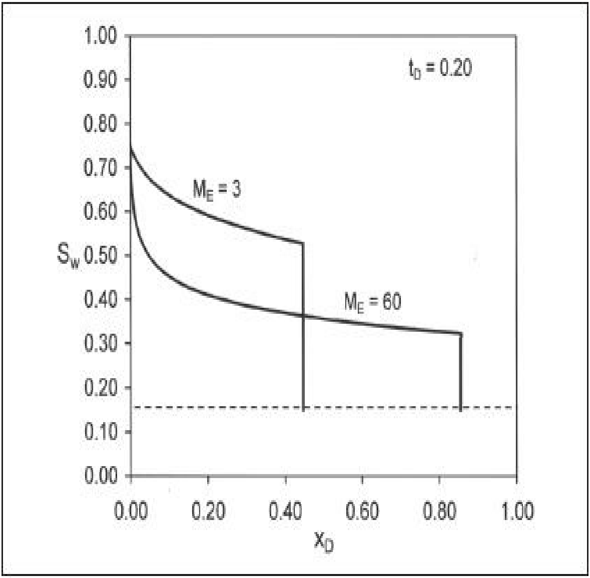

FIGURE 8.2.2 A comparison of water saturation profiles at $t_D = 0.20$.

8.2c

Figure 8.2.3 compares the oil recovery curves for the two waterfloods. The superiority of the waterflood performance at the lower mobility ratio is evident.

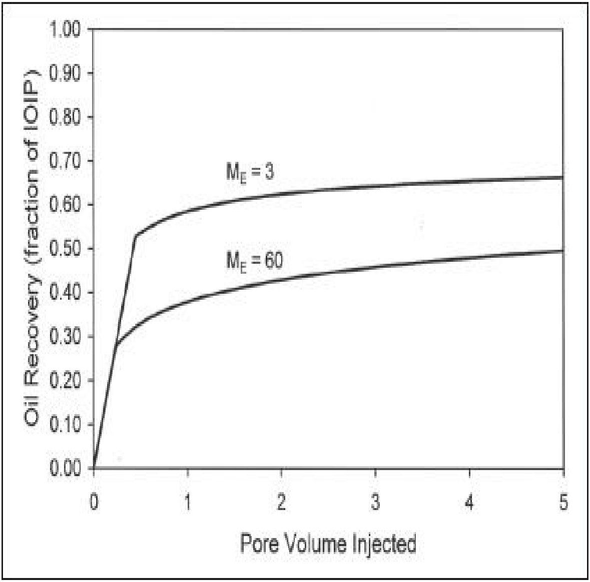

FIGURE 8.2.3 A comparison of oil recovery curves.

The oil viscosity in this waterflood is only 100 cp and there is a marked deterioration in the waterflood performance. The viscosities of heavy oils are considerably higher than 100 cp, say 500 to 1000 cp. At such high oil viscosities, the waterflood will be essentially doomed to failure.

PROBLEM 8.3

$$M_E = 0.03$$

$$\mu_w = 100cp$$

$$\left(\frac{df_w}{dS_w}\right)_{S_{wf}} = 1.675$$

Before breakthrough, the distance traveled by the front is given by

$$x_D = t_D \left(\frac{df_w}{dS_w}\right)_{S_{wf}} = 1.675 t_D \qquad (8.3.1)$$

$$t_D = 0.20,\ x_D = 1.675 \times 0.20 = 0.335$$

$$t_{DBT} = \frac{1}{1.675} = 0.597$$

$$R_{BT} = \frac{t_{DBT}}{1 - S_{wirr}} = \frac{0.597}{1 - 0.15} = 0.702$$

The waterflood performance indices at this favorable mobility ratio of 0.03 are superior to those at the unfavorable mobility ratios of 3 and 60. The frontal saturation is higher, the water breakthrough is delayed, the breakthrough oil recovery is higher, and the waterflood is over at water breakthrough, with considerable savings in time and money. These differences are apparent in the comparative plots in

figures 8.3.1, **8.3.2**, and **8.3.3**.

8.3a

Figure 8.3.1 shows a comparison of the approximate fractional flow curves at the three mobility ratios. Note the shift in the curve to the right as the mobility ratio is reduced from 3 to 0.03. The result of this shift is a higher S_{wf} and a higher S_{wav} from the tangent construction.

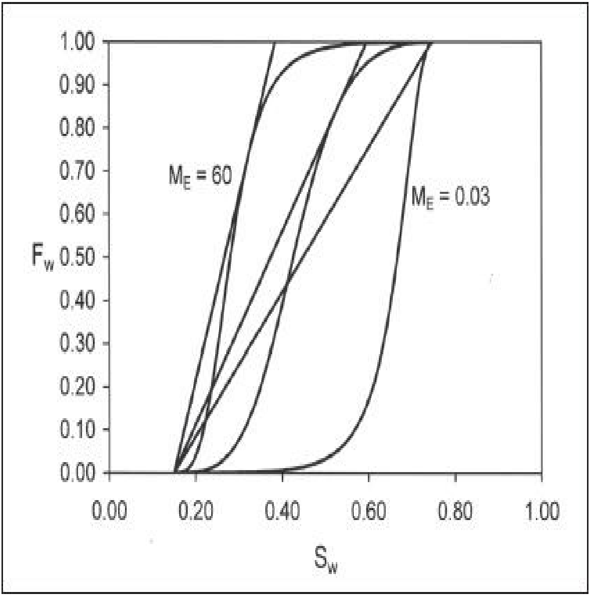

FIGURE 8.3.1 A comparison of the approximate fractional flow curves for $M_E = 0.03$, 3, and 60.

8.3b

Figure 8.3.2 compares the water saturation profiles at $t_D = 0.20$ for the three waterfloods. Note the higwer S_{wf} at the mobility ratio of 0.03 than at the other two mobility ratios. At this mobility ratio, S_{wf} is essentially equal to $(1-S_{or})$ and the displacement is piston-like, albeit with a leaky piston since residual oil is left behind.

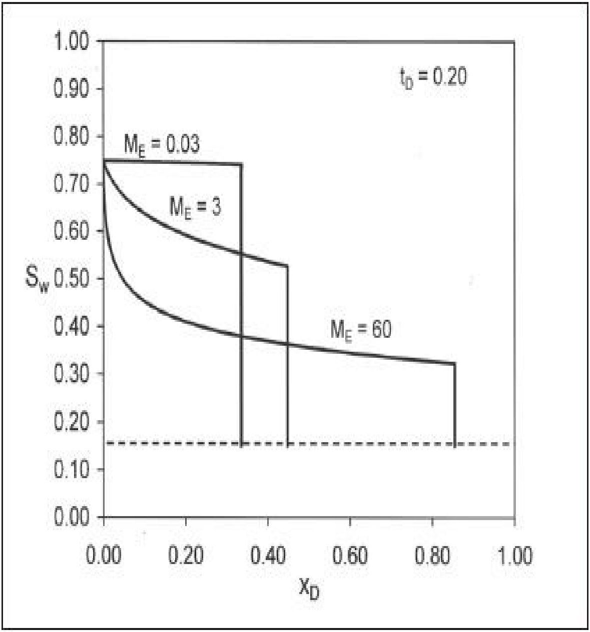

FIGURE 8.3.2 A comparison of water saturation profiles at $t_D = 0.20$ for $M_E = 0.03$, 3, and 60.

8.3c

Figure 8.2.3 compares the oil recovery curves for the three waterfloods. The superiority of the waterflood performance at the favorable mobility ratio of 0.03 is evident. The water breakthrough is delayed and the waterflood is over at water breakthrough as all the oil that can be recovered has been recovered with considerable savings in project time. Of course, you know that time is money.

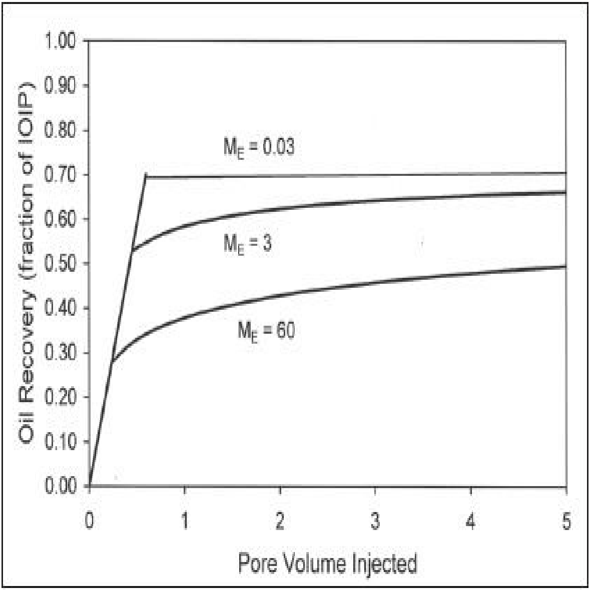

FIGURE 8.3.3 A comparison of the oil recovery curves for $M_E = 0.03$, 3, and 60.

The performance of this waterflood at the favorable mobility ratio of 0.03

clearly demonstrates why mobility control is highly desirable in any displacement. The reason for the use of polymers to increase the viscosity of the injected fluid is to achieve a favorable mobility ratio for the displacement and thereby improve the oil recovery and shorten the project life.

PROBLEM 8.4

$$q = 500 \text{ STB/D}$$
$$L = 2{,}000 \text{ ft}$$
$$A = 2{,}800 \text{ ft}^2$$
$$\phi = 0.25$$
$$S_{wirr} = 0.20$$
$$S_{or} = 0.15$$
$$\mu_o = 2 \text{ cp}$$
$$\mu_w = 1 \text{ cp}$$
$$PV = AL\phi = 2800 \times 2000 \times 0.25 = 1{,}400{,}000 \text{ ft}^3 = 249{,}332 \text{ RB}$$
$$HCPV = PV(1 - S_{wirr}) = 1{,}400{,}000(1 - 0.20) = 1{,}120{,}000 \text{ ft}^3 = 199{,}466 \text{ RB}$$
$$IOIP = \frac{HCPV}{B_o} = \frac{199{,}466}{1.5} = 132{,}977 \text{ STB}$$

8.4a

FIGURE 8.4.1 shows the curve fit of analytical models to the sparse experimental relative permeability curves. The model fits are good. The analytical equations are

$$k_{rw} = 0.60 S^{2.1}$$

$$k_{ro} = 0.70(1-S)^2$$

Where

$$S = \frac{S_w - S_{wirr}}{1 - S_{wirr} - S_{or}}$$

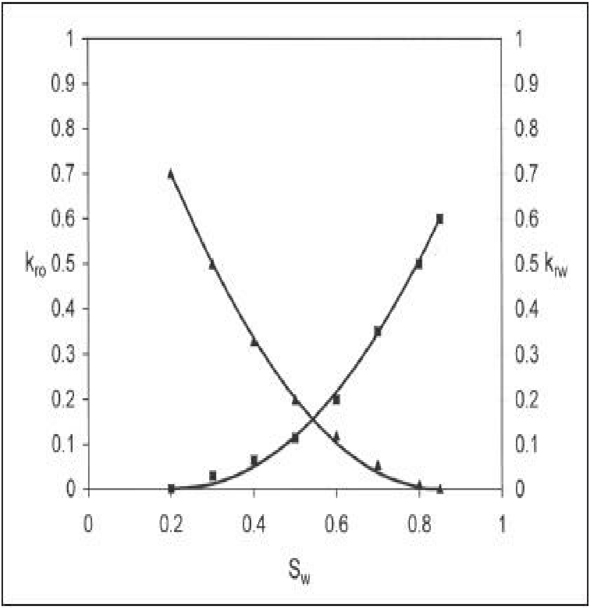

FIGURE 8.4.1 Curve fit of relative permeability curves.

These analytical models are used in subsequent calculations.

FIGURE 8.4.2 shows the

approximate fractional flow curve with the Welge tangent construction.

$$\left(\frac{df_w}{dS_w}\right)_{S_{wf}} = 2.0$$

$$S_{wf} = 0.60$$

$$S_{wav} = 0.70$$

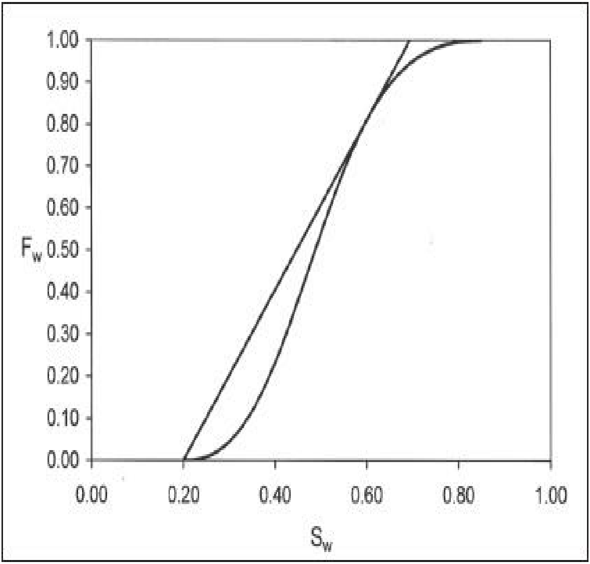

FIGURE 8.4.2 Tangent construction.

Before breakthrough, the distance traveled by the front is given by

$$x_D = t_D \left(\frac{df_w}{dS_w} \right)_{S_{wf}} = 2t_D \quad (8.4.1)$$

$$t = 150 \text{ days}$$

$$t_D = \frac{5.615 q B_w t}{PV} = \frac{5.615 \times 500 \times 1 \times 150}{1{,}400{,}000} = 0.301$$

$$t_D = 0.301,\ x_D = 2 \times 0.301 = 0.602$$

$$x = x_D L = 0.602 \times 2{,}000 = 1{,}204 \text{ ft}$$

FIGURE 8.4.3 shows the water saturation profile at 150 days of injection.

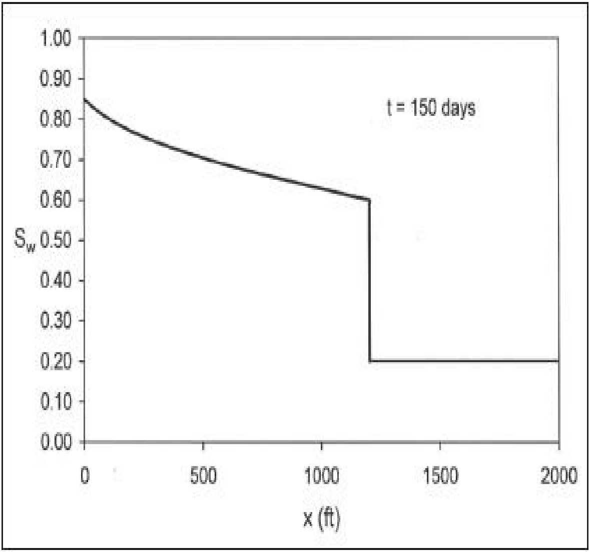

FIGURE 8.4.3 Water saturation profile at 150 days of injection.

8.4b

$$t_{DBT} = \frac{1}{2.0} = 0.50$$

$$t_{BT} = \frac{t_{DBT} \times PV}{qB_w} = \frac{0.50 \times 249,332}{500 \times 1} = 249.33 \text{ days}$$

8.4c

$$R_{BT} = \frac{S_{wav} - S_{wir}}{1 - S_{wirr}} = \frac{0.70 - 0.20}{1 - 0.20} = 0.625$$

Alternatively,

$$R_{BT} = \frac{t_{DBT}}{1 - S_{wirr}} = \frac{0.50}{1 - 0.20} = 0.625$$

$$N_p = R_{BT} \times IOIP = 0.625 \times 132,977 = 83,111 \text{ STB}$$

8.4d

$$WOR = \frac{B_o}{B_w}\left[\frac{f_w(S_{w2})}{1-f_w(S_{w2})}\right] = \frac{1.5}{1}\left[\frac{f_w(S_{w2})}{1-f_w(S_{w2})}\right] = \frac{30}{1} \qquad \textbf{(8.4.2)}$$

$$f_w(S_{w2}) = \frac{30B_w}{B_o+30B_w} = \frac{30\times 1}{1.5+30\times 1} = 0.952$$

$$S_{w2} = 0.704$$

$$W_i = 1.192$$

$$N_{pD} = S_{w2} - S_{wirr} + W_i\left[1-f_w(S_{w2})\right] = 0.704 - 0.20 + 1.192(1-0.952)$$
$$= 0.561$$

$$R = \frac{N_{pD}}{1-S_{wirr}} = \frac{0.561}{1-0.20} = 0.701$$

$$N_p = R \times IOIP = 0.701 \times 132{,}977 = 93{,}217 \text{ STB}$$

8.4e

$$Q_i = \frac{W_i \times PV}{B_w} = \frac{1.192 \times 249,332}{1} = 297,204 \text{ STB}$$

8.4f

$$t = \frac{Q_i}{q} = \frac{297,204}{500} = 594.41 \text{ days}$$

PROBLEM 8.5

S_{wirr}=0.20
S_{or}=0.70
S_{wf}=0.40

8.5a

$$x_D = t_D \left(\frac{df_w}{dS_w} \right)_{S_{wf}} \quad (8.5.1)$$

For 0.20 S_w 0.40

$$\left(\frac{df_w}{dS_w}\right)_{S_w} = \frac{0.70-0.00}{0.40-0.20} = 3.5$$

$$t_D = 0.20,\ x_D = 0.20 \times 3.5 = 0.70$$

For 0.40 S_w 0.70

$$\left(\frac{df_w}{dS_w}\right)_{S_w} = \frac{1-0.70}{0.70-0.40} = 1.0$$

$$t_D = 0.20,\ x_D = 0.20 \times 1.0 = 0.20$$

FIGURE 8.5.1 shows the saturation distribution at $t_D = 0.20$.

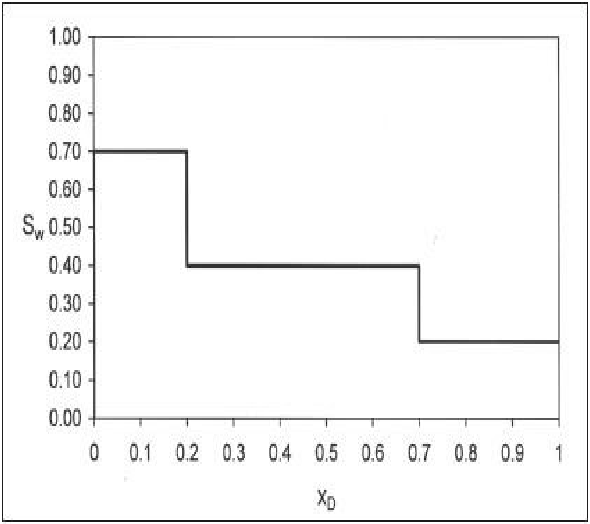

FIGURE 8.5.1 Wetting phase saturation profile at $t_D = 0.20$.

8.5b

$$t_{DBT} = \frac{1}{3.5} = 0.286$$

8.5c

$$R_{BT} = \frac{t_{DBT}}{1 - S_{wirr}} = \frac{0.286}{1 - 0.20} = 0.358$$

8.5d

The time when the second front arrives at the outlet is given by

$$t_D = 1/\left(\frac{df_w}{dS_w}\right)_{S_w=0.70} = 1/1 = 1.0$$

$$S_{wav} = 0.70$$

$$R = \frac{S_{wav} - S_{wir}}{1 - S_{wirr}} = \frac{0.70 - 0.20}{1 - 0.20} = 0.625$$

FIGURE 8.5.2 shows the recovery curve.

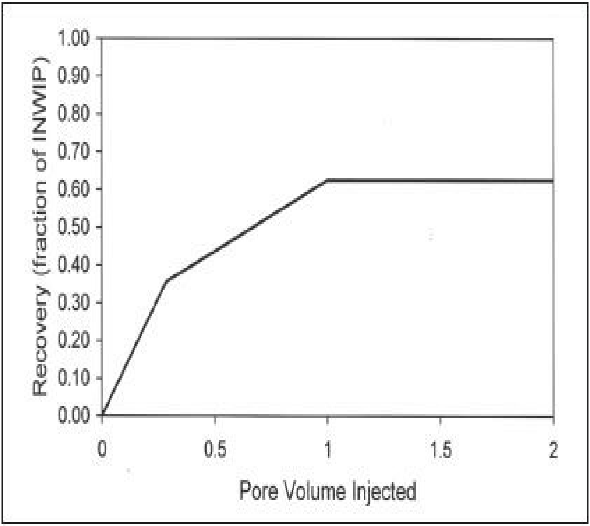

FIGURE 8.5.2 Recovery curve.

8.5e

The physical system is a favorable mobility ratio displacement in a two-layer heterogeneous reservoir in which the permeability of the bottom layer is greater than that of the top layer.

8.5f

If we neglect the effect of capillary pressure,

$$P_w(x_D,0.20)=P_{nw}(x_D,0.20)=P(x_D,0.20) \quad (8.5.2)$$

For 0x_D 0.20, Darcy's law gives

$$\frac{\partial P}{\partial x_D}=-\frac{q\mu_w f_w(S_w=0.70)}{kk_{wr}A}=-C_1 \quad (8.5.3)$$

For 0.20 *D* 0.70, Darcy's law gives

$$\frac{\partial P}{\partial x_D} = -\frac{q\mu_w f_w(S_w = 0.40)}{kk_{rw}(S_w = 0.40)A} = -C_2 \quad (8.5.4)$$

For 0.70*D*1, Darcy's law gives

$$\frac{\partial P}{\partial x_D} = -\frac{q\mu_{nw}}{kk_{nwr}A} = -C_3 \quad (8.5.5)$$

$$P(1, 0.20) = 1 \quad (8.5.6)$$

where C_1, C_2, and C_3 are constants. Eq. (8.5.5) can be integrated to obtain the pressure profile in the third segment, using the boundary condition of Eq. (8.5.6). This profile is used to determine the boundary condition for the second segment. Using this boundary condition, Eq.(8.5.4) is then integrated to obtain the pressure profile in the second segment. This profile is used to calculate the boundary condition for the first segment. Eq.(8.5.3) can be integrated to obtain the pressure profile in the first segment. Because the mobility ratio is favorable, $C_1 C_2 C_3$. **FIGURE 8.5.3** shows a qualitative sketch of the pressure profile for $C_1 = 5$, $C_2 = 3$, $C_3 = 1$.

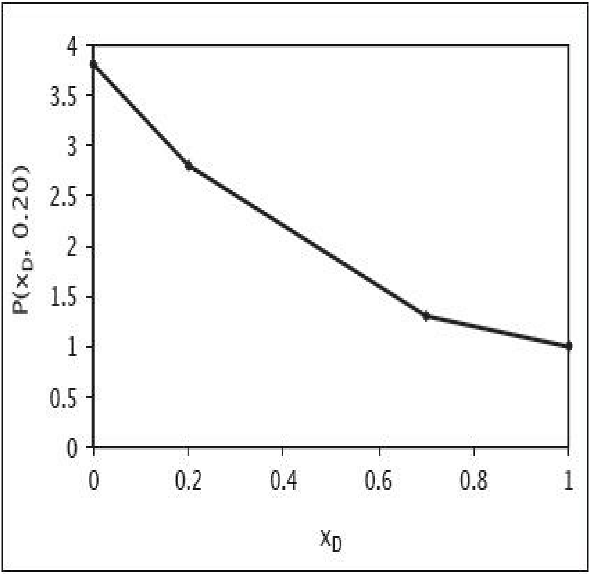

FIGURE 8.5.3 Qualitative sketch of the pressure profile at $t_D = 0.20$.

PROBLEM 8.6

$L = 5.0$ cm
$d = 3.0$ cm
$\varphi = 0.15$
$\rho_s = 2.666$ g/cm^3
$k = 150$ mD
$\mu_o = 10$ cp
$\rho_o = 0.85$ g/cm^3
$\mu_1 = 1$ cp
$\rho_w = 1.05$ g/cm^3
$\delta P = 48.13$ psi

$$A = \pi\left(\frac{d}{2}\right)^2 = \pi\left(\frac{3}{2}\right)^2 = 7.069\ \text{cm}^2$$

$$V_b = A \times L = 7.069 \times 5 = 35.343\ \text{cm}^3$$

$$V_p = \phi \times V_b = 0.15 \times 35.343 = 5.301\ \text{cm}^3$$

$$k_{ri} = \frac{k_i}{k} = \frac{q_i \mu_i L}{kA\Delta P} \tag{8.6.1}$$

Application of unit conversions to Eq. (8.6.1) gives

$$k_{ri} = \frac{k_i}{k} = \frac{(q_i/3600)\mu_i L}{(k/1000)A(\Delta P/14.696)} = 4.0822\frac{q_i \mu_i L}{kA\Delta P} \tag{8.6.2}$$

$$S_w = \frac{W - \rho_s V_b(1-\phi) - \rho_o V_p}{V_p(\rho_w - \rho_o)} \tag{8.6.3}$$

For example,

$$q_o = 98.82\ \text{cm}^3/\text{hr}$$

$$q_w = 140.63\ \text{cm}^3/\text{hr}$$

$$k_{ro} = 4.0822\frac{q_i \mu_i L}{kA\Delta P} = 4.0822 \times \frac{98.82 \times 10 \times 5}{150 \times 7.069 \times 48.13} = 0.3953$$

$$k_{rw} = 4.0822\frac{q_i \mu_i L}{kA\Delta P} = 4.0822 \times \frac{140.63 \times 1 \times 5}{150 \times 7.069 \times 48.13} = 0.0562$$

$$W = 85.1270\ \text{g}$$

$$S_w = \frac{W - \rho_s V_b (1-\phi) - \rho_o V_p}{V_p(\rho_w - \rho_o)}$$

$$= \frac{85.1270 - 2.666 \times 35.343(1-0.15) - 0.85 \times 5.301}{5.301_p(1.05-0.85)}$$

$$= 0.5000$$

Figure 8.6.1 shows the relative permeability curves from the steady state experiment.

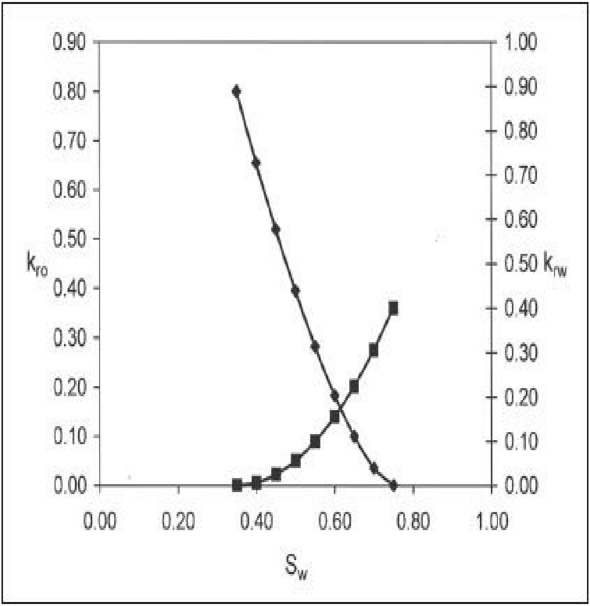

FIGURE 8.6.1 Steady state relative permeability curves.

PROBLEM 8.7

$q = 30\ \text{cm}^3/\text{hr}$

$L = 54.6\ \text{cm}$

$d = 4.8\ \text{cm}$

$A = 18.0956\ \text{cm}^2$

$\varphi = 0.3034$

$K = 3.37\ \text{D}$

$\mu_0 = 108.37\ \text{cp}$

$\mu_w = 1.01\ \text{cp}$

$p_0 = 0.959\ \text{g/cm}^3$

$p_w = 0.996\ \text{g/cm}^3$

$\sigma = 26.7\ \text{dynes/cm}$

$$R_{BT} = 0.4214$$
$$R_{final} = 0.567$$
$$S_{wirr} = 0.1221$$
$$k_{o@S_{wirr}} = 3.09 \text{ D}$$
$$k_{or} = 3.09 / 3.37 = 0.917$$
$$S_{or} = 0.38$$
$$k_{wr} = 0.180$$
$$(q / \Delta P)_s = 0.010306 \text{ cm}^3 / (\text{sec.atm})$$

8.7a

FIGURE 8.7.1 shows the raw experimental data.

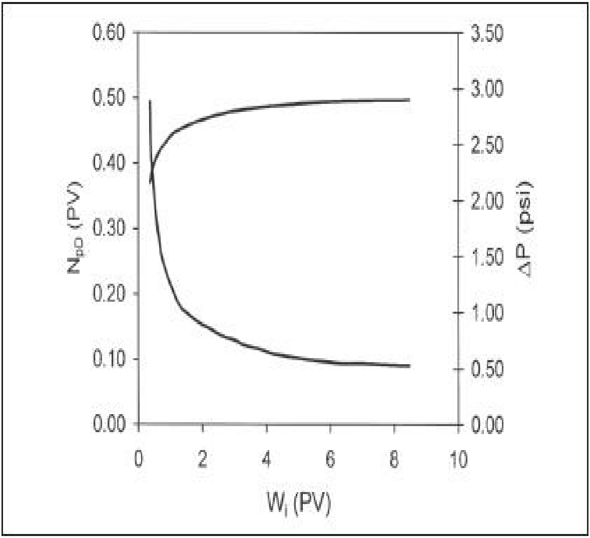

FIGURE 8.7.1 Raw experimental data for unsteady state relative permeability measurements.

8.7b

FIGURES 8.7.2 and 8.7.3 show the

curve fits of N_{pD} versus $\ln W_i$ and $\ln\left(\frac{1}{W_i I_r}\right)$ versus $\ln\left(\frac{1}{W_i}\right)$.

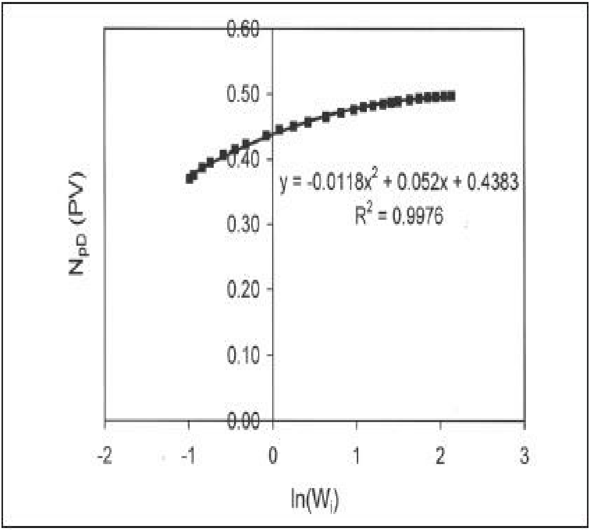

FIGURE 8.7.2 Curve fit for N_{pD} versus $\ln W_i$.

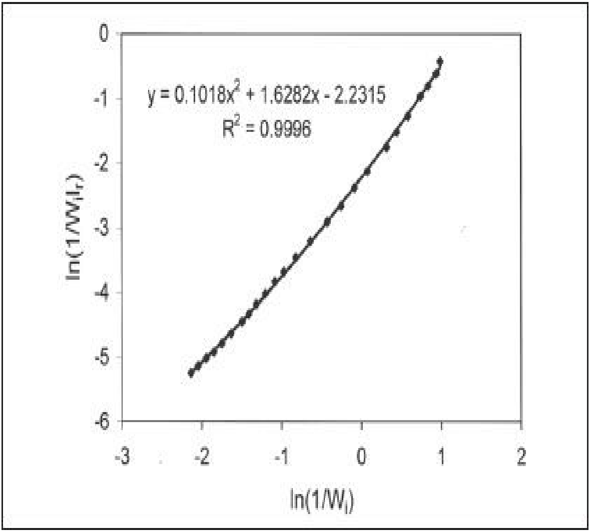

FIGURE 8.7.3 Curve fit of $\ln(1/W_i I_r)$ versus $\ln(1/W_i)$.

8.7c

The curve fit equations are

$$N_{pD} = 0.4383 + 0.052 \ln W_i + 0.0118 (\ln W_i)^2$$

$$\ln\left(\frac{1}{W_i I_r}\right) = -2.2315 + 1.6282 \ln\left(\frac{1}{W_i}\right) + 0.1018 \left[\ln\left(\frac{1}{W_i}\right)\right]^2$$

These equations can be differentiated analytically to obtain

$$f_{nw2} = \frac{dN_{pD}}{dW_i} = \frac{0.052 - (2)(0.0118)\ln W_i}{W_i}$$

$$\frac{f_{nw2}}{k_{rnw}} = \frac{d\left(\frac{1}{W_i I_r}\right)}{d\left(\frac{1}{W_i}\right)}$$

$$= \left[\frac{1.6282}{\left(\frac{1}{W_i}\right)} + \frac{(2)(0.1018)\ln\left(\frac{1}{W_i}\right)}{\left(\frac{1}{W_i}\right)}\right] e^{\left(-2.2315 + 1.6282\ln\left(\frac{1}{W_i}\right) + 0.1018\left[\ln\left(\frac{1}{W_i}\right)\right]^2\right)}$$

$$k_{rw} = k_{ro}\frac{\mu_w}{\mu_o}\left(\frac{1}{f_{o2}} - 1\right)$$

FIGURE 8.7.4 shows the calculated relative permeability curves.

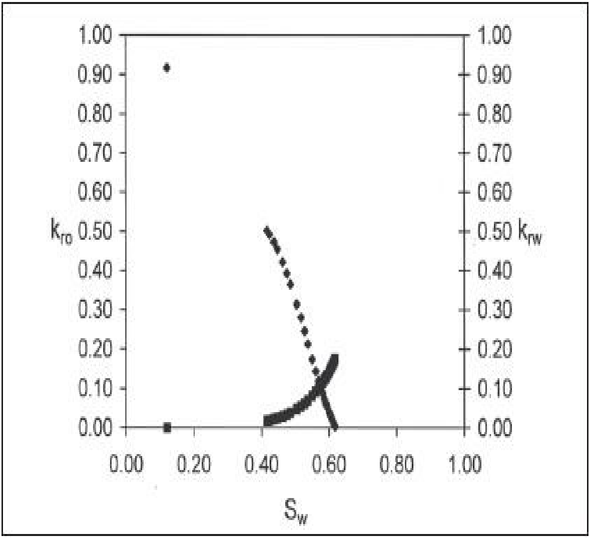

FIGURE 8.7.4 Computed relative permeability curves.

8.7d

FIGURE 8.7.5 shows the experimental data fitted to analytical relative permeability models. The fit is good.

The analytical models are

$$k_{rw} = 0.180 S^{4.5}$$

$$k_{ro} = 0.917\left(1 - S^{1.55}\right)$$

where

$$S = \frac{S_w - S_{wirr}}{1 - S_{wirr} - S_{or}}$$

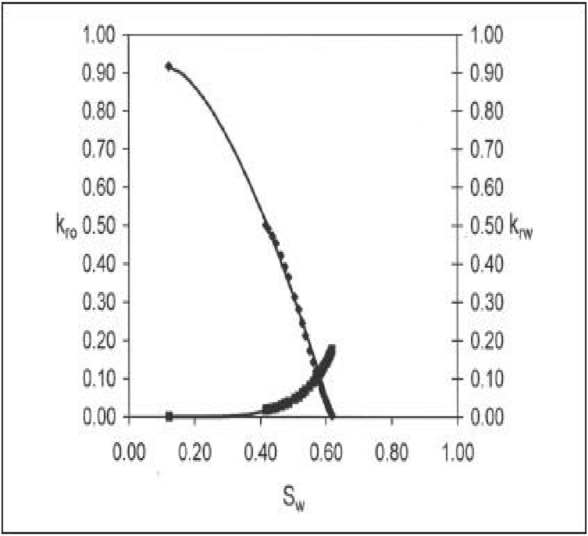

FIGURE 8.7.5 A comparison of the analytical model and the experimental relative permeability curves.

8.7e

The true fractional flow curve measured

in the experiment is shown in FIGURE 8.7.6.

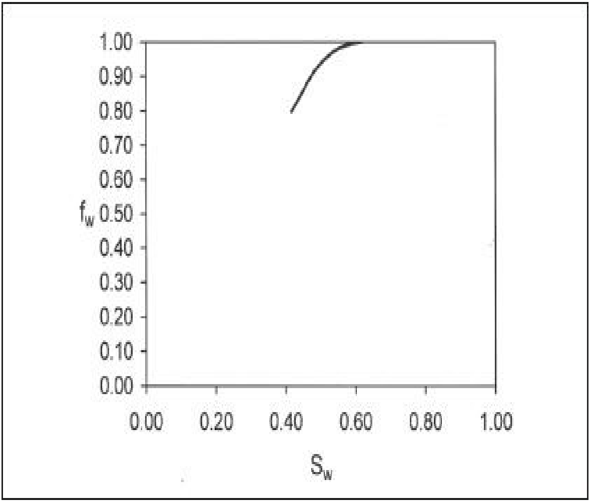

FIGURE 8.7.6 True fractional flow curve measured in the unsteady state experiment.

8.7f

The unsteady state experiment lasted 84.65 hours.

PROBLEM 8.8

$q_w = 200\ \text{cm}^3/\text{hr}$

$q_o = 50\ \text{cm}^3/\text{hr}$

$\mu_w = 1$ cp

$\mu_o = 10$ cp

$$f_w = \frac{q_w}{q_w + q_o} = \frac{200}{200+50} = 0.80$$

$P_5 = 1$ atm

Core 1

$$L = 20 \text{ cm}$$

$$\text{d} = 5 \text{ cm}$$

$$A = \pi\left(\frac{d}{2}\right)^2 = \pi\left(\frac{5}{2}\right)^2 = 19.635 \text{ cm}^2$$

$$k = 100 \text{ mD}$$

Core 2

$$L = 20 \text{ cm}$$

$$\text{d} = 5 \text{ cm}$$

$$A = \pi\left(\frac{d}{2}\right)^2 = \pi\left(\frac{5}{2}\right)^2 = 19.635 \text{ cm}^2$$

$$k = 50 \text{ mD}$$

8.8a

At $f_w = 0.80$

$S_{w1} = 0.31$

$K_{ro1} = 0.26$

$S_{w2} = 0.558$

$K_{ro2} = 0.27$

8.8b

Darcy's law for multiphase flow gives

$$\Delta P_o = \frac{q_o \mu_o L}{k k_{ro} A} \tag{8.8.1}$$

Application of unit conversions to Eq. (8.8.1) gives

$$\Delta P_o = \frac{(q_o / 3600)\mu_o L}{(k / 1000)k_{ro} A} = 0.2778 \frac{q_o \mu_o L}{k k_{ro} A} \tag{8.8.2}$$

$$P_{o4} - P_{o5} = 0.2778 \frac{q_o \mu_o (L_2 / 2)}{k_2 k_{ro2} A} = 0.2778 \times \frac{50 \times 10 \times (20/2)}{50 \times 0.27 \times 19.635} = 5.240 \text{ atm}$$

$$P_{o4} = P_{o5} + 5.240 = 1 + 5.240 = 6.240 \text{ atm absolute}$$

$$P_{o3} - P_{o5} = 0.2778 \frac{q_o \mu_o L_2}{k_2 k_{ro2} A} = 0.2778 \times \frac{50 \times 10 \times 20}{50 \times 0.27 \times 19.635} = 10.479 \text{ atm}$$

$$P_{o3} = P_{o5} + 10.479 = 1 + 10.479 = 11.479 \text{ atm absolute}$$

$$P_{o2} - P_{o3} = 0.2778 \frac{q_o \mu_o (L_1/2)}{k_1 k_{ro1} A} = 0.2778 \times \frac{50 \times 10 \times (20/2)}{100 \times 0.26 \times 19.635} = 2.721 \text{ atm}$$

$$P_{o2} = P_{o3} + 2.721 = 11.479 + 2.721 = 14.200 \text{ atm absolute}$$

$$P_{o1} - P_{o3} = 0.2778 \frac{q_o \mu_o L_1}{k_1 k_{ro1} A} = 0.2778 \times \frac{50 \times 10 \times 20}{100 \times 0.26 \times 19.635} = 5.441 \text{ atm}$$

$$P_{o1} = P_{o3} + 5.441 = 11.479 + 5.441 = 16.921 \text{ atm absolute}$$

The gauge pressures are

$$P_{o1} = 15.921 \text{ atm guage}$$

$$P_{o2} = 13.200 \text{ atm guage}$$

$$P_{o3} = 10.479 \text{ atm guage}$$

$$P_{o4} = 5.240 \text{ atm guage}$$

$$P_{o5} = 0 \text{ atm guage}$$

8.8c

To enable the pressure gauges to sense the oil pressure and not the water pressure, the pressure taps should be instrumented with oil-wet semi-permeable membranes that are saturated with oil and are in contact with the core. The stems of the pressure gauges also should be filled with oil.

8.8d

Core 1 is oil wet for the following reasons:

- The end-point relative permeability to oil is less than the end-point relative permeability to water. This is an indication that the core is preferentially oil wet. See Section 8.5.3 for explanation.
- The intersection of the oil and water relative permeability curves occurs at S_w = 0.37 0.50 (Craig's rule of thumb).
- S_{wjrr} =0.15 is low and falls within Craig's rule of thumb for oil-wet reservoirs.

Core 2 is water wet for the following

reasons:

- The end-point relative permeability to water is less than the-end point relative permeability to oil. This is an indication that the core is preferentially water wet. See Section 8.5.3 for explanation.
- The intersection of the oil and water relative permeability curves occurs at $S_w = 0.51 > 0.50$ (Craig's rule of thumb).
- $S_{wirr} = 0.35$ is high and falls within Craig's rule-of-thumb for water-wet reservoirs.

PROBLEM 8.9

8.9a

TABLE 8.9.1 shows the dimensional matrix.

TABLE 8.9.1 Dimensional Matrix.

	μ_w x_1	D_p x_2	σ x_3	u x_4	ρ_o x_5	μ_o x_6	ρ_w x_7	$\Delta\rho g$ x_8
M	1	0	1	0	1	1	1	1
L	–1	1	0	1	–3	–1	–3	–2
T	–1	0	–2	–1	0	–1	0	–2

8.9b

The rank of the dimensional matrix is 3 because the determinant of the following 3×3 submatrix is not zero.

$$\det\begin{bmatrix} 0 & 1 & 0 \\ 1 & 0 & 1 \\ 0 & 2 & -1 \end{bmatrix} = -1 \neq 0$$

$$N = 8$$

$$r = 3$$

Number of independent dimensionless group = $N - r = 5$.

8.9c

The dimensional matrix can be reduced to the following row echelon form by row operations:

$$\begin{bmatrix} 1 & 0 & 0 & -1 & 2 & 1 & 2 & 0 \\ 0 & 1 & 0 & 0 & -1 & 0 & -1 & -2 \\ 0 & 0 & 1 & 1 & -1 & 0 & -1 & 1 \end{bmatrix}$$

The solution to the dimensional analysis problem is

$$x_1 = x_4 - 2x_5 - x_6 - 2x_7$$

$$x_2 = x_5 + x_7 + 2x_8$$

$$x_3 = -x_4 + x_5 + x_7 - x_8$$

$$x_4 = x_4$$

$$x_5 = x_5$$

$$x_6 = x_6$$

$$x_7 = x_7$$

$$x_8 = x_8$$

The solution in matrix form is

$$\begin{matrix} \mu_w \\ D_p \\ \sigma \\ u \\ \rho_o \\ \mu_o \\ \rho_w \\ \Delta\rho g \end{matrix} \begin{bmatrix} x_1 \\ x_2 \\ x_3 \\ x_4 \\ x_5 \\ x_6 \\ x_7 \\ x_8 \end{bmatrix} = \begin{bmatrix} 1 \\ 0 \\ -1 \\ 1 \\ 0 \\ 0 \\ 0 \\ 0 \end{bmatrix} x_4 + \begin{bmatrix} -2 \\ 1 \\ 1 \\ 0 \\ 1 \\ 0 \\ 0 \\ 0 \end{bmatrix} x_5 + \begin{bmatrix} -1 \\ 0 \\ 0 \\ 0 \\ 0 \\ 1 \\ 0 \\ 0 \end{bmatrix} x_6 + \begin{bmatrix} -2 \\ 1 \\ 1 \\ 0 \\ 0 \\ 0 \\ 1 \\ 0 \end{bmatrix} x_7 + \begin{bmatrix} 0 \\ 2 \\ -1 \\ 0 \\ 0 \\ 0 \\ 0 \\ 1 \end{bmatrix} x_8$$

The initial set of independent dimensionless groups is

$$\pi_1 = \frac{\mu_w u}{\sigma}$$

$$\pi_2 = \frac{\rho_o \sigma D_p}{\mu_w^2}$$

$$\pi_3 = \frac{\mu_o}{\mu_w}$$

$$\pi_4 = \frac{\rho_w \sigma D_p}{\mu_w^2}$$

$$\pi_5 = \frac{\Delta \rho g D_p^2}{\sigma}$$

We need to transform the initial set of dimensionless groups into more meaningful and familiar dimensionless groups.

Choose $x_4 = 1$

$$\Pi_1 = \frac{\mu_w u}{\sigma} = \pi_1$$

Choose $x_5 = 1$, $x_7 = -1$

$$\Pi_2 = \frac{\rho_o}{\rho_w} = \frac{\pi_2}{\pi_4}$$

Choose $x_6 = 1$

$$\Pi_3 = \frac{\mu_o}{\mu_w} = \pi_3$$

Choose $x_4 = 1$, $x_7 = 1$

$$\Pi_4 = \frac{\rho_w u D_p}{\mu_w} = \pi_1 \times \pi_4$$

Choose $x_8 = 1$

$$\Pi_5 = \frac{\Delta \rho g D_p^2}{\sigma} = \pi_5$$

Thus,

$$k_{rw} = f_1\left(S_w, \Gamma, \theta, \frac{\mu_w u}{\sigma}, \frac{\rho_o}{\rho_w}, \frac{\mu_o}{\mu_w}, \frac{\rho_w u D_p}{\mu_w}, \frac{\Delta \rho g D_p^2}{\sigma} \right)$$

Similarly,

$$k_{ro} = f_2\left(S_w, \Gamma, \theta, \frac{\mu_w u}{\sigma}, \frac{\rho_o}{\rho_w}, \frac{\mu_o}{\mu_w}, \frac{\rho_w u D_p}{\mu_w}, \frac{\Delta \rho g D_p^2}{\sigma} \right)$$

PROBLEM 8.10

Γ: Pore structure or the morphology of the porous medium. Does it affect the relative permeability curves obtained by the steady state method? Yes. How? See Section 8.5.7.

θ: Wettability.
Does it affect the relative permeability curves obtained by the steady state method? Yes. How? See Section 8.5.3.

$\dfrac{\mu_w u}{\sigma}$: Capillary number.

Does it affect the relative permeability curves obtained by the steady state method? Yes, depending on its magnitude. How? Capillary number is a measure of the ability to mobilize residual phases in a porous medium. If the capillary number is high enough, residual phases will be reduced thereby increasing the range of wetting and nonwetting phase saturations for which the relative permeability curves are nonzero. However, if the capillary number is low, as in a normal waterflood, it will have no effect on the relative permeability curves.

$\frac{\rho_o}{\rho_w}$: Ratio of inertia forces in the nonwetting and wetting phases.

Does it affect the relative permeability curves obtained by the steady state method? No. Why? For the slow flow in porous media, the inertia force is usually negligible. This is the underlying premise for Darcy's law normally used to describe flow in porous media.

$\frac{\mu_o}{\mu_w}$: Ratio of viscous forces in the nonwetting and wetting phases.

Does it affect the relative permeability curves obtained by the steady state method? No. Why? In the steady state experiment, there is no displacement of one fluid by another as the two fluids are mixed and co-injected. The instability normally caused by adverse viscosity ratio in a displacement is absent. See Section 8.5.5. It should be noted that this dimensionless group will affect the relative permeability curves obtained by the unsteady state method.

$\frac{\rho_w u D_p}{\mu_w}$: Reynolds number in the wetting phase. Ratio of inertia to viscous forces in the wetting phase.

Does it affect the relative permeability curves obtained by the steady state method? No. Why? For the slow flow in porous media, the inertia force is usually negligible.

$\frac{\Delta \rho g D_p^2}{\sigma}$: Eötvös number. Ratio of gravity and interfacial or capillary forces at the pore scale.

Does it affect the relative permeability curves obtained by the steady state method? No. Why? For the slow flow in porous media, the inertia force is usually negligible. Because of the small pore dimension, the capillary force far exceeds the gravity force. Therefore, this number is negligibly small and will have no effect on the relative permeability curves. To see how small this number can be, let us calculate it for a typical steady state relative permeability experiment.

$$\rho_w = 1 \text{ g/cm}^3$$

$$\rho_o = 0.8 \text{ g/cm}^3$$

$$\sigma = 35 \text{ dynes/cm}$$

$$g = 981 \text{ cm/s}^2$$

$$D_p = 5\ \mu\text{m} = 5\times10^{-4}\text{ cm}$$

$$\frac{\Delta\rho g D_p^2}{\sigma} = \frac{(1-0.8)\times981\times\left(5\times10^{-4}\right)^2}{35} = 1.401\times10^{-6}$$

PROBLEM 8.11

8.11a

FIGURE 8.11.1 shows the polymer saturation profiles to be expected before breakthrough.

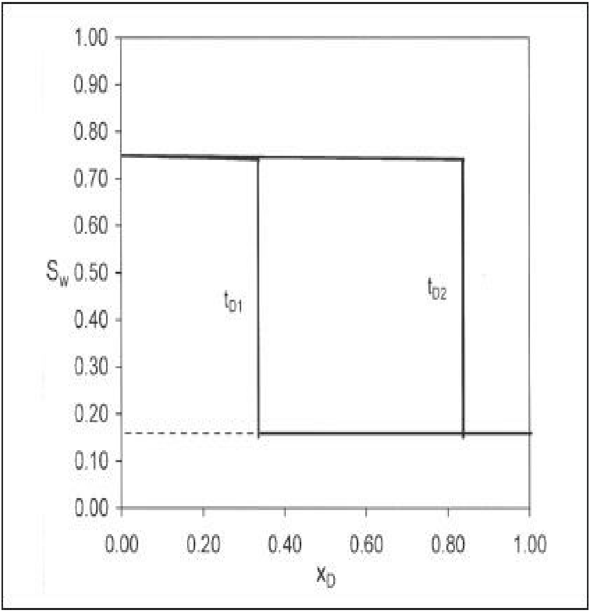

FIGURE 8.11.1 Polymer saturation profiles before breakthrough.

8.11b

FIGURE 8.11.2 shows the expected oil

recovery curve.

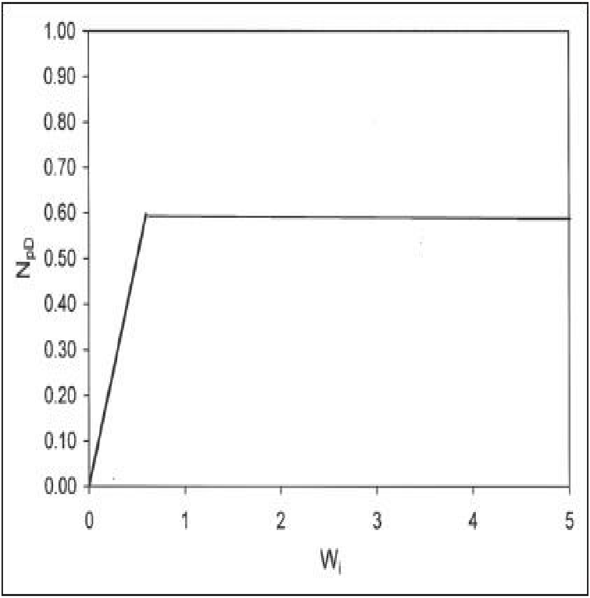

FIGURE 8.11.2 Oil recovery curve.

8.11c

The colleague’s suggestion is a bad idea because the data from a favorable mobility ratio displacement are not suitable for calculating the relative permeability curves by the JBN method. There are two reasons for this problem.

1. The saturation window for the unsteady state method is

$$\frac{k_{ro}}{k_{rw}}=\frac{\mu_o f_{o2}}{\mu_w\left(1-f_{o2}\right)} \tag{8.11.1}$$

. For the polymerflood,

$$f_{o2}=\frac{dN_{pD}}{dW_i} \tag{8.11.2}$$

.

Therefore, the saturation window is lost.

2. Two of the key equations for the unsteady state method are

$$\frac{dN_{pD}}{dW_i} = 0 \quad (8.11.3)$$

$$f_{o2} = \frac{dN_{pD}}{dW_i} \quad (8.11.2)$$

For the polymerflood, after breakthrough,

$$\frac{dN_{pD}}{dW_i} = 0 \quad (8.11.3)$$

There are no data available to calculate the ratio of the relative permeability curves after breakthrough, which is the basis for the unsteady state method.

PROBLEM 8.12

8.12a

If the core is oriented horizontally, the injected gas could migrate to the top due to gravity segregation. If that happens, the result of the measurement will be wrong.

8.12b

To overcome the problem of gravity segregation, the core should be oriented vertically with the gas injected at the top and the produced fluids drained from the bottom.

8.12c

See Figure 8.2 in Volume 2 for typical drainage relative permeability curves.

PROBLEM 8.13

8.13a

$$\text{USBM Wettability Index} = \log(A_1/A_2)$$

where

A_1 = the area under the capillary pressure curve for oil displacing water

A_2 = the area under the capillary pressure curve for water displacing oil

From the given centrifuge data, A_2»A_1. Therefore, $\log(A_1/A_2)$0. This indicates that the medium is preferentially oil wet. One can estimate a numerical value for the USBM wettability index as follows. From the centrifuge data, $A_2 \approx 1.5\ A_1$. Therefore, $\log(A_1 / A_2) \approx \log(1 / 2) = -0.18$.

8.13b

The relative permeability curves for a preferentially oil wet medium typically shows a high-end point value for water which is comparable to or even higher than the end-point value for oil. Also, based on Craig's rule of thumb, the relative permeability curves for an oil-wet medium usually intersect at a water saturation less than 0.50. These considerations are the basis for the sketch of the relative permeability curves shown in **FIGURE 8.13.1**.

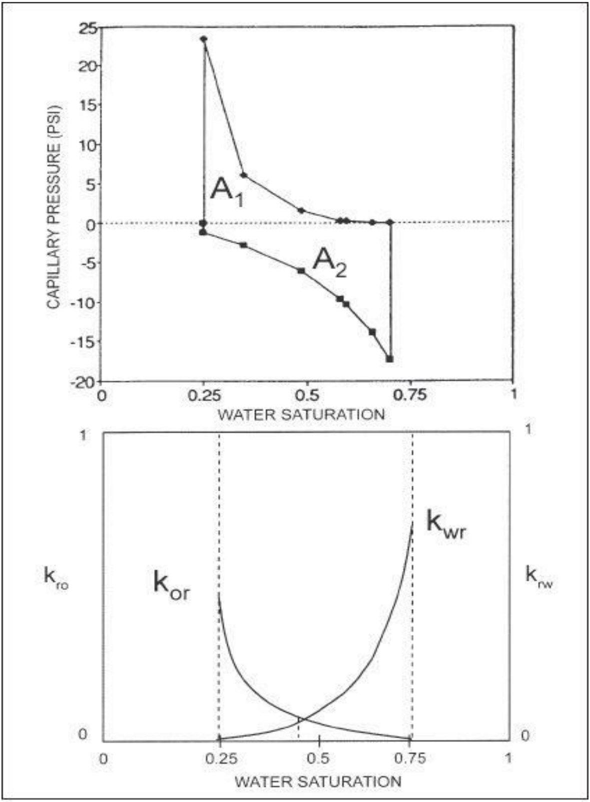

FIGURE 8.13.1 Relative permeability curves for oil-wet medium.

PROBLEM 8.14

8.14a

Darcy's law gives

$$q = \frac{k_w A}{\mu_w}\left(\frac{P_1 - P}{x}\right) \tag{8.14.1}$$

$$q = \frac{k_o A}{\mu_o}\left(\frac{P - P_2}{L - x}\right) \tag{8.14.2}$$

where P is the pressure at the front. Also,

$$(P_1 - P) + (P - P_2) = (P_1 - P_2) \tag{8.14.3}$$

Substituting Eqs.(8.14.1) and (8.14.2)

into (8.14.3) gives

$$\frac{q\mu_w x}{k_w A}+\frac{q\mu_o(L-x)}{k_o A}=(P_1-P_2) \tag{8.14.4}$$

From Eq.(8.14.4)

$$\frac{q}{A}=\frac{P_1-P_2}{\mu_w x/k_w+\mu_o(L-x)/k_o} \tag{8.14.5}$$

The interstitial velocity of the front is given by

$$\frac{dx}{dt}=\frac{q}{\phi A(1-S_{wirr}-S_{or})}=\frac{P_1-P_2}{\phi(1-S_{wirr}-S_{or})[\mu_w x/k_w+\mu_o(L-x)/k_o]} \tag{8.14.6}$$

Eq.(8.14.6) can be rearranged as

$$\frac{dx}{dt} = \frac{\left[k_w\left(P_1 - P_2\right)/\mu_w\right]/\left[\phi\left(1 - S_{wirr} - S_{or}\right)\right]}{\left[x + M\left(L - x\right)\right]} \quad (8.14.7)$$

where

$$M = \frac{k_w}{\mu_w} \times \frac{\mu_o}{k_o} \quad (8.14.8)$$

In Darcy units,

$$P_1 = \rho_w g h_w / 1.0133 \times 10^6 \quad (8.14.9)$$

$$P_2 = \rho_o g h_o / 1.0133 \times 10^6 \quad (8.14.10)$$

Substituting Eqs.(8.14.9) and (8.14.10) into (8.14.7) gives

$$\frac{dx}{dt}=\frac{\left[k_w\left(\rho_w h_w-\rho_o h_o\right)/1.0133\times10^6\mu_w\right]/\left[\phi\left(1-S_{wirr}-S_{or}\right)\right]}{\left[x+M\left(L-x\right)\right]} \tag{8.14.11}$$

Eq.(8.14.11) is of the form

$$\frac{dx}{dt}=\frac{\text{constant}}{\left[x+M\left(L-x\right)\right]} \tag{8.14.12}$$

where

$$\text{constant}=\left[k_w\left(\rho_w h_w-\rho_o h_o\right)/1.0133\times10^6\mu_w\right]/\left[\phi\left(1-S_{wirr}-S_{or}\right)\right] \tag{8.14.13}$$

8.14b

Separate variables and integrate Eq. (8.14.12) to obtain

$$\frac{1}{2}x^2 + MLx - \frac{1}{2}Mx^2 + C = \text{constant} \times t \qquad (8.14.14)$$

Application of the initial condition, $x = 0$ at $t = 0$ gives $C = 0$. Eq.(8.14.14) becomes

$$\frac{1}{2}(1-M)x^2 + MLx = \text{constant} \times t \qquad (8.14.15)$$

When the water arrives at the oil tank, $x = L$, and Eq.(8.14.15) becomes

$$\frac{1}{2}(1-M)L^2 + ML^2 = \frac{1}{2}(1+M)L^2 = \text{constant} \times t \qquad (8.14.16)$$

The time the front arrives at the oil tank is obtained from Eq.(8.14.16) as

$$t_{arrival} = \frac{(1+M)L^2/2}{\text{constant}} \tag{8.14.17}$$

$$L = 100 \text{ cm}$$

$$\phi = 0.25$$

$$k = 500 \text{ mD} = 0.50 \text{ D}$$

$$S_{wirr} = 0.20$$

$$S_{or} = 0.15$$

$$k_{or} = 0.70$$

$$k_{wr} = 0.60$$

$$\rho_w = 1.0 \text{ g/cm}^3$$

$$\rho_o = 0.85 \text{ g/cm}^3$$

$$\mu_w = 1.0 \text{ cp}$$

$$\mu_o = 0.50 \text{ cp}$$

$$h_w = 300 \text{ cm}$$

$$h_o = 20 \text{ cm}$$

$$g = 981 \text{ cm/s}^2$$

$$M = \frac{kk_{wr}}{\mu_w} \times \frac{\mu_o}{kk_{or}} = \frac{(0.50)(0.60)}{1} \times \frac{0.50}{(0.50)(0.70)} = 0.4286$$

$$\text{constant} = \frac{(0.50)(0.60)}{1}(981)\left(\frac{1.0\times 300 - 0.85\times 20}{1.0133\times 10^6}\right) \times \frac{1}{0.25(1-0.20-0.15)} = 0.5058$$

$$t_{arrival} = \frac{(1+M)L^2/2}{\text{constant}} = \frac{(1+0.4286)100^2/2}{0.5058} = 14{,}121.9 s = 3.92 \text{ hrs}$$

PROBLEM 8.15

8.15a

Darcy's law gives

$$q_w = -\frac{kk_{rw}A}{\mu_w}\frac{\partial P_w}{\partial x} \tag{8.15.1}$$

$$q_o = -\frac{kk_{ro}A}{\mu_o}\frac{\partial P_o}{\partial x} \tag{8.15.2}$$

Capillary pressure constraint is

$$P_o - P_w = P_c\left(S_w\right) \tag{8.15.3}$$

For incompressible fluids, for countercurrent flow,

$$q_w + q_o = 0 \tag{8.15.4}$$

$$\phi A \frac{\partial S_w}{\partial t} + \frac{\partial q_w}{\partial x} = 0 \tag{8.15.5}$$

Eqs.(8.15.1) through (8.15.5) can be combined to obtain the required partial differential equation as

$$\phi \frac{\partial S_w}{\partial t} + \frac{k}{\mu_o} \frac{\partial}{\partial x}\left(k_{ro} F_w \frac{dP_c}{dS_w} \frac{\partial S_w}{\partial x} \right) = 0 \tag{8.15.6}$$

where

$$F_w = \frac{1}{1 + \frac{k_{ro}\mu_w}{k_{rw}\mu_o}} \tag{8.15.7}$$

8.15b

The initial condition is

$$S_w(x,0)=S_{wirr} \quad (8.15.8)$$

The boundary conditions are

$$S_w(0,t)=1-S_{or} \quad (8.15.9)$$

At $x = L$, $q_w = 0$. This condition leads to

$$\frac{dP_c}{dS_w}\frac{\partial S_w}{\partial x}=0 \text{ at } x=L \quad (8.15.10)$$

8.15c

Let

$$x_D=\frac{x}{L} \quad (8.15.11)$$

$$P_c(S_w) = \frac{\sigma \cos\theta}{\sqrt{k/\phi}} J(S_w) \tag{8.15.12}$$

$$S_{wD} = \frac{S_w - S_{wirr}}{1 - S_{wirr} - S_{or}} \tag{8.15.13}$$

Substituting Eqs.(8.15.11) through (8.15.13) into (8.15.6) gives

$$\phi(1 - S_{wirr} - S_{or})\frac{\partial S_{wD}}{\partial t} + \frac{k\sigma\cos\theta}{\mu_o L^2\sqrt{k/\phi}}\frac{\partial}{\partial x_D}\left(k_{ro}F_w\frac{dJ}{dS_{wD}}\frac{\partial S_{wD}}{\partial x_D}\right) = 0 \tag{8.15.14}$$

Let the dimensionless time for capillary imbibition be defined as

$$t_D = \frac{k\sigma\cos\theta}{\phi\left(1-S_{wirr}-S_{or}\right)\mu_o L^2\sqrt{k/\phi}}t = \left(\frac{k\sigma\cos\theta}{\left(1-S_{wirr}-S_{or}\right)\mu_o L^2}\sqrt{\frac{k}{\phi}}\right)t \tag{8.15.15}$$

Substituting Eq.(8.15.15) into (8.15.14) gives

$$\frac{\partial S_{wD}}{\partial t_D} + \frac{\partial}{\partial x_D}\left(k_{ro}F_w\frac{dJ}{dS_{wD}}\frac{\partial S_{wD}}{\partial x_D}\right) = 0 \tag{8.15.16}$$

The initial condition becomes

$$S_{wD}\left(x_D, 0\right) = 0 \tag{8.15.17}$$

The boundary conditions become

$$S_{wD}\left(0, t_D\right) = 1 \tag{8.15.18}$$

$$\frac{dJ}{dS_{wD}}\frac{\partial S_{wD}}{\partial x_D}=0 \text{ at } x_D=1 \quad (8.15.19)$$

8.15d

FIGURE 8.15.1 shows the sketch of the expected saturation profiles.

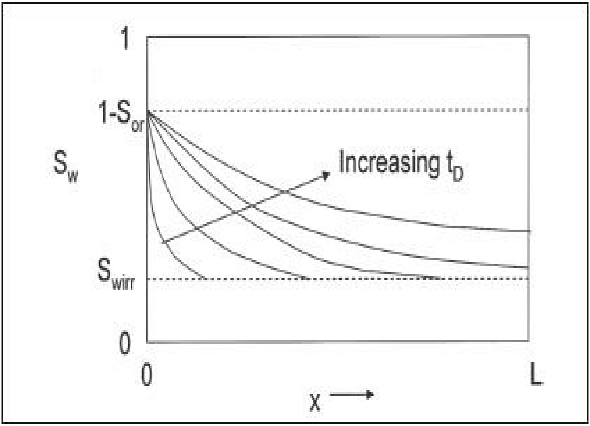

FIGURE 8.15.1 Expected saturation profiles.

PROBLEM 8.16

8.16a

Water will be spontaneously imbibed into the core and oil will be expelled from the core in a countercurrent fashion as time passes. Eventually, the imbibition will stop and some residual oil saturation will be left in the core.

8.16b

Darcy's law gives

$$q_w = -\frac{kk_{rw}A}{\mu_w}\left(\frac{\partial P_w}{\partial x} + \rho_w g\right) \quad (8.16.1)$$

$$q_o = -\frac{kk_{ro}A}{\mu_o}\left(\frac{\partial P_o}{\partial x} + \rho_o g\right) \tag{8.16.2}$$

Capillary pressure constraint is

$$P_o - P_w = P_c(S_w) \tag{8.16.3}$$

For incompressible fluids, for countercurrent flow,

$$q_w + q_o = 0 \tag{8.16.4}$$

$$\phi A \frac{\partial S_w}{\partial t} + \frac{\partial q_w}{\partial x} = 0 \tag{8.16.5}$$

Eqs.(8.16.1) through (8.16.5) can be combined to obtain the required partial differential equation as

$$\phi\frac{\partial S_w}{\partial t}+\frac{k}{\mu_o}\frac{\partial}{\partial x}\left(k_{ro}F_w\frac{dP_c}{dS_w}\frac{\partial S_w}{\partial x}\right)-\frac{k(\rho_w-\rho_o)}{\mu_o}\frac{d(k_{ro}F_w)}{dS_w}\frac{\partial S_w}{\partial x}=0 \quad (8.16.6)$$

where

$$F_w=\frac{1}{1+\frac{k_{ro}\mu_w}{k_{rw}\mu_o}} \quad (8.16.7)$$

8.16c
The initial condition is

$$S_w(x,0)=S_{wirr} \quad (8.16.8)$$

The boundary conditions are

$$S_w(0,t)=1-S_{or} \quad (8.16.9)$$

At $x = L$, $q_w = 0$. This condition leads to

$$\frac{dP_c}{dS_w}\frac{\partial S_w}{\partial x} = (\rho_w - \rho_o)g \text{ at } x = L \tag{8.16.10}$$

8.16d

Let

$$x_D = \frac{x}{L} \tag{8.16.11}$$

$$P_c(S_w) = \frac{\sigma \cos\theta}{\sqrt{k/\phi}} J(S_w) \tag{8.16.12}$$

$$S_{wD} = \frac{S_w - S_{wirr}}{1 - S_{wirr} - S_{or}} \tag{8.16.13}$$

Substituting Eqs.(8.16.11) through

(8.16.13) into (8.16.6) gives

$$\phi\left(1-S_{wirr}-S_{or}\right)\frac{\partial S_{wD}}{\partial t}+\frac{k\sigma\cos\theta}{\mu_o L^2\sqrt{k/\phi}}\frac{\partial}{\partial x_D}\left(k_{ro}F_w\frac{dJ}{dS_{wD}}\frac{\partial S_{wD}}{\partial x_D}\right)$$
$$-\frac{k\left(\rho_w-\rho_o\right)g}{\mu_o L}\frac{d\left(k_{ro}F_w\right)}{dS_{wD}}\frac{\partial S_{wD}}{\partial x_D}=0$$

(8.16.14)

Let the dimensionless time for capillary imbibition be defined as

$$t_D=\frac{k\sigma\cos\theta}{\phi\left(1-S_{wirr}-S_{or}\right)\mu_o L^2\sqrt{k/\phi}}t=\left(\frac{k\sigma\cos\theta}{\left(1-S_{wirr}-S_{or}\right)\mu_o L^2}\sqrt{\frac{k}{\phi}}\right)t$$

(8.16.15)

Substituting Eq.(8.16.15) into (8.16.14) gives

$$\frac{\partial S_{wD}}{\partial t_D}+\frac{\partial}{\partial x_D}\left(k_{ro}F_w\frac{dJ}{dS_{wD}}\frac{\partial S_{wD}}{\partial x_D}\right)$$
$$-\left(\frac{k(\rho_w-\rho_o)gL}{\sigma\cos\theta}\sqrt{\frac{k}{\phi}}\right)\frac{d(k_{ro}F_w)}{dS_{wD}}\frac{\partial S_{wD}}{\partial x_D}=0 \tag{8.16.16}$$

Let

$$N_g=\frac{(\rho_w-\rho_o)gL}{\sigma\cos\theta}\sqrt{\frac{k}{\phi}} \tag{8.16.17}$$

Substituting Eq.(8.16.17) into (8.16.17) gives

$$\frac{\partial S_{wD}}{\partial t_D}+\frac{\partial}{\partial x_D}\left(k_{ro}F_w\frac{dJ}{dS_{wD}}\frac{\partial S_{wD}}{\partial x_D}\right)-N_g\frac{d(k_{ro}F_w)}{dS_{wD}}\frac{\partial S_{wD}}{\partial x_D}=0 \tag{8.16.18}$$

The initial condition becomes

$$S_{wD}(x_D, 0) = 0 \tag{8.16.19}$$

The boundary conditions become

$$S_{wD}(0, t_D) = 1 \tag{8.16.20}$$

$$\frac{dJ}{dS_{wD}} \frac{\partial S_{wD}}{\partial x_D} = \frac{(\rho_w - \rho_o) g L}{\sigma \cos\theta} \sqrt{\frac{k}{\phi}} = \mathrm{N}_g \text{ at } x_D = 1 \tag{8.16.21}$$

8.16e

FIGURE 8.16.1 shows a sketch of the expected water saturation profiles.

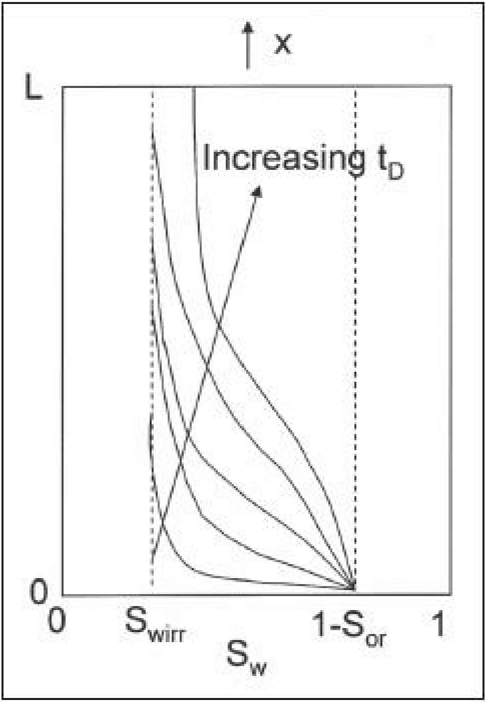

FIGURE 8.16.1 Water saturation profiles.

8.16f

FIGURE 8.16.2 shows a sketch of the expected oil recovery curve.

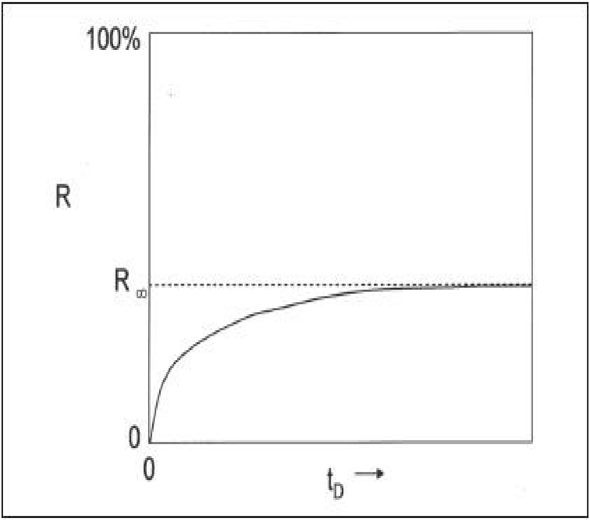

FIGURE 8.16.2 Oil-recovery curve.

PROBLEM 8.17

8.17a

TABLE 8.17.1 shows the dimensional matrix.

TABLE 8.17.1 Dimensional Matrix.

	μ_w x_1	L x_2	t x_3	μ_o x_4	$\sigma\cos\theta$ x_5	k/ϕ x_6
M	1	0	0	1	1	0
L	−1	1	0	−1	0	2
T	−1	0	1	−1	−2	0

8.17b

The rank of the dimensional matrix is 3 because the determinant of the following 3×3 submatrix is not zero.

$$\det\begin{bmatrix} 1 & 0 & 0 \\ -1 & 1 & 0 \\ -1 & 0 & 1 \end{bmatrix} = 1 \neq 0$$

$$N = 6$$

$$r = 3$$

Number of independent dimensionless group = $N - r = 3$.

8.17c

The dimensional matrix can be reduced to the following row echelon form by row operations:

$$\begin{bmatrix} 1 & 0 & 0 & 1 & 1 & 0 \\ 0 & 1 & 0 & 0 & 1 & 2 \\ 0 & 0 & 1 & 0 & -1 & 0 \end{bmatrix}$$

The solution to the dimensional analysis problem is

$$x_1 = -x_4 - x_5$$

$$x_2 = -x_5 - 2x_6$$

$$x_3 = x_5$$

$$x_4 = x_4$$

$$x_5 = x_5$$

$$x_6 = x_6$$

The solution in matrix form is

$$\begin{matrix} \mu_w \\ L \\ t \\ \mu_o \\ \sigma\cos\theta \\ k/\phi \end{matrix} \begin{bmatrix} x_1 \\ x_2 \\ x_3 \\ x_4 \\ x_5 \\ x_6 \end{bmatrix} = \begin{bmatrix} -1 \\ 0 \\ 0 \\ 1 \\ 0 \\ 0 \end{bmatrix} x_4 + \begin{bmatrix} -1 \\ -1 \\ 1 \\ 0 \\ 1 \\ 0 \end{bmatrix} x_5 + \begin{bmatrix} 0 \\ -2 \\ 0 \\ 0 \\ 0 \\ 1 \end{bmatrix} x_6$$

8.17d

The initial set of independent dimensionless groups is

$$\pi_1 = \frac{\mu_o}{\mu_w}$$

$$\pi_2 = \frac{t\sigma\cos\theta}{\mu_w L}$$

$$\pi_3 = \frac{\sqrt{k/\phi}}{L}$$

8.17e

The proposed dimensionless time for capillary imbibition is

$$t_D = \pi_2 \times \pi_3 = \left(\frac{\sigma\cos\theta}{\mu_w L^2}\sqrt{\frac{k}{\phi}}\right)t \tag{8.17.1}$$

Substituting the numerical value for *scosθ* into Eq.(8.17.1) along with the appropriate unit conversions gives

$$t_D = \left(\frac{35 \times 1}{\mu_w \times 0.01 \times L^2} \sqrt{\frac{k \times 9.869 \times 10^{-9}}{\phi}} \right) t \times 60 = 20.8620 \left(\frac{1}{\mu_w L^2} \sqrt{\frac{k}{\phi}} \right) t \tag{8.17.2}$$

We need to replot the recovery data versus the proposed dimensionless time. If the hypothesis is correct, the recovery data from the three experiments will plot as one curve.

$$\mu_w = 0.9 \text{ cp}$$

$$L_1 = 5.08 \text{ cm}$$

$$k_1 = 1.475 \text{ D}$$

$$\phi_1 = 0.291$$

$$t_{D1} = 20.8620\left(\frac{1}{0.9 \times 5.08^2}\sqrt{\frac{1.475}{0.291}}\right)t = 2.0223t$$

$$L_2 = 11.05 \text{ cm}$$

$$k_2 = 1.545 \text{ D}$$

$$\phi_2 = 0.289$$

$$t_{D2} = 20.8620\left(\frac{1}{0.9 \times 11.05^2}\sqrt{\frac{1.545}{0.289}}\right)t = 0.4389t$$

$$L_3 = 7.75 \text{ cm}$$

$$k_3 = 0.075 \text{ D}$$

$$\phi_3 = 0.223$$

$$t_{D3} = 20.8620\left(\frac{1}{0.9\times 7.75^2}\sqrt{\frac{0.075}{0.223}}\right)t = 0.2238t$$

FIGURE 8.17.1 shows the recovery data for the three experiments plotted versus the proposed dimensionless time for capillary imbibition. They plot as one curve. The hypothesis is verified.

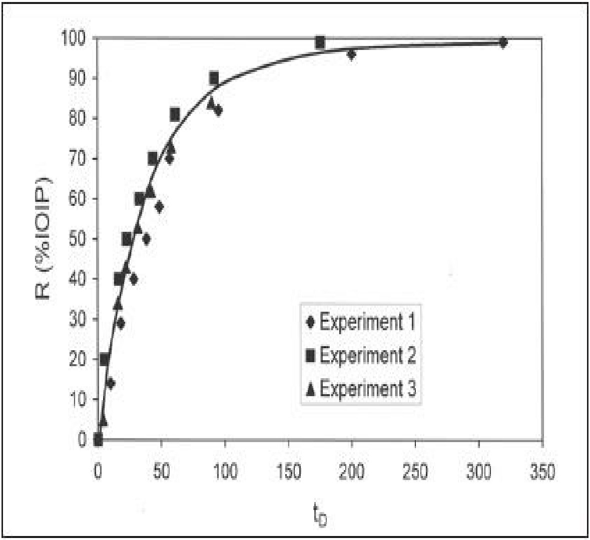

FIGURE 8.17.1 Oil-recovery curves for the three experiments.

PROBLEM 8.18

L = 1 ft = 30.48 cm

d = 2 in = (2/12)x30.48 = 5.08 cm

$A = \pi(d/2)^2 = \pi p(5.08/2)^2 = 20.2683\ cm^2$

k = 1 D

Ø = 0.20

σ = 30 dynes/cm

$\rho_w = 1\ g/cm^3$

$\rho_o = 0.9\ g/cm^3$

μ_w = 1 cp

μ_o = 10 cp

S_{wirr}=0–25

S_{Or}=0.15

K_{wr} = 0.05

K_{or}=0.90

8.18a

$$\Delta P_w = \frac{q_w \mu_w L}{k k_{wr} A} \qquad (8.18.1)$$

$$q_w = 1\ \text{cm}^3/\text{min} = (1/60)\ \text{cm}^3/\text{s}$$

Substituting the numerical values into Eq.(8.18.1) gives

$$\Delta P_w = \frac{q_w \mu_w L}{k k_{wr} A} = \frac{(1/60)\times 1\times 30.48}{1\times 0.05\times 20.2683} = 0.5013\ \text{atm} = 7.37\ \text{psi}$$

8.18b

$$q_w = q_o = 1\ \text{cm}^3/\text{min}$$

$$F_w = \frac{1}{1 + \frac{k_{ro}\mu_w}{k_{rw}\mu_o}} = \frac{1}{2} \qquad (8.18.2)$$

$$\frac{k_{ro}}{k_{rw}} \times \frac{\mu_w}{\mu_o} = 1 \qquad (8.18.3)$$

$$\frac{k_{ro}}{k_{rw}} \times \frac{\mu_w}{\mu_o} = \frac{0.90\left(\frac{0.85 - S_w}{0.60}\right)^{1.2}}{0.05\left(\frac{S_w - 0.25}{0.60}\right)^{4.2}} \times \frac{1}{10} = 1 \qquad (8.18.4)$$

Eq.(8.18.4) can be solved iteratively to obtain $S_w = 0.7076$.

8.18c

The partial differential equation for the wetting phase is given by

$$\frac{\partial S_w}{\partial x} = \frac{\frac{q_w \mu_w}{k_{rw}} - \frac{q_o \mu_o}{k_{ro}}}{kA\left(\frac{dP_c}{dS_w}\right)} \tag{8.18.5}$$

The boundary condition is

$$S_w = 0.85 \quad \text{at } x = L \tag{8.18.6}$$

We consider the steady state condition after injecting oil for a long time such that no more water is produced. Only oil is flowing in the core. Thus at steady state, $q_w = 0$, and the partial differential equation becomes the following ordinary differential equation:

$$\frac{dS_w}{dx} = -\frac{\dfrac{q_o \mu_o}{k_{ro}}}{kA\left(\dfrac{dP_c}{dS_w}\right)} \tag{8.18.7}$$

After substituting the expressions for k_{ro}, P_c, and the numerical values for the various parameters, Eq.(8.18.6) becomes

$$\frac{dS_w}{dx} = 0.1596\left(\frac{S_w - 0.25}{0.85 - S_w}\right)^{1.2} \tag{8.18.8}$$

After separating variables and rearranging, Eq.(8.18.8) can be integrated to give

$$\int_{0.25}^{S_w} 6.2649\left(\frac{0.85-S_w}{S_w-0.25}\right)dS_w = x + x_o \qquad (8.18.9)$$

where x_0 is an integration constant. Application of the boundary condition gives

$$\int_{0.25}^{0.85} 6.2649\left(\frac{0.85-S_w}{S_w-0.25}\right)dS_w = 27.0451 = 30.48 + x_o \qquad (8.18.10)$$

$$x_o = 27.0451 - 30.4800 = -3.4349$$

The water saturation profile is then given by

$$x = 3.4349 + \int_{0.25}^{0.85} 6.2649\left(\frac{0.85-S_w}{S_w-0.25}\right)dS_w \qquad (8.18.11)$$

The integral on the right side of Eq.

(8.18.11) can be performed numerically for various values of S_w to calculate the steady state water saturation profile shown in **FIGURE 8.18.1**, plotted in dimensionless form.

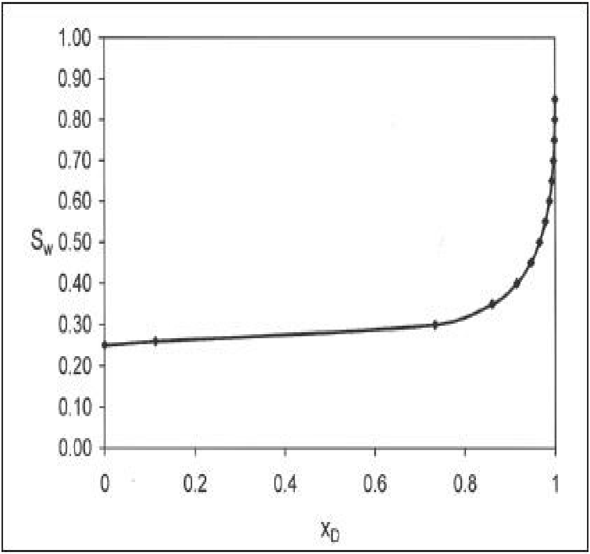

FIGURE 8.18.1 Steady state water saturation profile showing capillary end effect.

PROBLEM 8.19

8.19a

FIGURE 8.19.1 shows the water saturation profiles together with the porosity along the sandpack. Clearly, the variation of the porosity along the sandpack is an indication that the sandpack is not homogeneous.

It should be observed that the sandpack has its lowest porosity and by inference its lowest permeability in the vicinity of $x_D = 0.45$. From our knowledge of capillarity, it is not surprising that this section of the sandpack has retained more water as the flood progresses than the neighboring sections, resulting in the anomalously high water saturation at late times.

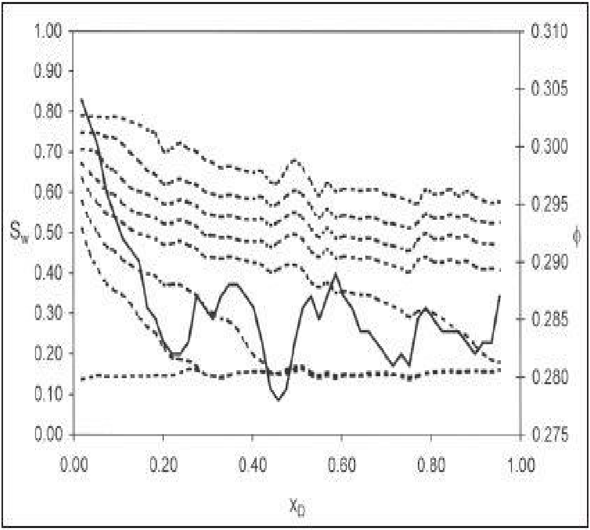

FIGURE 8.19.1 Water saturation and porosity profiles for the waterflood in the water-wet sandpack.

8.19b

FIGURE 8.19.2 shows the similarity transformation in the spirit of Figure 8.11. All the data essentially plot as one curve thereby providing the experimental verification of the theory of immiscible displacement in porous media.

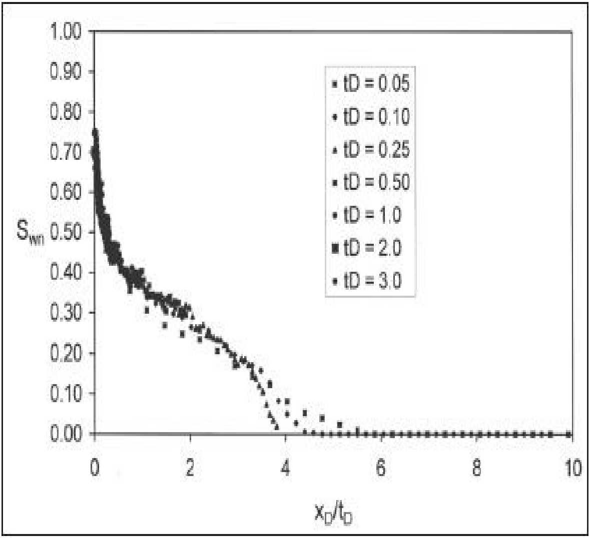

FIGURE 8.19.2 Similarity transformation for the waterflood in the water-wet sandpack.

8.19c

The true fractional flow curve is given by

$$f_w = \int \frac{x_D}{t_D} dS_w + C \tag{8.19.1}$$

$$f_w = 1 \text{ at } S_w = 1 - S_{or} \tag{8.19.2}$$

where C is an integration constant. **FIGURE 8.19.3** shows the true fractional flow curve computed for this flood and tabulated in TABLE 8.19.1. It should be observed that the true fractional flow curve at low water saturations does not have the S shape of the approximate fractional flow curve. It is also nonlinear. The Welge tangent line is only an approximation of this curve, which is satisfactory in many cases. For this flood, $S_{or} = 0.21$.

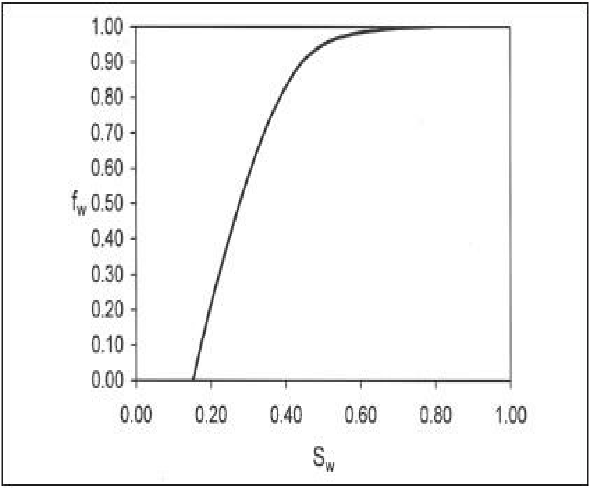

FIGURE 8.19.3 True fractional flow curve for the waterflood in the water-wet sandpack.

TABLE 8.19.1 Computed True Fractional Flow Curve.

S_w	f_w	S_w	f_w	S_w	f_w	S_w	f_w	S_w	f_w	S_w	f_w
0.150	0.000	0.411	0.847	0.411	0.848	0.487	0.939	0.545	0.970	0.613	0.987
0.153	0.007	0.411	0.848	0.412	0.849	0.487	0.939	0.545	0.970	0.615	0.987
0.155	0.016	0.412	0.849	0.414	0.852	0.489	0.941	0.546	0.970	0.619	0.988
0.159	0.032	0.414	0.852	0.416	0.855	0.490	0.942	0.547	0.970	0.624	0.988
0.168	0.075	0.416	0.855	0.416	0.855	0.490	0.942	0.547	0.971	0.625	0.988
0.171	0.089	0.416	0.855	0.421	0.865	0.491	0.942	0.547	0.971	0.626	0.988
0.174	0.103	0.421	0.865	0.421	0.865	0.491	0.943	0.549	0.971	0.626	0.989
0.182	0.135	0.421	0.865	0.423	0.869	0.492	0.943	0.551	0.972	0.627	0.989
0.185	0.148	0.423	0.869	0.424	0.869	0.492	0.944	0.551	0.972	0.628	0.989
0.193	0.184	0.424	0.869	0.424	0.870	0.493	0.944	0.559	0.974	0.631	0.989
0.193	0.185	0.424	0.870	0.425	0.871	0.493	0.945	0.561	0.975	0.632	0.989

continues on next page

S_w	f_w	S_w	f_w	S_w	f_w	S_w	f_w	S_w	f_w	S_w	f_w
0.195	0.195	0.425	0.871	0.425	0.872	0.494	0.945	0.562	0.975	0.634	0.989
0.214	0.272	0.425	0.872	0.427	0.874	0.495	0.945	0.562	0.975	0.639	0.990
0.220	0.295	0.427	0.874	0.428	0.876	0.495	0.946	0.568	0.976	0.645	0.990
0.221	0.298	0.428	0.876	0.429	0.878	0.495	0.946	0.570	0.977	0.648	0.991
0.240	0.370	0.429	0.878	0.430	0.879	0.497	0.947	0.571	0.977	0.650	0.991
0.253	0.415	0.430	0.879	0.434	0.887	0.500	0.949	0.572	0.977	0.651	0.991
0.254	0.419	0.434	0.887	0.435	0.887	0.500	0.949	0.574	0.978	0.652	0.991
0.259	0.437	0.435	0.887	0.435	0.888	0.501	0.950	0.574	0.978	0.653	0.991
0.268	0.471	0.435	0.888	0.437	0.891	0.507	0.953	0.575	0.978	0.657	0.992
0.273	0.486	0.437	0.891	0.438	0.891	0.510	0.955	0.575	0.978	0.657	0.992
0.283	0.522	0.438	0.891	0.440	0.894	0.511	0.955	0.575	0.978	0.658	0.992
0.284	0.524	0.440	0.894	0.441	0.895	0.514	0.957	0.576	0.979	0.658	0.992
0.295	0.559	0.441	0.895	0.441	0.896	0.516	0.958	0.577	0.979	0.665	0.993
0.295	0.560	0.441	0.896	0.441	0.896	0.517	0.958	0.580	0.980	0.667	0.993
0.296	0.565	0.441	0.896	0.442	0.897	0.518	0.959	0.581	0.980	0.669	0.993
0.297	0.568	0.442	0.897	0.442	0.897	0.518	0.959	0.583	0.980	0.676	0.994
0.304	0.587	0.442	0.897	0.443	0.899	0.519	0.959	0.583	0.980	0.677	0.994
0.309	0.603	0.443	0.899	0.443	0.899	0.519	0.959	0.584	0.980	0.678	0.994
0.309	0.605	0.443	0.899	0.444	0.899	0.521	0.960	0.585	0.981	0.679	0.994
0.310	0.606	0.444	0.899	0.445	0.900	0.523	0.961	0.585	0.981	0.682	0.994
0.317	0.630	0.445	0.900	0.452	0.909	0.524	0.961	0.587	0.981	0.698	0.996
0.320	0.638	0.452	0.909	0.452	0.909	0.525	0.962	0.588	0.981	0.698	0.996
0.326	0.655	0.452	0.909	0.454	0.911	0.525	0.962	0.588	0.981	0.699	0.996
0.330	0.665	0.454	0.911	0.459	0.916	0.526	0.962	0.589	0.982	0.704	0.996
0.337	0.684	0.459	0.916	0.461	0.917	0.526	0.962	0.589	0.982	0.705	0.996
0.339	0.690	0.461	0.917	0.462	0.918	0.527	0.963	0.591	0.982	0.708	0.996
0.348	0.716	0.462	0.918	0.462	0.918	0.528	0.963	0.593	0.983	0.710	0.997
0.349	0.717	0.462	0.918	0.463	0.919	0.528	0.963	0.594	0.983	0.712	0.997
0.350	0.720	0.463	0.919	0.464	0.920	0.529	0.963	0.594	0.983	0.722	0.997
0.350	0.721	0.464	0.920	0.465	0.921	0.530	0.964	0.595	0.983	0.722	0.997
0.354	0.730	0.465	0.921	0.470	0.925	0.530	0.964	0.596	0.983	0.737	0.998
0.358	0.740	0.470	0.925	0.470	0.925	0.531	0.964	0.596	0.983	0.739	0.998
0.360	0.745	0.470	0.925	0.471	0.926	0.531	0.965	0.597	0.984	0.745	0.998
0.362	0.749	0.471	0.926	0.471	0.926	0.534	0.966	0.597	0.984	0.746	0.998
0.368	0.763	0.471	0.926	0.474	0.929	0.535	0.966	0.598	0.984	0.747	0.998
0.370	0.767	0.474	0.929	0.475	0.929	0.535	0.966	0.599	0.984	0.748	0.998
0.374	0.775	0.475	0.929	0.475	0.929	0.537	0.967	0.600	0.984	0.758	0.999
0.375	0.777	0.475	0.929	0.475	0.930	0.537	0.967	0.600	0.984	0.769	0.999
0.375	0.778	0.475	0.930	0.475	0.930	0.537	0.967	0.601	0.984	0.777	1.000
0.379	0.784	0.475	0.930	0.476	0.930	0.537	0.967	0.602	0.985	0.785	1.000
0.380	0.786	0.476	0.930	0.476	0.931	0.538	0.967	0.604	0.985	0.786	1.000
0.395	0.819	0.476	0.931	0.477	0.932	0.540	0.968	0.605	0.985	0.786	1.000
0.399	0.826	0.477	0.932	0.478	0.932	0.541	0.968	0.606	0.985	0.786	1.000
0.400	0.829	0.478	0.932	0.478	0.932	0.541	0.968	0.606	0.985	0.790	1.000
0.403	0.833	0.478	0.932	0.482	0.936	0.541	0.968	0.607	0.985	0.790	1.000
0.403	0.834	0.482	0.936	0.483	0.936	0.541	0.969	0.607	0.986		
0.405	0.837	0.483	0.936	0.483	0.937	0.542	0.969	0.609	0.986		
0.408	0.843	0.483	0.937	0.484	0.937	0.543	0.969	0.609	0.986		
0.409	0.844	0.484	0.937	0.485	0.938	0.544	0.970	0.610	0.986		
0.410	0.846	0.411	0.847	0.487	0.939	0.545	0.970	0.610	0.986		

8.4d

FIGURE 8.19.4 compares the simulated and experimental water saturation profiles. The agreement is good. The numerical simulator is a finite difference model for incompressible fluids developed by the author and coded in Excel/VBA. The model assumes a homogeneous porous medium. Therefore, it cannot capture the wiggles in the experimental saturation profiles caused by heterogeneity of the sandpack. The numerical model does capture the experimental inlet boundary condition in which the water saturation is observed to buildup toward $(1–S_{or})$ in contrast to Buckley-Leverett model in with the inlet water saturation is fixed at $(1 - S_{or})$.

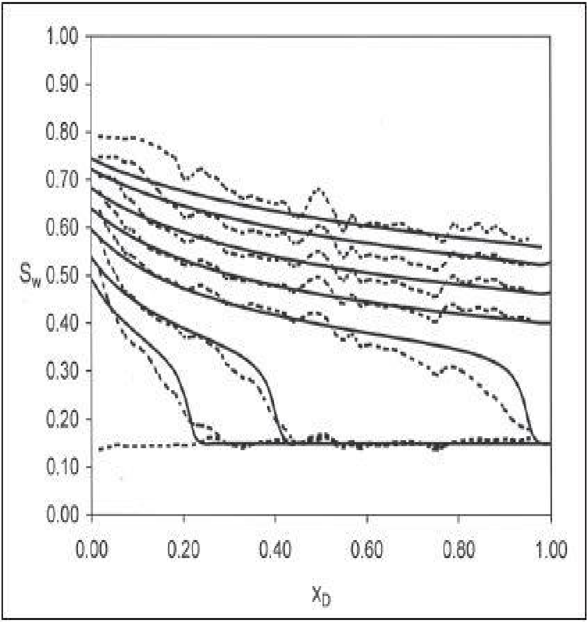

FIGURE 8.19.4 Comparison of the simulated and experimental water saturation profiles for the waterflood in the water-wet sandpack.

FIGURE 8.19.5 shows a comparison of the simulated and the experimental oil-recovery curves. The agreement is good.

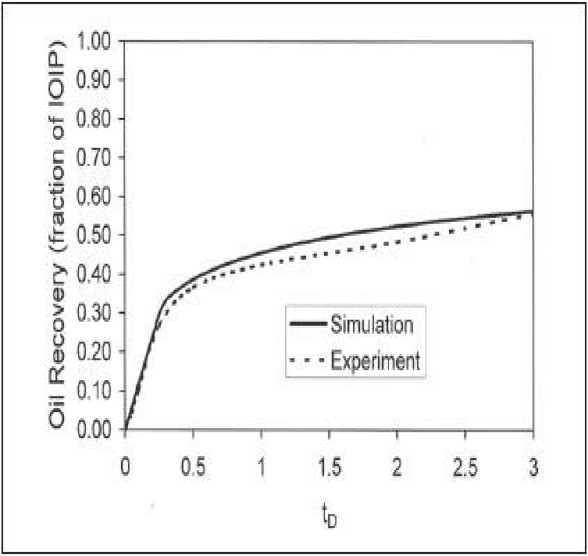

FIGURE 8.19.5 Comparison of the simulated and experimental oil-recovery curves for the waterflood in the water-wet sandpack.

FIGURE 8.19.6 shows the relative permeability curves that gave the best match. The relative permeability models are

$$k_{rw} = 0.35 S_e^{2.7} \tag{8.19.3}$$

$$k_{ro} = 0.98 \left(1 - S_e\right)^{1.2} \tag{8.19.4}$$

where S_e is given by

$$S_e = \frac{S_w - S_{wirr}}{1 - S_{wirr} - S_{or}} \tag{8.19.5}$$

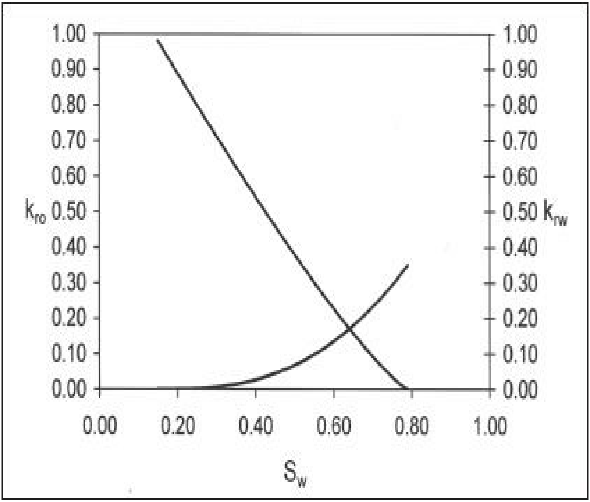

FIGURE 8.19.6 Relative permeability curves that gave the best history match for the waterflood in the water-wet sandpack.

FIGURE 8.19.7 shows the oil pressure profiles at various dimensionless times. The profiles are in good agreement with those typically observed in corefloods in which the core holder is instrumented with pressure transducers to measure the pressures along the core. **FIGURE 8.19.8**, from the author's archives, shows such experimental pressure profiles. In this experiment, the sandpack was 216.8 cm long and the core holder was instrumented with 12 pressure transducers spaced equally from the inlet to the outlet. The simulated pressure profiles of Figure 8.19.7 are in good qualitative agreement with experimental profiles of Figure 8.19.8.

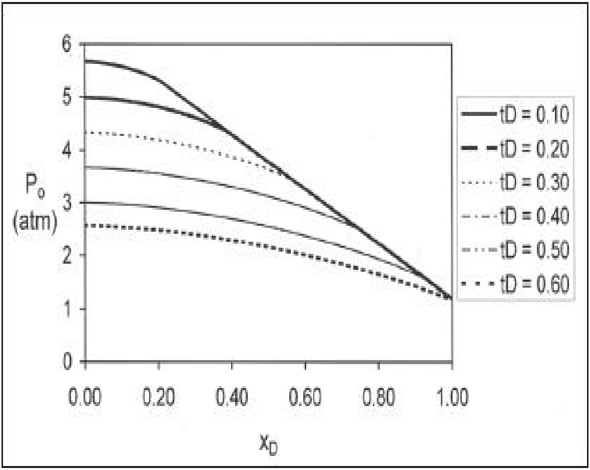

FIGURE 8.19.7 Pressure profiles in the oil phase for the waterflood in the water-wet sandpack.

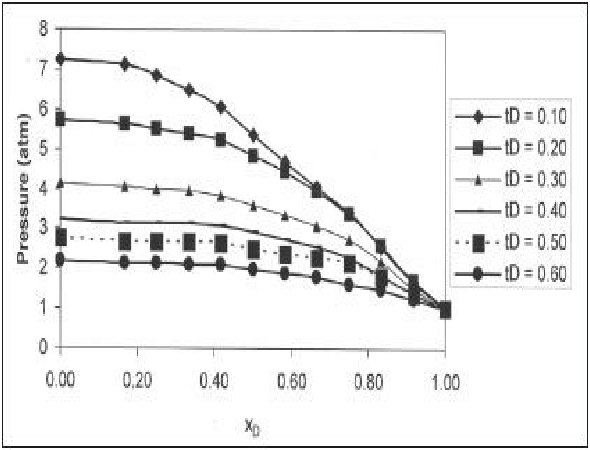

FIGURE 8.19.8 Experimental pressure profiles for a coreflood.

FIGURE 8.19.9 shows the true and approximate fractional flow curves along with the Welge tangent line. In this case, the Welge tangent line is a reasonable approximation of the true fractional flow curve at low water saturations.

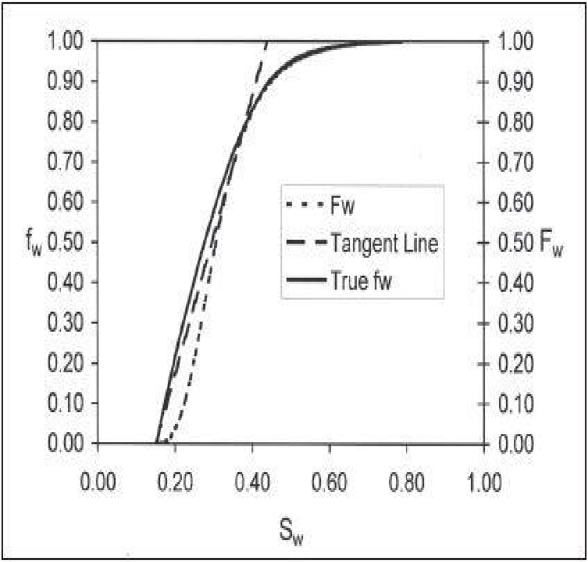

FIGURE 8.19.9 Comparison of the true and approximate fractional flow curves for the waterflood in the water-wet sandpack.

PROBLEM 8.20

8.20a

FIGURE 8.20.1 shows the water saturation profiles together with the porosity along the sandpack for the waterflood in the oil-wet sandpack. Again, the variation of the porosity along the sandpack is an indication that the sandpack is not homogeneous.

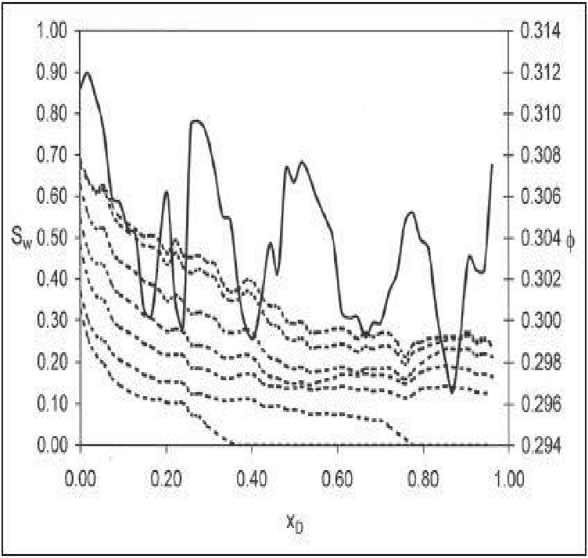

FIGURE 8.20.1 Water saturation and porosity profiles for the waterflood in the oil-wet sandpack.

8.20b

FIGURE 8.20.2 shows a comparison of the similarity transformations for the waterflood in the water-wet and oil-wet sandpacks. It can be clearly seen that the waterflood efficiency in the water-wet sandpack is higher than that in the oil-wet sandpack. At low values of x_D/t_D, which corresponds to large values of t_D, each waterflood tends toward a residual oil saturation, with the residual oil saturation in the water-wet system being lower than that in the oil-wet system.

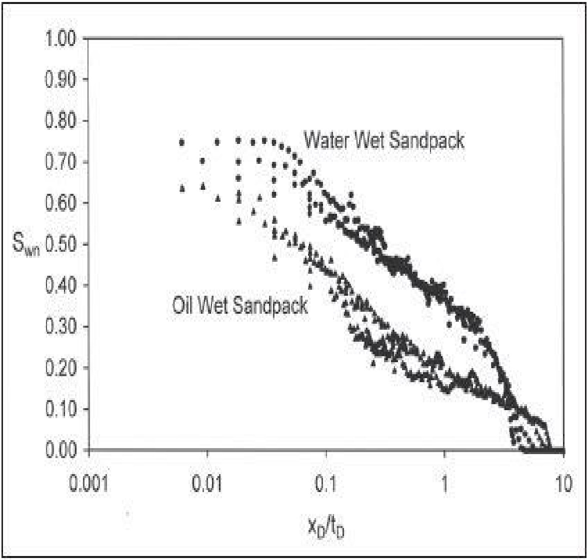

FIGURE 8.20.2 Comparison of the similarity transformations for the waterfloods in the water-wet and oil-wet sandpacks.

8.20c

[FIGURE 8.20.3](#) compares the true

fractional flow curves for the two waterfloods. Clearly, the waterflood in the water-wet sandpack is more efficient than in the oil-wet sandpack. The residual oil saturation in the oil-wet system is 40% compared to 21% in the water-wet system.

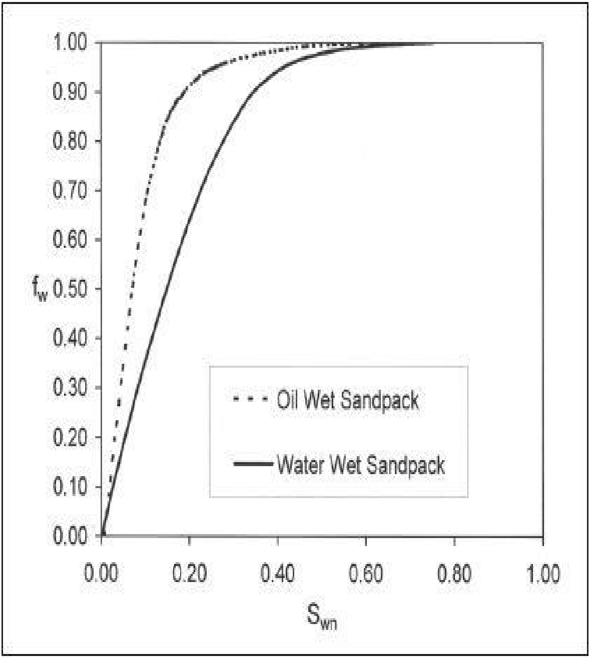

FIGURE 8.20.3 Comparison of the true fractional flow curves for the waterfloods in the water-wet and oil-wet sandpacks.

8.20d

FIGURE 8.20.4 compares the simulated and experimental water saturation profiles. The agreement is good.

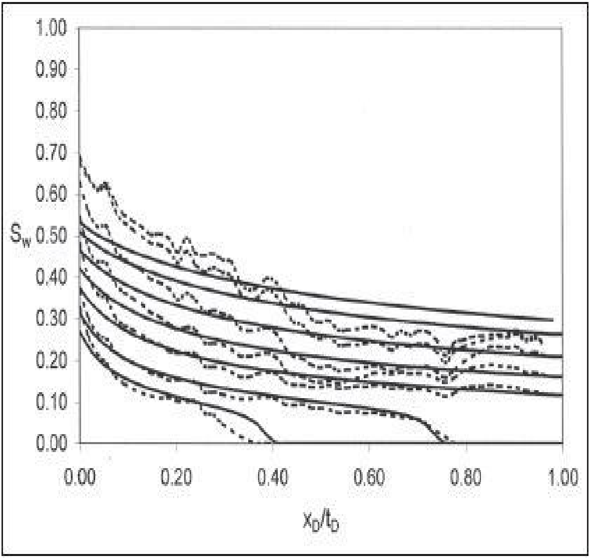

FIGURE 8.20.4 Comparison of the simulated and experimental water saturation profiles for the waterflood in the oil-wet sandpack.

FIGURE 8.20.5 shows a comparison of the simulated and the experimental oil recovery curves. The agreement is good.

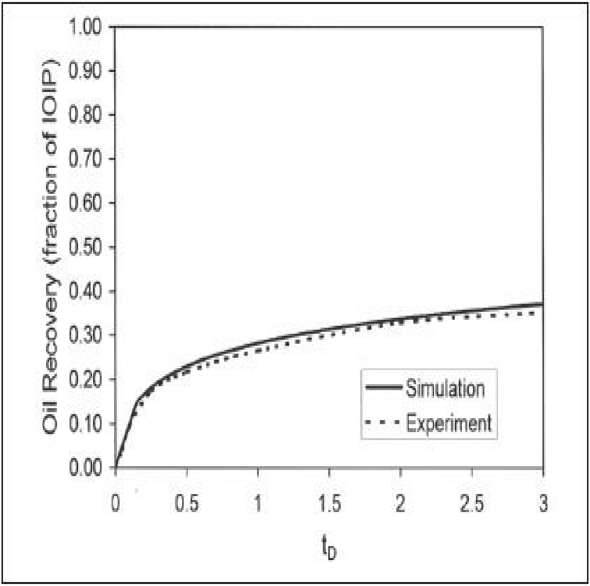

FIGURE 8.20.5 Comparison of the simulated and experimental oil-recovery curves for the waterflood in the oil-wet sandpack.

FIGURE 8.20.6 compares the relative permeability curves that gave the best match for each waterflood. The relative permeability models for the oil-wet is system are

$$k_{rw} = 0.55 S_e^2 \quad (8.21.1)$$

$$k_{ro} = 0.98\left(1 - S_e\right)^{1.5} \quad (8.21.2)$$

where S_e is given by

$$S_e = \frac{S_w - S_{wirr}}{1 - S_{wirr} - S_{or}} \quad (8.21.3)$$

As expected the relative permeability curves for the oil-wet sandpack are shifted to the left of the curves for the water-wet sandpack. The end-point relative permeability to water is higher in the oil-wet system than in the water-wet system. The relative permeability curves for the oil-wet system intersect at S_{wn} less than 50%, an indication that the relative permeability curves are consistent with Craig's rule of thumb.

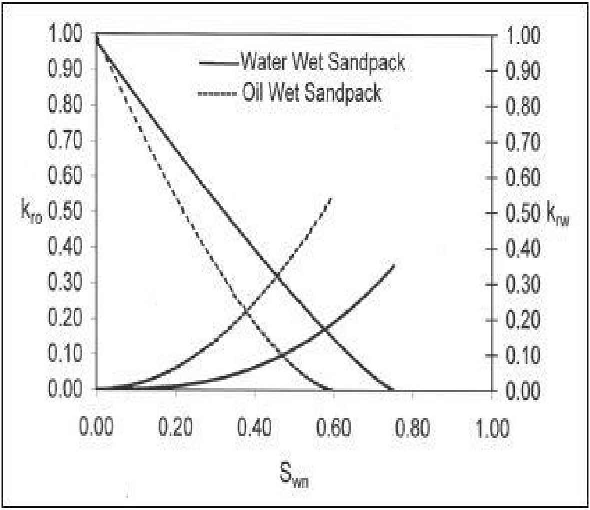

FIGURE 8.20.6 Comparison of the relative permeability curves for the water-wet and oil-wet sandpacks.

FIGURE 8.20.7 shows the true and approximate fractional flow curves along with the Welge tangent line. In this case, the true fractional flow curve, the approximate fractional flow curve, and the Welge tangent line are essentially the same. This is generally the case in inefficient immiscible displacements.

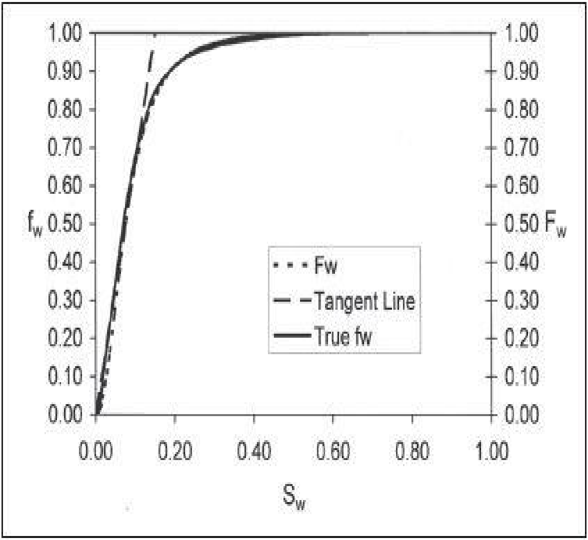

FIGURE 8.20.7 Comparison of the true and approximate fractional flow curves for the waterflood in the oil-wet sandpack.

PROBLEM 8.21

8.21a

FIGURE 8.21.1 shows the oil saturation profiles together with the porosity along the sandpack for the favorable mobility immiscible displacement. The displacement is essentially piston-like with an average irreducible water saturation of 15% left behind.

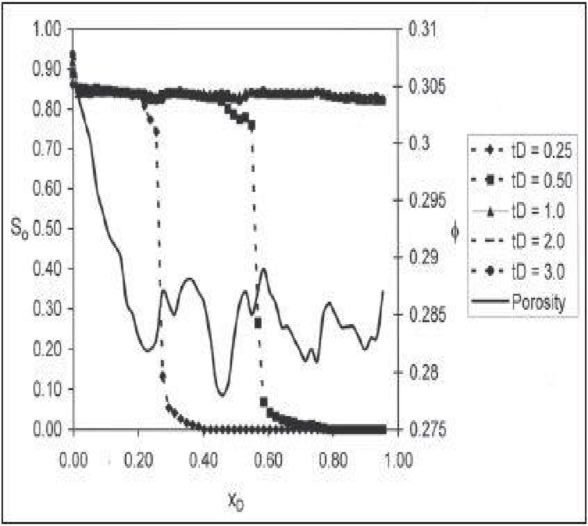

FIGURE 8.21.1 Water saturation and porosity profiles for the favorable mobility ration displacement.

8.21b

FIGURE 8.21.2 shows the water-recovery curve. The water recovery is complete at oil breakthrough.

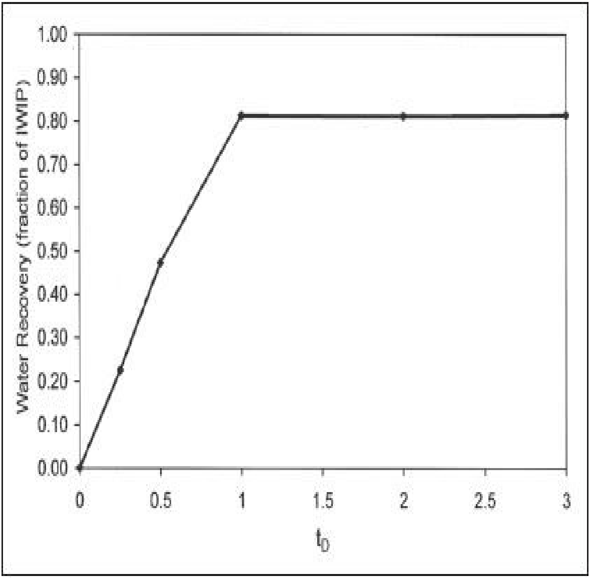

FIGURE 8.21.2 Recovery curve for the favorable mobility ration displacement.

8.21c

FIGURE 8.21.3 shows the similarity

transformation for the favorable mobility ratio displacement. All the data plot as one curve that is characteristic of the displacement.

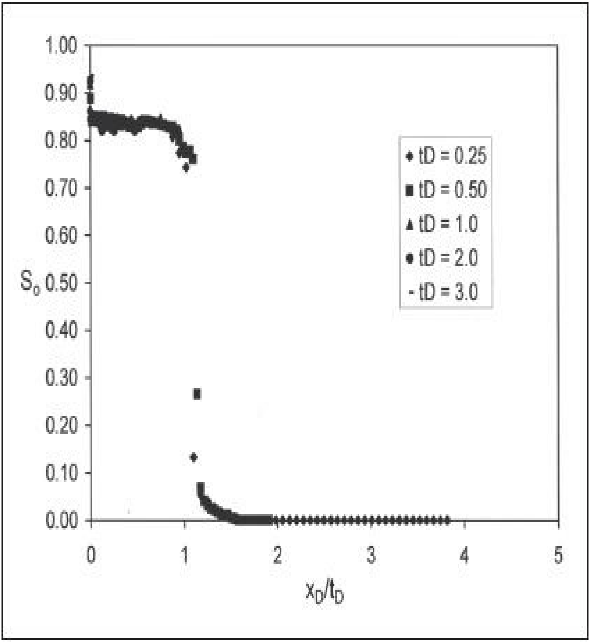

FIGURE 8.21.3 Similarity transformation for the favorable mobility ratio displacement.

8.21d

FIGURE 8.21.4 shows the true fractional flow curve for the favorable mobility ratio displacement.

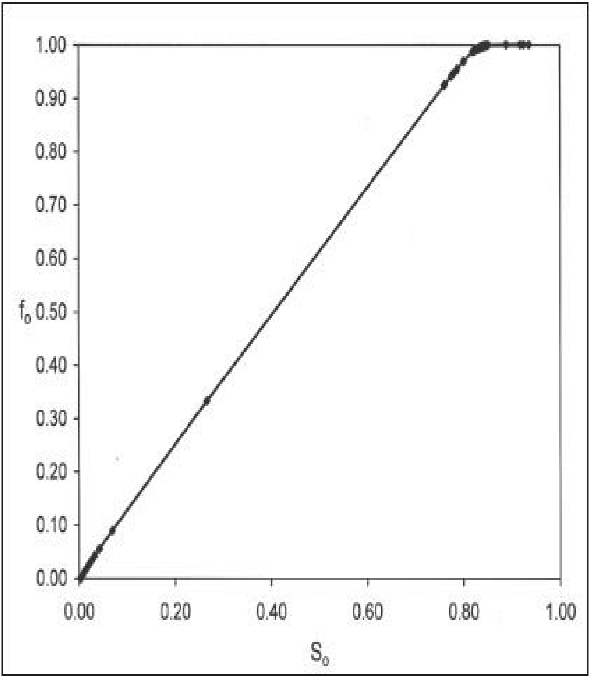

FIGURE 8.21.4 True fractional flow curve for the favorable mobility ratio displacement.

8.21e

The relative permeability curves are

$$k_{ro} = 0.55 S_e^2 \qquad (8.21.4)$$

$$k_{rw} = \left(1 - S_e\right)^{1.5} \qquad (8.21.5)$$

where S_e is given by

$$S_e = \frac{S_o}{1 - S_{wirr}} \qquad (8.21.6)$$

FIGURE 8.21.5 shows the following graphs: (1) the relative permeability curves versus oil saturation, (2) the approximate fractional flow curve for oil versus oil saturation, (3) the true fractional flow curve for oil versus oil saturation, and (4) the Welge tangent line. In this case, the Welge tangent line is essentially the same as the true fractional flow curve. This is generally true for favorable mobility ratio displacements.

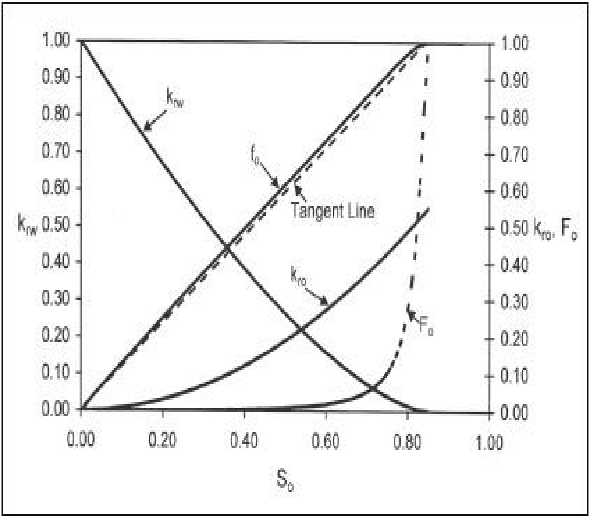

FIGURE 8.21.5 Summary graphs for the favorable mobility ratio displacement.

APPENDIX B SOLUTIONS

PROJECT 1

1a, b, c

FIGURE B1.1 shows the *GR* and caliper logs in the first track, the shallow and deep resistivity logs in the second track, and the neutron and density logs in the third track.

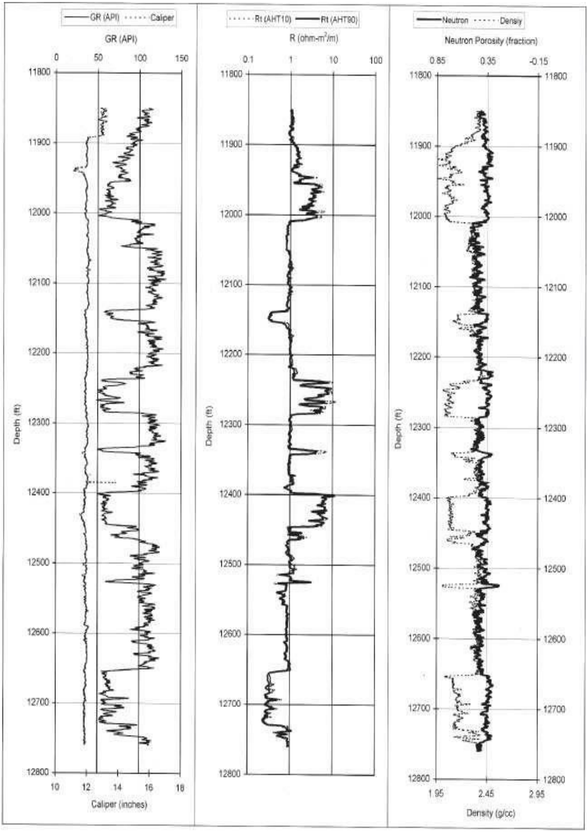

FIGURE B1.1 *GR*, Caliper, AHT10, AHT90, Neutron, and Density plots.

A pattern is clearly visible in the third track in which the density log swings to the left of the neutron in sands and swings to the right of the neutron in shales. This pattern is helpful in distinguishing sands from shales.

1d

The shale volume is calculated from the *GR* as

$$V_{sh} = \frac{GR - GR_{sa}}{GR_{sh} - GR_{sa}} \tag{B1.1}$$

with GR_{sa} = 60 API units and GR_{sh} = 110 API units. **FIGURE b1.2** shows the log of V_{sh} in the third track. The low values of V_{sh} correspond to sands and the high values correspond to shales. The pattern of V_{sh} indicates that the sands can best be described as shaly sands.

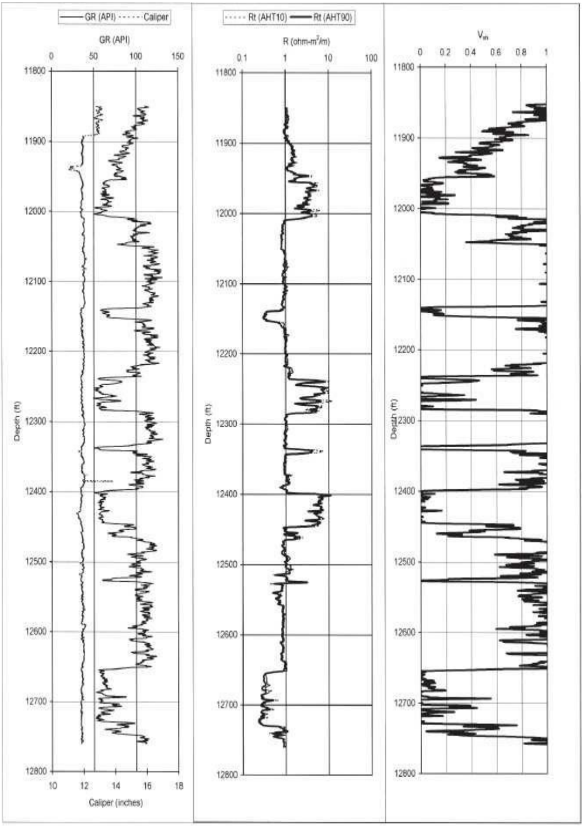

FIGURE B1.2 *GR*, Caliper, AHT10, AHT90, V_{sh} plots.

1e

The density porosity is calculated from the bulk density as

$$V_{sh} = \frac{\sigma_m - \rho_b}{\sigma_m - \rho_f} \quad \text{(B1.2)}$$

with ρ_m = 2.66 g/cc and ρf = 0.80 g/cc. FIGURE b1.3 shows a comparison of the density and neutron porosities in the third track. A clear pattern is visible. The density and neutron porosities agree in sands but differ in shales with the neutron porosity being higher in shales than in sands as expected.

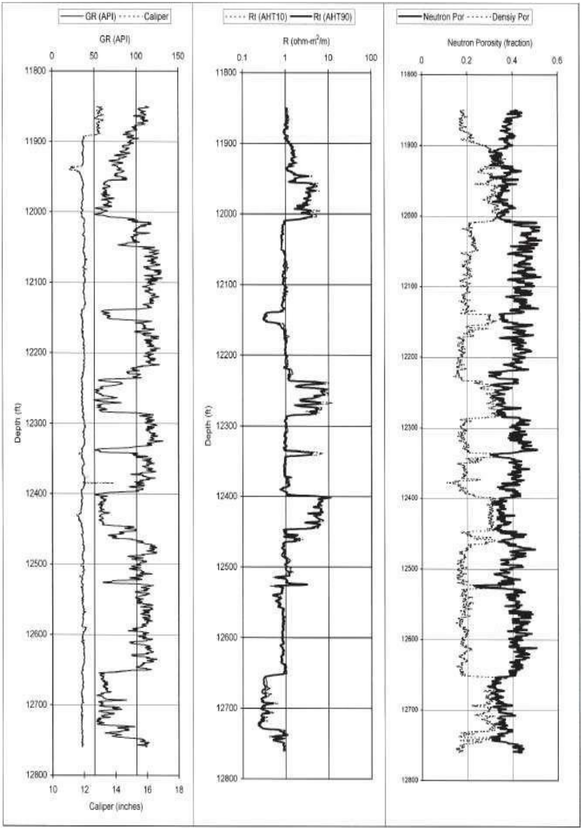

FIGURE B1.3 *GR*, Caliper, AHT10, AHT90, neutron, and density porosity plots.

1f

The water saturation was calculated using Archie's equations assuming clean sands:

$$F = \frac{a}{\phi^m} \qquad \text{(B1.3)}$$

$$S_w = \left(\frac{F R_w}{R_t} \right)^{\frac{1}{n}} \qquad \text{(B1.4)}$$

with $a = 1$, $m = 2$, $n = 2$, and $R_w = 0.04$ ohm-m. FIGURE B1.4 shows the calculated water saturation in track 3. This water saturation estimate is pessimistic for shaly sands and will be refined in a future project.

1g

The logs were analyzed using the combinations of the GR, deep resistivity, and density and neutron porosity patterns to identify the 7 sands and their fluid contents shown in **TABLE B1.1**.

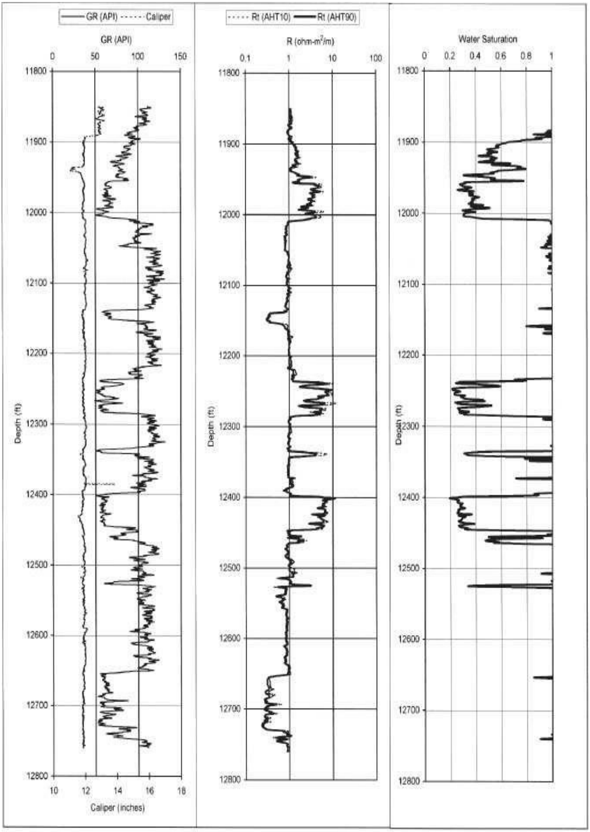

FIGURE B1.4 *GR*, Caliper, AHT10, AHT90, and water saturation plots.

TABLE B1.1 Summary of Preliminary Log Analyses.

Sand #	Fluid Content	Top (ft MD)	Bottom (ft MD)	Gross Thickness (ft MD)	$\bar{\phi}$	$\bar{S}_w$
1	Hydrocarbon	11888.0	12008.5	121.0	0.3033	0.4771
2	Water	12138.5	12153.5	15.5	0.2990	1.0
3	Hydrocarbon	12237.0	12284.5	48.0	0.3114	0.3184
4	Hydrocarbon	12335.0	12341.5	7.0	0.3140	0.3598
5	Hydrocarbon	12398.0	12464.0	66.5	0.2896	0.3872
6	Hydrocarbon	12523.5	12528.0	5.0	0.3055	0.5801
7	Water	12652.0	12746.5	95.0	0.2860	1.0

PROJECT 2

2a

The results of the Monte Carlo sampling are summarized in **TABLE B2.1**. Because of the stochastic nature of the simulation, your numbers will not be identical to those in the TABLE. However, if your simulation is correct, the statistical averages should be similar to those in the TABLE. These include the mean, standard deviation, P90, P50, and P10. The minimum and maximum values can be significantly different from those in the TABLE because they are not statistical averages.

TABLE B2.1 Summary of Results for Monte Carlo Sampling.

	N (MMSTB)	N_r (MMSTB)	NCF (MMS)
Minimum	610	148	1336
Maximum	5945	1838	18359
Standard Deviation	872	293	2856
P90	1293	366	3391
P50	2285	665	6272
P10	3559	1098	10349

2b

The histograms and expectation curves are shown in **FIGURES B2.1** through **B2.13**.

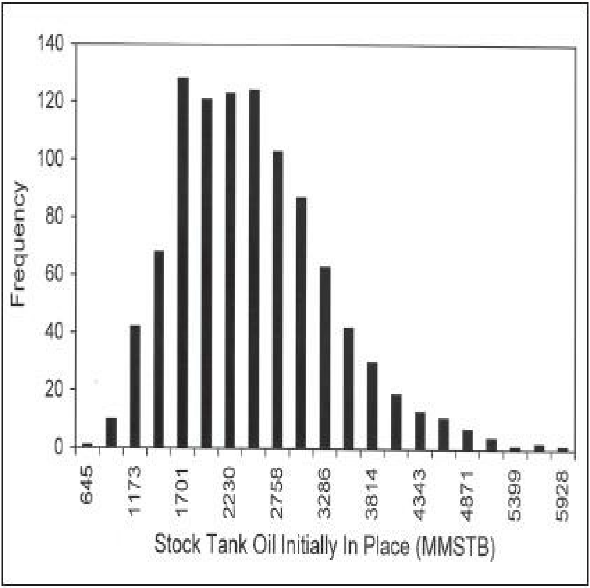

FIGURE B2.1 STOIIP histogram (Monte Carlo sampling).

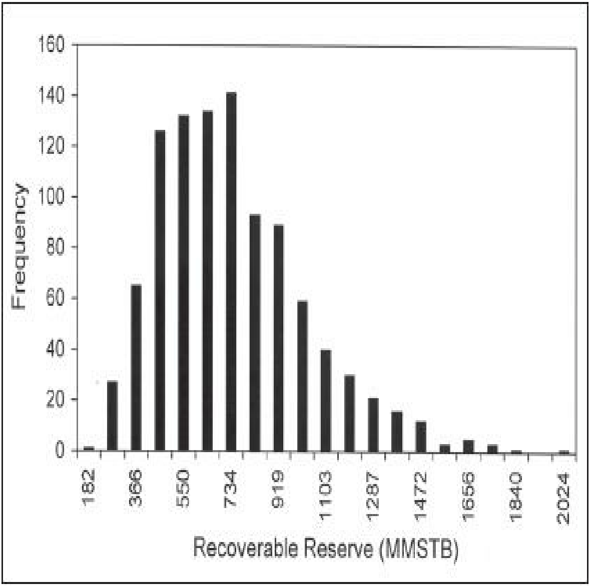

FIGURE B2.2 Recoverable reserve histogram (Monte Carlo sampling).

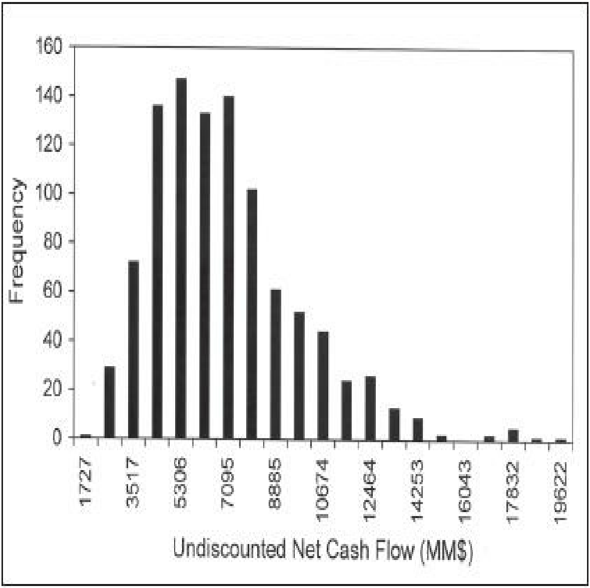

FIGURE B2.3 Undiscounted net cash flow histogram (Monte Carlo sampling).

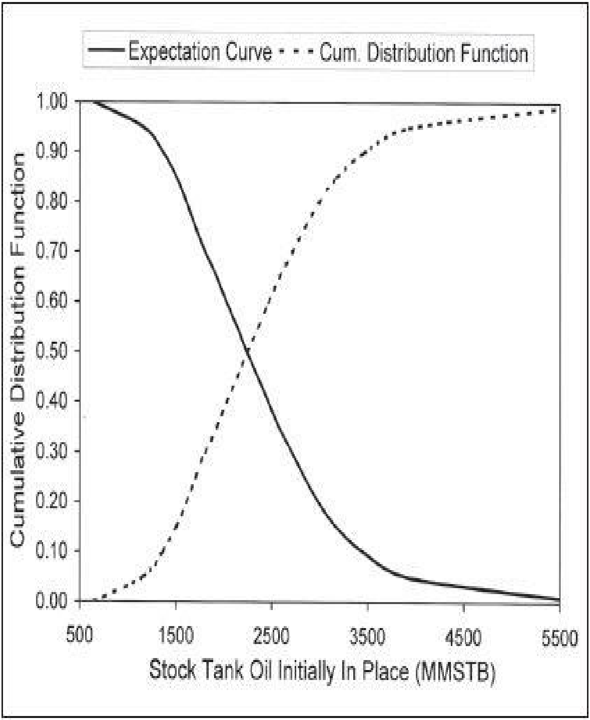

FIGURE B2.4 Cumulative distribution function and expectation curve for STOIIP (Monte Carlo sampling).

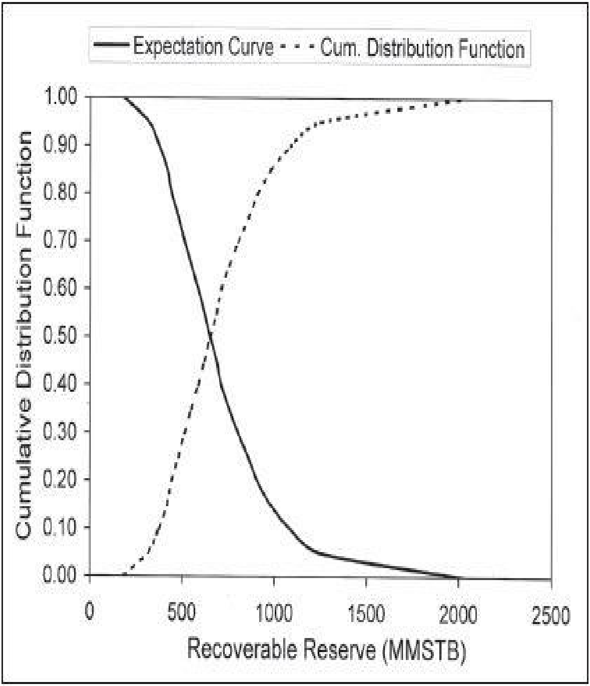

FIGURE B2.5 Cumulative distribution function and expectation curve for recoverable reserve (Monte Carlo sampling).

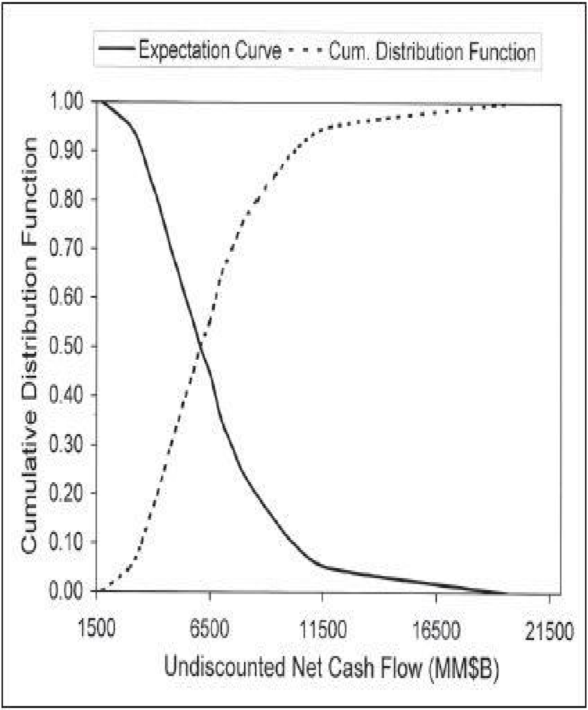

FIGURE B2.6 Cumulative distribution function and expectation curve for undiscounted net cash flow (Monte Carlo sampling).

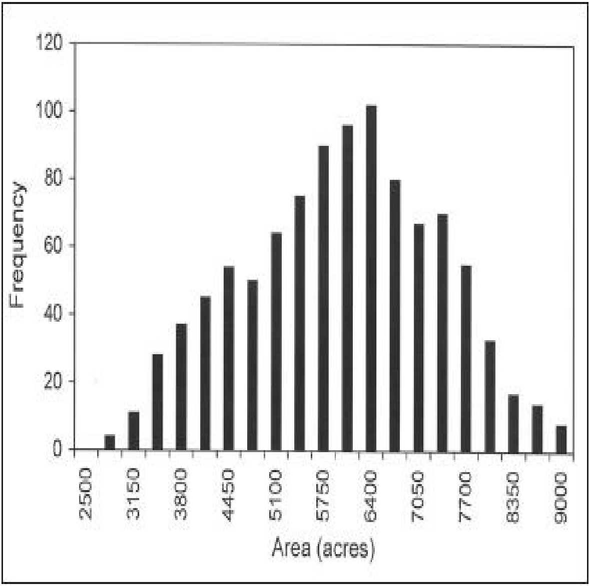

FIGURE B2.7 Area histogram (Monte Carlo sampling).

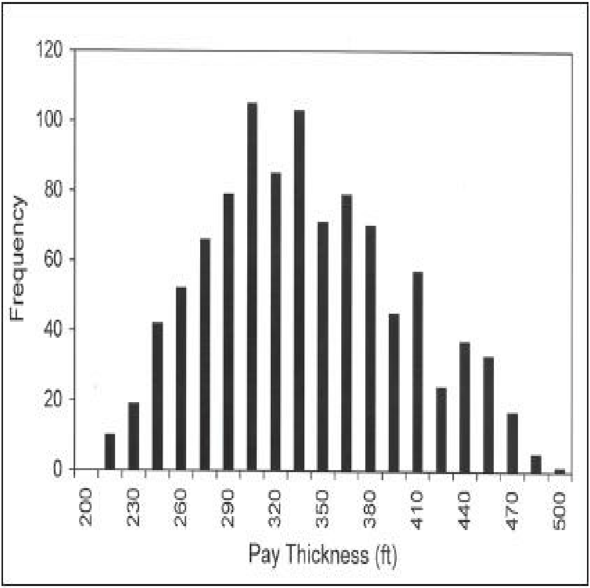

FIGURE B2.8 Pay thickness histogram (Monte Carlo sampling).

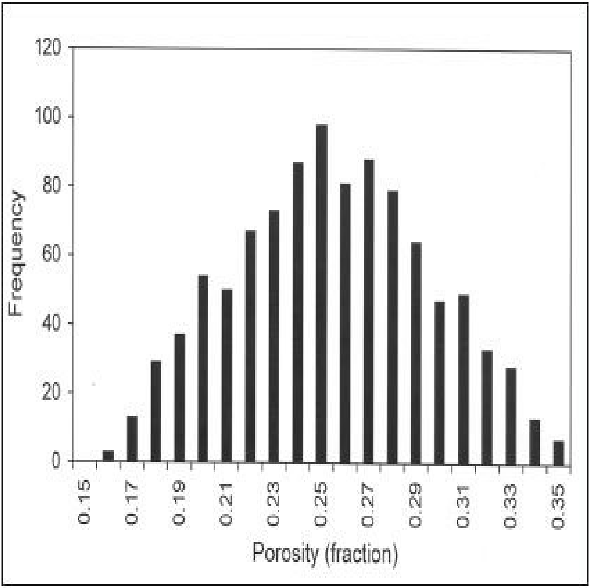

FIGURE B2.9 Porosity histogram (Monte Carlo sampling).

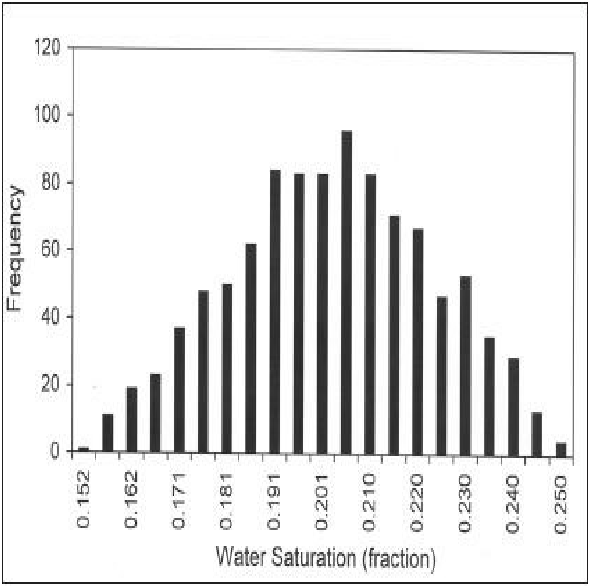

FIGURE B2.10 Water saturation histogram (Monte Carlo sampling).

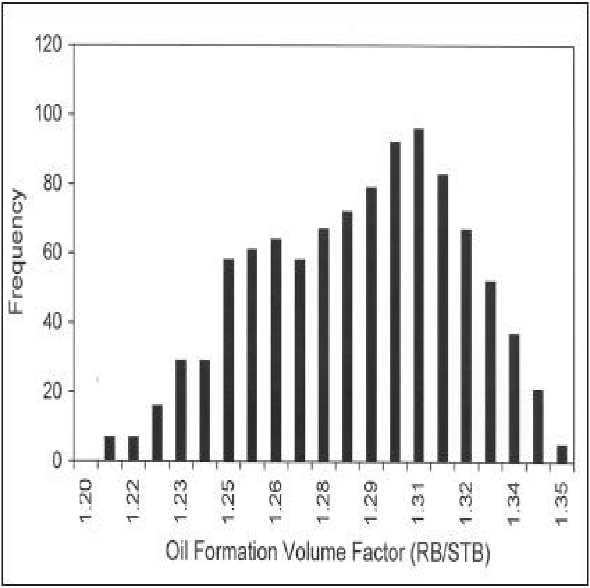

FIGURE B2.11 Oil formation value histogram (Monte Carlo sampling).

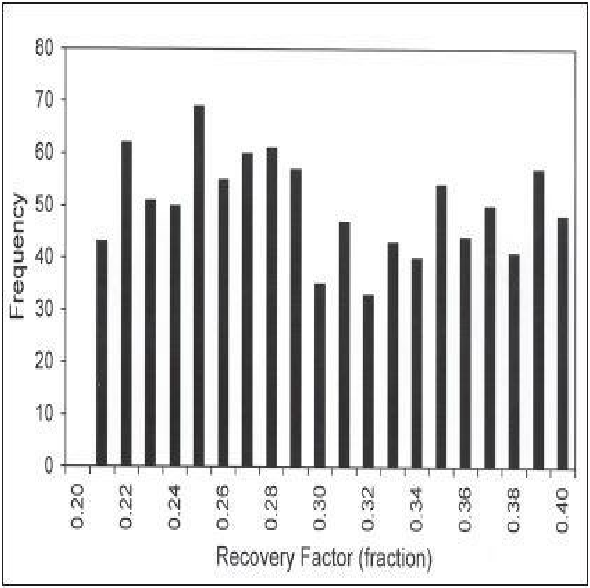

FIGURE B2.12 Recovery factor histogram (Monte Carlo sampling).

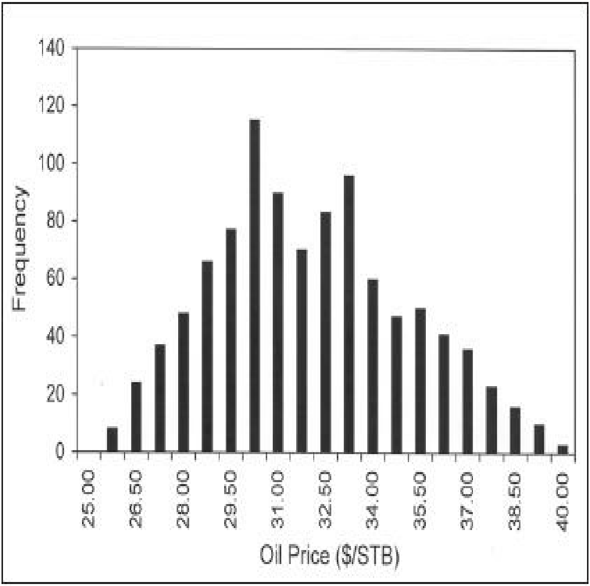

FIGURE B2.13 Oil price histogram (Monte Carlo sampling).

2c

The Monte Carlo sampling method is inefficient. This is apparent from the fact that the triangular distributions are not truly triangular. In particular, the uniform distribution of the recovery factor is anything but uniform. It is likely that 1000 iterations may not be sufficient to converge to the solution for this sampling method. This can be verified by increasing the number of iterations to 5000 and comparing the results to those for 1000 iterations.

PROJECT 3

3a

The results of the Latin Hypercube sampling are summarized in **TABLE b3.1**. Because of the stochastic nature of the simulation, your numbers will not be identical to those in the TABLE. However, if your simulation is correct, the statistical averages should be similar to those in the TABLE. These include the mean, standard deviation, P90, P50, and P10. The minimum and maximum values can be significantly different from those in the TABLE because they are not statistical averages.

TABLE B3.1 Summary of Results for Monte Carlo Sampling.

	N (MMSTB)	N_r (MMSTB)	NCF (MM$)
Minimum	667	136	1349
Maximum	5596	1996	19327
Standard Deviation	872	298	2862
P90	1367	374	3502
P50	2260	668	6170
P10	3570	1108	10520

3b

The histograms and expectation curves are shown in **FIGURE B3.1** through **B3.13**.

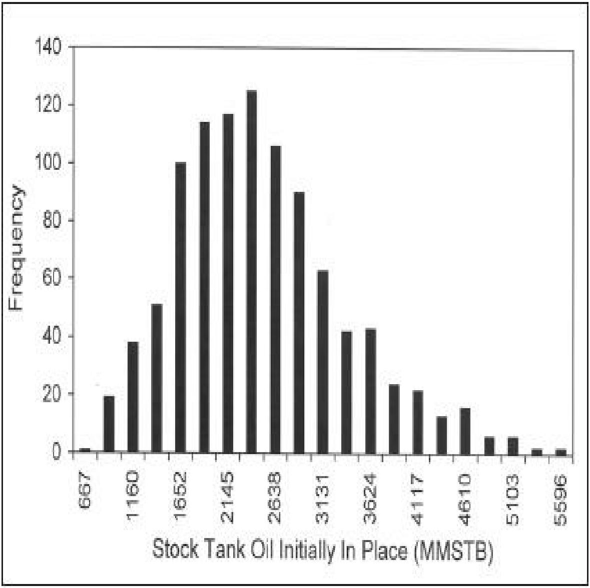

FIGURE B3.1 STOIIP histogram (Latin Hypercube sampling).

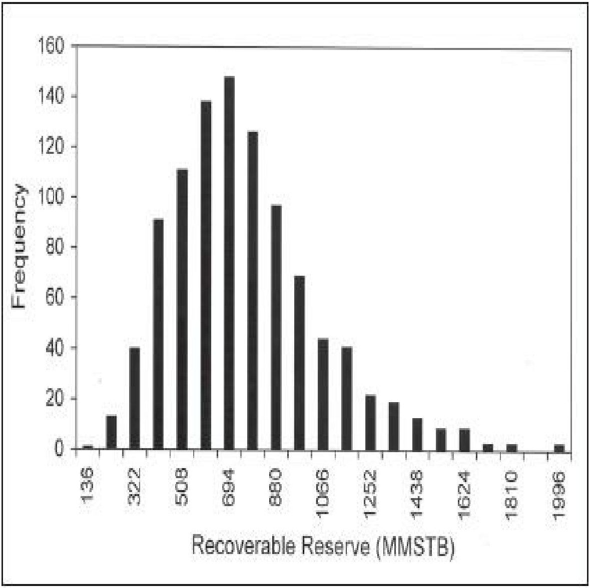

FIGURE B3.2 Recoverable reserve histogram (Latin Hypercube sampling).

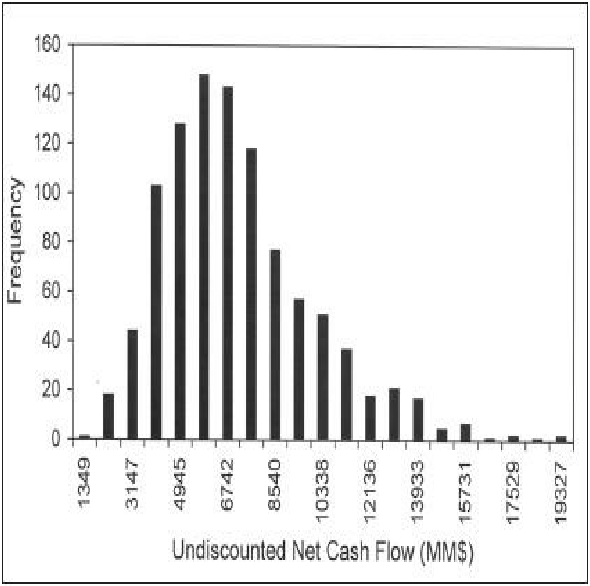

FIGURE B3.3 Undiscounted net cash flow histogram (Latin Hypercube sampling).

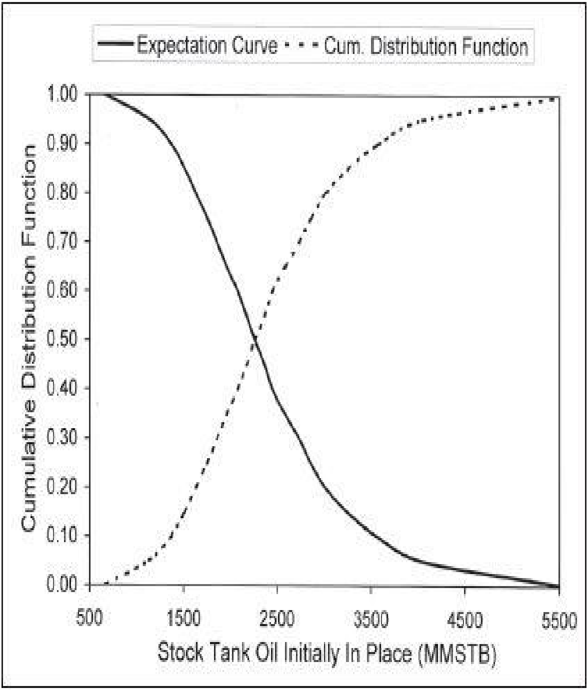

FIGURE B3.4 Cumulative distribution function and expectation curve for STOIIP (Latin Hypercube sampling).

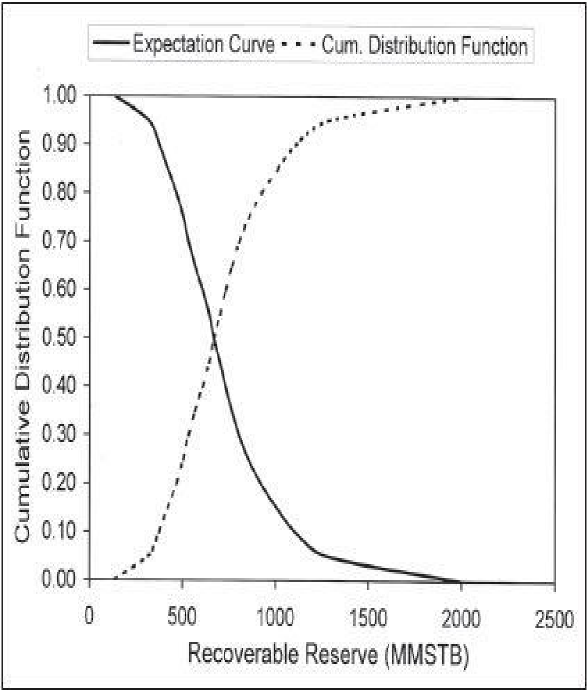

FIGURE B3.5 Cumulative distribution function and expectation curve for recoverable reserve (Latin Hypercube sampling).

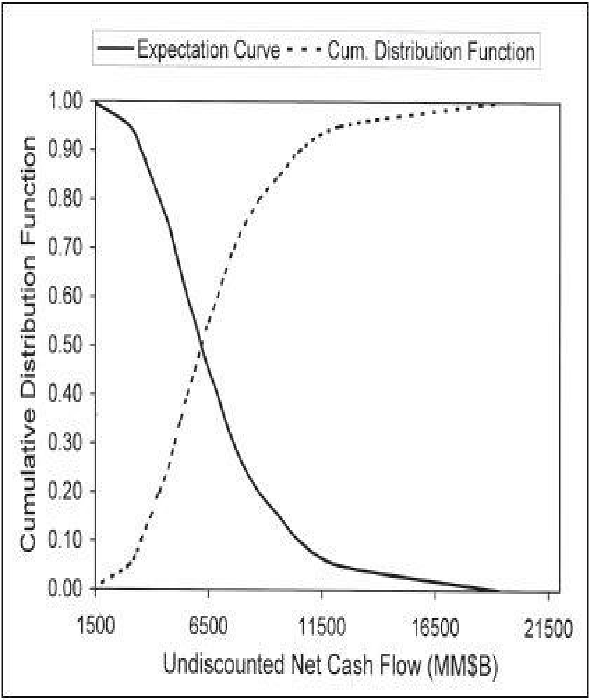

FIGURE B3.6 Cumulative distribution function and expectation curve for undiscounted net cash flow (Latin Hypercube sampling).

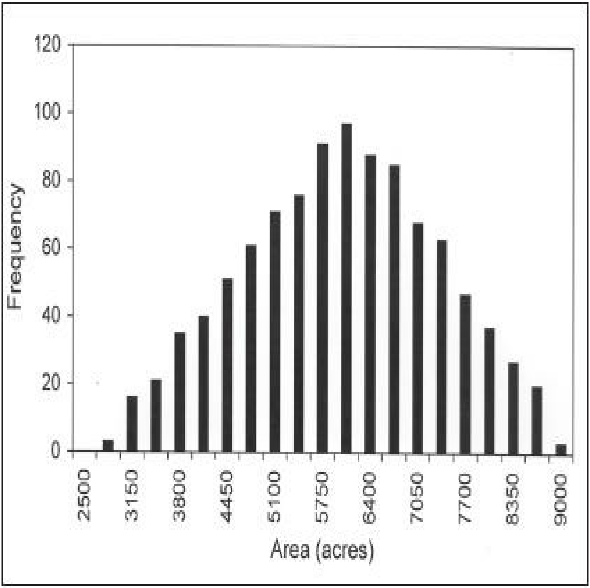

FIGURE B3.7 Area histogram (Latin Hypercube sampling).

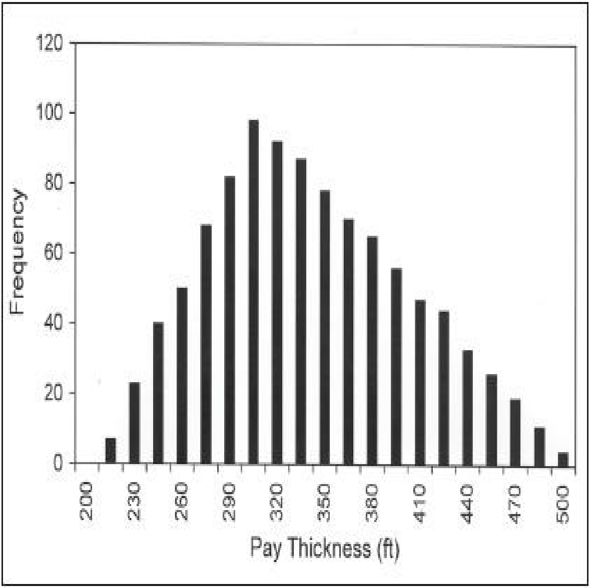

FIGURE B3.8 Pay thickness histogram (Latin Hypercube sampling).

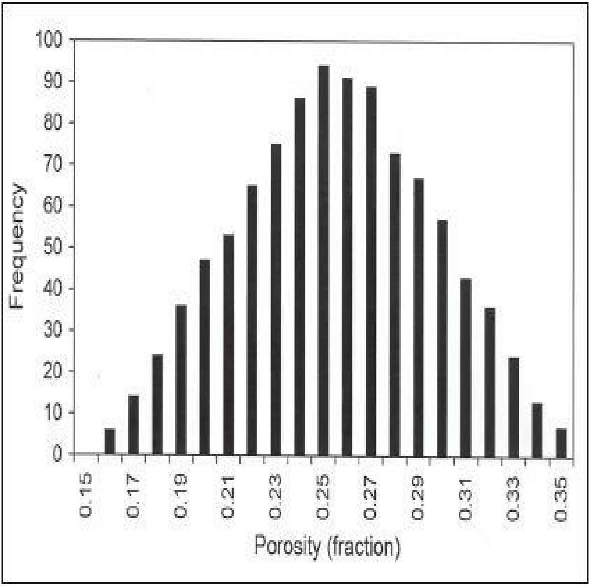

FIGURE B3.9 Porosity histogram (Latin Hypercube sampling).

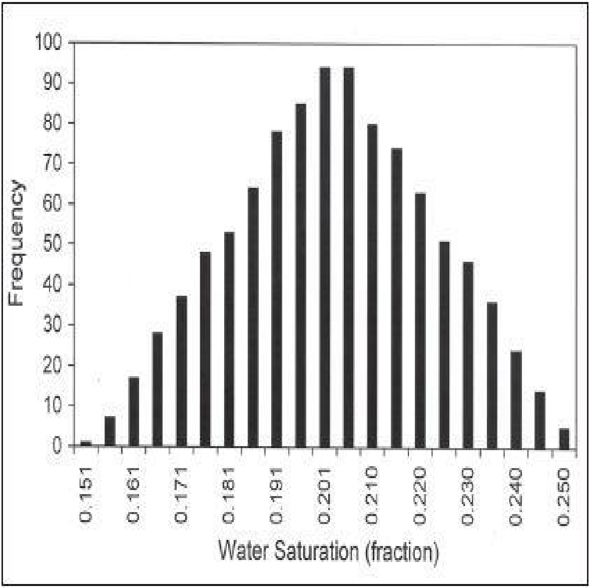

FIGURE B3.10 Water saturation histogram (Latin Hypercube sampling).

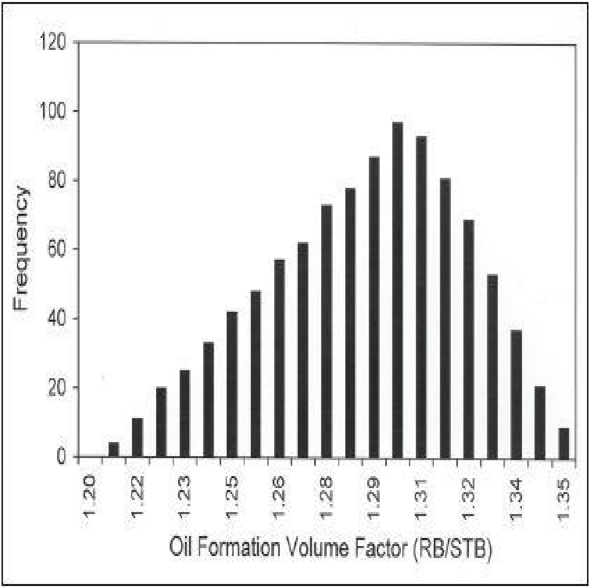

FIGURE B3.11 Oil formation value histogram (Latin Hypercube sampling).

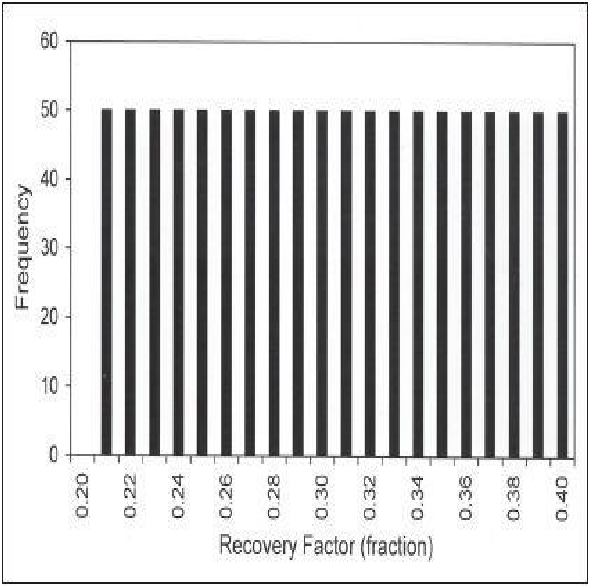

FIGURE B3.12 Recovery factor histogram (Latin Hypercube sampling).

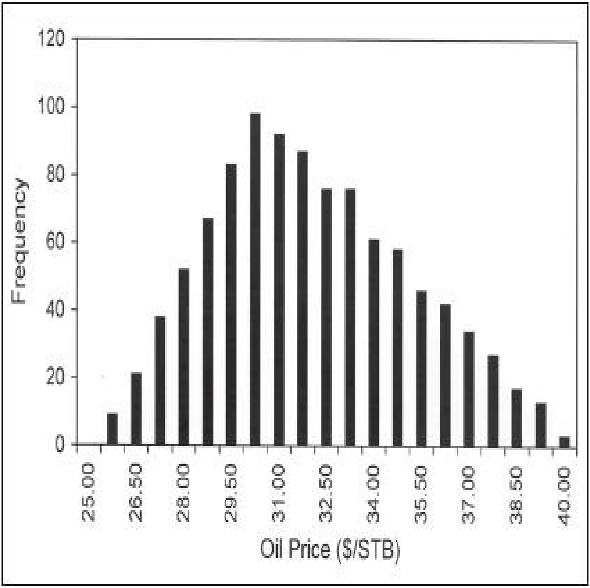

FIGURE B3.13 Oil price histogram (Latin Hypercube sampling).

3c

The Latin Hypercube sampling method is

very efficient. This is apparent from the fact that the triangular distributions are truly triangular. In particular, the uniform distribution of the recovery factor is truly uniform. For this sampling method, 1000 iterations are sufficient for the simulation to converge to the solution. This can be verified by increasing the number of iterations beyond 1000 and comparing the results to those for 1000 iterations. It will be found that the results are essentially the same as for 1000 iterations.

PROJECT 4

4a

The measured depth is different from the true vertical depth because of well deviations. The measured depth is always longer than the true vertical depth. Normally, the true vertical depth is calculated from the measured depth using deviation surveys. In the absence of deviation surveys for this project, a simple linear regression is used to relate the two depths as shown in **FIGURE B4.1**. The regression equation is

$$TVD = 0.9933MD - 19.1799 \quad \text{(B4.1)}$$

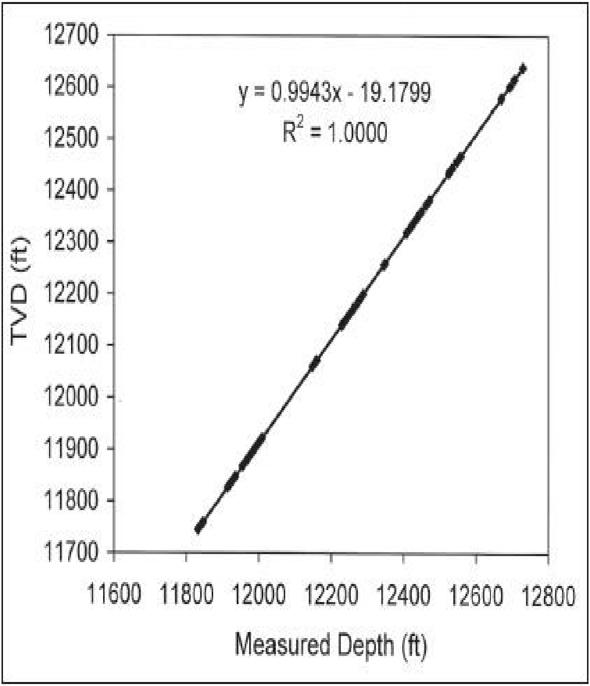

FIGURE B4.1 Graph of true vertical depth versus measured depth.

4b

FIGURE B4.2 shows the static pressure log along with the *GR* and resistivity logs. It can be seen that pressure data were acquired in six of the seven sands encountered in the well. No pressure data were acquired in Sand 6.

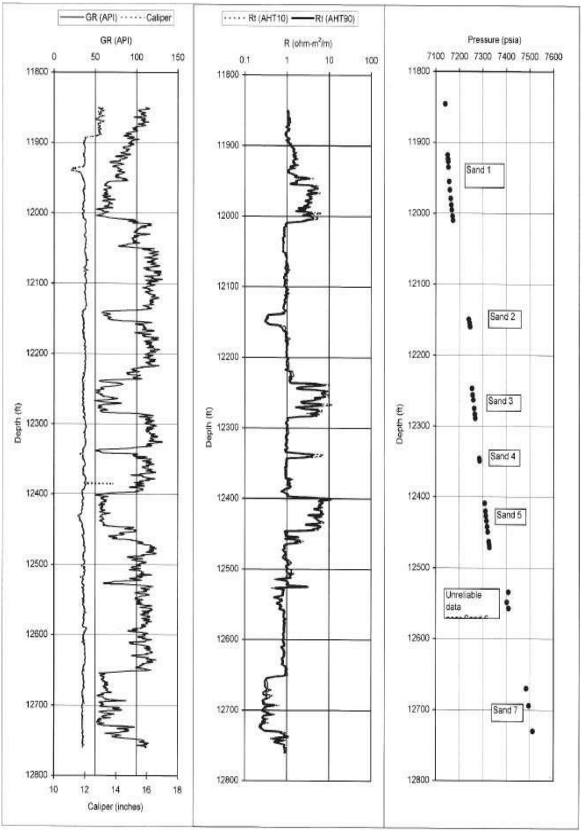

FIGURE B4.2 Overview of pressure data.

4c

FIGURE B4.3 shows the detailed static pressure analysis. The pressure equations for the sands are as follows.

Sand 1—Gas Cap:

$$TVD = 6.4676P - 34417.3455 \quad \text{(B4.2)}$$

Sand 1—Oil Rim:

$$TVD = 3.3129P - 11840.5454 \quad \text{(B4.3)}$$

Sand 2:

$$TVD = 2.2936P - 4546.8600 \quad \text{(B4.4)}$$

Sands 3, 4, and 5:

$$TVD = 2.9904P - 9534.1153 \quad \text{(B4.5)}$$

Sand 7:

$$TVD = 2.1367P - 3412.3661 \quad \text{(B4.6)}$$

It should be observed that Sands 3, 4, and 5 lie along the same pressure line. This is evidence that the three sands are in hydraulic communication.

The fluid gradients and densities can be calculated from the pressure equations. For example, for the gas cap, solving Eq.(B4.2) for pressure gives

$$P = 0.1546TVD + 34417.3455 \quad \text{(B4.7)}$$

The fluid gradient is given by

$$Gradient = 0.1546 \text{ psi/ft TVD}$$

The fluid specific gravity is related to the fluid gradient by

$$0.433\gamma = Gradient = 0.1546 \quad \text{(B4.8)}$$

The fluid specific gravity is given by

$$\gamma = 0.1546 / 0.433 = 0.357$$

The fluid density is given by

$$\rho_f = \gamma \times \rho_w = 0.357 \times 1 = 0.357 \text{ g/cc}$$

The gas-oil contact is assumed to occur at the intersection of the pressure lines for the gas cap and the oil rim. This assumes a zero displacement pressure for the gas-oil capillary pressure curve. Solving Eqs.(B4.2) and (B4.3) simultaneously gives the gas-oil contact as

$$GOC = 11868.42 \text{ ft TVD}$$

$$GOC = (11868.42 + 19.1799) / 0.9943 = 11955.75 \text{ ft MD}$$

From log analysis,

$$GOC = 11950.00 \text{ ft MD}$$

$$GOC = 0.9943 \times 11950.00 = 11862.71 \text{ ft TVD}$$

The agreement between the estimates of the gas-oil contact from pressure analysis and log analysis is good.

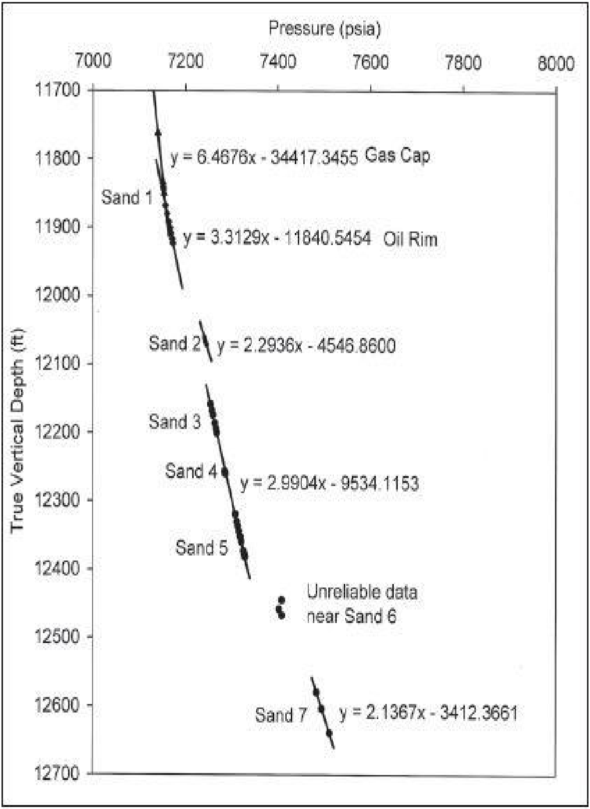

FIGURE B4.3 Detailed static pressure analysis.

4d

TABLE B4.1 shows the fluid types in the seven sands. The fluid types were inferred from the fluid gradients and densities obtained from the pressure analysis except in Sand 6 for which no pressure data were available. The fluid type for Sand 6 was inferred from the density-neutron porosity crossover shown in **FIGURE B4.4**. See Figure 2.24 in Volume 1 for examples of density-neutron porosity crossovers in gas zones.

TABLE B4.1 Fluid Contents of the Various Sands.

Sand #	Fluid Type	Fluid Gradient (psi/ft TVD)	Fluid Density (g/cc)	Top (ft TVD)	Bottom (ft TVD)	Gross Thickness (ft TVD)	Top (ft MD)	Bottom (ft MD)	Gross Thickness (ft MD)
1	Gas	0.1546	0.357	11801.06	11862.71	66.88	11888.00	11950.00	67.26
1	Oil	0.3019	0.697	11867.94	11920.87	52.94	11955.26	12008.50	53.24
2	Water	0.4360	1.007	12050.13	12065.05	14.91	12138.50	12153.50	15.00
3	Oil	0.3344	0.772	12148.07	12195.30	47.23	12237.00	12284.50	47.50
4	Oil	0.3344	0.772	12245.51	12251.97	6.46	12335.00	12341.50	6.50
5	Oil	0.3344	0.772	12308.15	12373.78	65.62	12398.00	12464.00	66.00
6	Gas			12432.94	12437.41	4.47	12523.50	12528.00	4.50
7	Water	0.4680	1.081	12560.70	12654.67	93.96	12652.00	12746.50	94.50

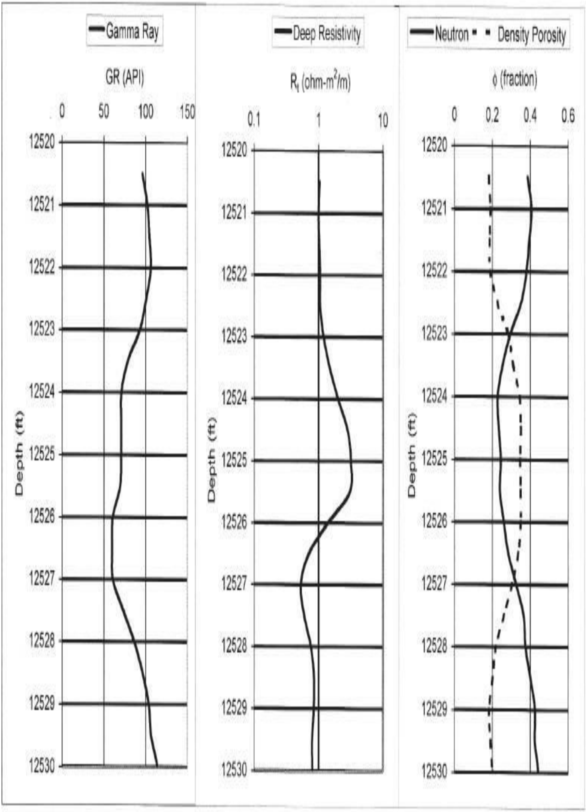

FIGURE B4.4 Density-neutron porosity crossover in Sand 6.

PROJECT 5

5a

The core data were posted in the spreadsheet containing the log data as requested.

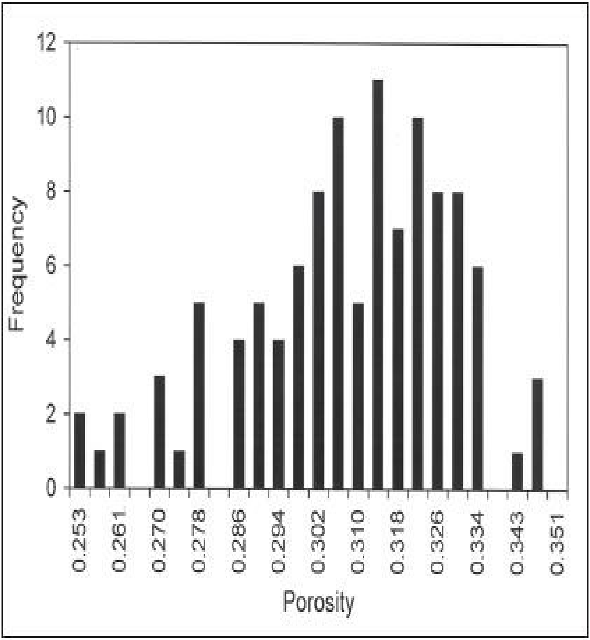

FIGURE B5.1 Core porosity histogram.

5b

[figures B5.1](), [B5.2](), and [B5.3]() show the core porosity histogram, permeability histogram, and the grain density histogram. The mean grain density is 2.663 g/cc with a standard deviation of 0.024 g/cc. This mean grain density was used to calibrate the density porosity for all subsequent log analyses.

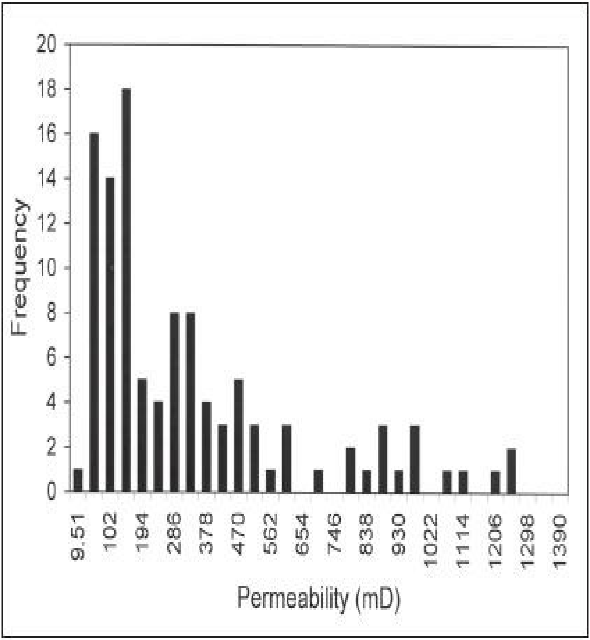

FIGURE B5.2 Core permeability histogram.

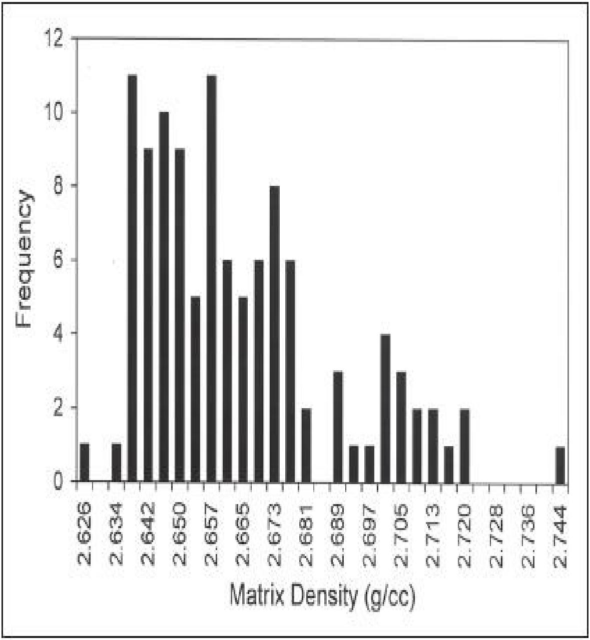

FIGURE B5.3 Core grain density histogram.

FIGURE B5.4 shows the poro-perm plot for Sand 1. The linear relationship is moderately strong with $R^2 = 0.54$. FIGURE b5.5 shows the poro-perm plots for the gas cap and the oil rim. It is clear that the quality of the reservoir rock in the oil rim is higher than in the gas cap. The permeability equations for the gas cap and the oil rim are

$$k = 5.8621 \times 10^7 \phi^{11.052} \tag{B5.1}$$

$$k = 1.5709 \times 10^9 \phi^{12.794} \tag{B5.2}$$

FIGURE B5.6 shows a comparison of the water saturation from Archie's equation and from core analysis.

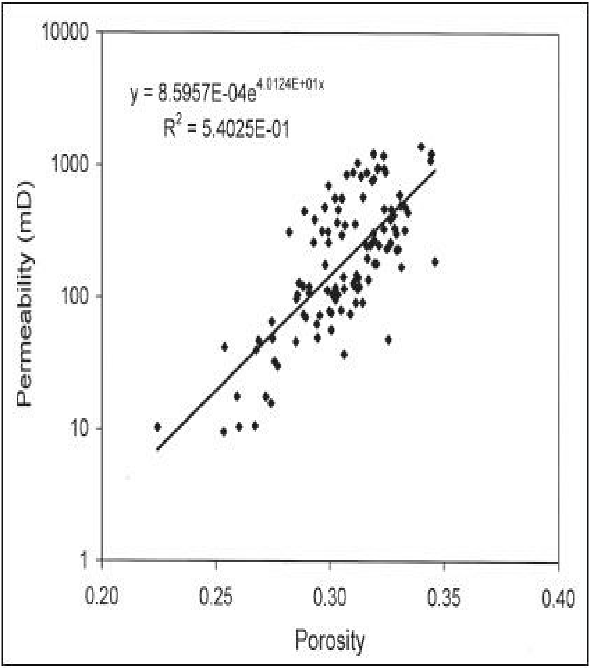

FIGURE B5.4 Core poro-perm plot for Sand 1.

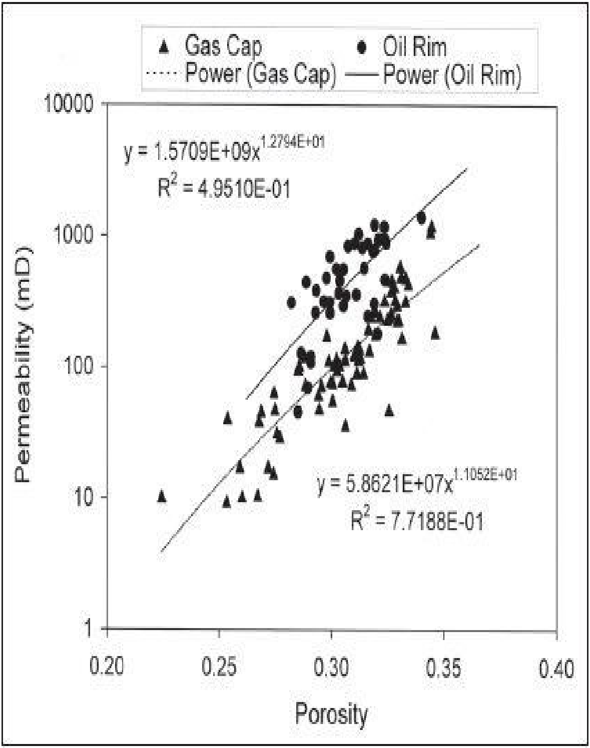

FIGURE B5.5 Core poro-perm plot for gas cap and oil rim.

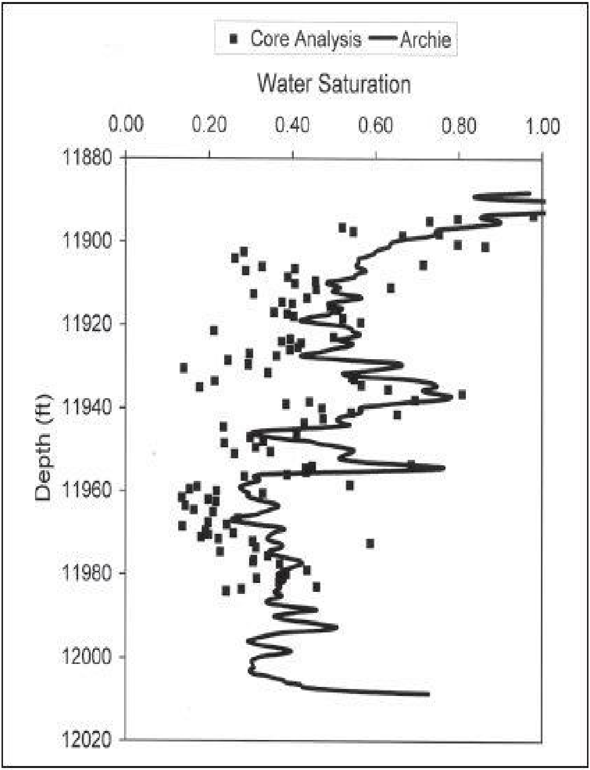

FIGURE B5.6 A comparison of water saturation from Archie's equation and core analysis.

5c

FIGURE B5.7 shows a comparison of the density porosity and the core porosity after the density porosity calibration with ρ_m = 2.663 g/cc and ρ_f = 0.80 g/cc. The agreement is good.

5d

FIGURE B5.8 shows the final density porosity log for Sands 1 and 2 along with the neutron porosity. It should be observed that the density porosity and the neutron porosity agree in sands but disagree in shales. This is as it should be. There is no evidence of a water-oil contact in Sand 1. The nearest water zone is in Sand 2, which is separated from Sand 1 by 129.26 ft TVD of shale.

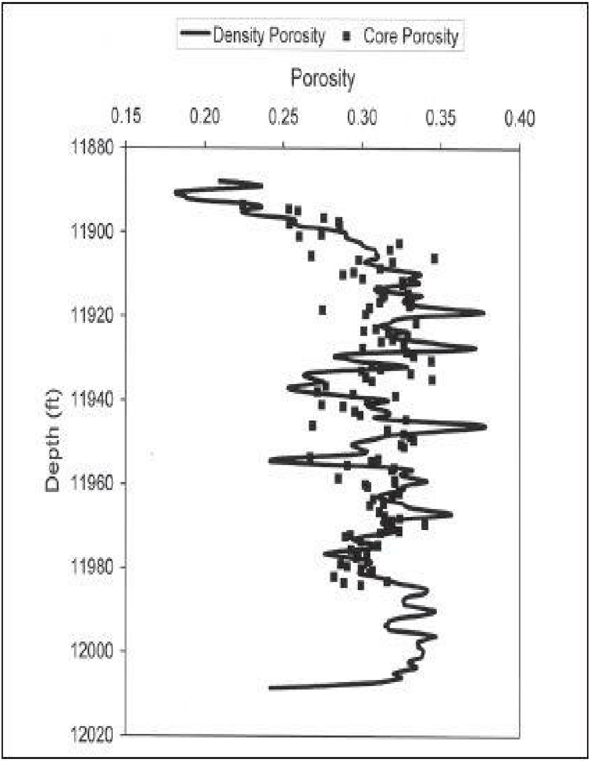

FIGURE B5.7 A comparison of density porosity and core porosity for Sand 1.

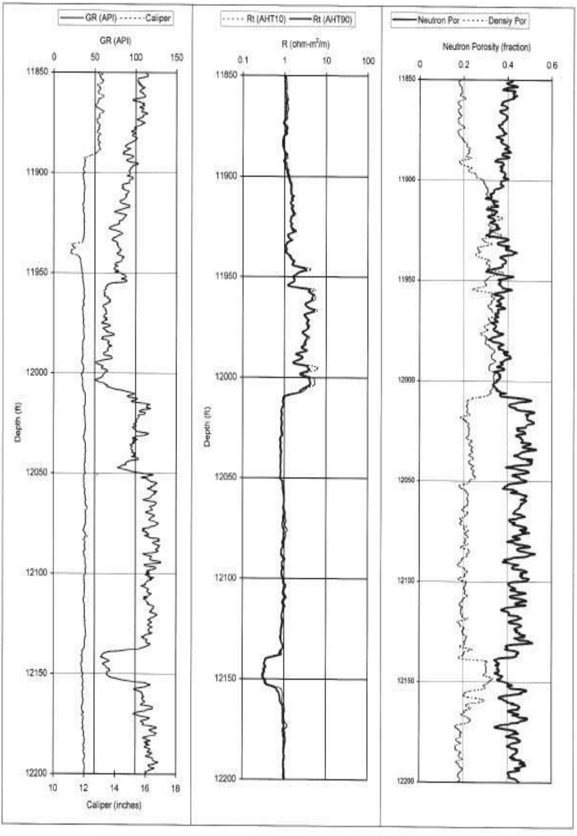

FIGURE B5.8 Final porosity log for for Sands 1 and 2.

5e

FIGURE B5.9 shows the permeability log computed with Eq.(B5.1) for the gas cap and (B5.2) for the oil rim along with the core data. The agreement is good.

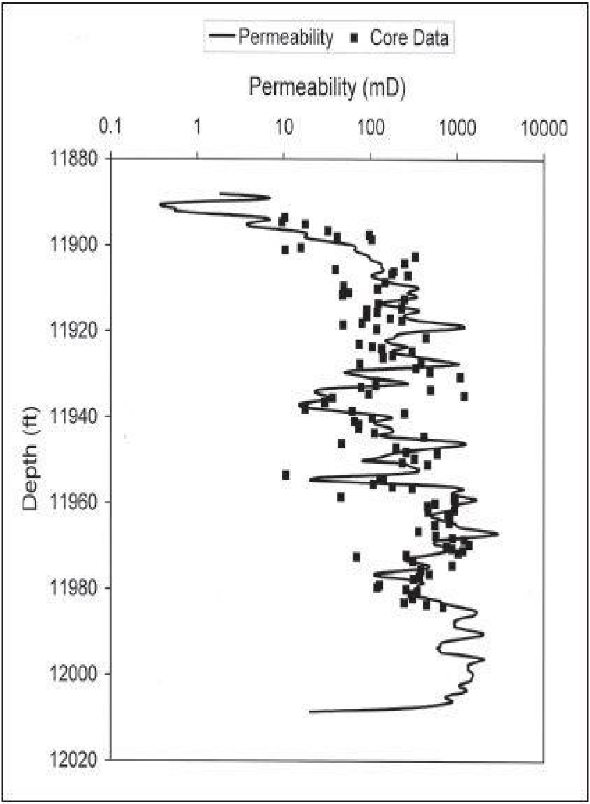

FIGURE B5.9 Permeability log for for Sand 1.

PROJECT 6

6a

FIGURE B6.1 shows the Pickett plot for Sand 2. The equation is

$$R_t = \frac{a \times R_w}{\phi^m} = \frac{1 \times 0.0419}{\phi^{1.7648}} \tag{B6.1}$$

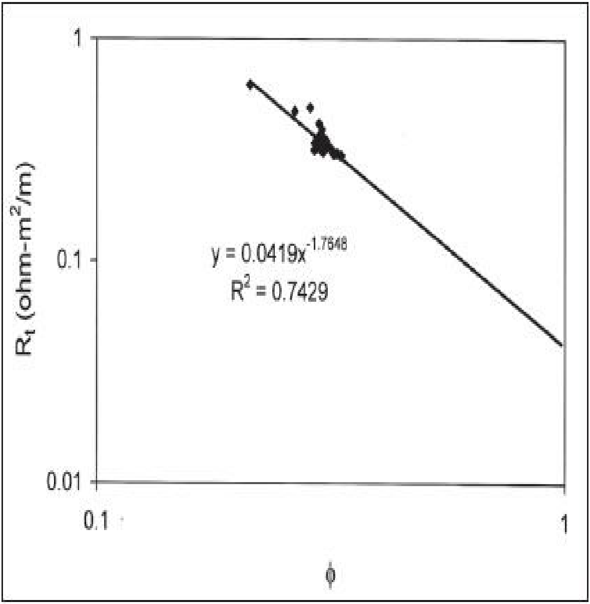

FIGURE B6.1 Pickett plot for Sand 2.

From Eq.(B6.1), for Sand 2,

$$R_w = 0.0419 \text{ ohm-m}$$
$$m = 1.7648$$

The water resistivity from this sand is used in the log analysis for Sand 1.

6b

FIGURE B6.2 through **B6.5** show the resistivity index plots for Cores 18, 63, 105, and 121. The average water saturation exponent is $n = 1.7662$. **FIGURE B6.6** shows the formation resistivity factor plot from the core data, which gives $a = 1.0113$ and $m = 1.7704$.

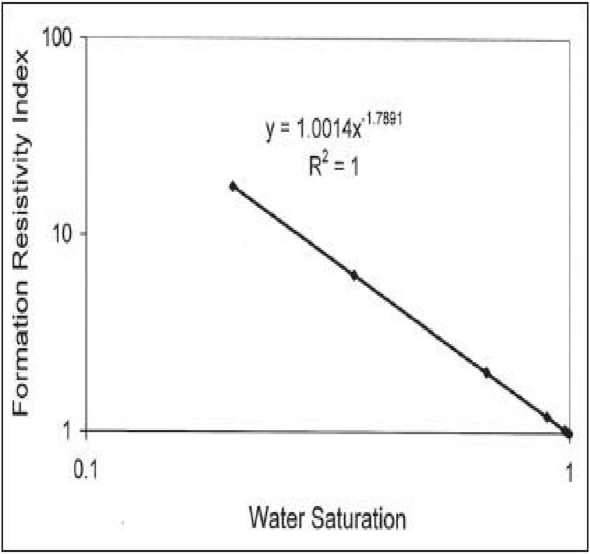

FIGURE B6.2 Resistivity index versus water saturation for Core 18.

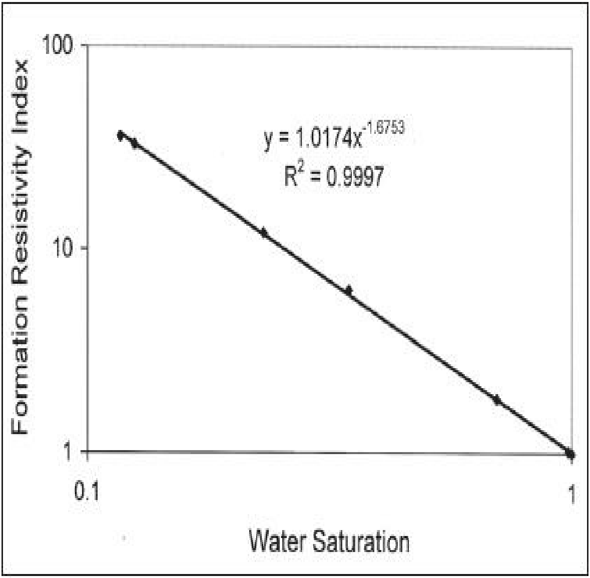

FIGURE B6.3 Resistivity index versus water saturation for Core 63.

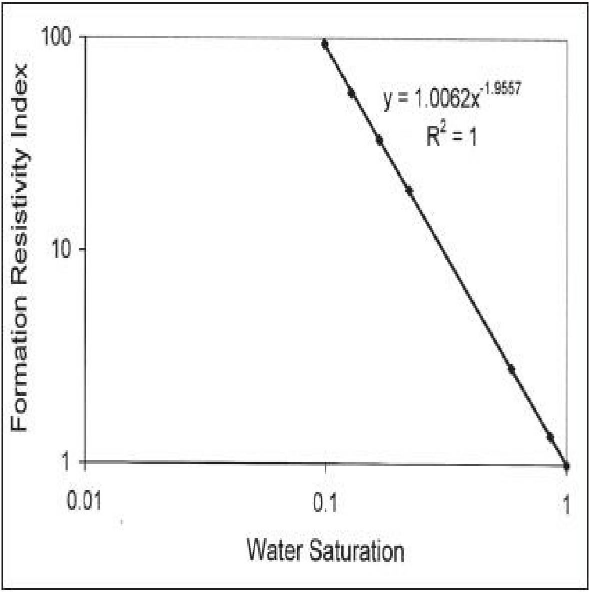

FIGURE B6.4 Resistivity index versus water saturation for Core 105.

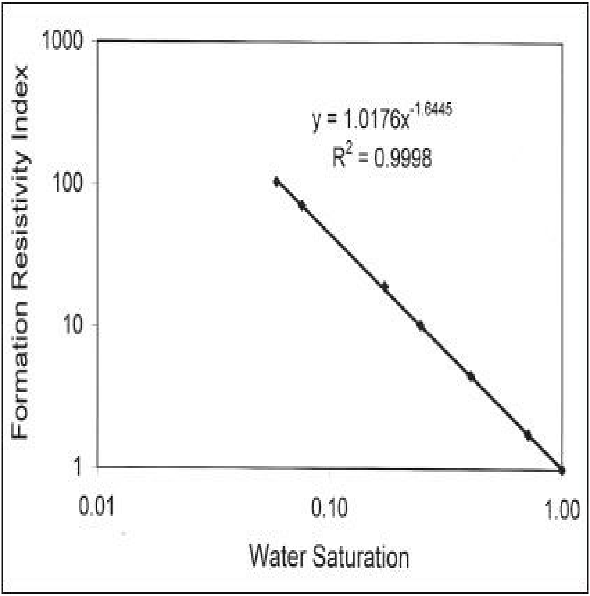

FIGURE B6.5 Resistivity index versus water saturation for Core 121.

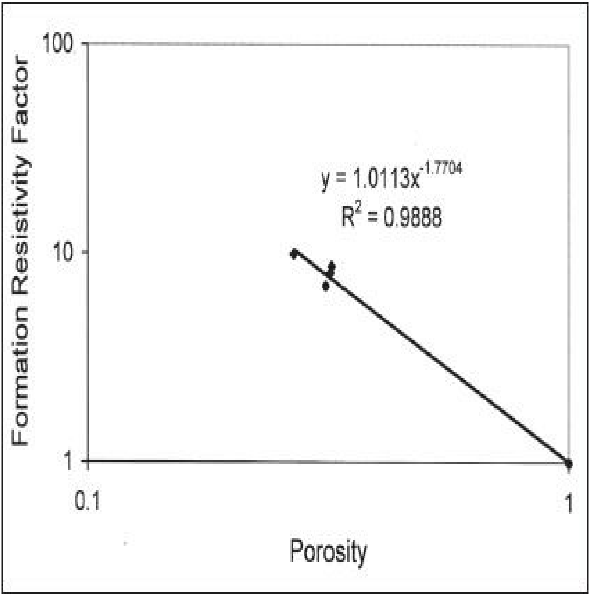

FIGURE B6.6 Formation resistivity factor versus porosity for core data.

6c

The water saturation equation for the

Indonesia shaly sand model is

$$S_w = R_t^{-\frac{1}{n}} \left(\frac{V_{sh}^{\left(1-\frac{V_{sh}}{2}\right)}}{\sqrt{R_{sh}}} + \frac{\phi^{\frac{m}{2}}}{\sqrt{AR_w}} \right)^{-\frac{2}{n}} \quad \text{(B6.2)}$$

Eq.(B6.2) was used to calculate the water saturation in Sand 1 using the following parameters:

$n = 1.7662$
$m = 1.7704$
R_{sh} = 1.0227 ohm-m (average resistivity of the shale above Sand 1)
$R_w = 0.0419$ ohm-m
$A = 1.0$ (worst case scenario)

V_{sh} from gamma ray log

FIGURE B6.7 shows a comparison of the water saturation from the Indonesia model and Archie's equation with a = 1, m = 1.7704, and n = 1.7662. Both estimates agree in the oil rim but differ in the gas cap which is more shaly than the oil rim. If a clean sand was assumed, the hydrocarbon pore volume in the gas cap would be underestimated by

$$Error\% = \frac{\bar{S}_{wI} - \bar{S}_{wA}}{1 - S_{wI}} \times 100 = \frac{0.2997 - 0.4689}{1 - 0.2997} \times 100 = -24.16\%$$

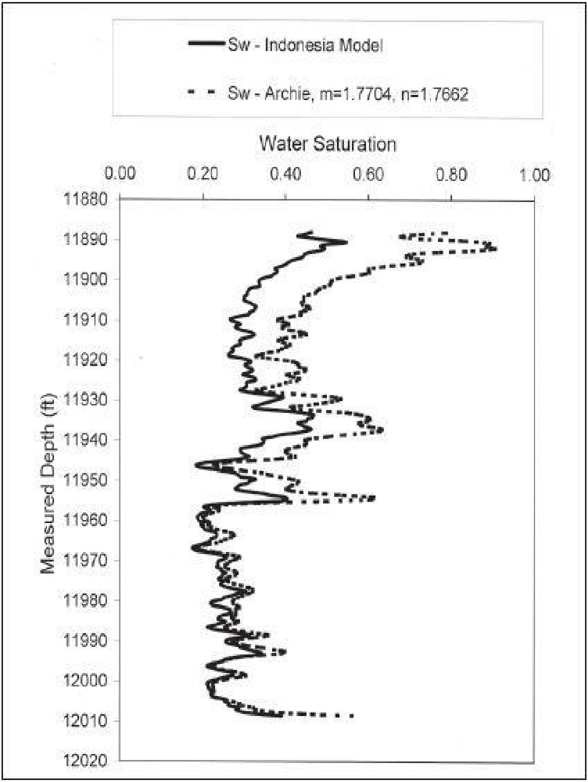

FIGURE B6.7 A comparison of the water saturation logs from the Indonesian model and Archie's equation.

The hydrocarbon pore volume in the oil rim would be underestimated by

$$Error\% = \frac{\bar{S}_{wI} - \bar{S}_{wA}}{1 - S_{wI}} \times 100 = \frac{0.2438 - 0.2704}{1 - 0.2438} \times 100 = -3.52\%$$

PROJECT 7

7a

FIGURE B7.1 shows a comparison of the shale volume estimates from gamma ray and particle size analysis. The agreement between the two is reasonable given that these are two independent estimates of the shale volume.

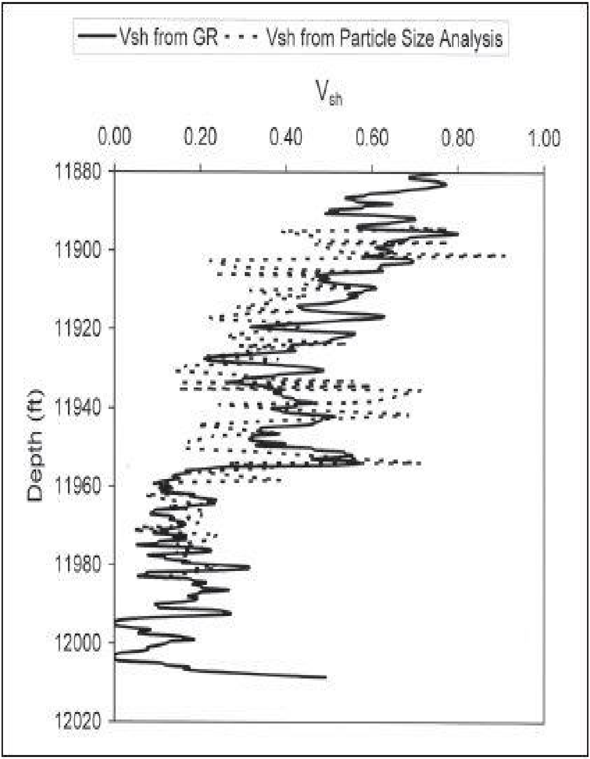

FIGURE B7.1 A comparison of V_{sh} from gamma ray and particle size analysis.

7b

FIGURE B7.2 shows a comparison of the mean grain size and the median grain size from core analysis. Both agree indicating a normal distribution for the grain size distribution.

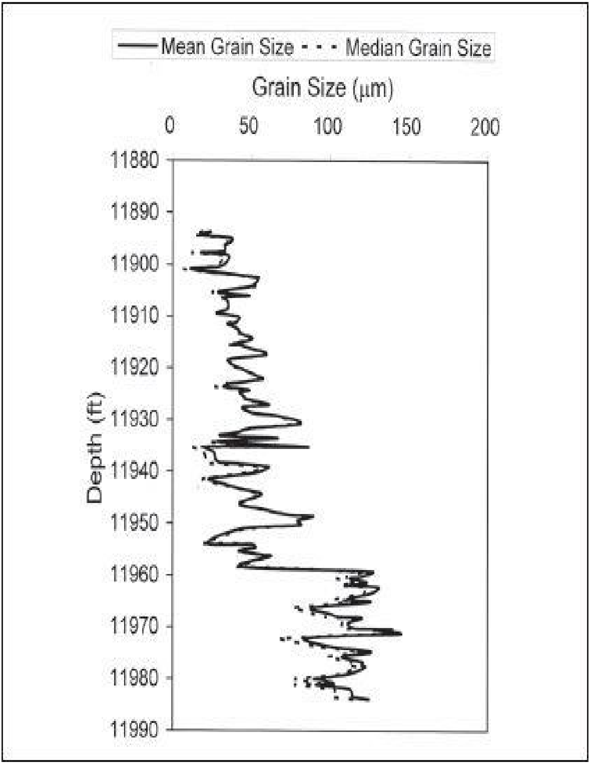

FIGURE B7.2 A comparison of the mean grain size and median grain size for core data.

7c

FIGURE B7.3 shows the specific surface area from core analysis based on the mean grain size. The equation is

$$S = \frac{3(1-\phi)}{D_m \times (0.0001/2)} \ \mathrm{cm^2/cm^3} \qquad \text{(B7.1)}$$

It can be observed that the specific surface area of the grains is higher in the gas cap than in the oil rim. This is further evidence of the poorer quality of the reservoir rock in the gas cap than in the oil rim.

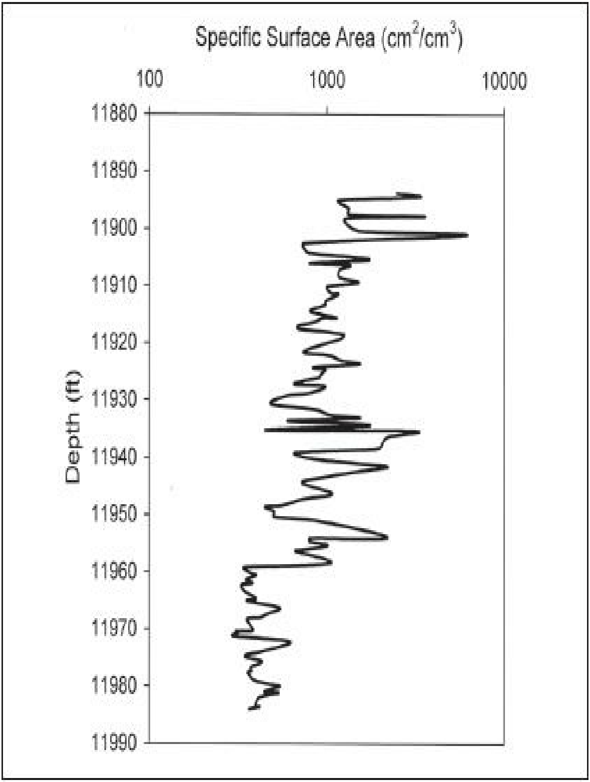

FIGURE B7.3 Specific surface area log for Sand 1.

7d

FIGURE B7.4 shows a comparison of the permeability from core analysis and from the Carman-Kozeny equation. The Carman-Kozeny equation is

$$k = \frac{\phi^3}{CS^2} \times \frac{1000}{9.689 \times 10^{-9}} \text{ mD} \tag{B7.2}$$

where C is the Carman-Kozeny constant. For this shaly sand, $C = 30$ compared to 5 typically used to estimate the permeability for clean sand. The agreement between the core permeability and the estimates from the Carman-Kozeny equation is good.

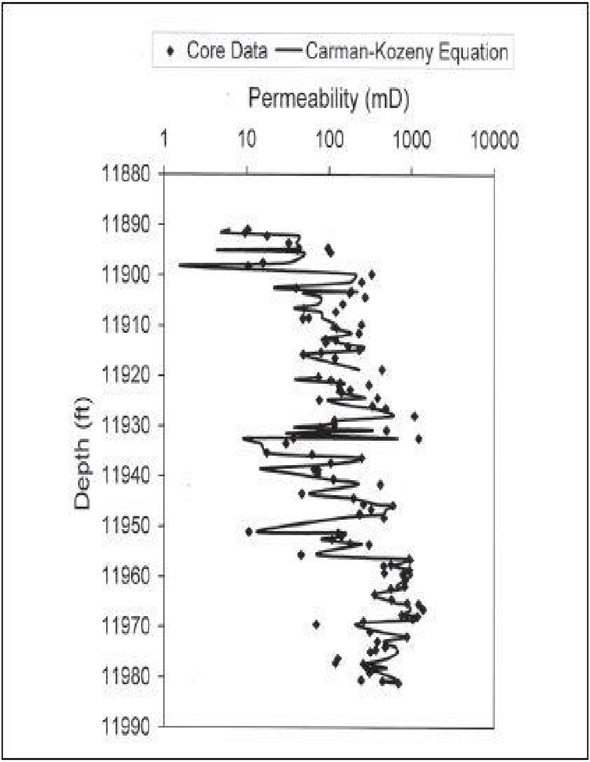

FIGURE B7.4 A comparison of the permeability from core data and the Carman-Kozeny equation.

7e

FIGURE B7.5 shows a comparison of the specific surface area for the gas cap and the oil rim. The equations for the gas cap and oil rim are

$$S = 7.5032\phi^{-4.0908} \quad \text{(B7.3)}$$

$$S = 73.608\phi^{-1.3648} \quad \text{(B7.4)}$$

Eqs. (B7.3) and (B7.4) were used to calculate the permeability in the gas cap and the oil rim. **FIGURE B7.6** shows the permeability log for Sand 1 from the poro-perm method and from the Carman-Kozeny equation. The agreement between the two is very good.

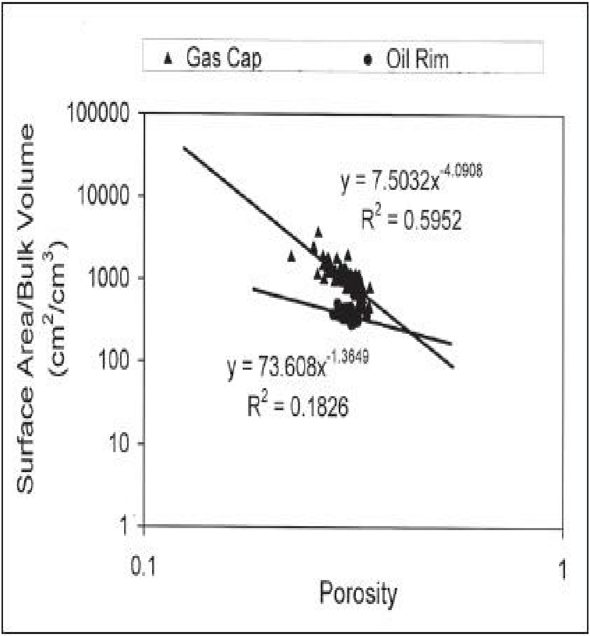

FIGURE B7.5 A comparison of the specific surface area for the gas cap and the oil rim in Sand 1.

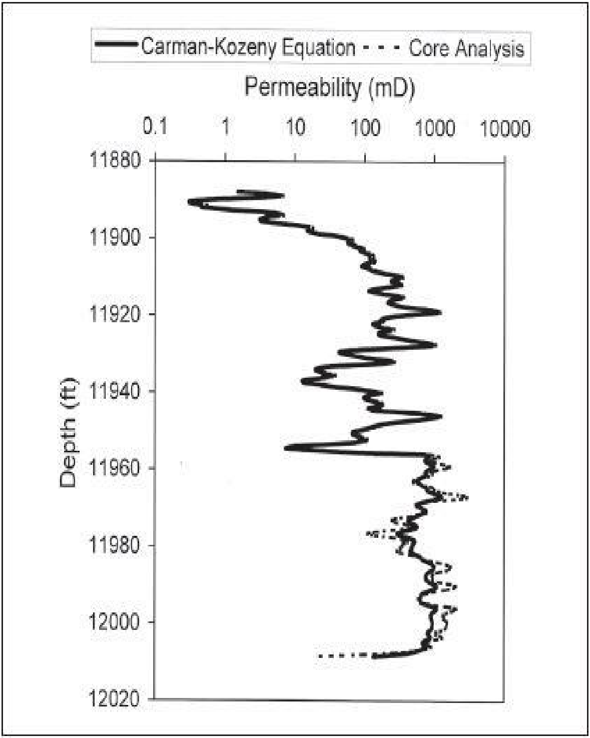

FIGURE B7.6 A comparison of the permeability for Sand 1 from the poro-perm method and the Carman-Kozeny equation.

PROJECT 8

8a

FIGURE b8.1 shows the air-water capillary pressure curves for Cores 18, 63, 105, and 121. All the curves show a zero displacement pressure.

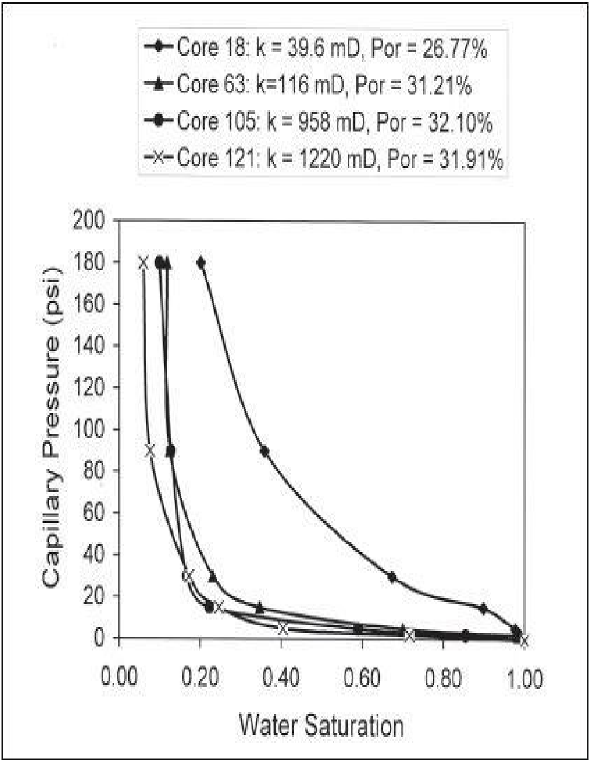

FIGURE B8.1 Air-water capillary pressure curves for Cores 18, 63, 105, and 121.

8b

FIGURE B8.2 shows the Leverett *J*-functions for Cores 18, 63, 105, and 121. They do not plot as one curve. Therefore, the cores have different pore structures.

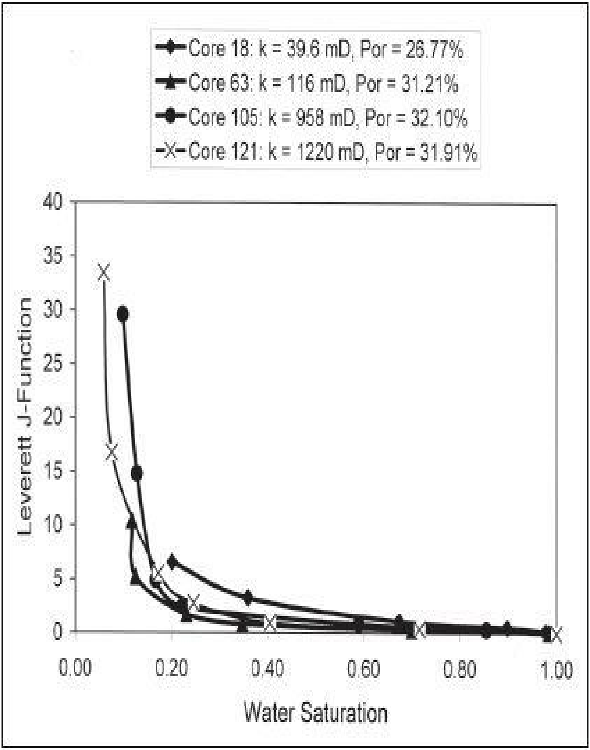

FIGURE B8.2 Leverett *J*-functions for Cores 18, 63, 105, and 121.

8c

FIGURE B8.3 through **B8.6** show the curve fits for the Leverett *J*-functions for Cores 18, 63, 105, and 121, where S^* is an adjustable parameter to obtain the best fit. The saturation equations for the curve fits are as follows:

Core 18:

$$S_w - 0.15 = 0.8873 e^{-0.4352 J} \qquad \text{(B8.1)}$$

Core 63:

$$S_w - 0.04 = 0.2760 J^{-0.6034} \qquad \text{(B8.2)}$$

Core 105:

$$S_w - 0.07 = 0.3596 J^{-0.7430} \qquad \text{(B8.3)}$$

Core 121:

$$S_w - 0.00 = 0.4128 J^{-0.5616} \tag{B8.4}$$

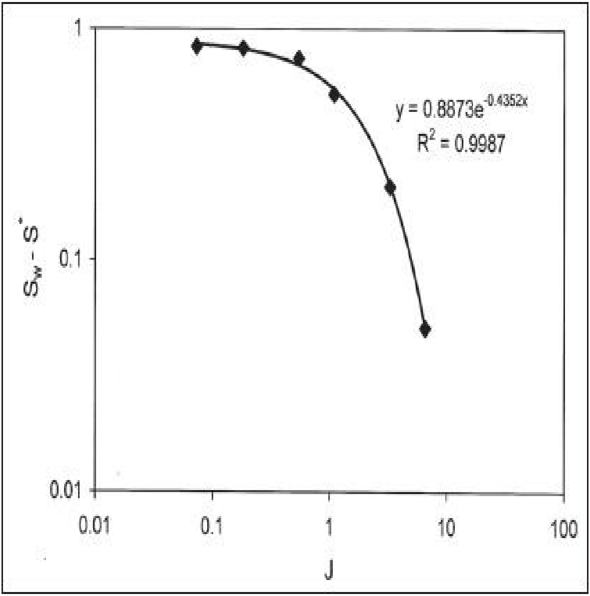

FIGURE B8.3 S_w versus J curve fit for Core 18.

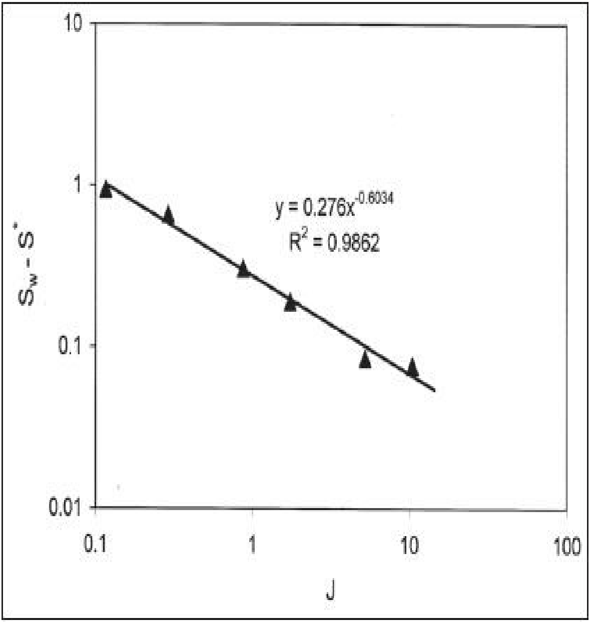

FIGURE B8.4 S_w versus J curve fit for Core 63.

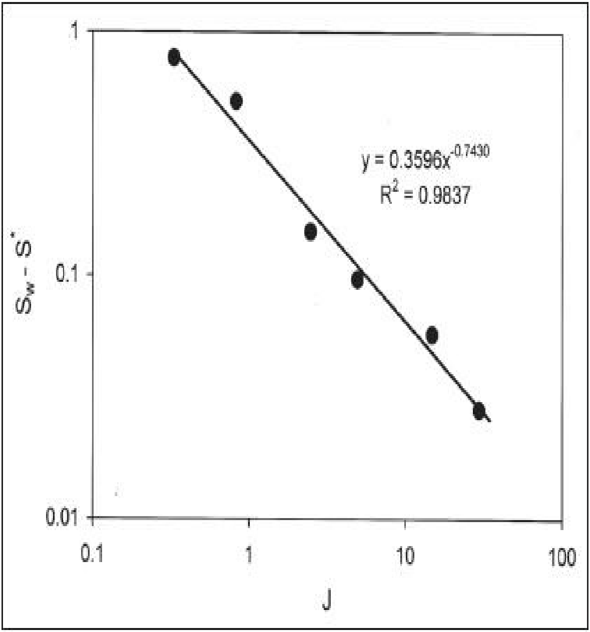

FIGURE B8.5 S_w versus J curve fit for Core 105.

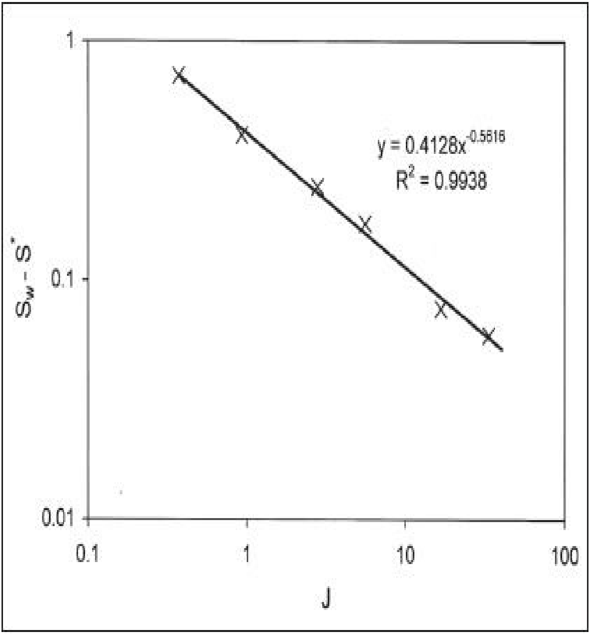

FIGURE B8.6 S_w versus J curve fit for Core 121.

PROJECT 9

9a

FIGURE b9.1 shows the pressure-depth lines for the water, oil, and gas in Sand 1.

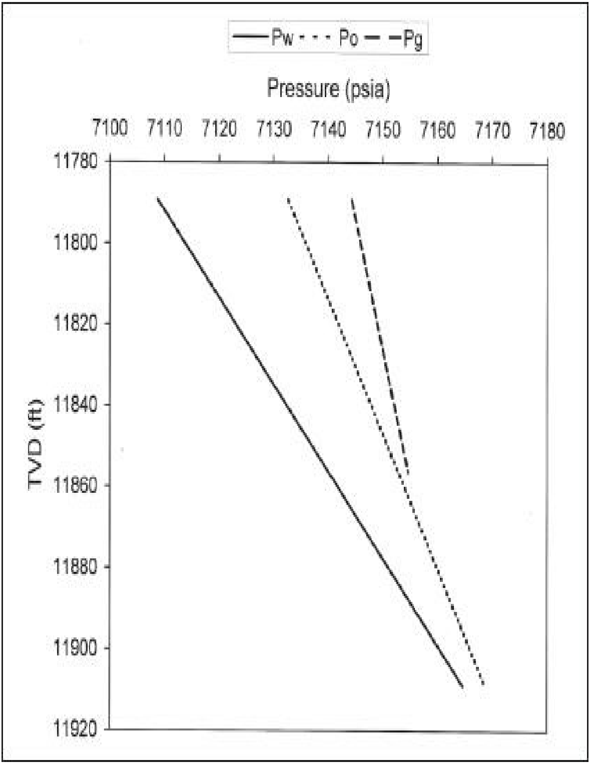

FIGURE B9.1 Pressure lines for water, oil, and gas in Sand 1.

9b

FIGURE B9.2 shows the gas-water and the oil-water capillary pressure lines for Sand 1. The two capillary pressure lines are separated at the oil-water contact by the oil-gas capillary pressure since there are three phases at this depth.

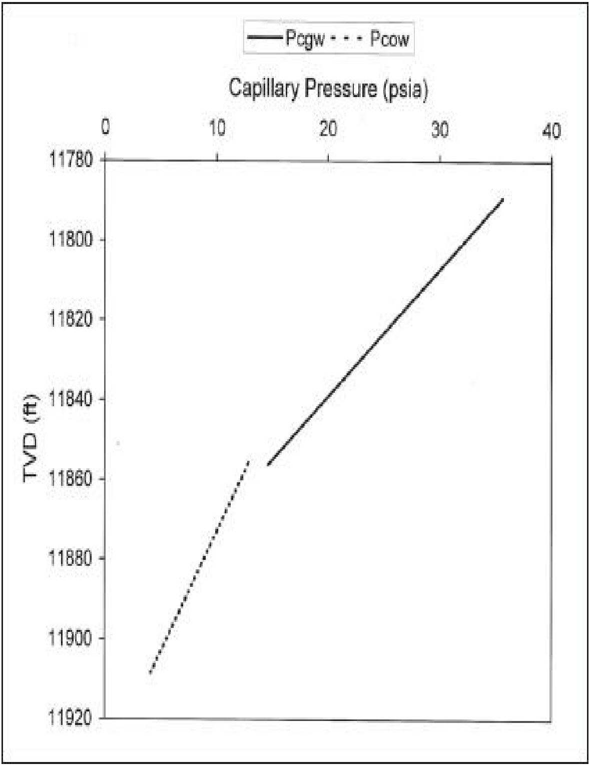

FIGURE B9.2 Gas-water and oil-water capillary pressure lines for Sand 1.

9c

FIGURE B9.3 shows the Leverett *J*-function for Sand 1 for σ_{gw} = 50 dynes/cm, σ_{ow} = 15 dynes/cm, and $\cos\theta$ = 1.

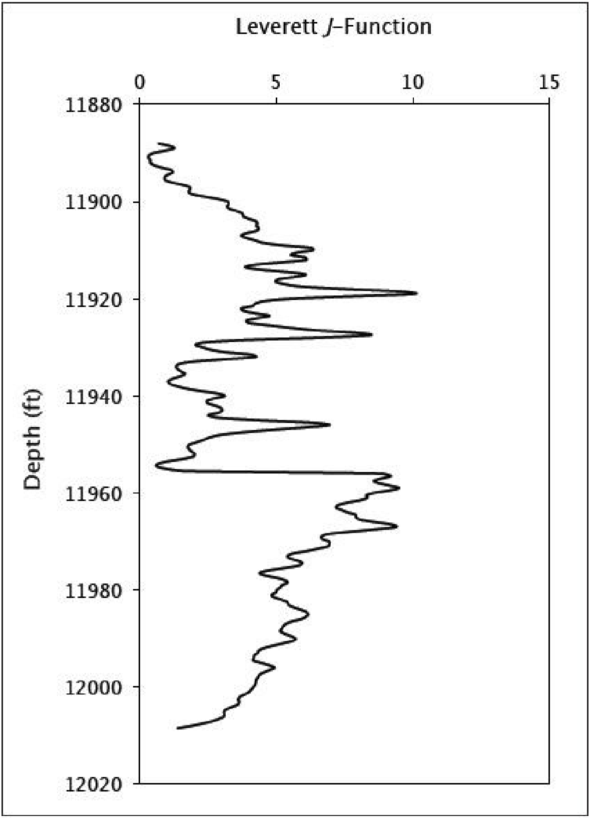

FIGURE B9.3 Leverett *J*-function for Sand 1.

9d

Eqs.(B8.1) through (B8.4) were used in conjunction with the Leverett *J*-function of Figure B9.3 to map the water saturation in Sand 1. The equation from each core was used to map the water saturation in a different segment of Sand 1 as follows:

> Eq.(B8.1) from Core 18: 11888.00 – 11931.00 ft MD
> Eq.(B8.2) from Core 63: 11931.50 – 11955.50 ft MD
> Eq.(B8.3) from Core 105: 11956.00 – 11968.00 ft MD
> Eq.(B8.4) from Core 121: 11968.50 – 12008.50 ft MD

9e

FIGURE B9.4 shows a comparison of the water saturation distributions from the Indonesia shaly sand model, Archie's equation, and capillary pressure data. It can be observed that the capillary pressure data give water saturation distribution in the oil rim that is much lower than those of the other two methods. It also gives the water saturation distribution at the top of the gas cap that is essentially the same as Archie's equation. It should be noted that there was no water zone in Sand 1 but one was created to demonstrate the method of water saturation estimation by the capillary pressure method. Under favorable conditions with an underlying water zone, the capillary pressure method can give a very reliable initial water saturation distribution in a petroleum reservoir.

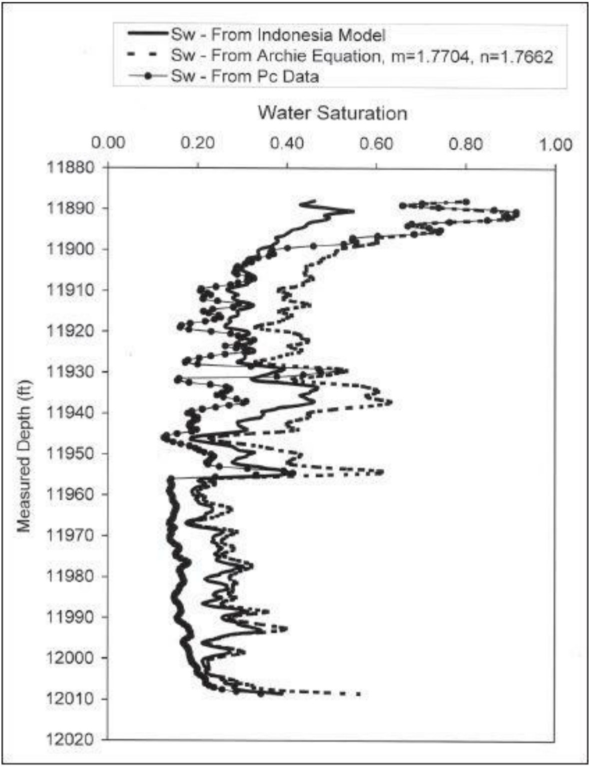

FIGURE B9.4 A comparison of the water saturation estimates from the Indonesian model, Archie's equation, and capillary pressure data.

PROJECT 10

FIGURE B10.1 shows a picture of the fluid distributions in Sand 1. Such a picture often is used in conjunction with log analysis to give an overview of fluid distributions in the sands penetrated by the well.

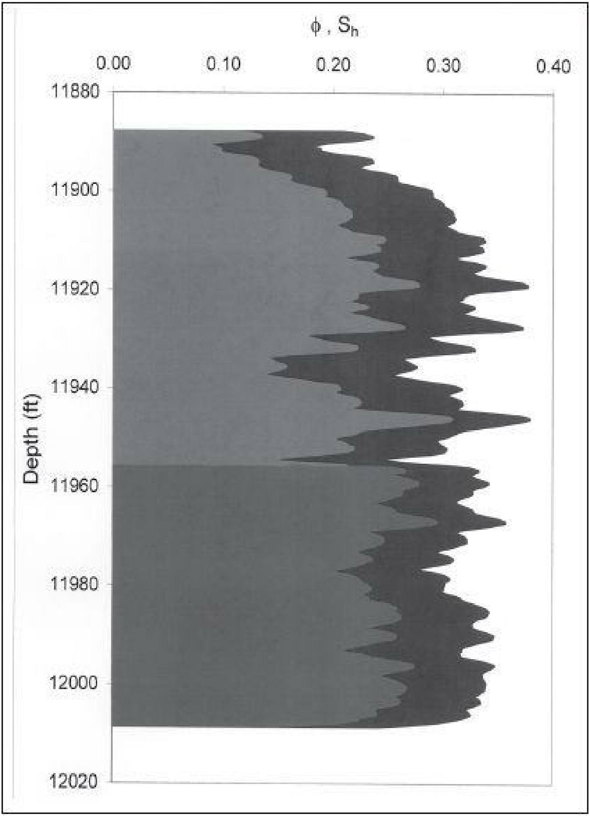

FIGURE B10.1 Fluid distribution in Sand 1.

PROJECT 11

11a

For the gas cap,

$$A = 8000 \text{ acres}$$

$$h = 66.88 \text{ ft}$$

$$\bar{\phi} = 0.2997$$

$$\bar{S}_w = 0.3332$$

$$T = 133.5°\text{F} = 133.5 + 460 = 593.5°\text{R}$$

$$P = 7260 \text{ psia}$$

$$\gamma_g = 0.80$$

$$T_{pc} = 444°\text{R}$$

$$T_{pr} = 593.5/444 = 1.34$$

$$P_{pc} = 650 \text{ psia}$$

$$P_{pr} = 7260/650 = 11.17$$

$$Z = 1.25$$

$$B_{gi} = 0.02827\frac{ZT}{P_i} = \frac{(0.02827)(1.25)(593.5)}{7260} = 2.889\times10^{-3}\ \frac{\text{res cu ft}}{\text{scf}}$$

$$G = 43560\frac{Ah\bar{\phi}\left(1-\bar{S}_w\right)}{B_{gi}}$$

$$= \frac{(43560)(8000)(66.88)(0.2997)(1-0.3332)}{2.889\times10^{-3}} = 1612\times10^{9}\ \text{scf}$$

11b

For the oil rim,

$$A = 8000 \text{ acres}$$

$$h = 52.94 \text{ ft}$$

$$\bar{\phi} = 0.3210$$

$$\bar{S}_w = 0.2438$$

$$B_{oi} = 1.45 \text{ RB/STB}$$

$$N = STOIIP = 7758 \frac{Ah\bar{\phi}\left(1-\bar{S}_w\right)}{B_{oi}}$$

$$= \frac{(7758)(8000)(52.94)(0.3210)(1-0.2438)}{1.45} = 550 \times 10^6 \text{ STB}$$

11c

The amount of gas in solution is given by

$$G_{solution} = R_{si} \times N = 1065 \times 550 \times 10^6 = 586 \times 10^9 \text{ scf}$$

PROJECT 12

12a

FIGURE B12.1 shows the correlation for the water saturation from the Indonesia shaly sand model with porosity. The equation is

$$S_w = 0.8246 - 1.7059\phi \qquad \text{(B12.1)}$$

TABLE b12.1 shows a summary of the Monte Carlo simulation using Latin Hypercube Sampling (Project 4).

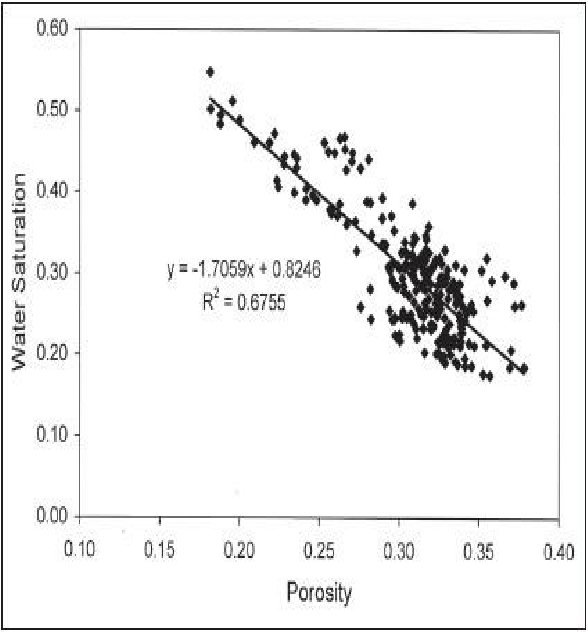

FIGURE B12.1 Water saturation versus porosity correlation from the Indonesian model.

TABLE B12.1 Summary of Monte Carlo Simulation.

	N (MMSTB)	N_r (MMSTB)	NCF (MM$)
Minimum	158	38	756
Maximum	866	320	7987
Standard Deviation	140	51	1229
P90	274	76	1671
P50	453	132	2949
P10	652	209	4699

12b

FIGURE B12.2 through **B12.4** show the expectation curves for the STOIIP, recoverable oil reserve, and undiscounted net cash flow.

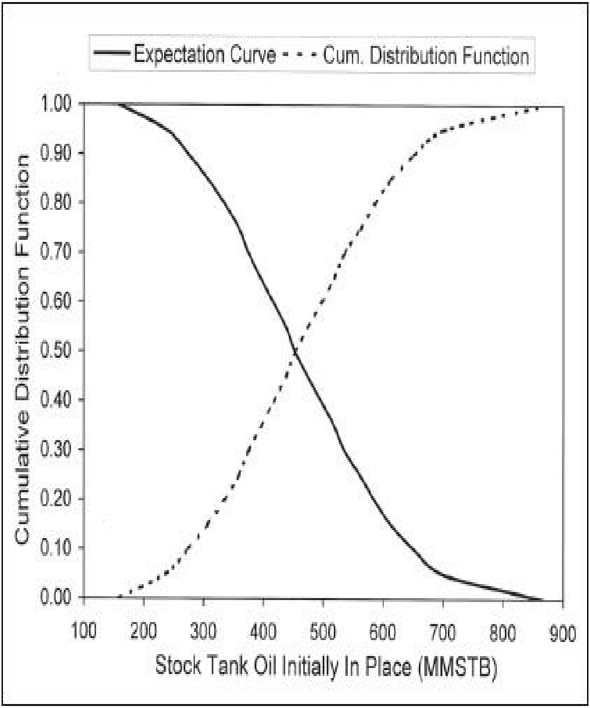

FIGURE B12.2 Expectation curve for STOIIP.

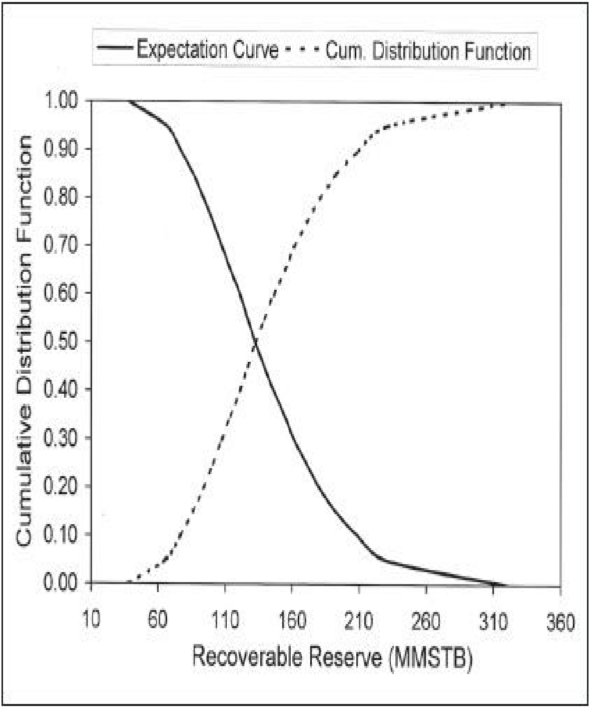

FIGURE B12.3 Expectation curve for recoverable oil reserve.

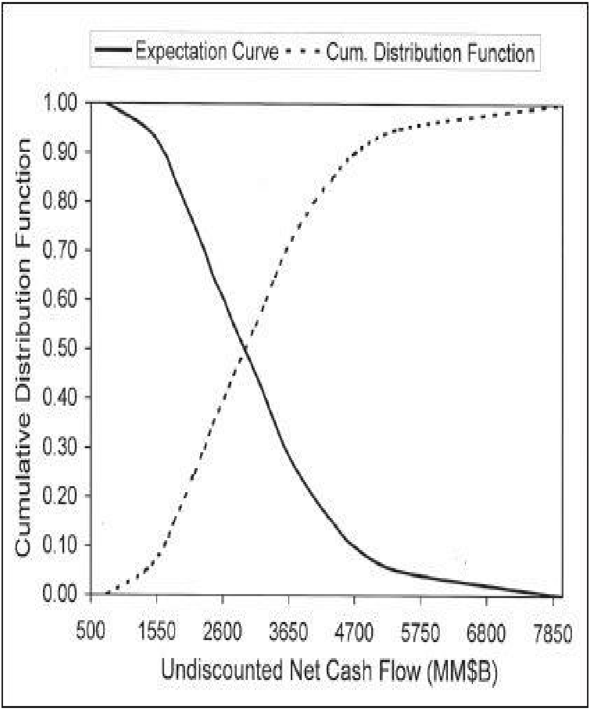

FIGURE B12.4 Expectation curve for undiscounted net cash flow.

12c

Based on the expectation curve for the STOIPP, there is 27% probability that the initial oil in place is at least 550×10^6 STB.

PROJECT 13

$\mu^{nw} = \mu^{o} = 10$ cp

$\mu^{w} = 1$ cp

$B^{o} = 1.45$ RB/STB

$B^{w} = 1.0$ RB/ STB

$R^{s} = 1065$ scf/STB

13a

$S_{wirr} = 0.161$

$S_{Or} = 0.200$

FIGURE B13.1 shows the relative permeability curves obtained from the service company. Note that the base permeability used to define relative permeability is the effective permeability to oil at the irreducible water saturation.

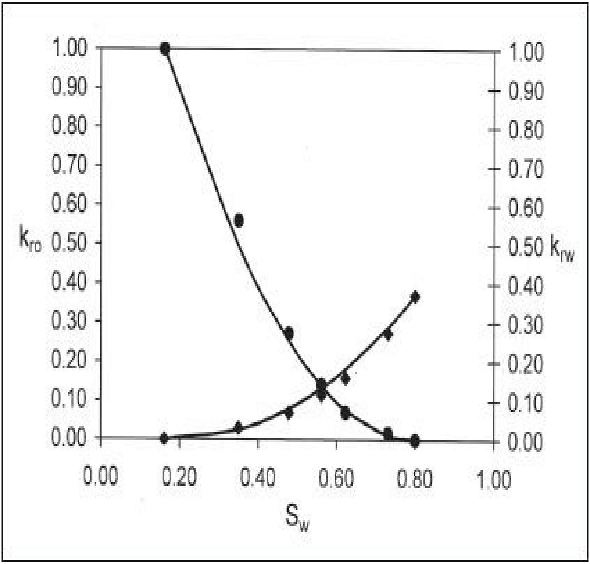

13b,c

FIGURE b13.2 shows the relative permeability curves rescaled with the base permeability equal to the absolute permeability of Core 125 along with the Corey curve fits. The Corey equations are

$$k_{rw} = 0.224 S_e^{2.3} \qquad \text{(B13.1)}$$

$$k_{ro} = 0.606 (1 - S_e)^{1.9} \qquad \text{(B13.2)}$$

where S_e is defined as

$$S_e = \frac{S_w - S_{wirr}}{1 - S_{wirr} - S_{or}} \qquad \text{(B13.3)}$$

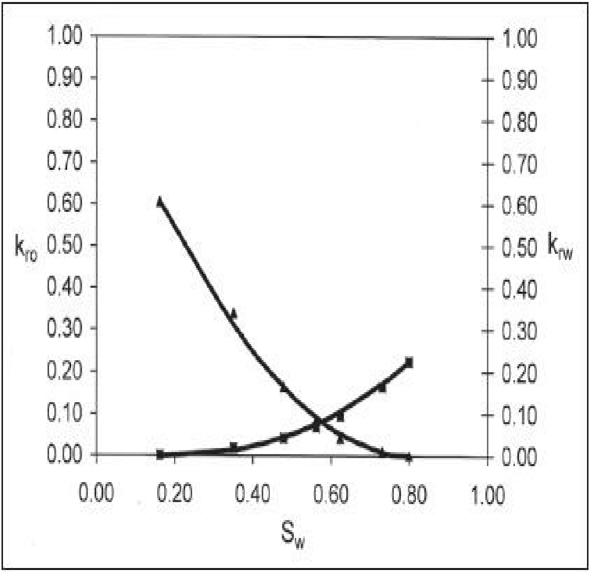

FIGURE B13.2 Rescaled relative permeability curves for Core 125 based on the absolute permeability of the core.

13d,e

FIGURE B13.3 shows the approximate fractional flow curve along with the

Welge line. Note that the Welge line is pivoted at $S_{wi} = 0.2438$, which is higher than $S_{wirr} = 0.161$.

$$S_{wf} = 0.455$$

$$S_{wav} = 0.567$$

$$\left(\frac{df_w}{dS_w}\right)_{S_{wf}} = 2.96$$

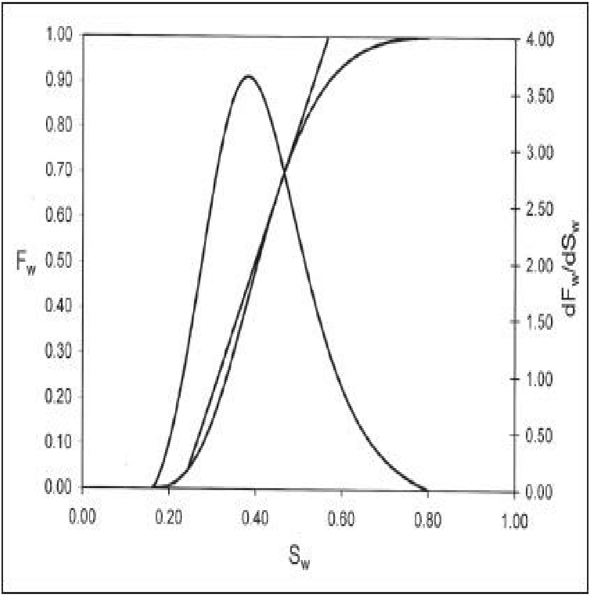

FIGURE B13.3 Approximate fractional flow curve with the Welge tangent line.

13f

The end-point mobility ratio for the

waterflood = 3.70.

13g

FIGURE B13.4 shows the water saturation profiles along with the initial and irreducible water saturations.

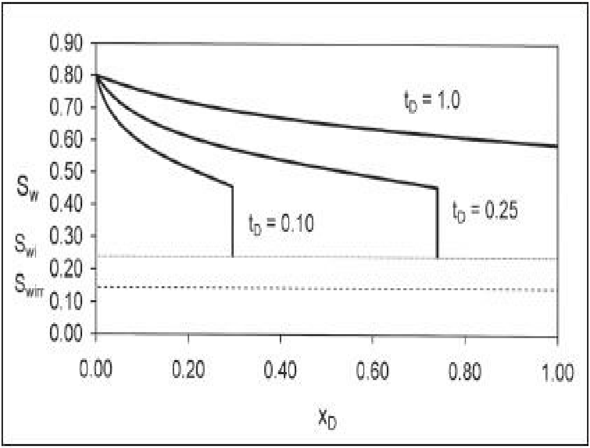

FIGURE B13.4 Water saturation profiles at $t_D = 0.10, 0.25,$ and 1.0.

13h

$t_{DBT} = 0.3378$

13i

$R_{BT} = 0.4276$

13j

FIGURE B13.5 shows the oil recovery curves.

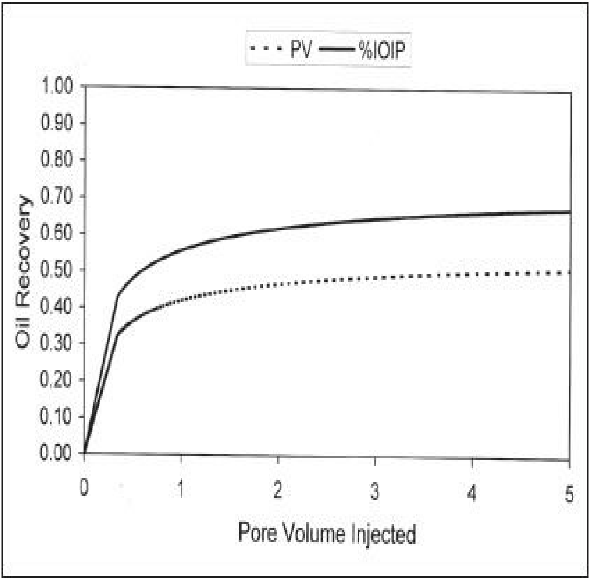

FIGURE B13.5 Oil-recovery curves.

13k

$\boldsymbol{A} =$ 8,000 acres

$\boldsymbol{L} =$ 37,335 ft

$\boldsymbol{W} =$ 9,334 ft

$\boldsymbol{h} =$ 52.94 ft

$\boldsymbol{V_p}$ =5,921,978,515 ft^3 = 1,054,671,151 RB

$\boldsymbol{B_0}$ = 1.45 RB/STB

$\boldsymbol{B_w}$ = 1.0 RB/STB

$\boldsymbol{A_x}$ = 494,132 ft^2

u = 1.215 ft/D

q=106,923 STB/D

Q_{wBT} = 391,978,986 RB

$\boldsymbol{W_{pBT}}$ = 16,822,470 RB

N_{pBT} = 258,728,632 STB

$\boldsymbol{t_{BT}} =$ 3,332.39 days = 9.13 years

FIGURE B13.6 shows the oil, gas, and water production rates. **FIGURE B13.7** shows the water cut along with the oil production rate. The water cut is over 90% after 20 years of production. **FIGURE B13.8** shows the cumulative oil, gas, and water productions along with the cumulative water injection volume.

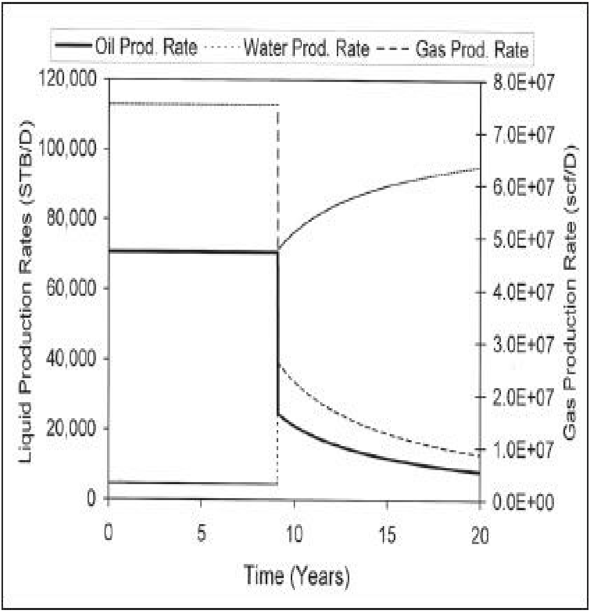

FIGURE B13.6 Production rates.

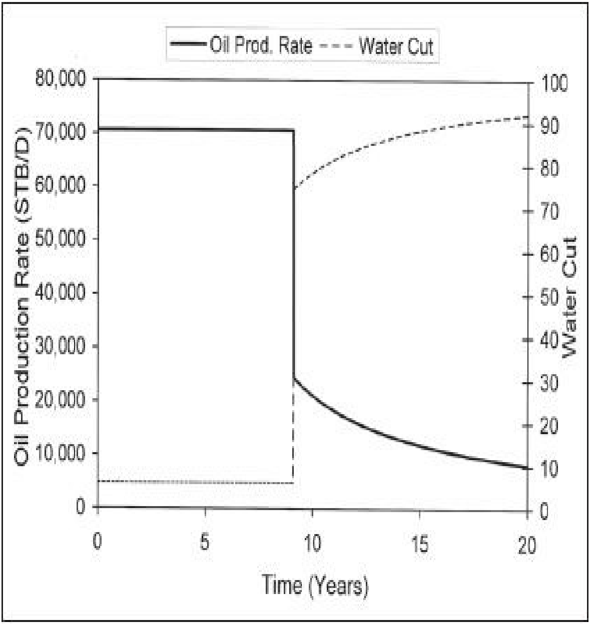

FIGURE B13.7 Water cut.

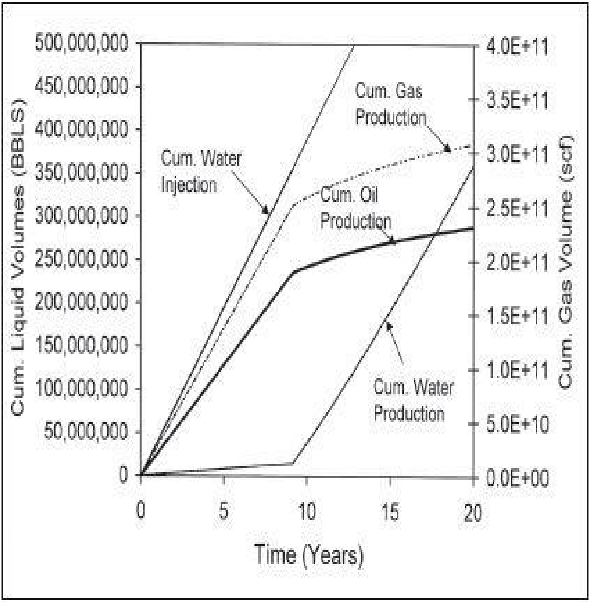

FIGURE B13.8 Cumulative production and injection volumes.

13l

Oil recovery factor after 20 years of

production = 52%

ABOUT THE AUTHOR

Dr. Ekwere J. Peters has over 35 years of petroleum engineering experience in field operations, petrophysics, higher education, and research. He was the holder of the Frank W. Jessen Endowed Professorship and the George H.

Fancher, Jr. Endowed Professorship in Petroleum Engineering at the University of Texas at Austin where he was a faculty member for over 31 years. From 1997–2001, he was the Chairman of the Department of Petroleum & Geosystems Engineering where he provided administrative and academic leadership to the highly ranked department.

At the University of Texas, he taught courses in introduction to the petroleum industry, drilling and well completions, production technology and design, advanced pressure transient analysis, petroleum fluid properties, and advanced petrophysics. He has conducted numerous short courses for the petroleum industry in the Unites

States, Canada, Nigeria, Mexico, Venezuela, Brazil, Japan, Indonesia, Ecuador, and Trinidad & Tobago. A recognized expert in flow through porous media and petrophysics, he has published papers on various aspects of petroleum engineering based on the results of original research.

Dr. Peters established a reputation as an excellent teacher early in his academic career and consistently received very high ratings for teaching effectiveness at the University of Texas and at industry short courses. He has won numerous awards for teaching and professional excellence including the prestigious Texas Excellence Teaching Award, the Petroleum Engineering

Teaching Excellence Award in the Cockrell School of Engineering, the Society of Petroleum Engineers International Distinguished Achievement Award for Petroleum Engineering Faculty, and the Society of Petroleum Engineers Distinguished Member Award.

His previous petroleum industry affiliations were with Shell-BP Petroleum Development Company Ltd (Nigeria) in drilling and well completions; United Petro Laboratories, Calgary as the manager of a PVT and Core Analysis Laboratory and Amoco Production Company, Houston in pressure transient analysis in tight gas sands. Currently, he is a senior consultant at Afren USA, Inc., Woodlands, where he oversees the company's educational initiatives.

He holds a BSc, 1st class honors, degree in Engineering from Leicester University, an MS and a PhD in Petroleum Engineering from the University of Alberta, and is a registered professional engineer in Texas.

E-mails:

ejpeters@mail.utexas.edu; Ekwere.Peters@yahoo.com